

**Development of carbamate modified PEI for delivery of a
granzyme B inhibitor gene to protect against cytotoxic lymphocyte
killing**

Wei Cheng

Imperial College London

Section of Immunobiology, Division of Immunology and Inflammation,

Department of Medicine, Faculty of Medicine

Thesis submitted for the degree of PhD

DECLARATION OF ORIGINALITY

This is to certify that to the best of my knowledge, the work presented in this thesis is my own, and it has not been previously submitted for a degree or diploma at any other higher education institution. Any assistance or advice rendered in preparing this thesis has been duly acknowledged.

COPYRIGHT DECLARATION

The copyright of this thesis rests with the author and is made available under a Creative Commons Attribution Non-Commercial No Derivatives licence. Researchers are free to copy, distribute or transmit the thesis on the condition that they attribute it, that they do not use it for commercial purposes and that they do not alter, transform or build upon it. For any reuse or redistribution, researchers must make clear to others the licence terms of this work.

ACKNOWLEDGEMENTS

I would like to express my sincerest gratitude to my supervisors Professor Philip G Ashton-Rickardt in Imperial College London and Dr. Yi Yan Yang in the Institute of Bioengineering and Nanotechnology (IBN), Singapore for their excellent guidance and supervision throughout the course of my PhD studies. The completion of thesis would not have been possible without their kind patience, unwavering support and encouragement at all stages of my training. In addition, I am indebted to our collaborator Dr. James L. Hedrick from the IBM Almaden Research Centre for the stimulating discussions and his insightful and constructive advice to various aspects of my research.

Deep appreciation goes out to all the past and present members in Professor Ashton-Rickardt's lab, namely: Dr. Lihui Wang for her invaluable suggestion on experimental design and planning, as well as animal work supervision; Dr. Dean Heathcote for his generous help during the gene transfection and plasmid amplification experiments; Dr. Susan Byrne for her excellent guidance through the Real Time PCR training; Dr. Emma Salisbury, Dr. Philip Muller, Dr. Jeff Temblay, Dr. Onjee Choi and Dr. Elena Lovo for their continuous encouragement and inspiration throughout my research. And appreciation also goes to those of the Drug and Gene Delivery Group at IBN, Agency of Science, Technology and Research (A*STAR, Singapore), especially: Dr. Chuan Yang for his ingenious design of the polymers; Dr. Zhan Yuin Ong, Dr. Nikken Wiradharma and Ms Pei Yun Teo for their unwavering support on various technical aspects of my project; Dr. Shujun Gao for his assistance in the intravenous injection of polymer/DNA complexes into mice; Mr. Xiyu Ke for training in dissecting the mice; Ms Amalina Bte Ebrahim Attia, Dr. Ashlynn Lee, Dr. Jeremy Tan, Dr. Majad Khan, Ms Sangeetha Krishnamurthy, Dr. Shrinivas Venkataraman, Dr. Shaoqiong Liu, Mr Xin Ding, and Dr. Yan Li for the great camaraderie as well as unreserved sharing of knowledge and technical expertise. In addition, technical advice and materials support from Professor Peter E. Lobie from Cancer Science Institute of Singapore, and Dr. Jessica Ponti from European Commission, Unit Nanobiosciences is gratefully acknowledged. I would also very much like to gratefully appreciate the invaluable support and assistance provided by the administrative and technical staff in the Section of Immunobiology, Division of Inflammation and Immunology, Department of Medicine, Faculty of Medicine in Imperial College London and in IBN, for their help in creating such conducive and harmonious environments for me to work in.

Moreover, the financial support from A*STAR Graduate scholarship (overseas) granted by A*STAR, Singapore is sincerely acknowledged.

Last but not least, I would like to extend my deepest appreciation to my family and friends for their constant support, understanding and encouragement during my graduate studies.

ABSTRACT

Cytotoxic T lymphocytes (CTLs) and natural killer (NK) cells protect vertebrates by killing infected or transformed cells using granzyme B (GrB) to induce apoptosis. However, GrB-induced apoptosis causes inflammatory disease and allograft rejection and is an important disease target. The aim of this project is to prevent apoptosis of the target cells by delivering a plasmid encoding GrB inhibitor proteinase inhibitor-9 (PI-9) using cationic polymers. Polyethylenimine (PEI, branched, Mw 25 kDa) gives high gene transfection efficiency in many cell lines, but it is highly cytotoxic. To reduce its cytotoxicity, we modified PEI by blocking primary amines through nucleophilic addition between primary amine and a protected functionalized cyclic carbonate, generating a carbamate linkage through the ring-opening of the cyclic carbonate. Different hydrophobic-groups or sugar functionalized carbonates were substituted onto PEI and the optimum substitution ratios to achieve high gene transfection efficiency and minimal cytotoxicity in various cell lines were determined. Among these polymers, PEI with 7 or 20 of 56 primary amine groups substituted by mannose had similar gene binding ability as unmodified PEI, leading to almost 100% transfection efficiency of a GFP plasmid in HEK293T cells as well as a large decrease in cytotoxicity. However, PEI with all primary amine groups blocked was unable to form complexes with DNA, and gene transfection was negligible. The PI-9 encoding plasmid was transfected into HEK293T cells effectively using the optimally modified PEIs, protecting up to 80% HEK293T cells from killing by human natural killer-like YT cells. Furthermore, PEI with 25 primary amine groups substituted by mannose successfully delivered PI-9 plasmid into Balb/3T3 fibroblasts and protected them from killing by GrB. Therefore, the carbamate-mannose modified PEI/PI-9 encoding plasmid complexes have potential clinical utility in the prevention of allograft rejection and inflammatory disease caused by GrB.

TABLE OF CONTENTS

DECLARATION OF ORIGINALITY	2
COPYRIGHT DECLARATION	3
ACKNOWLEDGEMENTS	4
ABSTRACT	6
List of Tables	12
List of Figures	13
List of Schemes	16
List of Abbreviations	17
CHAPTER 1: INTRODUCTION	20
1.1 Different types of transplant pathology, risk factors, and current status of treatments.....	20
1.1.1 Different types of transplant pathology	20
1.1.2 Risk factors of AAR and CAR.....	21
1.1.3 Current status of treatments	22
1.1.3.1 Treatments for AAR.....	22
1.1.3.2 Treatments for CAR.....	23
1.1.3.3 The urgent need to develop new treatment methods to tackle CAR.....	24
1.2 The role of GrB in CTL and NK mediated killing.....	25
1.3 Regulation of GrB by serine protease inhibitors.....	27
1.3.1 Cytotoxic lymphocytes could protect themselves from self-inflicted damage	27
1.3.2 Serine protease inhibitors.....	28
1.3.2.1 Spi6 protects CTLs.....	28
1.3.2.2 Spi6 protects DCs.....	29
1.3.2.3 Spi6 and Spi2A protect CD8 ⁺ memory T cells	29
1.3.2.4 PI-9 protects human CTLs and NK cells	30
1.3.2.5 PI-9 protects accessory cells	30
1.4 The role of GrB in allograft rejection, and the strategies to block GrB.....	30
1.5 Gene therapy: Major developments and current status	33
1.6 Barriers limiting gene delivery and solutions to overcome them.....	34

1.6.1 DNA packaging	35
1.6.2 Extracellular stability	37
1.6.3 Cellular uptake and endosomal escape	38
1.6.4 Intracellular trafficking	40
1.6.5 DNA unpacking	41
1.6.6 Biocompatibility	42
1.7 Methods of gene delivery.....	43
1.7.1 Viral	44
1.7.2 Non-viral	48
1.7.2.1 Cationic liposomes.....	48
1.7.2.2 Cationic polymers	50
1.7.2.2.1 Poly-L-lysine.....	50
1.7.2.2.2 Poly(ethylenimine).....	51
1.7.2.2.3 Dendrimers.....	53
1.7.2.2.4 Biodegradable polymers	54
1.8 Summary and Concluding remarks.....	55
CHAPTER 2: HYPOTHESIS AND AIMS	57
CHAPTER 3: RATIONAL DESIGN OF CARBAMATE-MODIFIED PEI FOR MITIGATED CYTOTOXICITY AND ENHANCED GENE TRANSFECTION EFFICIENCY.....	61
3.1 Introduction.....	61
3.2 Materials and Methods.....	61
3.2.1 Materials	61
3.2.2 Synthesis of carbamate-modified PEI.....	62
3.2.3 Cell culture.....	62
3.2.4 Preparation, particle size and zeta potential analyses of polymer/nucleic acids complexes	62
3.2.5 Gel retardation assay	63
3.2.6 DNA binding assay	63
3.2.7 <i>In vitro</i> gene expression	63
3.2.8 Confocal imaging for GFP expression in HepG2 cells	64

3.2.9 Cellular trafficking.....	64
3.2.10 siRNA transfection and real-time reverse transcription-polymerase chain reaction (RT-PCR) analysis.....	65
3.2.11 Cytotoxicity test.....	66
3.2.12 Organ specific luciferase gene expression in mice.....	66
3.2.13 Statistical analysis.....	67
3.3 Results and Discussion.....	68
3.3.1 Polymer synthesis and characterization.....	68
3.3.2 Size and zeta potential of polymer/DNA complexes.....	75
3.3.3 DNA binding.....	78
3.3.4 <i>In vitro</i> GFP gene expression in various cell lines.....	82
3.3.4.1 <i>In vitro</i> GFP gene expression in HepG2.....	82
3.3.4.1.1 Confocal imaging of GFP gene expression in HepG2.....	86
3.3.4.1.2 Intracellular trafficking of polymer/DNA complexes in HepG2.....	87
3.3.4.2. <i>In vitro</i> GFP gene expression in other cell lines.....	88
3.3.5 <i>In vitro</i> luciferase gene expression assay.....	91
3.3.6 Cytotoxicity test.....	96
3.3.6.1 Cytotoxicity test for HepG2, HeLa and NIH3T3 cells.....	96
3.3.6.2 Cytotoxicity test in other cell lines.....	100
3.3.7 siRNA mediated Bcl-2 knockdown in HeLa cells.....	103
3.3.8 Viability of HeLa cells after being treated with polymer/siRNA complexes.....	104
3.3.9 <i>In vivo</i> organ-specific luciferase expression in mice.....	105
3.4 Conclusion.....	107
CHAPTER 4: DELIVERY OF A GRANZYME B INHIBITOR GENE USING CARBAMATE-MANNOSE MODIFIED PEI TO PROTECT AGAINST NK CELL KILLING.....	109
4.1 Introduction.....	109
4.2 Materials and Methods.....	109
4.2.1 Materials.....	110
4.2.2 Synthesis of protected mannose-functionalized cyclic carbonate (MTC-ipman) and MTC-ipman modified PEI.....	110

4.2.3 Cell culture.....	110
4.2.4 Preparation, particle size and zeta potential analyses of polymer/DNA complexes	110
4.2.5 Gel retardation assay.....	111
4.2.6 <i>In vitro</i> gene transfection	111
4.2.7 Confocal imaging for GFP expression in HEK293T cells.....	112
4.2.8 Cytotoxicity test.....	112
4.2.9 Characterization of GrB expression level in YT cells	112
4.2.10 <i>In vitro</i> protection of HEK293T cells from YT cell killing by transfection with polymer/PI-9 encoding plasmid DNA complexes.....	113
4.3 Results and Discussion	114
4.3.1 Polymer synthesis and composition.....	114
4.3.2 Size and zeta potential of polymer/DNA complexes	115
4.3.3 DNA binding ability of polymers	116
4.3.4 <i>In vitro</i> GFP transfection efficiency.....	116
4.3.5 Cytotoxicity of unmodified and carbamate-mannose modified PEIs	118
4.3.6 Protection of HEK293T cells from GrB mediated killing	120
4.4 Conclusions.....	122
CHAPTER 5: CARBAMATE-MANNOSE MODIFIED PEI DELIVERY OF A GRANZYME B INHIBITOR GENE TO MOUSE FIBROBLAST BALB/3T3 CELLS TO PROTECT AGAINST GRB MEDIATED KILLING	
124	
5.1 Introduction.....	124
5.2 Materials and Methods.....	124
5.2.1 Materials	124
5.2.2 Synthesis of mannose-functionalized cyclic carbonate (MTC-ipman) and mannose-modified bPEI-25 in the absence of DBU	125
5.2.3 Cell culture.....	125
5.2.4 DNA handling, transformation of bacteria with recombinant DNA, and maxiprep	126
5.2.5 Generation of stable cell transfectants	127
5.2.6 Preparation, particle size and zeta potential analyses of polymer/DNA complexes	129
5.2.7 Titration experiments	129

5.2.8 Gel retardation assay.....	129
5.2.9 <i>In vitro</i> GFP gene transfection.....	130
5.2.10 Cytotoxicity test.....	130
5.2.11 Mixed Lymphocyte Reaction (MLR).....	131
5.2.12 <i>In vitro</i> protection of Balb/3T3 cells from YT cell or allo-specific CTL killing by transfection with polymer/PI-9 encoding plasmid DNA complexes	132
5.2.13 Statistical Analysis.....	133
5.3 Results and Discussion	133
5.3.1 Polymer synthesis	133
5.3.2 Buffering Capacity.....	135
5.3.3 Size and zeta potential of polymer/DNA complexes	135
5.3.4 DNA binding ability of polymers	137
5.3.5 Cytotoxicity of unmodified and carbamate-mannose modified PEIs	138
5.3.6 <i>In vitro</i> GFP gene transfection efficiency	139
5.3.7 Protection of Balb/3T3 cells from allo-specific CTL and YT cell killing	141
5.4 Future work.....	150
5.5 Conclusions.....	151
CHAPTER 6: CONCLUSIONS AND FUTURE PERSPECTIVES	153
LIST OF PUBLICATIONS AND PRESENTATIONS.....	157
REFERENCES	158
APPENDIX A.....	174
1. Synthesis of sugar-functionalized cyclic carbonate (MTC-ip-sugar) (Figure S1)	174
2. Synthesis of hydrophobic groups-functionalized cyclic carbonate (MTC-benzyl, MTC-ethyl, and MTC-urea)	175
3. Synthesis of sugar-modified PEI (25 kDa)	178
4. Synthesis of hydrophobic groups functionalized carbamate-modified PEI.....	178
5. Characterization of monomers and polymers using ¹ H NMR spectroscopy.....	179
APPENDIX B.....	180

List of Tables

Table 1. Targeting ligands utilized to promote cellular uptake.

Table 2. (a) Mannose-PEI conjugates synthesized and used in this thesis. (b) Summary of the NMR analysis of the mannose- modified PEI (25 kDa) polymers.

Table 3. (a) Galactose/Glucose-PEI conjugates synthesized and used in this thesis. (b) Summary of the NMR analysis of the Galactose/Glucose-modified PEI (25 kDa) polymers.

Table 4. (a) Hydrophobic groups-PEI conjugates synthesized and used in this thesis. (b) Summary of the NMR analysis of the hydrophobic groups-modified PEI (25 kDa) polymers.

Table 5. The concentrations of various polymers used to deliver 4 μg luciferase DNA intravenously per mouse, and the polymer to mouse weight/weight ratios.

Table 6. Compositions, nitrogen contents, and ^1H NMR analysis of carbamate-mannose modified PEI.

Table 7. Compositions and nitrogen contents of carbamate-mannose modified PEI synthesized without the DBU catalyst, and their buffering capacity.

List of Figures

Figure 1. Granzyme A and B (GrA and GrB)-mediated cell death pathways.

Figure 2. Barriers to gene delivery—Design requirements for gene delivery systems.

Figure 3. Generic strategy for engineering a virus into a vector.

Figure 4. Granzyme B (GrB) which was released from the cytotoxic granules of the host cytotoxic T lymphocytes (CTL)/NK cells entered the target cell (indicated by the black arrow) and could trigger cell apoptosis.

Figure 5. ^1H NMR spectrum of polymer **B** in D_2O .

Figure 6. ^1H NMR spectra of PEI-TMC at conjugation degrees of 1, 8, 25 and 100 (a, b, c and d respectively) in MeOD.

Figure 7. Particle size (A, B, C, D) and zeta-potential (E, F, G, H) of polymer/DNA complexes at various N/P ratios specified.

Figure 8. Electrophoretic mobility of DNA in polymer/DNA complexes.

Figure 9. DNA binding analyzed as a decrease in fluorescence of SYBR green dye added to polymer/DNA complexes.

Figure 10. *In vitro* GFP gene transfection efficiency in HepG2 cells mediated by the various polymers at various N/P ratios indicated.

Figure 11. (A) Confocal images of HepG2 cells after incubation with unmodified or modified PEI/DNA complexes formed at various N/P ratios. (B) GFP gene delivered by the polymers could be expressed in HepG2 cells over a time of 6 days, however the expression diminished to very low level at day 10 after transfection.

Figure 12. Cellular trafficking of DNA.

Figure 13. *In vitro* GFP gene transfection efficiency in HeLa cells mediated by polymers at various N/P ratios indicated.

Figure 14. *In vitro* GFP gene transfection efficiency in NIH3T3 cells mediated by polymers at various N/P ratios indicated.

Figure 15. *In vitro* GFP gene transfection efficiency in MCF7 (A) and 4T1 cells (B) mediated by polymers at various N/P ratios indicated.

Figure 16. *In vitro* luciferase expression levels in HepG2 cells, mediated by polymers at various N/P ratios indicated.

Figure 17. *In vitro* luciferase expression levels in (A) MCF7, (B) 4T1, (C) HMSC, and (D) keratinocytes, mediated by polymers at various N/P ratios indicated.

Figure 18. Viability of HepG2 cells (A, B, C), HeLa cells (D), and NIH3T3 cells (E) after incubation with polymer/DNA complexes at various N/P ratios in comparison to unmodified PEI/DNA complexes.

Figure 19. Viability of (A) MCF7, (B) 4T1, (C) HMSC, and (D) keratinocytes after incubation with polymer/DNA complexes at various N/P ratios in comparison to unmodified PEI/DNA complexes.

Figure 20. Down-regulation of Bcl-2 mRNA in HeLa cells at siRNA concentration of 100 nM and N/P 50.

Figure 21. Viability of HeLa cells after being treated with polymer/siRNA complexes at various N/P ratios.

Figure 22. *In vivo* organ specific luciferase gene expression induced 72 h after i.v. injection of selected polymers complexed with luciferase gene at various N/P ratios.

Figure 23. *In vitro* GFP transfection in HEK293T cells.

Figure 24. Confocal microscopic images of GFP-transfected HEK293T cells.

Figure 25. Viability of HEK293T cells after incubation with unmodified PEI/DNA and carbamate-mannose modified PEI/DNA complexes at various concentrations.

Figure 26. Intracellular staining of GrB in YT cells under standard cell culture condition.

Figure 27. Viability of HEK293T cells after incubation with YT cells for 4 h.

Figure 28. ^1H NMR spectra of PEI-mannose at conjugation degrees of 6, 12.5 and 25 (a, b and c respectively) in D_2O .

Figure 29. Particle size (A) and zeta potential (B) of polymer/DNA complexes at various N/P ratios as specified.

Figure 30. Electrophoretic mobility of DNA in polymer/DNA complexes.

Figure 31. Viability of Balb/3T3 cells after incubation with unmodified PEI/DNA and carbamate-mannose modified PEI/DNA complexes at various concentrations.

Figure 32. *In vitro* GFP transfection in viable Balb/3T3 cells.

Figure 33. Expression profiles of intracellular GrB (A) and cell surface CD8 (B) markers of B6 CTLs.

Figure 34. “Missing self” hypothesis.

Figure 35. Viability of Balb/3T3 cells after incubation with YT cells for 8 h.

Figure S1. (A) Synthesis of protected mannose-functionalized cyclic carbonate (MTC-ipman). (B) Chemical structures of sugar-functionalized cyclic carbonates.

Figure S2. Synthesis of functional MTC-urea (a) and MTC-ethyl (b) monomers.

List of Schemes

Scheme 1. Synthesis procedures and structures of PEI-mannose conjugate.

Scheme 2. Single-step carbamate modification of branched PEI (PEI-TMC, PEI-ethyl, PEI-benzyl and PEI-urea).

List of Abbreviations

2ME	beta-mercaptoethanol
5-FU	5-fluorouracil
A*STAR	Agency for Science, Technology and Research
AAR	acute allograft rejection
AAVs	adeno-associated viruses
ADCC	antibody-dependent cellular cytotoxicity
APC	antigen-presenting cell
ASOR	asialoorosomuroid
ATG	antithymocyte globulin
BOS	bronchiolitis obliterans syndrome
CAD	caspase-activated deoxyribonuclease
Calcein-AM	Calcein-acetoxymethyl
CAR	chronic allograft rejection
CD	cyclodextrins
CHAR	chronic heart allograft rejection
CMV	cytomegalovirus
CNI	calcineurin inhibitors
CTL	cytotoxic T lymphocyte
DBU	1,8-Diazabicyclo[5,4,0]undec-7-ene
DC	dendritic cells
DCM	dichloromethane
dDC	donor dendritic cells
DMEM	Dulbecco's Modified Eagle Medium
DMF	dimethylformamide
DOGS	di-octadecyl-amido-glycyl-spermine
DOSPA	2,3-dioleoyloxy- <i>N</i> -[2(sperminecarboxamido)ethyl]- <i>N,N</i> -dimethyl-1-propanaminium trifluoroacetate
DOTMA	2,3- <i>bis</i> (oleyl)oxipropyl-trimethylammonium chloride
DOTAP	1,2-dioleoyl-3-trimethylammonium propane
DOPE	dioleoylphosphatidylethanolamine
ds	double stranded
DSP	dithiobis(succinimidylpropionate)
DTBP	dimethyl 3,3'-dithiobispropionimidate
EPR	enhanced permeation and retention
FACS	fluorescence-activated cell sorting
FBS	fetal bovine serum
GFP	Green Fluorescent Protein
GrB	granzyme B
GVHD	graft-versus-host diseases
HCPT	10-hydroxycamptothecin
hGH	human growth hormone
HLA	Human Leukocyte Antigen
HMSC	human mesenchymal stem cell
HMW	high molecular weight
HSCT	hematopoietic stem cell transplant
HSVs	herpes simplex viruses
HSV-1	HSV type 1
HSV-TK	herpes simplex virus thymidine kinase

IACUC	Institutional Animal Care and Use Committee
IL	interleukin
ipman	2,3;5,6-di-O-isopropylidene-D-mannofuranose
ISHLT	International Society for Heart and Lung Transplantation
ITIM	immune-receptor tyrosine-based inhibitory motif
ITRs	inverted terminal repeats
i.v.	intravenous
IVT	<i>in vitro</i> transcribed
kb	kilo bases
KIRs	Killer immunoglobulin-like receptors
KO	knock out
LCMV	Lymphocytic choriomeningitis virus
LCST	Lower Critical Solution Temperature
LDH	lactate dehydrogenase
LFA1	leukocyte function-associated antigen 1
LUPM	light units per minute
LMW	low molecular weight
ManPEI	mannosylpolyethylenimine
MEM	Minimum Essential Medium Eagle
MHC	Major Histocompatibility Complexes
MLR	Mixed Lymphocyte Reaction
MTC	methylcarboxytrimethylene carbonate
MTC-ipman	mannose-functionalized cyclic carbonate
MTC-OH	5-Methyl-5-carboxyl-1,3-dioxan-2-one
MTT	1-(4,5-dimethylthiazol-2-yl)-3,5-diphenylformazan, thiazolyl blue formazan
MW	molecular weight
NCR	natural cytotoxicity receptors
NIPAM	N-isopropylacrylamide
NK	natural killer
NLS	nuclear localization signal
NOD	non-obese diabetic
NPC	nuclear pore complexes
PAGA	Poly(a-[4-aminobutyl]-l-glycolic acid)
PAMAM	poly(amidoamine)
PBS	phosphate-buffered saline
PDGF	platelet derived growth factor
PDMAEMA	poly(2-(dimethylamino)ethyl methacrylate)
PECAM	platelet endothelial cell adhesion molecule
PEG	poly(ethylene glycol)
PEI	polyethylenimine
PI	Propidium Iodide
PI3-K	phosphatidylinositol 3-kinase
PI-9	proteinase inhibitor-9
PIC	polyion complex
PLGA	poly(lactide-co-glycolide)
PLL	poly(lysine)
pMHC	peptide major histocompatibility complex
PPI	poly(propylenimine)
PVP	polyvinyl pyrrolidone

RCL	reactive center loop
RLU	relative light units
RME	receptor-mediated endocytosis
RNAi	RNA interference
ROS	reactive oxygen species
RSV	respiratory syncytial virus
RT-PCR	real-time reverse transcription-polymerase chain reaction
SCID	severe combined immunodeficiency
SCID-X1	X-linked severe combined immunodeficiency
SCR	subclinical rejection
serpin	serine protease inhibitor
shRNA	small hairpin RNA
siRNA	small interfering RNA
SPDP	N-succinimidyl 3-(2-pyridyldithio)propionate
Spi6	serine protease inhibitor 6
TCR	T cell receptor
TGF β	Transforming growth factor β
THF	tetrahydrofuran
TMC	trimethylene carbonate
TNFR	tumor necrosis factor receptor
Tregs	regulatory T cells
WT	wildtype

CHAPTER 1: INTRODUCTION

1.1 Different types of transplant pathology, risk factors, and current status of treatments

1.1.1 Different types of transplant pathology

Organ transplantation often brings hope to patients with irreversible diseases such as end-stage organ failure. However, various complications post transplantation often hamper the survival of the transplanted organs. Statistics reported by the Registry of the International Society for Heart and Lung Transplantation (ISHLT) showed that as many as 55% of lung transplant recipients are treated for acute allograft rejection in their first year after transplantation, and only 50% of lung recipients are alive 5 years after transplantation [1]. Moreover, taking renal transplants as an example, different forms of kidney allograft pathology exist. One of them, the spontaneous graft rupture, which is common in the latter half of the first week post transplantation, is usually caused by the hyperplasia of lymph nodes compressing intra-renal veins, causing intra-renal venous hypertension and rupture [2]. Although this complication has been cured since the introduction of cyclosporine, an immunosuppressant drug, acute allograft rejection (AAR) and chronic allograft rejection (CAR) still persist as threats to the allograft survival and functioning. A typical difference between AAR and CAR is the length of persistence of syndromes. Subclinical Rejection (SCR) is histologically proven AAR in the absence of immediate functional deterioration, while CAR is persistent SCR of 2 years or more duration and implying continuous immunologic activation [3]. Being an indolent but progressive form of primarily immunologic injury to the allograft, CAR compromises organ function more slowly than AAR. Furthermore, according to the Banff working classification of kidney transplant pathology, interstitial infiltration, tubulitis and intimal arteritis are regarded as the principal indications of AAR, while interstitial fibrosis, tubular atrophy and tubular loss suggest the presence of CAR [4]. According to the degrees of severity of the pathological symptoms, Banff scheme also classifies both AAR and CAR into three grades. Therefore, the AAR and CAR are defined not only by the duration of pathology post transplantation, but also largely by the pathological changes integrated with clinical data. Although the literature suggests that the clinical symptoms of CAR are dependent on the function of the specific organ allograft, and no uniform criteria have been set for all kinds of allografts, the most common histological manifestation of CAR is progressive muscular arteries obliteration [5], infiltration of immunocytes, interstitial and tubular atrophy, graft arteriosclerosis, and marked interstitial fibrosis [6]. All in all, the various forms of post-

transplantation complications greatly compromised the success of the transplant surgery as well as the patient welfare. Adaptive immune responses to the allo-antigens on the graft, which are perceived as foreign by the recipient, are the main barrier to successful transplant survival. These responses can be mediated by antibodies, CD8 T cells, CD4 T cells, or by both CD8 and CD4 T cells. T cell responses to the highly polymorphic Major Histocompatibility Complexes (MHC) molecules on the transplanted cells destroy the grafted tissue, which could only be prevented by perfect matching the MHC type of the donor and the recipient [7].

1.1.2 Risk factors of AAR and CAR

Researchers have come up with a series of factors that could aid the prediction the onset of AAR. Firstly, it was shown that Human Leukocyte Antigen (HLA) (also referred to as MHC) mismatching between the donor and recipient, especially at the HLA-DR, HLA-B, and HLA-A loci, had significant correlation with the risk of AAR, especially in the lung transplants [8, 9]. Both donor and recipient dendritic cells (DC) capture and display the donor-antigens on their HLA molecules, and present them to the recipient T cells, triggering robust immune responses. Secondly, viral or bacterial infection has always been shown to stimulate the immune system and trigger allo-reactivity after the solid organ transplantation. Community-acquired respiratory tract infections with human influenza virus, respiratory syncytial virus (RSV), rhinovirus, coronavirus, etc. were reported to cause high incidence of acute lung transplant rejection [10, 11]. Furthermore, *Chlamydia pneumonia* infection was proven to cause AAR and bronchiolitis obliterans syndrome (BOS), a condition of progressive airflow obstruction that made survival at 5 years after lung transplantation only 50% [12]. Thirdly, AAR has a lot to do with the recipient factors. Genetic variation in the innate pattern recognition receptors in the donor may have a positive influence on the AAR, for example, an augmented acute rejection was observed in a patient with a variant in CD14 molecule, which stimulated the innate immune response [13]. Another example illustrating this point would be a multidrug-resistant genotype (MDR1 C3435T), which was shown to predispose the patient to persistent AAR, despite consistent immunosuppressive treatment [14]. All in all, although the precise mechanisms contributing to AAR are uncertain, it seems a complex interplay between genetic and environmental factors might modulate the incidence and severity of AAR.

Similarly, a list of risk factors has been identified to be associated with the occurrence of CAR. First of all, the immune-mediated factor, often triggered by AAR, is the most significant risk factor for CAR [15]. The heightened and ongoing immune responses due to

therapeutic withdrawal of immunosuppressive drugs to minimize their side effects, patient non-compliance [16], or development of cytotoxic anti-HLA antibodies in the recipient body [17] all suggest that allo-immune responses resulting from AAR gradually lead to chronic rejection. Secondly, the donor-related factors are critical in CAR development. For example, donor age-related replicative senescence often led to cellular exhaustion and organ dysfunction [18]; donor brain death-associated electrolytes abnormalities, overproduction of cytokines and overexpression of allo-antigens could cause chronic graft failure [19]; bad donor organ quality due to complications associated with hypertension or diabetes mellitus of the donor was also proven to be significant hurdle to long term graft survival [20]. The third risk factor for CAR was identified to be the nephrotoxicity associated with calcineurin inhibitors (CNI). Calcineurin is a key enzyme in the T-cell signal transduction cascade, activation of which leads to T cell activation and potent immune reaction [21]. CNI such as cyclosporine and tacrolimus chronically used post transplantation as immunosuppressant often lead to renal and systemic vasoconstriction, progressive arteriolar hyalinosis and downstream glomerulosclerosis [22], and eventually organ failure. Last but not least, cytomegalovirus (CMV) infection often accelerates CAR, which is associated with up-regulation of transforming growth factor β (TGF β), platelet derived growth factor (PDGF) in endothelial cells and connective tissue growth factor within fibroblasts [23]. Thus, similar to AAR, both immune and non-immune factors form the non-exclusive list of CAR etiology.

1.1.3 Current status of treatments

1.1.3.1 Treatments for AAR

Various immunosuppressive therapies have substantially reduced the risk of acute lung rejection, for example, high-dose methylprednisolone, antithymocyte globulin (ATG), or alemtuzumab is used to treat cellular rejection, while intravenous immunoglobulin, plasmapheresis, or rituximab is usually employed for humoral rejection treatment [24]. For cellular rejection mitigation, studies from the 90s have shown promising alleviation of lung AAR by administration of pulse-steroids such as 500 mg of methylprednisolone intravenously per day, for at least three doses followed by an oral prednisone taper [25, 26]. Moreover, muromonal-CD3 (Orthoclone OKT3) was shown to be an effective therapy for steroid-resistant, high-grade, or relapsing acute lung rejection during the first 6 months after transplantation, when used together with antimicrobial prophylaxis [27]. Another promising example of treating cellular acute rejection is the administration of a CD154-specific monoclonal antibody

(hu5C8) to prevent CD154-CD40 interaction leading to endothelial and antigen-presenting cell (APC) activation and interaction with T cells, and this method enabled successful renal transplantation in outbred, MHC-mismatched rhesus monkeys without acute rejection [28]. Additionally, for the humoral rejection, successful clinical trials during 2005 to 2007 showed that intravenous immune globulin and rituximab (an anti-CD20 monoclonal antibody causing B cell depletion) treatment of 20 patients after renal transplantation enabled the 12-month survival rates of grafts and patients to be 94% and 100% respectively [29]. Despite the apparently high treatment efficacy of the immunosuppressant for AAR, their advantages are usually traded off by the serious side-effects such as severe infections and malignancy owing to systemic and chronic use of immunosuppressive therapy causing paralysis of normal immune surveillance function [30]. Specifically, corticosteroids and cyclosporine had the most negative impact on weight gain, blood pressure and lipids function; tacrolimus was positively correlated with diabetes mellitus; sirolimus and everolimus greatly increased the chance of post-transplant hyperlipidaemia; and CNI was one class of the immunosuppressive agents most linked with post-transplant malignancies [31]. Therefore, these immunosuppressive therapies to AAR should be considered carefully during clinical usage, in order not to let their side effects override their potential efficacy.

1.1.3.2 Treatments for CAR

Despite some success in alleviating AAR, CAR remains as the major obstacle in long-term graft survival. Statistics showed that about 40%-50% patients undergoing renal graft surgery developed chronic allograft nephropathy [5]. Currently, the exact mechanisms underlying CAR are unknown, and therefore no targeted clinical evidence-based treatment strategies exist. However, several animal models has been developed, such as rodent models for heart CAR, swine models for lung CAR, and so on, with an aim to identify and analyze individual immunological and non-immunological contributing factors with the hope to translate effective clinical therapies from bench to bedside [32]. After many years of exploration, several preventative and treatment measures have been practiced in reality, and are explained as follows:

The first preventative measure is to minimize the development of symptoms associated with AAR, due to the direct link between AAR and CAR. Tacrolimus was shown to reduce interstitial infiltration, whereas mycophenolate was able to reduce tubulitis, and the combination of them effectively eliminated SCR in a trial involving 961 kidney biopsies from

patients receiving kidney-pancreas transplantation [3]. In addition, due to the strong association between pre-sensitization and development of humoral-driven CAR, pre-treatment of sensitized patients using plasmapheresis combined with intravenous immunoglobulin or rituximab was shown to effectively prevent the onset of rejection syndromes [33]. Another cause of the CAR lies in the toxicity associated with the CNI. Therefore, a minimization or complete withdrawal strategy, such as a CNI-free immunosuppression therapy based on sirolimus, mycophenolate mofetil and steroids appeared to slow the rate of renal function loss, though only with a short follow-up [34]. Finally, antiviral treatment, diet, smoking ban and patient good compliance also contribute to healthy blood pressure, proteinuria, lipids, glucose and weight, and better results of clinical transplantation [35].

Other than the drug-mediated immunosuppression to treat CAR, induction of immunological tolerance to the antigens expressed on the graft cells by modulating the recipient immune cells could help avoid rejection and the need for lifelong treatment with immunosuppressive drugs [36]. Joffre et al. showed that by injecting *in vitro* allo-antigen stimulated donor specific regulatory CD4⁺CD25⁺Foxp3⁺ T cells (Tregs), long-term bone marrow, skin and cardiac allografts were well tolerated in mice pre-treated with clinically acceptable levels of irradiation [37]. Moreover, another group delved into the mechanisms of the donor specific Tregs contributing to CAR prevention. They recently conducted a similar BM transplantation study but demonstrated that injected donor regulatory T cells wane away after 9 weeks, and the nevertheless long-term allograft tolerance suggested that the donor Tregs were only for induction but not maintenance of the tolerance status [38]. Rather, the persistent CAR avoidance was likely caused by two reasons: the depletion of donor-specific CD4⁺ T cells after *in vivo* depletion of donor Tregs using diphtheria toxin, and the induction of the emergence of host Tregs with similar specificity by the injected Tregs, thus ensuring persistence of tolerance [38]. Therefore Tregs are potential highly useful agents in inducing self-perpetuating tolerance to the allograft. Further investigations regarding the application of Tregs in clinical settings such as treating the graft-versus-host diseases (GVHD) are needed.

1.1.3.3 The urgent need to develop new treatment methods to tackle CAR

Having analyzed all the preventative and treatment strategies above, currently, although better immunosuppressive strategies result in short-term improvement of allograft survival, they have severe side effects leading to immune system paralysis, they do not target specific pathways of CAR, and sometimes they may even be implicated in the process of CAR in terms

of calcineurin toxicity [39, 40]. Therefore, there is an urgent need to develop novel anti-CAR strategies that are safer and more effective. Two strategies have been proposed in my lab to tackle this problem: co-stimulation blockage [41] and granzyme B (GrB) inhibition. Co-stimulation blockade was recently used in practice with promising short-term results but it was unable to prevent CAR. Therefore my lab proposed to use a GrB inhibition strategy to boost the tolerogenic effect of co-stimulation blockade. This strategy has two advantages. First, neither co-stimulation blockade nor GrB inhibition causes vascular disease, which is the major component of CAR. This is an important merit as one of the main issues with current immunosuppressive strategies is their vascular toxicity [42]. Secondly, immune-suppression by inhibiting GrB has the advantage that it is specific for the CTLs and NK cells [43]. This means that rejection by GrB is prevented but protective T helper cell and antibody immunity is left intact. Therefore GrB inhibition has the potential for immunosuppression without immunodeficiency and susceptibility to infection.

1.2 The role of GrB in CTL and NK mediated killing

Rejection of the allografts generally involves antibody and T cell responses, and among them, T cell effector mechanisms contribute to rejection to a major extent. Cytotoxic T Lymphocytes (CTL, includes CD8 and certain CD4 cells) and Natural Killer (NK) cells are sentinels of the immune system and they eliminate foreign and infected cells in a quick and potent way. Foreign antigens in non-lymphoid tissues all over the body are captured by DCs (professional APC), processed by the DCs into peptides and displayed on the MHC molecules on DCs cell surface. The DCs then migrate to the secondary lymphoid organs and present them to the naïve T cells. When the T cell receptor (TCR) of a naïve T cell recognizes the foreign antigen-MHC complex on a DC, with the help of co-stimulatory signals offered by the DC, a cascade of intracellular signaling activates the naïve T cell, which then rapidly proliferates (clonal expansion), and migrates to the sites of antigen presence to induce the death of the target cells and produce various cytokines [44]. The best understood CTL population, CD8 cells, effectively causes lysis of the infected or malignant cells, while CD4 T helper cells produce cytokines which either directly aid the killing of the target cells or stimulate and augment other T effector cells function and B cell antibody production [45]. For NK cells, activation of their activating receptors and lack of signals for their inhibitory receptors trigger NK-mediated killing of the target cells [46]. Specifically, the absence of inhibitory signals derived from the binding to self peptide-MHC molecules resulting in NK cell activation and allograft rejection is called “missing self” response of NK cells [47].

There are two pathways of lymphocyte mediated contact dependent cytotoxicity. The first pathway is triggered by the tumor necrosis factor receptor (TNFR) family Fas, and the second one is calcium dependent exocytosis of cytotoxic granules in the CTL and NK cells to induce apoptosis of target cells, which is the focus of this thesis. Cytotoxic granules residing in the cytosol of CTL and NK cells contain at least three distinct classes of cytotoxic effector protein: perforin, which polymerizes in the target cell membrane and induce trans-membrane pore formation; granzymes, which are serine proteases; and granulysin, which induces apoptosis in target cells and has antimicrobial action [48]. There are five granzymes encoded by the human genome and ten encoded by the mouse genome, among which GrB is the most extensively studied granzyme in inducing target cell death [49]. Upon recognition of the foreign antigen on the target cell surface, granule contents are rapidly released into the lymphocyte-target cell synapse, then GrB binds to the mannose-6-phosphate receptor on the target cell surface and enters the target cell through pores made by perforin [43]. Once inside the target cell, GrB triggers apoptosis by caspase-dependent or independent pathways [50]. Briefly, GrB directly cleaves and activates pro-apoptotic protein Bid, which trans-locates to the mitochondria and causes release of cytochrome c, which in turn activates a cascade of caspases, and leads to cleavage and activation of the ubiquitous cellular cysteine protease caspase-3 [51]. Caspase-3 could also be cleaved and activated directly by GrB without the involvement of mitochondria. Then a caspase proteolytic cascade is activated, which eventually activates the caspase-activated deoxyribonuclease (CAD), the enzyme believed to finally degrade the cellular DNA and cause cell death [48]. For the caspase-independent pathway, GrB could directly cleave and activate proteins crucial to cellular structure and function, such as nuclear lamins, which leads to dismantling of the target cell [52]. It can also induce cell death by stimulating mitochondria to generate reactive oxygen species (ROS). Thus, both caspase-dependent and independent pathways work together to ensure the most effective clearance of foreign or infected cells and maintenance of the maximal functionality of the various body systems. A schematic picture of GrB mediated cell death pathways is shown as Figure 1.

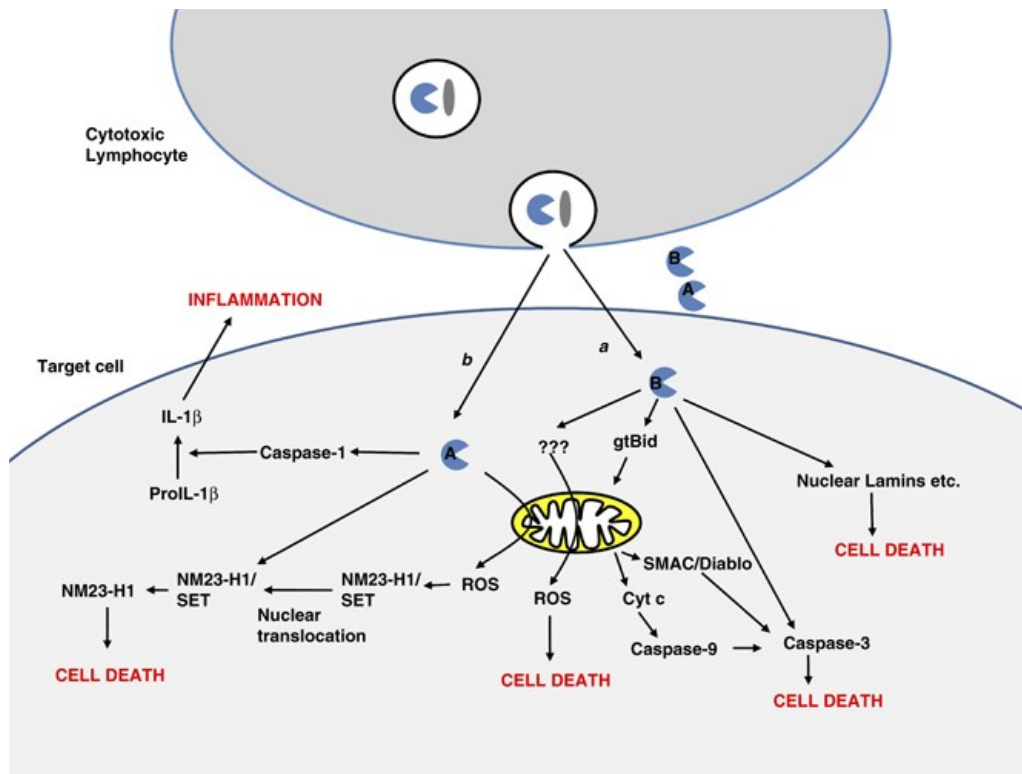


Figure 1. Granzyme A and B (GrA and GrB)-mediated cell death pathways. After recognizing foreign cells, activated CTLs release granzymes (designated by A and B, blue molecules) and perforin (designated by the gray spindle molecule) into the lymphocyte–target cell synapse. Perforin causes pore formation on target cell membrane and facilitates the entry of granzymes into the target cell cytoplasm. (a) Once inside the target cell, GrB induces cell death through a number of pathways. GrB-mediated cleavage of Bid leads to mitochondrial permeability and release of cytochrome c, which initiates caspase activation. SMAC/Diablo is also released from mitochondria, and it augments caspase activity by preventing caspase inhibition by endogenous inhibitors. GrB also directly cleaves and activates caspase-3. Moreover, GrB can induce cell death without the activation of caspases through the induction of ROS from mitochondria as well as through the direct cleavage of structural proteins, such as nuclear lamins. (b) GrA acts directly on mitochondria to induce the production of ROS. ROS induces the translocation of the SET complex to the nucleus, which inhibits the endonuclease NM23-H1. GrA cleaves and inactivates SET in the nucleus, which leaves active NM23-H1 to cleave the DNA. In addition, GrA induces inflammation through the production of IL-1 β through a caspase-1-dependent mechanism. Reproduced with permission from [53]. Copyright © 2009, Rights Managed by Nature Publishing Group.

1.3 Regulation of GrB by serine protease inhibitors

1.3.1 Cytotoxic lymphocytes could protect themselves from self-inflicted damage

Given the effectiveness of the granule exocytosis-induced cell death, it is not surprising that GrB could potentially turn against CTLs and NK cells and make them susceptible to self-

inflicted damage. In fact, it has been reported that GrB resides in compartments other than the lytic granules in CTLs, and up to one-third of them is secreted directly via constitutive secretory pathway rather than from lytic granules with the purpose of bystander killing of targets [54]. Also, GrB could be misdirected into the cytoplasm of the CTL, and cause suicidal death of the CTL. Another possible mechanism of GrB inflicting self-destruction could be explained by the fratricide killing theory, where CTLs infected by viruses such as human T lymphotropic virus 1 and expressing peptide major histocompatibility complex (pMHC) are subjected to killing by other CTLs [55-57]. In addition, NK cells were observed to die due to its residential GrB leakage [58]. However, despite the potential self-inflicted injury, CTLs and NK could still effectively function to kill damaged and foreign cells without killing themselves. Therefore, it has been proposed that cytotoxic lymphocytes can protect themselves from self-inflicted damage, by expressing physiologically important inhibitors of executioner proteases that keep both themselves and other immune cells intact [59].

1.3.2 Serine protease inhibitors

1.3.2.1 *Spi6* protects CTLs

Regulation of the serine proteases is mainly achieved through inhibitors of serine protease inhibitor (serpin) family, which are usually located in the cytoplasm of the cells. Serpins regulate the proteolytic activities of serine proteases by acting like suicide substrates. Briefly, when a serpin interacts with a serine protease, they form a 1:1 complex where the C-terminal reactive center loop (RCL) with a similar structure as the serine protease substrate undergoes a conformational change that distorts the serine protease and irreversibly locks the serpin-serine protease complex, rendering the protease incapable of killing [60]. Through the study of serine protease inhibitor 6 (*Spi6*) knock out (KO) mice, our lab demonstrated that *Spi6* acted as a classic suicide substrate by inhibiting ectopic or misdirected GrB, prevented CTLs from self-inflicted injury and maintained their effector function [61]. Actually, the complexes formed by GrB and *Spi6* were clearly observed in western blots of proteins isolated from wildtype (WT) CTLs cytoplasm, but were absent in *Spi6* KO CTLs cytoplasm. Also, when challenged with Lymphocytic choriomeningitis virus (LCMV), the size of CTL pool in the *Spi6* KO mice shrank to 10-20% of that in the WT mice, and the elimination of LCMV in the *Spi6* KO mice was severely compromised as a result of large extent of CTLs apoptosis. Subsequently, the restoration of CTLs number and function by crossing *Spi6* KO and GrB KO mice suggest that *Spi6* was indeed a potent inhibitor of GrB. Additionally, the observation that

fewer cytotoxic granules were present in the CTLs of the Spi6 KO mice compared to those of the WT mice coincide with a study suggesting that Spi6 was also responsible for maintaining the integrity of the cytotoxic granules [62].

1.3.2.2 Spi6 protects DCs

Since DCs are professional APCs that stimulate the proliferation and activation of naïve CD8⁺ T cells into CTLs for elimination of infected or foreign cells, they are in a dangerous position to be exposed to collateral damage mediated by perforin and GrB. It was suggested that pMHC on the DCs might induce killing by the CTLs that were primed by them. A study further demonstrated that *in vitro* killing of pMHC-expressing DCs by LCMV-specific CTLs was perforin dependent, and GrB was involved in the process [63]. However, Spi6 was shown to be up-regulated upon DCs activation by inflammatory mediators, and overexpression of Spi6 protected DCs from GrB mediated killing by CTLs [64]. The protective role of Spi6 in DCs ensures that the professional APCs could function effectively to present the foreign antigen to the naïve CD8⁺ T cells and initiate a robust adaptive immune response to the damaged or foreign cells.

1.3.2.3 Spi6 and Spi2A protect CD8⁺ memory T cells

Not only cytotoxic lymphocytes are protected from misdirected GrB by Spi6, but CD8⁺ memory T cells which are important in maintaining a reactive state upon antigen recurrence benefit from serpins. As CD8⁺ memory T cells were thought to be a direct progeny of CTLs after their clonal expansion and receding [65], research has shown that there are two different serpins expressed in CTLs that control memory T cell survival through different mechanisms. The first serpin is Spi6 [66]. Although the pool size of memory CD8⁺ T cells was the same in Spi6 KO and WT mice, the seeming dispensability of Spi6 in memory CD8⁺ T cells survival was due to low GrB expression in memory cell precursors, making them resistant to GrB mediated self-destruction. However, high doses of LCMV re-infection in Spi6 KO mice diminished the memory T cell population almost completely, suggesting that Spi6 was crucial to the memory cell responses by ensuring the appropriate size of the CTL clonal burst after re-infection [67]. Additionally, the serpin directly responsible for the development of memory T cells after infection with LCMV was found to be Spi2A. Spi2A is a cross-class-specific serpin inhibitor of pro-apoptotic cysteine cathepsins, and transgenic and knockdown experiments showed that Spi2A up-regulation protected memory T lymphocyte precursors directly from cathepsin B-mediated programmed cell death [68, 69].

1.3.2.4 PI-9 protects human CTLs and NK cells

Another serpin, proteinase inhibitor 9 (PI-9), which is the human homolog of Spi6, is widely expressed in CD4/CD8 T cells, NK cells, B cells and myeloid cells in human, exerting a protective role against GrB mediated apoptosis [70]. PI-9 was demonstrated to be physically associated with the cytoplasmic surface of the GrB containing cytotoxic granules in the activated human CTLs and NK cells, in order to inactivate GrB immediately upon its leaking into the cytoplasm. Also, PI-9 level in proliferating but non-degranulating T cells and activated NK cells was almost constant, suggesting that there was sufficient PI-9 to protect against the leaking GrB. However, PI-9 was up-regulated in response to GrB production and secretion, indicating that granule exocytosis was associated with increasing entry of GrB into the T cell cytoplasm, and higher PI-9 level ensures the cell viability [70]. Furthermore, functional assay of PI-9 transduced CTLs lysing target cells expressing an anti-CD3 mAb (OKT3) showed that overexpression of PI-9 enhanced the potency of human CTLs, probably due to protection of CTLs from GrB mediated self-infliction.

1.3.2.5 PI-9 protects accessory cells

PI-9 not only protects human CTLs and NK cells from GrB killing, but is also evidently expressed in accessory cells (DCs, B cells, and macrophages). In particular, it is abundant in thymic DCs, tonsillar DCs, and DC subsets purified from peripheral blood. Although the close association of DCs and activated CTLs might result in inadvertent killing of DCs, elimination of DCs in WT mice was rare, probably due to protective mechanisms of serpins. Several transgenic mouse models, though, showed that elimination of antigen-specific DCs by cognate CTLs was possible, and expression of PI-9 in DCs prevented GrB mediated apoptosis during the antigen presentation to CTLs [63, 71]. The expression of PI-9 in thymic medullary DCs was essential in ensuring their survival during the positive and negative selection of thymocytes, which expressed GrB and had cytotoxic potential [70]. Moreover, the PI-9 expression level in B cells, monocytes and granulocytes was not as high as that in CTLs or DCs, suggesting a delicate balance between protection against traces of ectopic PI-9 and being cleared by the killer cells once become infected or malignant. In conclusion, the presence and subcellular localization of PI-9 could successfully protect accessory cells from misdirected GrB during an immune response.

1.4 The role of GrB in allograft rejection, and the strategies to block GrB

Clinical studies demonstrated that GrB expression in infiltrating lymphocytes correlated strongly with the speed and severity of rejection [72]. Histological studies also showed abundant amount of GrB and perforin in many types of acutely rejecting allografts [73-75]. In fact, increased GrB and perforin mRNA in the peripheral blood mononuclear cells from kidney allograft recipients were regarded as biomarkers for the renal AAR [76]. Moreover, in solid organ transplants, GrB was shown to act with perforin to induce rapid cell death of human endothelial cells *in vitro*, and GrB alone degraded extracellular proteins of the endothelial cells important for adhesion-mediated chondrocyte cell survival [77]. Further, it was reported that clinically, antibody-mediated rejection occurred in only 5.6-23% of rejecting ABO-matched kidney allografts, 30–60% of ABO-mismatched kidney allografts, and 3–28% of heart allografts [78, 79]. Therefore, a more substantial contribution of allograft rejection in the clinic was made by T cell-mediated rejection, and the perforin-GrB cytotoxic effector pathway could be the main mechanism of this type of allograft killing and rejection.

Recent published data have shown that in the donor grafts, donor dendritic cells (dDC) are potent inducers of tolerance to allograft under conditions of co-stimulation blockage [41]. However, CTLs and NK cells of the host use the granule exocytosis pathway to destroy donor cells, including dDC. As discussed in Section 1.1.3.3, means to prevent allograft rejection which is safer and more effective is urgently needed. Our strategy is thus to prevent apoptosis of donor cells and dDC by inhibiting GrB after co-stimulation blockade, and my thesis will focus on GrB inhibiting strategies. Current pharmacological inhibitors of GrB are unsatisfactory as they are non-cell permeable and toxic. Therefore, it is rational to develop new clinically useful GrB inhibitors with high cell permeability and low toxicity. Indeed, a novel, potent and selective GrB inhibitor has been discovered by Willoughby et al. to block CTL mediated apoptosis with an IC_{50} of 3 micromolar [43], however, the inhibitor was based on the four amino-acid peptide GrB substrate IEPD and synthetically costly. Moreover, delivery of Spi6 or PI9 protein to tackle inflammatory disease was only effective against extracellular GrB, due to the technical difficulty in delivering intracellular proteins to the cytoplasm [59]. Since GrB exerts its apoptotic function only when entering the target cell cytoplasm, the difficulty of serpin protein to enter the cells would significantly limit the effectiveness of protein therapy to alleviate allograft rejection. Considering all the above-stated difficulties in GrB inhibitor protein/peptide development and delivery, and the fact that no major improvements have been made in the last few decades regarding the overall allograft survival rates following protein

therapies, novel forms of immunomodulation is thus justified. In this thesis, we explore such a strategy involving gene therapy.

We hypothesized that using gene delivery vectors to deliver DNA encoding PI-9 gene into the dDC or other donor cells could achieve GrB inhibition and prevent cytotoxic lymphocyte killing. The idea of delivering GrB inhibitor gene was inspired by cancer vaccination studies using DCs in cancer patients [80]. The whole array of viral (including adenovirus, retrovirus, lentivirus, adeno-associated virus, poxvirus and herpesvirus) and nonviral methods (including gene gun, lipoplexes and electroporation) were applied to *ex vivo* generated DCs to deliver plasmid DNA or *in vitro* transcribed (IVT) RNA to make the DCs as cancer vaccines [81, 82]. Although efficient transfection of human DCs has been achieved with viral vectors due to the natural efficiency of viruses at infecting and transferring genetic cargos into cells, their application has been limited by the immunogenicity of viral particles, toxicity associated with residual viral gene products upon transduction, and the unfavorable economics of large scale industrial production [83]. As a result, the clinical application of viral vectors may seem more feasible in theory rather than in practice, at least for the time being. In contrast, non-viral methods, although without the safety and ethical concerns associated with viruses, have generally resulted in inefficient gene transfer, and/or low cell viability. Nevertheless, genes are easier and cheaper to synthesize in large scale *in vitro* compared to protein/peptides, and genetic engineering of DCs has made them successful in suppressing tumor growth in quite a few studies [84-88]. Therefore delivery of GrB inhibitor PI-9 gene to the dDC or donor cells might as well achieve promising results.

Another factor favoring the idea of genetic engineering of the dDC or donor cells to prevent them against cytotoxic lymphocyte killing came from the observation that gene silencing via RNA interference such as small interfering RNA (siRNA) or small hairpin RNA (shRNA) in DCs played a role in preventing immune rejection. Depending on the maturation status, phenotype and source of origin, DC can both prime the adaptive immune response and induce immunological tolerance [89, 90]. Specifically, donor-specific, allogeneic tolerogenic immature DCs can enhance the survival of transplanted grafts [91, 92]. However, NF- κ B activity (especially conferred by RelB protein in the mammalian NF- κ B family) has been revealed to be associated with DC maturation and Th1 responses [93-96]. Hence, delivery of inhibitors of NF- κ B activation such as RelB siRNA was shown to block the maturation of DCs,

resulting in reduced expression of T cell stimulatory molecules, such as MHC class II, CD80 and CD86 molecules [97], and reduced immune responses against the transplanted organs.

In conclusion, the relatively easier and more feasible nucleic acids (DNA, siRNA and shRNA) delivery to cure allograft rejection compared to the expensive and difficult GrB inhibitor peptide/protein intracellular delivery prompted me to develop a safe and effective gene carrier to deliver PI-9 gene cargo to the target cells in order to protect them from GrB triggered apoptosis. Since the key bottleneck in gene therapy is the lack of safe and efficient delivery systems, the primary objective of this thesis is thus to develop novel gene delivery vectors that could be evaluated in the setting of prevention of GrB and promotion of organ survival post transplantation. In order to achieve this, firstly, the barriers at gene delivery vehicle-cellular interaction level for the successful *in vivo* gene delivery will be examined and the strategies to overcome them will be discussed. These would cast a light on the rationale behind the designs of modern, multifunctional genetic carriers. Then the various types of gene delivery methods will be briefly reviewed, and the merits and limitations of each type of the vectors will be investigated. Prominent examples of cationic polymer based vectors are given special attention since the vectors used in this study are cationic polymers. Finally, a conclusion and justification of non-viral vectors to specifically suit PI-9 gene delivery for GrB inhibition and allograft rejection prevention will be presented.

1.5 Gene therapy: Major developments and current status

Gene therapy has brought hope to numerous genetic diseases such as hemophilia [98], cystic fibrosis [99] and even cancer [100]. Therapeutic action is achieved via knocking down erroneous genes or over-expressing therapeutic genes through gene delivery, which to date remains a limiting challenge [101]. Gene delivery vectors could be generally divided into two major categories: viral and non-viral. Viral vectors are extremely effective at delivering genes, however, their disadvantages such as relatively low gene loading capacity, immunogenicity, and safety issues impede their wide spread clinical adoption [102]. The first successful retroviral vector mediated gene therapy was reported in 2000 for the treatment of severe combined immunodeficiency (SCID) in infants [103]. Several other retroviral gene therapies followed, but the effect was short lived as some patients developed leukemia-like disorders owing to the retroviral insertion near the promoter of a proto-oncogene [104]. Moreover, the death of the 18-year old Jesse Gelsinger from fatal inflammatory responses to adenoviral vector treatment of ornithine transcarbamylase deficiency in 1999 aptly illustrated the danger

of a bad gene therapy introducing high dose of viruses [105]. Alternatively, non-viral gene delivery vectors are receiving a tremendous amount of attention because they are relatively inexpensive, reproducible and synthetically modular [106-111]. However their lower gene transfection efficiencies compared to viral vectors act as a hurdle to their clinical usage. For example, although lipid-based vectors are one of the most commonly used non-viral vectors for gene therapy (6.4%) [112], the incidence of successful clinical trials performed to date is disappointingly low. Among the non-viral carriers, cationic polymeric systems have been extensively investigated. In particular, branched polyethylenimine (PEI, Mw 25 kDa) has been shown to be one of the most efficient synthetic gene delivery carriers *in vitro* [106, 113], and it has been long used as the gold standard for *in vitro* gene transfection. However, various issues related to its biocompatibility, general toxicity etc. hindered its successful *in vivo* application. Therefore, an urgent demand for developing safe and efficient gene vectors exists before the immense potential of gene therapy can be fully realized.

1.6 Barriers limiting gene delivery and solutions to overcome them

Understanding the various biological barriers that gene delivery face at the cellular level is fundamental to formulating ingenious design strategies of the gene carriers in order to overcome these barriers. Here the delivery of DNA plasmids will be the subject of the topic, since RNA interference (RNAi) concept is relatively new and the delivery method for siRNA/shRNA is largely adopted from the DNA delivery technology. Generally, the chronological sequence of challenges that a plasmid faces during its journey towards the nucleus is as follows: (1) DNA packaging, (2) extracellular stability, (3) cellular uptake and endosomal escape, (4) intracellular trafficking, (5) DNA unpackaging, and (6) biocompatibility (Figure 2). Each step will be analyzed in detail in the following six subsections. Moreover, strategies employed by polymeric gene carriers to overcome them will be briefly discussed here due to the vast volume of information available for different types of vectors.

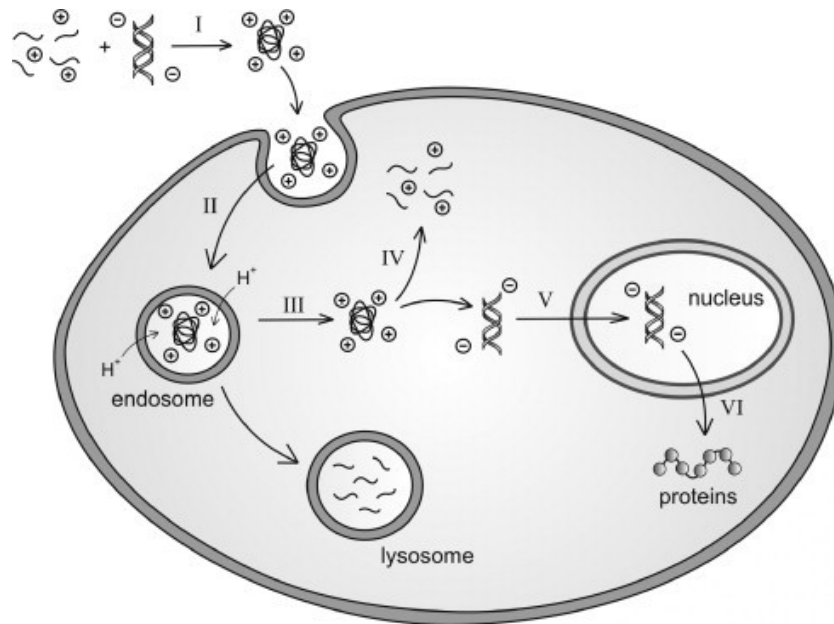


Figure 2. Barriers to gene delivery—Design requirements for gene delivery systems include the ability to (I) package therapeutic genes; (II) enter cells; (III) escape the endo-lysosomal pathway; (IV) efficient DNA release from the vector; (V) traffic through the cytoplasm and into the nucleus; (VI) successful gene expression; and (VII) remain biocompatible. Image reproduced with permission from [114]. Copyright (2007) Elsevier.

1.6.1 DNA packaging

Before entering the target cell, a naked DNA plasmid is susceptible to degradation by the numerous serum nucleases in the cell culture medium or the extracellular milieu, and it needs protection against the enzymatic degradation. Additionally, the negative charge constituted by the phosphate groups on DNA makes it likely to be repelled from the plasma membrane, which contains negatively charged proteoglycans and phospholipids. The molecular topography of the plasmid DNAs (often several kilo base pairs long) makes them easily condensed into small nanosize particles when complexed with a cationic carrier. The advantages of packaging and condensation of DNA by cationic agents are three fold: firstly, the vulnerable naked DNA is protected from nuclease degradation effectively [115]; secondly, the negative charge of DNA is neutralized, hence DNA is not likely to subject to charge repulsion by the anionic plasma membrane of the cell [116]; and lastly, due to the charge screening effect, the size of the DNA is able to be collapsed to micro- or nano-scale, which facilitates its cellular internalization by phagocytosis or receptor-mediated endocytosis (RME) [117].

DNA is packaged based on three mechanisms: electrostatic interaction, non-electrostatic interaction, and encapsulation. The entropy-driven spontaneous electrostatic interaction between cationic vectors and anionic DNA is the most common gene carrier design rationale. Polycationic polymers such as poly(2-(dimethylamino)ethyl methacrylate) (PDMAEMA), branched or lineal PEI, poly(propylenimine) (PPI), poly(amidoamine) (PAMAM), and poly(lysine) (PLL) all possess various degrees of primary, secondary, tertiary and/or quaternary amines which are protonated at certain degrees at physiological pH [114] and able to condense negatively charged DNA via electrostatic interaction. At an optimum N/P ratio (ratio of protonatable polymer amine groups to nucleic acid phosphate groups), efficient DNA condensation and gene transfection could occur. However, the net positive charges of the polymer/DNA complexes have drawbacks. Firstly, it was well documented that cationic nanoparticles disrupted lipid bilayers [118, 119] and induced oxidative stress inside the cell resulting in high cytotoxicity. Also, a very strong binding force between carrier and DNA makes unpacking and release of the DNA cargo inside the cell difficult, resulting in low gene transfection efficiency. Therefore, a careful balance is needed when designing the cationic carrier to allow both easy condensation of the DNA molecule and effective DNA release intracellularly to achieve its therapeutic goal.

Cationic charge on the polymer/DNA complex is a double edged sword. Therefore, alternative gene packing strategies using non-electrostatic interactions namely hydrogen bonding and/or van der Waals interactions to bind and condense DNA were developed by researchers, and typical examples include polyvinyl pyrrolidone (PVP) [120] and lipopolythioureas [121]. These polymers, after interacting with DNA, not only protect them from enzymatic degradation, but at the same time increase the surface hydrophobicity of the nanoparticle, enhancing the cellular uptake of complexes.

Encapsulation within biodegradable spherical vehicles is an alternative means for DNA packaging. Poly(phosphoester) [122], poly(β -amino ester) [123], poly(lactide-co-glycolide) (PLGA) [124] are typical examples of biodegradable gene carriers due to the ester bonds in their backbone which are prone to hydrolytic degradation so that the polymer is broken into shorter segments for more efficient clearance from the body. Moreover, biodegradable polymers enable localized, controlled and sustained DNA release at the site of action via sustained diffusion through the polymer matrix, whose kinetics is coupled to that of degradation of the polymer matrix itself [125]. Thus the biodegradable polymers have

applications in tissue engineering, where broadening the range of DNA release rate to allow long-term expression of therapeutic proteins for specific growth regulation is an absolute advantage. However, the encapsulation approach is not without limitations. Apart from low encapsulation efficiency, potential degradation of DNA cargo in the low pH environment during the hydrolyzing event, and incomplete DNA release, current methods available for encapsulation usually incur high shear stresses and exposure to organic solvents and extreme temperatures that can damage the DNA [126, 127]. Strategies to overcome the former problems could be mixing the polymers using encapsulation for DNA packaging with polymers using electrostatic interaction to pack DNA. For example, the presence of 0.25% of a triblock copolymer PLGA-PEG-PLGA exhibited a 10-fold enhancement in cellular transgene expression when used together with polycationic protamine/DNA complexes [128].

1.6.2 Extracellular stability

One potential problem of cationic polymer as an *in vivo* gene carrier is that they could encounter negatively charged macromolecules such as serum proteins like albumin, which may absorb onto the positively-charged nanoparticle and weaken the electrostatic interactions between the vector and the DNA cargo, as well as screen the inter-particle electrostatic repulsive forces, eventually lead to aggregation of the nanoparticles over time. A remedy to this is to develop “core-shell” nanoparticles which contain poly(ethylene glycol) (PEG) and a polycation block. When mixing with DNA in water, the electrostatic interaction between DNA and the cationic segment causes them to spontaneously complex into a compact “polyplex” structure, while PEG moieties form a protective outer layer that shields the positive charge of the polyplex core, and at the same time provides steric hindrance to the undesirable protein absorption in the surroundings [129]. One study showed that in the case of PEG-grafted PEIs, the stability of the nanoparticles and effective transfection efficiency is contingent upon the optimal length and amount of PEG side chains, as PEG side chains shorter than 350 kDa enabled satisfactory stability, while those longer than 350 kDa provided too much steric hindrance, causing interrupted gene delivery to the cells [130]. Therefore, a fine balance must be stricken between providing enough stability and not over-obstructing the positive charges of the polymer resulting less efficient DNA binding and transfection.

One shortcoming of PEG-modified polycation/DNA nanoparticles lies in their propensity to easily dissociate under physiological environments due to the strong hydrophilicity of PEG, hence unpredictable behavior *in vivo* could happen [131]. The

counteracting strategy was adding another layer of chemical stability: disulfide cross linking. As is shown in the work by Miyata et al., the stability of PEG-PLL block copolymer was enhanced by post-DNA-complexation disulfide cross-linking. A sodium dextran sulfate displacement assay showed that disulfide bond cross-lined polyplexes were more stable compared to the non-cross-lined counterparts by demonstrating less dissociation in a non-reductive environment [132]. Although the disulfide bonds provided an extra level of stability to the complexes extracellularly, they could be easily cleaved under the intracellular reductive environment into two thiol groups (–SH) through the action of glutathione, one of the most abundant cytosolic peptides in mammalian cells, facilitating DNA release [133].

In addition, besides PEGylation, other hydrophilic moieties have been employed to improve the colloidal stability of polycationic vectors, for example, poly(methyl acrylate), PVP, and sugars [102, 120].

1.6.3 Cellular uptake and endosomal escape

When cationic polymer/DNA complexes reach negatively charged cell membrane, they bind to the anionic proteoglycans electrostatically and are taken up via non-specific endocytosis through a mechanism that is still unclear [134]. But during *in vivo* applications, positive charges of the nanoparticle are usually shielded by PEG to ensure stability. Therefore, cell-targeting ligands are usually chemically conjugated to the polymers to increase cellular uptake and confer cell specificity, making the nanoparticle “smart” [129]. The cell-specific recognition of the ligands upon binding to their cognate cell surface receptors induces RME, which is important in treating lots of diseases involving a specific cell type, as uptake of the therapeutic DNA complexes via cell surface receptors exclusively expressed or over expressed on certain cell types could significantly reduce the side effects of the treatments. Table 1 lists some examples of the conventional ligands to be conjugated onto the polymers to provide selective targeting to cell types displaying the appropriate receptors.

Table 1. Targeting ligands utilized to promote cellular uptake.

Targeting ligand	Target receptor	Target cell type(s)	Ref
<i>Carbohydrates:</i>			
Galactose	Asialoglycoprotein receptor	Hepatocytes	[135]
Mannose	Mannose receptor	Dendritic cells, macrophages	[136]

Glucose	Glucose transporter	Cancer cells	[137]
<i>Endogenous ligands:</i>			
Folate	Folate receptor	Cancer cells	[138]
Transferrin	Transferrin receptor	Cancer cells	[139]
<i>Antibodies:</i>			
Anti-platelet endothelial cell adhesion molecule (PECAM) antibody	PECAM receptor	Endothelial cells	[140]
Anti-HER2 antibody	Human epidermal growth factor receptor	Cancer cells	[141]
<i>Cell penetration Peptides:</i>			
RGD	Integrin receptor	Endothelial cells	[142, 143]
EGF peptides	Human epidermal growth factor receptor	Cancer cells	[144]
HAIYPRH (T7)	Transferrin receptor	Cancer cells	[145]

Different pathways by which the nanoparticles are internalized include phagocytosis, macropinocytosis, clathrin-mediated endocytosis, caveolae-mediated endocytosis, and clathrin- and caveolae- independent endocytosis, and it is these different pathways that determine the intracellular itinerary of the nanoparticles. Factors such as cell type, polyplex type, and polyplex formulation conditions are primary determining factors of the internalization pathway and subsequent travel route [146]. Currently, clathrin-mediated endocytosis is the most characterized pathway of uptaking nanoparticles, during which clathrin-coated pits pinch off the cell membrane and fuse with early endosomes, with a concomitant drop of pH from neutral to around 6 [147]. Vesicle acidification occurs further when endosomes mature to late endosomes and lysosomes, with reduction of pH to around 5. Thus, the ability for the polymer/DNA complexes to escape from enzymatic degradation in the low pH environment in the endosomes is paramount to successful gene delivery.

To address this issue, various techniques were employed to disrupt the endosome membrane in order to allow successful release of the genetic material into the cytoplasm.

Firstly, some polymers were conjugated with membrane disruptive (fusogenic) proteins/peptides like melittin [148] and KALA [149]. Fusogenic peptides undergo structural transition from random coils at neutral pH to α -helical conformation at acidified pH to disrupt the endosomal membrane and allow endosomal escape of the genetic cargo. The second group includes polymers possessing excess protonable amine groups which provide superior buffering capacities. A typical example is PEI. The success of PEI for gene transfection is primarily attributed to its high positive charge density and its composition of primary, secondary, and tertiary amines. While primary amines are protonated at physiological pH 7.4 to allow PEI to bind and condense negatively charged DNA effectively into nanosize complexes via electrostatic interactions, the secondary and tertiary amines are able to sequester protons in the endosomes. The buffering effect leads to influx of chloride ions, which causes osmotic swelling and finally the rupture of the endosomes---a phenomenon known as the “proton sponge” hypothesis [150]. Moreover, people use endosomolytic agents such as chloroquine during *in vitro* gene transfection to allow the nanoparticles to escape from the endosomes. Chloroquine not only swells and disrupts endosomes, but also competitively dissociates DNA from the polycation by electrostatic interactions, and protects DNA from intracellular nuclease degradation [151]. The fourth group of polymers designed to enable endosomal release is conjugated with alkylated carboxylic acid groups, where the carboxyl groups contain buffering capacity in sequestering protons and the hydrophobic alkyl groups interact with the endosomal membrane to enhance vesicle release [152].

1.6.4 Intracellular trafficking

Once released out of the endosome into the cytosol, the polyplexes face a hostile environment where nucleolytic enzymes are abundant to degrade the nucleic acids. Moreover, it was reported that part of the cytoskeleton, the cross-linked actin filaments could significantly hinder the diffusion of free DNA greater than 250 bp [153]. Although the exact mechanism by which DNA travels to the nucleus and be expressed is still under investigation, researchers have suggested that DNA travels on the microtubule network driven by dynein motor proteins to reach the nucleus [154]. Various approaches have been utilized by researchers to promote DNA transport into the nucleus. Firstly, nuclear localization signal (NLS), some of which are peptide sequences borrowed from viruses (e.g. SV40 and TAT), was frequently conjugated to polymers or linear DNA molecules or directly complexed with DNA via electrostatic interaction [155, 156]. These peptides recognize and bind to the import proteins like importins in the cytosol, which mediate active shuttling of the polyplexes or DNA cargo through the

nuclear pore complexes (NPC), which would otherwise exclude the passive diffusion of molecules larger than 39 nm [157]. A similar but less investigated nuclear transport method involves intracellular carbohydrate-binding receptors (i.e. lectins). Certain carbohydrates on the polymers, upon recognizing their cognate lectins, could activate energy- and signal-dependent processes to transport the DNA into the nucleus through NPC [158]. Conflicting results are present in the literature regarding the usage of certain types of carbohydrate, but the ease and economy of synthesis [159, 160], and the biocompatibility of the sugar molecule clearly provide the advantages of this technique in vector design. Moreover, it has been shown that increased gene transfection efficiency was observed when the gene transfection occurs shortly before cell division (i.e. S and G2 phases), probably due to the transient breakdown of nuclear membrane during mitosis, allowing easy DNA entry into the nucleus [161]. However, this behavior has limited clinical application since most cells in the body are non-dividing, also, successful exploitation of the mitosis behavior has vector dependency [162].

1.6.5 DNA unpacking

During the DNA delivery process, the dissociation of the DNA cargo from the polymer and the escape of the DNA from the endosome happen not necessarily concurrently. In some cases, the DNA might still be bound to the polymer after escaping into the cytosol. Actually, inefficient unpacking of DNA from the polymer may result in unsatisfactory gene delivery efficiency [132]. The competitive displacement of DNA molecules by anionic agents such as mRNA, heparin, proteoglycans and/or genomic DNA has been proposed as the major mechanism for the intracellular DNA unpacking from polyplexes, despite the fact that the exact mechanism and location of the event are still unclear [102, 163, 164]. Generally, introducing disulfide bonds or ester bonds into the polymeric delivery vehicle is the primary means to facilitate intracellular DNA release. Disulfide bonds could be introduced between cationic ligands and the polymer backbone, so that DNA bound to the ligands extracellularly could be easily released upon reductive bond cleavage by glutathione in the cytosol [165]. Alternatively, disulfide bonds along the backbone of the cationic polymer, upon reduction, could result in both efficient DNA release and reduced cytotoxicity associated with lower molecular weight (MW) polymers [166]. The idea of incorporation of hydrolytically-sensitive ester bonds is similar to that of the disulfide bonds except that it is the water molecules that act as cleaving agents, and the cleavage could occur as soon as the polymer contacts the physiological environments. Thus, premature release of DNA is a concern, and further studies investigating the relationship between structural and chemical requirements (MW, crosslinking

density, etc.) and sustained DNA release are absolutely necessary [114]. Moreover, another strategy to achieve efficient and controlled release of DNA is through thermo-responsive polymers. These polymers are characterized by a relaxed hydrophilic “coil” phase and a collapsed hydrophobic “globule” phase, which are separated by a transition temperature called the Lower Critical Solution Temperature (LCST) [167]. Thermo-responsive polymers with LCSTs lower than body temperature could deliver tightly condensed DNA molecules intracellularly. Then an induced temperature drop (for example, via external applied cooling pad) could result in conformational change of the polymer to the relaxed phase and facilitate DNA release. A typical example is the poly(N-isopropylacrylamide) (NIPAM)-based polymers, which could be used to enhance gene transfection efficiency in a temperature and N/P ratio dependent manner [168]. However, the enhancement was only modest so far, and a series of factors such as cationic character, endosomal escape capacity, the suitable LCST range need to be further explored for optimization of the polymer design.

1.6.6 Biocompatibility

Achieving biocompatibility is one of the biggest challenges in synthetic gene delivery vector design. The notion of biocompatibility comes two-fold. Firstly, the vector has to be stable within the blood stream (i.e. not interacting with anionic blood components and aggregate, not activating the complement system, and/or not being recognized and cleared by the reticuloendothelial system) [169]. As discussed in section 1.6.2, PEG incorporation into the polymers is the most widely used strategy for stability enhancement as it provides a hydrophilic shell that masks the cationic residues on the polymer which absorb competing anionic biomolecules in the blood, and it provides steric stability to the polymer. Moreover, the inherent solubility, biodegradability, and potential targeting capacity of oligosaccharides make them appropriate alternatives to PEG stabilizers [114]. For example, cyclodextrins (CD) (compounds made of sugar molecules linked together in a ring) not only enhanced the stability and reduced the toxicity of polycations such as PEI and PLL by shielding their surface charges, they also had a topology of toroid with hydrophobic interior and hydrophilic exterior, making them ideal for accommodating and enhancing solubility and bioavailability of hydrophobic compounds [170]. This property has been widely exploited for CD containing vector mediated gene delivery, for example, CD-PEI nanoparticles were observed to bind specifically to adamantine (a kind of polycarbon)-PEG conjugates, forming particles that are stable at physiological salt concentrations, and allowed high-affinity loading of gene delivery vehicles onto mice liver without eliciting immune responses or toxicity [171, 172]. The second criterion

of biocompatibility is that the vector must not elicit wide scale toxicity on the transfected cells. Although the exact mechanism of cytotoxicity remains to be explored, the prevailing hypothesis is that it is the high charge densities of the cationic polymeric carriers such as PEI, PLL, and PAMAM dendrimers that are the major cause behind cellular membrane damage and phospholipid reshuffling, which often lead to the activation of the apoptotic or necrotic pathways [173]. In order to overcome the potential cytotoxicity, the charge shielding effects of hydrophilic moieties such as PEG, PVP and carbohydrates have been extensively exploited in the design of cationic polymers for systemic gene delivery. In a study by Liu et al., a biodegradable hyper-branched PEI (25 kDa)-grafted polycaprolactone (570 kDa)-block-monomethoxyl poly(ethylene glycol) (2 kDa) copolymer was found to exhibit less toxicity in the A549 cell line and to induce less hemolysis compared to the 25 kDa PEI control [174]. In addition, MW was demonstrated to be directly related to both high cytotoxicity and high transfection efficiency, therefore a delicate balance must be achieved to ensure successful gene transfection while maintaining high cell viability. Efforts were made to design biodegradable polymers which allowed high MW polycations to be constructed with linkages such as disulfide bonds which were cleavable intracellularly and converted the high MW vectors into less toxic low MW constituents [175]. Furthermore, another counteracting approach to address the cytotoxicity problem was to use polymers derived from natural resources, such as cationic chitosan, due to their inherent biocompatible, biodegradable, and nontoxic properties. In fact, chitosan-incorporated nucleic acids delivery systems have achieved high nuclease resistance, endosomolytic activity and promising transfection efficiency, as demonstrated in lots of studies [176-178].

1.7 Methods of gene delivery

The delivery systems for gene can be generally divided into two categories: physical and carrier-based. The physical methods include electroporation, sonoporation [179], gene gun [180], scrape loading [181], microinjection [182], and so on, mostly with the aim of disrupting the plasma membrane to allow gene entry. Obviously, these seemingly aggressive methods are associated with widespread cell death resulting from cell membrane damage, laborious manipulation with single cells, difficulty in *in vivo* applications, and concerns over selectivity. Therefore, safer and more efficient gene delivery methods are needed. On the other hand, viral and non-viral gene carriers effectively package the genetic cargo to protect them from nuclease degradation and facilitate cellular uptake and intracellular trafficking processes elaborated in section 1.6, therefore they will be the focus of discussion in this section. Different types of

viral and non-viral vectors, the advantages and disadvantages associated with each of them will be evaluated.

1.7.1 Viral

Viral vectors generally have superior gene transfection efficiency, often several orders of magnitude higher than that of non-viral vectors, mainly benefited from centuries of selective evolutionary pressure [183]. From the review by Kay et al., recombinant viral vectors have a “split design” consisting of the vector DNA and the helper DNA. The vector DNA is constructed in a way that the coding regions of the viral genome are replaced by a therapeutic gene cassette, leaving the non-coding *cis*-acting gene regulatory sequences responsible for packaging of vector genome into the viral capsid and integration of vector genome into the host chromatin intact. It also includes a packaging domain (ψ). On the other hand, the helper vector contains essential viral genes for expression of viral replication and structural proteins, and it does not have the packing domain (ψ). When a recombinant virus transduces the target packaging cell, both the vector and the helper DNA are introduced into the cell, either as heterologous plasmid within the same virus, or by the vector virus and the helper virus respectively, or in a situation when the helper DNA has already been stably integrated into the host chromosomes of the transduced packaging cells. Then, the viral replication proteins expressed from the helper DNA enabled replication of the vector DNA, resulting in synthesis of many copies of the therapeutic genes, while the viral structural proteins recognize the packing domain (ψ) on the vector DNA and package the vector genome into the viral particles, leaving helper (ψ negative) DNA behind (Figure 3). In this way, the spatial segregation of the essential viral genes and the *cis*-acting elements enables the production of replication-defective viral particles able to selectively introduce the therapeutic genes into the target cells, hence retains the high efficiency of viral delivery of desirable genetic cargoes, and simultaneously increases the safety of the viral vector system by increasing the number of recombination events required to make the virus replication-competent again.

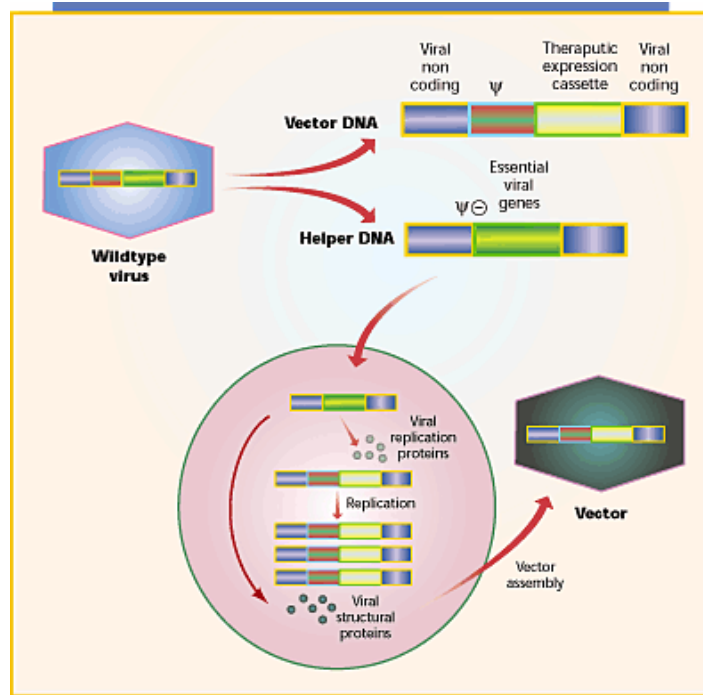


Figure 3. Generic strategy for engineering a virus into a vector. The helper DNA contains genes essential for viral replication which are placed in a heterologous/unrelated DNA context that can be delivered as a plasmid, helper virus or stably inserted into the host chromosomal DNA of the packaging cell. The helper DNA lacks the packaging domain (ψ) so it itself or its RNA cannot be packaged into a viral particle. The helper DNA of some vectors also lacks additional transfer functions, to increase safety. The vector DNA contains the therapeutic expression cassette and non-coding viral *cis*-acting elements that include a packaging domain. The viral proteins required for replication of the vector DNA are produced, leading to the synthesis of many copies of the vector genome. Viral structural proteins recognize the vector (ψ^+) but not the helper (ψ^-) DNA for packaging of the vector genome into a particle. Reproduced with permission from [184]. Copyright (2010) Nature Publishing Group.

Viral vectors such as retroviruses, lentiviruses, adenoviruses, adeno-associated viruses (AAVs) and herpes simplex viruses (HSVs) are the main clinically available gene delivery viruses and have been extensively reviewed by several groups [104, 184, 185]. They are generally classified into two categories: non-lytic viruses, such as retroviruses and lentiviruses, which produce virions from the cell membrane of the transduced cell, leaving the host cell relatively intact; and lytic viruses, such as adenovirus and HSVs, which destroy the infected cell after virions release [186]. Their respective structural design, mechanism of transduction, advantages and disadvantages will be discussed below.

Retroviruses are a class of lipid-enveloped viruses replicating in host cells via reverse transcription processes. The genome of the retrovirus is a positive sense, single-stranded RNA molecule of 7-11 kilo bases (kb), which upon entering the host cell, is reverse-transcribed into

linear double stranded DNA molecule by its own reverse transcriptase enzyme, and integrated into the host genome by its integrase enzyme. The host cell then treats the viral DNA as its own, transcribes and translates the “parasite” viral genes together with its own genome, allowing replication and assembly of new viral particles, which cause further infection. The *cis*-acting elements of the retrovirus locate at both ends of the viral genome, allowing up to 8 kb of therapeutic DNA to replace the viral genes, which are expressed by the transfection factors encoded by two heterologous helper DNA constructs. The location of *cis*-acting elements in the terminal regions as well as the property which allows viral genome integration into the host chromatin enabling stable expression of therapeutic genes have made retroviruses to be the most popular gene delivery vector in clinical trials up to now [187]. However, one limitation of retroviruses is that target cell mitosis must occur after viral entry so that nuclear membrane disruption during cell division could allow the viral gene to integrate into host chromatin. This limits the application of retroviruses for gene delivery to dividing cells such as tumor cells and *ex vivo* transduction of lymphocytes and hematopoietic progenitor cells [188]. In addition, the random insertion of retroviral gene into host genome might pose some potential danger in triggering cancer. For example, exciting news was released in 2000 regarding successful retroviral mediated gene delivery treatment of children suffering from a rare form of X-linked severe combined immunodeficiency (SCID-X1) caused by mutations in genes encoding γ -chain of several interleukin receptors, blocking T and NK cells differentiation [189]. The treatment however, showed complication in 2012 because two of the ten children developed a leukemia like condition, shown to be related to retroviral vector insertion near the LMO2 proto-oncogene promoter leading to aberrant overexpression of the oncogene [190]. Nevertheless, encouraging clinical trial results were reported, for example, a herpes simplex virus thymidine kinase (HSV-TK) suicidal gene was transferred into donor lymphocytes to treat allogeneic graft-versus-leukemia while limiting the possibility of ensuing GVHD [191].

Lentiviruses are another promising type of gene delivery vectors, which are different from retroviruses in the way of transporting their pre-integration complex into the nucleus of the target cell. Active transport by nuclear import machinery of the host cell is exploited by lentiviruses so that they could infect non-dividing cells, which greatly expands their tropism of infection. Research showed that lentiviral vectors were used to effectively transduce non-dividing, differentiated, and *ex vivo* dissociated epithelial tissues of rodents and humans origin [192]. Hybrid lentiviral vectors were derived from non-human lentiviruses such as simian,

feline, equine, caprine and bovine immunodeficiency viruses, with the hope that they would be more tolerated in clinical trials as they were not likely to be infectious to humans, although successful *in vivo* testing were still waited to be seen [193]. In addition, similar to the retroviruses, the lentiviruses post potential danger in activating transcription of proto-oncogenes via insertional mutagenesis.

Adenoviruses are non-enveloped virus containing about 36 kb viral double stranded (ds) DNA genome encoding over 50 polypeptides. Upon cell entry, the viral particle-contained protein facilitates endosomal escape allowing genome entry into the host nucleus. Then, viral genes essential for genome replication and structural protein synthesis were expressed, allowing encapsulation of newly replicated genomes into new viral particles. During the recombinant adenoviruses vector development, it was realized that although they could induce high transduction efficiency, even low-level transcription of the viral genes resulted in innate cytokine responses and antigen-dependent immune responses, causing destruction of transduced cells and high toxicity profiles in animals [194]. Therefore, a helper-dependent vector system was subsequently employed in which the helper virus contained all the virus genes essential for replication but lacked the packing signal, while the second virus contained the viral inverted terminal repeats (ITRs), the therapeutic genes and packaging signal allowing its genome to be selectively packaged into the new virions. Despite the fact that this process was labor intensive and hard to scale up, it substantially reduced cytotoxicity and induced promising therapeutic effects in pre-clinical trials in rodents [195].

AAVs are human parvoviruses that usually depend on a helper virus such as adenovirus to transduce cells and replicate. Upon entering the target cell nucleus, AAV carried genes either remain as episomal transgenes (>90%) or randomly integrate into the host genome (<10%) for transduction [184]. Currently, there is no known disease or obvious toxicity associated with AAV infection, which along with its broad tropism, is one of its greatest advantages in gene therapy. However, the largest drawback of AAV vectors lies in its limited packaging capacity, which is only about 5 kb [186]. Nevertheless, AAV seems to be a promising gene delivery system for phase I clinical trials. It has been involved in the treatment of cystic fibrosis, hemophilia B, α -antitrypsin deficiency, Leber congenital amaurosis, and so on, largely due to the fact that no hostile host cellular immune responses have yet been observed [196].

HSVs contain a large genome of linear dsDNA of 152 kb, which encodes at least 84 genes, at least half of which are nonessential HSV genes replaceable by foreign therapeutic genes [197]. HSV type 1 (HSV-1) is the most extensively studied and used herpes virus vector for gene delivery, which has benefits of highly efficient gene transduction and broad tropism. However, its use is limited by the lack of long term transgene expression in tissues such as brain and difficulties in targeting specific cells. Successful HSV mediated pre-clinical treatments in animal models of cancer [198] and epilepsy [199] were reported, but their test in clinical settings remains to be explored.

In summary, the viral vectors have superior gene delivery capabilities compared to the physical means and the non-viral vectors, however, their clinical applications are limited by problems such as high toxicity, restricted targeting of specific cell types, relatively low DNA loading capacity, immunogenicity, and high cost in production and packaging [182, 200]. Owing to these reasons, safer, non-viral gene delivery systems are becoming increasingly desirable to allow modern science and medicine to fully captivate the benefits brought about by gene therapy.

1.7.2 Non-viral

Comparing to the viral vector counterparts, non-viral gene vectors represent a simpler and safer alternative for gene delivery. Other advantages of non-viral vectors, especially synthetic non-viral vectors, include unlimited clone capacity, large-scale and cost-effective preparation, low immunogenicity, and the feasibility of repeated applications [201]. However, the main defect of non-viral vectors is their relatively lower gene transfection efficiencies compared to the viral vectors due to the various barriers of nucleic acids delivery and expression illustrated in section 1.6. Luckily, modern synthetic methodologies have made ingenious designs and modulations of the non-viral vectors' structures and properties to circumvent the various barriers and enhance their widespread applications. In this section, various types of non-viral vectors will be introduced, and their superiorities and drawbacks will be discussed.

1.7.2.1 Cationic liposomes

Cationic liposomes are a group of attractive non-viral gene delivery vectors extensively investigated by researchers worldwide. Typical advantages include lack of immunogenicity, safety, ability to pack large genetic cargos and ease of fabrication. They are usually composed

of a cationic lipid and a neutral helper lipid. Cationic lipids are amphiphilic, which are consisted of a positively charged head group and a hydrophobic lipid anchor, linked together via ester, ether, or alkyl linkages. The head group is usually a single amine group or multiple protonable amines, whose positive charge could effectively bind and condense the negatively charged DNA and enhance cellular uptake via interaction with the anionic cell membranes. In addition, multivalent head groups such as 2,3-dioleyloxy-*N*-[2(sperminecarboxamido)ethyl]-*N,N*-dimethyl-1-propanaminium trifluoroacetate (DOSPA) and di-octadecyl-amido-glycyl-spermine (DOGS) were proven to be more efficient in DNA condensation than the monovalent counterparts [202], although they are more prone to micelle formation causing less stable and more toxic complexes. The hydrophobic chains are usually made up of cholesterol or diacyl chains, whose alkyl chain length and saturation degree correlate negatively with the transfection efficiency of cationic lipids [203]. Specifically, an increased degree of unsaturation of alkyl chains could enhance membrane fluidity and fusogenicity, resulting in higher gene transfection. Furthermore, the linker group has direct correlation with the transfection efficiency and cytotoxicity of the lipid vector; for example, lipids with non-degradable ether linkages (2,3-*bis*(oleyl)oxipropyl-trimethylammonium chloride, DOTMA) are more toxic than those containing degradable ester linkages (1,2-dioleoyl-3-trimethylammonium propane, DOTAP), due to the fact that the latter is more biodegradable after releasing the DNA cargo inside the target cell [204]. But chemically unstable linkers could also compromise the stability of the lipoplexes in the physiological environment. Therefore a fine balance must be stricken between biodegradability and stability of the lipoplexes.

The neutrally charged helper lipid dioleoylphosphatidylethanolamine (DOPE) has gained much attention as it could improve the transfection performance of the cationic lipids such as DOTMA and DOTAP. Studies showed that equimolar mixture of DOPE and DOTMA could form a liposome that mediated higher levels of gene transfection *in vitro* than the single cationic lipids or than the mixture of DOTMA and another helper lipid DOPC [205]. The reason was due to the conformation transition of DOPE from a bilayer to a hexagonal structure under acidic pH, facilitating fusion or destabilization of endosomal membranes and enhancing gene escape from endosomes [206]. Additionally, cholesterol has been employed as a helper lipid which could greatly increase the stability of the lipoplexes and allow increased doses of DNA to be incorporated into the lipoplexes. An intravenous (i.v.) injection of stable cationic liposomes with cholesterol inclusion showed promising expression of a marker gene in mouse

lungs, significantly higher than that achieved by the cationic liposome/DOPE helper lipid counterpart [207]. In addition to the nature of lipids, other factors like stoichiometric ratio of cationic lipid and DNA, and method of formulation of the lipoplexes also have significant impact on the gene transfection efficiency and cytotoxicity of the vectors, which need to be taken into account when designing newer generation lipid carriers with greater safety and potency [208].

1.7.2.2 Cationic polymers

The complexes formed between cationic polymers and nucleic acids at appropriate ratios and conditions are referred to as polyplexes. They usually have nano-scale sizes and are homogeneous. Similar to the cationic liposomes, cationic polymers effectively protect the DNA from nuclease degradation, enhance cellular uptake, promote endosomal escape and nuclear transport of the genes when their properties are properly modulated. Here several most commonly used cationic polymer-based gene delivery vectors will be presented, including poly-L-lysine (PLL), poly(ethylenimine) (PEI), dendrimers, and biodegradable cationic polymers, and their merits together with faults will be discussed.

1.7.2.2.1 Poly-L-lysine

PLL is the first intensively studied peptide-based vector. Low MW PLL with a MW less than 3000 forms unstable complexes with DNA, as the number of primary ϵ -amines of lysine in the polypeptide backbone is not enough for electrostatically binding the nucleic acids [209]. However, high MW PLL is usually associated with high cytotoxicity, aggregation and precipitation [210]. Also, the relatively low transfection efficiencies of PLL are primarily caused by protonation of all the primary amines at physiological pH, rendering them unavailable for buffering in the acidic endosomes. To address this problem, chloroquine or fusogenic peptides were co-incubated with PLL/DNA complexes and were shown to improve gene transfection efficiency *in vitro*, although the *in vivo* success was limited due to the inherent toxicity of the endosomolytic agents [211]. Moreover, PEG was conjugated to PLL to screen the positive surface charges and act as a protecting hydrophilic shell, which could resolve the problems such as absorption of anionic serum proteins, rapid aggregation of the complexes, and high cytotoxicity due to the membrane disturbance property of the high cationic charges, and so on. Indeed, a PLL-PEG block copolymer designed by Kataoka's group self-assembled into a polyion complex (PIC) upon binding to DNA, which showed a significant reduction in zeta potential and cytotoxicity compared to the unmodified PLL, and

the PIC protected the DNA from enzymatic degradation, enabling a prolonged circulation time in the blood compared to the naked DNA [212, 213]. Furthermore, to address the problem of limited transfection efficiency, histidine was conjugated to PLL, and the imidazole head group of histidine ($pK_a \sim 6$) was proven to enhance endosomal buffering and escape of the polyplexes, enhancing the transfection efficiency [214].

Various targeting ligands have been conjugated to PLL to enhance cellular uptake and reduce unnecessary side effects at other cells. For example, Wu and Wu provided the first targeting strategy of PLL by conjugating asialoorosomucoid (ASOR) to PLL with N-succinimidyl 3-(2-pyridyldithio)propionate (SPDP) as a linker, and the resulting polymer could specifically target asialoglycoprotein receptor-expressing hepatocytes both *in vitro* and *in vivo* [215]. In addition, monoclonal antibody against leukemia-specific JL1 antigen was attached to PLL via disulfide bonds, and the resulting polymer could specifically delivery DNA into Molt 4 cells, a human leukemia T cell line, at a transfection efficiency significantly higher than PLL/DNA complexes [216]. Furthermore, folate was conjugated to PLL, making it a popular vehicle for delivery of anti-cancer therapeutics to the folate-receptor over-expressing malignant tumor cells. Actually, folate-PLL conjugate showed dramatically increased cellular uptake, and 6 times higher luciferase gene transfection efficiency in the KB cell line, which contains overexpressed folate receptors, compared to the unmodified PLL [217].

1.7.2.2.2 Poly(ethylenimine)

Among the polycationic polymers used for nucleic acid delivery, PEIs take a prominent stand due to its superior gene delivery potential. First described by Boussif et al. in 1995, branched PEI (Mw 25 kDa) has primary (25%), secondary (50%) and tertiary amines (25%), making every third atom of PEI a protonable amino nitrogen atom, which imparts the polymer with a high cationic charge density at physiological pH [106, 218]. This property allows PEI to effectively form electrostatic interactions with and ensnares negatively charged nucleic acids, and to change its degree of ionization over a broad pH range [219]. Once internalized into the cells via caveolae- or clathrin- dependent routes, due to the decreasing pH in the milieu as the PEI/DNA complexes move from earlier to late endosomes, the estimated percentage of protonated nitrogen of PEI could increase from 15% to 45%, and PEI thus facilitate the release of the nucleic acids from endosomes through the so called “proton sponge effect”, allowing uptake of DNA into the nucleus and achieving high gene transfer efficiency [220-222].

Since it was first reported in 1995, PEI has been used as the ‘gold standard’ for non-viral nucleic acids delivery due to its superior gene transfection capabilities. It enabled high gene transfection in many eukaryotic cell types, such as 3T3 (murine fibroblasts line), COS-7 (monkey kidney cell line), HepG2 (human hepatoma cell line), K-562 (human leukemia cell line), HeLa (human epithelial carcinoma), and MRC-5 (human lung epithelium cells); primary cells such as rat brain endothelial cells and chick embryonic neurons; and in various animal models [106, 223, 224]. Not only therapeutic DNA molecules, but also siRNA have been successfully transfected by various PEI and PEI derivatives *in vivo*. For example, PEI/DNA complexes mediated overexpression of the tumor suppressor gene p53 upon effective delivery led to a reduction of growth of metastatic lung cancer in a mouse model [225]; and systemic/intratumoral administration of PEI/siRNA complexes showed inhibition of subcutaneous liver and lung xenograft growth upon knockdown of RecQL1 DNA helicase [226].

Despite its high nucleic acids transfection efficiency, the high cationic charge density of PEI may lead to major drawbacks concerning toxicity/biocompatibility, complex aggregation and undesired non-specific complex interactions with cellular and non-cellular components, particularly *in vivo*, resulting in adverse effects such as liver necrosis, adhesion of aggregated platelets and shock after systemic injection of higher doses [169, 227, 228]. To improve the biocompatibility and abrogate the toxic effects, various modifications of PEI molecules have been introduced, aiming at shielding of PEI surface charge and altering the PEI/DNA complex architecture [219]. For instance, PEG [229], hyaluronic acid [230], chitosan [231], oligosaccharide such as mannose [232] and galactose [135] have been grafted onto PEI. Additionally, various other hydrophobic [233] or hydrophilic moieties [234] aiming at neutralizing the primary amine groups on PEI have been studied. For example, Wang et al. attached cystamine derivatives containing a reductive cleavable disulfide bond to the primary amines of PEI to reduce the polymer charge density and accelerate the intracellular release of the complexed DNA, achieving reduced cytotoxicity and up to 4.1-fold of the transfection efficiency of the unmodified PEI [235]. Thomas et al. modified PEI with the hydrophobic acetylated alanine, and observed a 2-fold increase in luciferase gene expression and reduced cytotoxicity in COS7 cells [236]. Similarly, the acetylation of PEI [237] and modification with N-isopropylacrylamide [238] also showed reduced cytotoxicity and enhanced transfection efficiency in HEK293 and HeLa cells, respectively. The transfection efficiency enhancement brought about by the hydrophobic groups has been suggested to be due to the increase of

polymer/DNA complex interactions with the cell membrane and therefore enhancement of complexes endocytosis.

PEI exist in many different MWs and structures, and generally, PEI with higher MW and higher degree of branching has been found to have more cytotoxicity and hemolytic properties, presumably due to their higher charge densities [239, 240]. The low molecular weight (LMW) counterparts, for example PEI 1.8 kDa, on the other hand is non-cytotoxic, but only had low gene transfection efficiency, due to weak DNA binding and insufficient protection from nuclease degradation of DNA [241]. Thus, researchers cross linked LMW PEI to form biodegradable high molecular weight (HMW) PEI to circumvent the low transfection efficiency problem [242]. Generally, among the various forms of PEI, branched 25 kDa, linear 22 kDa and 25 kDa PEIs have been regarded by researchers as prominent candidates for *in vitro* and/or *in vivo* gene delivery by exhibiting more favorable physicochemical characteristics, serum stability, and cytotoxicity profile [223, 224, 243-245]. And in this study, branched 25 kDa PEI was selected as the benchmark for investigation and evaluation of the non-viral vectors for PI-9 gene delivery for prevention of cytotoxic lymphocyte killing mediated allograft rejection.

1.7.2.2.3 Dendrimers

Dendrimers such as PAMAM are highly branched and symmetrical molecules with a tree like structure that consists of multiple branched monomers emanating radially from a central core. The number of branch points from the core to the periphery is called generation, with higher generation number indicating larger and more branched dendrimers [246]. Moreover, a higher generation number and associated higher charge density often lead to an enhancement in cellular uptake and gene transfection, and the undesirable cytotoxicity effects [247]. Additionally, the more interior branches have lower chain densities, and are ideal for loading small drug molecules, while the peripheral end groups provide points for DNA binding and surface modifications.

Various benefits are associated with dendrimers. For example, their high structural and chemical homogeneity makes reproducibility of pharmacokinetic data facile; their ability to be loaded with multiple drugs or ligands at both interiors and peripheries greatly increases the cargo loading capacity compared to linear polymers; their high ligand density on the surface favors ligand-receptor interaction and targeting; and the ability to fine-tune the bio-distribution

and pharmacokinetic properties by controlling dendrimers size and conformation, like varying generation number [248] is beneficial for *in vivo* studies. However, successful application of dendrimers as drug/gene carriers is limited by their low biocompatibility, as they cause toxic reactions in the biological host, and they are difficult to be degraded into smaller units for excretion in the urine or feces after metabolism. To circumvent the problems, taking PAMAM for example, PEG and sugars were attached to the dendrimer periphery to bring down the charge density of the amino-terminals and reduce the toxicity [107], and disulfide bonds were introduced into PAMAM to make the polymer biodegradable in the intracellular reductive environment [249].

1.7.2.2.4 Biodegradable polymers

Many polymers for gene delivery contain a backbone made by carbon-carbon bonds, or vinyl bonds, which are not spontaneously degraded into smaller constituents in the physiological environment. Thus, they are not eliminated easily after administration into the host body, or they are simply too large to be filtered out via the kidney. Their accumulation inside cells could cause severe cytotoxicity. To address this problem, cleavable linkages were introduced into backbones or side chains of cationic polymers, rendering them biodegradable. By doing so, the polymers generally demonstrated less cytotoxicity and greater transfection efficiency due to easier unpackaging and release of the genetic cargo in the cytosol.

Poly(a-[4-aminobutyl]-l-glycolic acid) (PAGA), a biodegradable PLL analogue, is synthesized via the polymerization of ϵ -carbobenzoxy (cbz)-L-lysine, whose α -amino group has been converted into a hydroxyl group [250]. After complexing with DNA, the complex was observed to completely dissociate within 24 h at 37°C, suggesting easy degradation of PAGA. In the meantime, there was higher transfection efficiency and no obvious cytotoxicity as compared to PLL [251]. Since its development, PAGA has been successfully applied to several *in vivo* studies. For instance, by delivering interleukin (IL)-4 and IL-10 encoded plasmid DNA using PAGA via mice tail veins, autoimmune diabetes was prevented in three quarters of the treated 32-week-old non-obese diabetic (NOD) mice six weeks after the treatment [252].

Another example of biodegradable polymer is the degradable PEIs, which are made by crosslinking LMW PEI using reducible linkages such as dithiobis(succinimidylpropionate) (DSP) and dimethyl 3,3'-dithiobispropionimidate (DTBP), and acid-labile imine linkage,

achieving lower cytotoxicity than the HMW counterparts, and enhanced gene transfection capability compared to the LMW prototype [253]. Research showed that when transferred from a medium of neutral pH to a medium of pH 4.5, 50% of the imine bonds were degraded within one hour, suggesting easy degradation of the synthetic polymer in the acidic endosomes [254]. Also, the imine-groups containing PEI had transfection efficiency comparable to the gold standard PEI 25 kDa and at the same time had significantly reduced cytotoxicity.

1.8 Summary and Concluding remarks

In conclusion, as discussed in this chapter, allograft rejection represents a big challenge for transplanted organ survival in the long run. Although immunosuppressive agents such as cyclosporine and tacrolimus promote short term alleviation of allograft rejection, they are not prominent in the long term, and they do not target specific pathways of CAR. There is therefore an urgent need to develop safer and more effective anti-allograft rejection strategies, one of which is gene therapy. PI-9 gene encodes a serine protease inhibitor which irreversibly binds to and inhibits GrB which is the main culprit of allograft rejection. Hence, a promising gene delivery vector is needed to deliver the PI-9 gene into the dDC or other donor cells to inhibit GrB and improve graft survival rates.

Synthetic non-viral vectors demonstrate clear advantages that they greatly mitigate problems such as immunogenicity and carcinogenicity associated with their viral counterparts. Moreover, the modern advanced synthetic chemistry makes large scale, cost effective and volatile production of synthetic non-viral vectors with well-defined and modulated chemical structures for gene delivery feasible. Cationic polymers are highly prominent among the various classes of non-viral gene delivery vectors due to their promising transfection efficiency, synthetic versatility and precision, and the ease of conjugating tailor-made functional groups such as ligands for cell/tissue targeting. Although currently adenovirus and retrovirus dominate the clinical trials of gene therapy, non-viral vectors are gaining more and more attention. Actually, it is encouraging that certain polymeric cationic vectors based on PEI and PLL have been employed in phase 1 or 2 clinical trials to combat cystic fibrosis, ovarian cancer and HIV virus infection [255]. The evidence for the safety and effectiveness of cationic polymers in clinical applications provided strong impetus for the continued development of safer and more effective polymeric gene delivery systems, aiming at better overcoming the various gene delivery barriers discussed in the section 1.6.

Furthermore, talking about the gene therapy for allograft rejection prevention using synthetic cationic polymeric vectors, one concern is that gene expression mediated by non-viral vectors is only transient as they do not integrate into the host chromosome like some of the viral counterparts. While this is a valid concern, non-viral vectors can still contribute to the cytotoxic lymphocyte killing inhibition and long-term survival of grafts, through careful design of the gene delivery regimes and methods. For example, renal pumps, and implanted biodegradable hydrogels or matrices could be employed to ensure slow, long-term release of the genetic cargo to achieve better therapeutic effects. They could also be part of a multi-component treatment strategy to boost the effect of immunosuppressive drugs. Moreover, the treatment could also occur during the *ex vivo* culture prior to transplantation to help combat the initial shock of acute rejection. And we believe that in the near future, widespread gene therapy using cationic polymers to fight various diseases would become a reality, with the help of ingenious synthetic polymer design.

CHAPTER 2: HYPOTHESIS AND AIMS

After reviewing the current status and various treatment methods of allograft rejection, and the benefits of using synthetically easy, reproducible, safe and potent non-viral gene delivery vectors for gene therapy in Chapter 1, we hypothesized that using well-designed gene delivery vectors to *ex vivo* deliver DNA encoding PI-9 gene into the dDC or other donor cells prior to transplantation could sequester GrB, inhibit cytotoxic lymphocyte killing mediated by GrB and improve graft survival rates (Figure 4, reproduced from [256]).

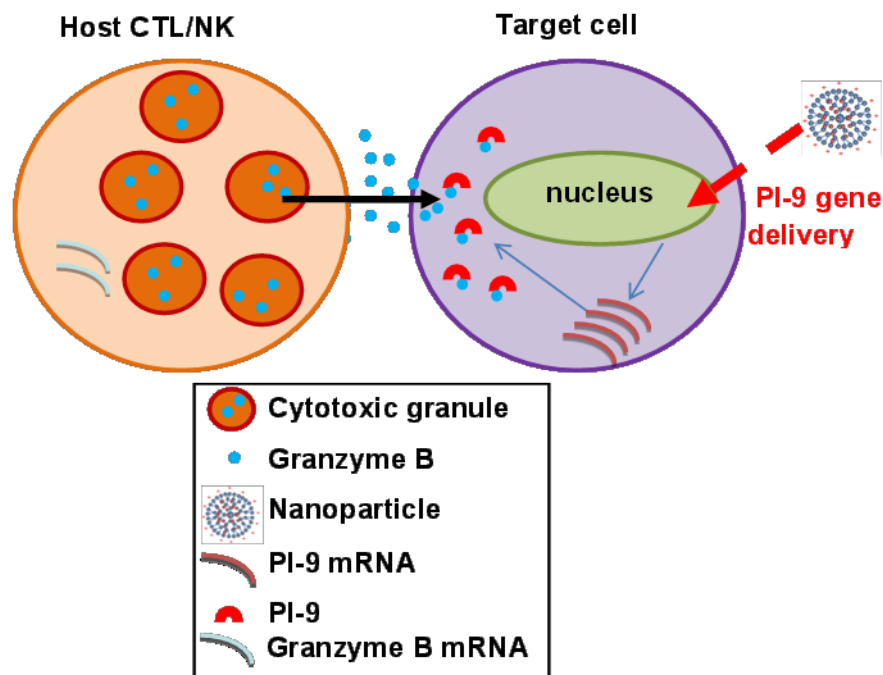


Figure 4. Granzyme B (GrB) which was released from the cytotoxic granules of the host cytotoxic T lymphocytes (CTL)/NK cells entered the target cell (indicated by the black arrow) and could trigger cell apoptosis. To prevent this, a plasmid encoding GrB inhibitor (i.e. proteinase inhibitor-9, PI-9) was delivered by nanoparticles (indicated by the red arrow) to prevent target cell apoptosis. When GrB was released from the host CTL/NK cells to the target cells, it would be inhibited by PI-9 protein, allowing survival of target cells. Reproduced with permission from [256], copyright © 2013, rights managed by Elsevier Ltd.

Among the various synthetic gene delivery vectors currently used in research or clinics, the gold standard branched PEI (25 kDa) is arguably one of the best in terms of achieving superior *in vitro* gene transfection efficiencies, which can be attributed to its high positive charge density for DNA binding and condensation as well as the unique proton sponge properties conferred by the high density of secondary and tertiary amines that participate in the endosomal buffering process, hence facilitating the liberation of DNA into the cytoplasm [182].

However, its clinical potential is limited by its notoriously high cytotoxicity, mainly attributed to its high positive charge density leading to problems such as complexes aggregation and disturbed cell membrane. Thus, a method to partially block the primary amines of PEI to reduce its positive charge has been proposed to effectively eliminate the associated problems.

To test our hypothesis, we explored the following specific aims:

(1) Rationally design and evaluate the gene transfection ability and cytotoxicity of novel cationic polymers based on the gold standard PEI (Mw 25 kDa), which has superior transfection efficiency but high cytotoxicity. The overall goal of this thesis is to design a novel class of modified PEIs with higher or comparable transfection efficiency but greatly mitigated cytotoxicity compared to unmodified PEI.

(2) Use the modified PEIs to deliver PI-9 gene as a strategy to protect various target cells from killing by GrB released from cytotoxic lymphocytes.

Work performed to address each specific aim is outlined in the following chapters: In Chapter 3, we designed and synthesized a variety of differentially modified PEI (25 kDa) to provide an *in vitro* proof-of-concept for the gene transfection efficiency and biocompatibility of this panel of modified PEIs. Traditionally, as discussed in Section 1.7.2.2.2, various functional groups were attached to the primary amines of PEI with an attempt to reduce cytotoxicity. However, despite having demonstrated to be somewhat less toxic, with comparable or elevated gene transfection efficiency to the unmodified PEI, the modified PEIs often face problems such as laborious synthetic process, relatively large polydispersities, complex molecular architectures, difficulty in reproduction, low yield and high cost of starting materials (in the case of amino acids). Therefore, the quest for novel materials with uncomplicated synthetic schemes, well-controlled MWs and narrow polydispersities for potential clinical gene therapy applications continues. In this chapter, a single step, spontaneous ring-opening event will be employed to modify primary amines on PEI using cyclic carbonates, in the presence or absence of DBU catalyst. Commercially available trimethylene carbonate (TMC) was conjugated onto PEI at various PEI:TMC ratios (1, 8, 25, 100) to identify the optimum substitution ratio for high transfection efficiency and low cytotoxicity, which was then applied to different substituted cyclic carbonates to determine which functional groups were the best suited for the purpose of this thesis [150]. Examples of functional groups on cyclic carbonates include Mannose, Galactose, Glucose, Ethyl, Benzyl,

Urea, and so on. Besides to reduce the positive charge of PEI, the rationale of incorporating hydrophobic groups such as TMC, Ethyl, Benzyl, and Urea into the polymer was to increase polymer/DNA complex interaction with cellular membranes and enhance complexes uptake and transfection efficiency [236]; and the purpose of employing sugar molecules was to provide targeting ability towards cells that over-express carbohydrate receptors. Moreover, other than physicochemical properties such as size, zeta potential, DNA binding, etc., *in vitro* gene transfection efficiency and cytotoxicity of these polymers were evaluated on a group of different cell lines comprising HepG2, HeLa, NIH3T3, MCF7, 4T1, HMSC, keratinocytes, and so on. A preliminary *in vivo* test of the polymers' potency and toxicity was also carried out via intravenous injection of the polyplexes into 6-7 weeks old Balb/c mice. As a result, several candidate polymers with satisfactory gene transfection efficiency and greatly mitigated cytotoxicity were selected for further application studies.

In Chapter 4, we examined the feasibility of using the modified PEIs to deliver the GrB inhibitor PI-9 gene into kidney cell line HEK293T to protect the cells from GrB mediated killing. Similar to Chapter 3, facile nucleophilic addition chemistry was employed to attach mannose-functionalized cyclic carbonates to the primary amines of branched PEI with MW of 25 kDa at varying substitution degrees. The ring-opening of the cyclic carbonate resulted in a carbamate linkage and a primary hydroxyl group together with mannose protected with acetyl, and after deprotection, five hydroxyl groups were generated, which could further mask the positive charge density of PEI/DNA complexes and bring down cytotoxicity. Additionally, as stated above, mannosylpolyethylenimine (ManPEI) conjugates are of particular interest for *in vitro* delivery of PI-9 gene, as the highly expressed mannose receptor on antigen-presenting DCs and macrophages could be potentially exploited for targeted gene transfer by RME. In fact, research has shown that DCs transfected with ManPEI/DNA complexes containing adenovirus particles are effective in activating T cells of T cell receptor transgenic mice in an antigen-specific fashion [232]. Here, roughly 7, 20, or 67 carbamate-mannose groups were attached onto PEI to determine the optimal balance of substituted to free primary amines to achieve high Green Fluorescent Protein (GFP)-reporter gene delivery and minimal undesirable adverse side effects on a model cell line HEK293T (human embryonic kidney cell line), where the unmodified PEI was used as a control. The selected modified PEI with the optimal mannose-attachment ratio were further used to deliver PI-9 encoding plasmid into HEK293T cells which were challenged by GrB mediated cell killing by YT cells (human NK-like leukemic cell line), so that the degree of protection provided by PI-9 gene delivery could be investigated.

In Chapter 5, the potential of using mannose modified PEIs to deliver PI-9 gene to mouse fibroblast cell line Balb/3T3 and protect the cells from killing by GrB secreted by allo-specific CTLs from B6 mice or YT cell line was examined. Based on the results in Chapter 4, three other ManPEI polymers were synthesized at PEI to mannose-functionalized cyclic carbonate (MTC-ipman) monomer conjugation ratios of 1:6, 1:12.5, and 1:25, as 1:75 ratio was proven inefficient for DNA complexation and transfection. Moreover, the synthesis of these three polymers was carried out in the same ring-opening reaction but without the use of catalyst, which further simplified the synthesis process. GFP-reporter gene was used to determine the gene transfection efficiency and cytotoxicity on Balb/3T3 cell line, and the results were compared to those of the unmodified PEI. Further, PI-9 was delivered by the modified polymers at optimal N/P ratios into Balb/3T3 cells which were then subjected to GrB mediated killing by allo-specific CTLs isolated from B6 mice or by YT cells. The different killing mechanisms by these two killer cells were compared. Additionally, the promising results also set a foundation for future *in vivo* work for measuring the longevity of the PI-9 transfected Balb/3T3 cells after i.v. injection.

Lastly, in Chapter 6, a conclusion of the thesis was presented.

The successful completion of this thesis has evidently established the molecularly well-defined and narrowly dispersed cationic polymers based on functional carbamate-modified PEIs prepared by facile one step ring-opening reaction as safe and efficient non-viral gene carriers. The promising findings presented here should provide the impetus for further preclinical evaluations of these polymers for gene delivery to lengthen the survival of various transplanted tissues.

CHAPTER 3: RATIONAL DESIGN OF CARBAMATE-MODIFIED PEI FOR MITIGATED CYTOTOXICITY AND ENHANCED GENE TRANSFECTION EFFICIENCY

3.1 Introduction

In Chapter 3, we designed and synthesized a variety of differentially modified PEI (25 kDa) to provide an *in vitro* proof-of-concept for the gene transfection efficiency and biocompatibility of this panel of modified PEIs.

Part of Chapter 3 has been published in *Advanced Healthcare Materials* [150], and was reproduced with permission from [150]. Copyright © 2013 WILEY-VCH Verlag GmbH & Co. KGaA, Weinheim.

Part of Chapter 3 has also been published in *Biomaterials* [256], and was reproduced with permission from [256]. Copyright © 2013, rights managed by Elsevier Ltd.

3.2 Materials and Methods

3.2.1 Materials

Trimethylene carbonate (TMC, Bohringer-Ingelheim, Germany) and branched PEI (MW of 25 kDa) were freeze-dried prior to use. 1,8-Diazabicyclo[5,4,0]undec-7-ene (DBU) was stirred over CaH₂ and distilled using vacuum before being transferred to a glove box. 1-(4,5-dimethylthiazol-2-yl)-3,5-diphenylformazan, thiazolyl blue formazan (MTT) for cytotoxicity assay, and other reagents for polymer synthesis were purchased from Aldrich and used without any other purification unless otherwise noted. Bcl-2 targeted siRNA duplex (sequence: sense 5'-GUA CAU CCA UUA UAA GCU G; antisense 5'-CAG CUU AUA AUG GAU GUA C), β -Actin targeted siRNA duplex, and scrambled siRNA (negative control) were purchased from Dharmacon (U.S.A). Luciferase substrate and 5 × lysis buffer were purchased from Promega (Singapore). GFP-reporter gene (encoding a red-shifted variant of wild-type GFP driven by the cytomegalovirus promoter) and luciferase-reporter gene (encoding the 6.4 kb firefly luciferase gene driven by the cytomegalovirus promoter) were obtained from Clontech (U.S.A.) and Carl Wheeler, Vical (U.S.A.) respectively. The plasmids were amplified in *Escherichia coli* DH5 α which was later purified using Endofree Giga plasmid purification kit from Qiagen. The BCA protein assay kit was from Pierce Biotechnology, Inc. (Singapore).

HepG2, HeLa, NIH3T3, MCF-7, 4T1, HMSC, and keratinocytes cell lines were purchased from ATCC (U.S.A.).

3.2.2 Synthesis of carbamate-modified PEI

All the carbamate-modified PEIs were synthesized by Dr. Chuan Yang in Dr. Yi Yan Yang's lab in IBN, A*STAR, Singapore. The various functional cyclic carbonates were used to modify primary amines on branched PEI 25 kDa through a single step, spontaneous ring-opening reaction, at different substitution ratios. The detailed procedures for the synthesis of the functional cyclic carbonate monomers (MTC-monomers) and MTC-monomer modified PEIs, and the characterization of the monomers and polymers using ^1H NMR spectroscopy were attached in the appendix.

3.2.3 Cell culture

HepG2, HeLa, NIH3T3, MCF7, 4T1, human mesenchymal stem cell (HMSC), and keratinocytes were cultured in Minimum Essential Medium Eagle (MEM, Invitrogen, Singapore, for HepG2), RPMI 1640 medium (Invitrogen, Singapore, for HeLa, MCF7, 4T1, HMSC, and keratinocytes), and Dulbecco's Modified Eagle Medium (DMEM, Invitrogen, UK, for NIH3T3). All media were supplemented with 10% (v/v) fetal bovine serum (FBS, Invitrogen, Singapore), streptomycin at 100 $\mu\text{g}/\text{mL}$, penicillin at 100 U/mL, L-glutamine at 2 mM, and 1 mM sodium pyruvate (Sigma-Aldrich, Singapore). MEM was further supplemented with 1 mM non-essential amino acids (Sigma-Aldrich, Singapore). Cells were cultured at 37 °C, under an atmosphere of 5% CO_2 and 95% humidified air. All cell lines were split using Trypsin/EDTA medium when reached 90% confluence.

3.2.4 Preparation, particle size and zeta potential analyses of polymer/nucleic acids complexes

The polymer was first dissolved in DNase/RNase-free water (Fermentas, Singapore). To form the complexes, an equivolume solution of siRNA/DNA was dripped into the polymer solution to achieve the intended N/P ratios (molar ratio of nitrogen content in the polymer to the phosphorus content of the nucleic acids) under gentle vortexing for about 5 s. The mixture was equilibrated at room temperature for 30 min to allow complete electrostatic interaction between the polymer and the nucleic acids, before being used for subsequent studies.

The particle sizes and zeta potentials of the post-equilibrated polymer/DNA complexes were measured by dynamic light scattering (Brookhaven Instrument Corp., Holtsville, New

York, U.S.A.) using a He–Ne laser beam at 658 nm, with a scattering angle of 90° and Zetasizer (Malvern Instrument Ltd., Worcestershire, UK) respectively. Immediately prior to the measurement, the polymer/DNA complexes in nuclease free water was diluted 10x in PBS to mimic the dilution in the physiological environment after i.v. administration. Particle size and zeta potential measurements were repeated for 3 runs per sample and reported as the mean \pm standard deviation of 3 readings.

3.2.5 Gel retardation assay

Various formulations of polymer/DNA complexes were prepared as described in section 3.2.4 with N/P ratios ranging from 1 to 30. Post equilibration, the complexes were electroporated on 1% agarose gel, which was stained with 5 μ L of 10 mg/mL ethidium bromide per 60 mL of agarose solution. The gel was run in 1 x TBE buffer at 110 V for 50 min, and then analyzed under a UV illuminator (Chemi Genius, Evolve, Singapore) to reveal the relative position of the complexed DNA to the naked DNA plasmid.

3.2.6 DNA binding assay

Polymer/DNA complexes were formed at increasing N/P ratios by gently mixing a fixed amount of plasmid with varying concentrations of polymer in nuclease-free water, as described in section 3.2.4. After incubating the mixture at room temperature for 30 min, an equivolume ratio of SYBR[®] Safe Green dye (Invitrogen, Singapore) was added. When SYBR[®] Safe Green dye intercalated with free DNA, it emitted fluorescence, which was measured by a TECAN microplate reader and calculated as relative fluorescence (%) = $(F_{\text{sample}} - F_{\text{blank}}) / (F_{\text{free DNA}} - F_{\text{blank}})$. Where F_{sample} is the fluorescence of the complex formed at a specific N/P ratio, F_{blank} is the fluorescence of the dye in nuclease free water and $F_{\text{free DNA}}$ is the fluorescence of free DNA read at excitation and emission wavelengths of 502 and 530 nm, respectively.

3.2.7 *In vitro* gene expression

The *in vitro* gene transfection efficiency of the polymer/DNA complexes was investigated using HepG2, HeLa, NIH3T3, MCF7, 4T1, HMSC and keratinocytes. Cells were seeded onto 24-well plates at a density of 1×10^5 cells per 500 μ L per well for GFP/luciferase gene delivery. After 24 h, the plating media were replaced with fresh growth media, followed by the drop-wise addition of 50 μ L of the complex solution (containing 1.75 μ g GFP plasmid DNA) or 50 μ L of complex solution (containing 2.5 μ g luciferase plasmid DNA) at various N/P ratios. Following 4 h of incubation, free complexes were removed by replacing the

medium in each well. After a further 68 h of incubation, the cell culture medium in each well was removed and the cells were rinsed once with 0.5 mL of phosphate-buffered saline (PBS, pH 7.4). For GFP protein expression analysis, 0.3 mL trypsin was added to detach cells in each well. Fresh growth medium (0.3 mL) was then added, and the cell suspension was centrifuged at 1500 rpm for 5 min. Two further cell-washing cycles of re-suspension and centrifugation were carried out in FACS buffer (PBS supplemented with 2% bovine serum albumin). The percentage of cells expressing GFP was then determined using a flow cytometer (FACSCalibur, BD Biosciences, USA) from 10000 events, and reported as mean \pm standard deviations of triplicates.

For luciferase expression assay, 0.2 mL of reporter lysis buffer (1x) was added to each well. The cell lysate collected after two cycles of freezing (-80 °C, 30 min) and thawing (room temperature, 30 min) was cleared by centrifugation at 14000 rpm for 5 min. After that, 20 μ L of supernatant was mixed with 100 μ L of luciferase substrate for the determination of relative light units (RLU) using a luminometer (Lumat LB9507, Berthold, Germany). The RLU readings were normalized against the protein concentration of the supernatant determined using the BCA protein assay to give the overall luciferase expression efficiency. In all *in vitro* gene expression experiments, naked DNA was used as a negative control, and unmodified PEI/DNA complexes prepared at the optimal N/P ratio (i.e. 10 for 25 kDa PEI), at which PEI induced high gene expression efficiency yet provided close to or more than 50% cell viability, were used as the positive control. Data were expressed as mean \pm standard deviations of four replicates.

3.2.8 Confocal imaging for GFP expression in HepG2 cells

HepG2 Cells were treated in similar fashion as described in Section 3.2.7 with polymer/GFP plasmid DNA complexes at intended N/P ratios (unmodified PEI: N/P 15; **K**:PEI-TMC(1:25): N/P 30 and 50). After 3, 6, and 10 days of transfection, the medium in the wells containing transfected cells was removed and the cells were washed once with PBS and fixed with paraformaldehyde for 15 min. Then, the cells were washed 3 times with PBS and imaged using a Motorized Zeiss AxioVert 200M inverted microscope (Carl Zeiss, Germany).

3.2.9 Cellular trafficking

Luciferase plasmid DNA was labelled with YOYO-1 Iodide (Invitrogen, Singapore) according to the manufacturer's instructions. Briefly, DNA (200 μ g) was mixed with 300 μ L of

1 μ M YOYO-1 and incubated at room temperature for 2.5 h in the dark. HepG2 cells were seeded onto 24-well plates at a density of 1×10^5 cells per 500 μ L per well at 24 h before treatment. The plating MEM media were then replaced with 0.5 mL of fresh growth media, followed by the dropwise addition of 50 μ L of the polymer/luciferase-gene-YOYO-1 complexes solution prepared at N/P 50 (containing 2.5 μ g labelled luciferase DNA). HepG2 cells were incubated with the complexes at 37 °C for 0.5, 2, 4, 6 or 24 h. Then, the medium in each well was discarded and the cells were washed with PBS three times and fixed in formalin containing 1% paraformaldehyde solution (300 μ L) for 15 min at 4 °C. After that, the cells in each well were washed with PBS for three times and stained with 300 μ L of Hoechst 33342 dye (5 μ g/mL in PBS) for 40 min at room temperature in the dark. After five runs of rinsing with cold PBS, the cells were visualized by confocal microscopy (LSM 5 DUO, Carl Zeiss, Jena, Germany) to reveal the relative positions of the DNA plasmids to the nuclei.

3.2.10 siRNA transfection and real-time reverse transcription-polymerase chain reaction (RT-PCR) analysis

The *in vitro* siRNA delivery property of the polymers was investigated using HeLa cell line. Cells were seeded onto 12-well plates at a density of 1×10^5 cells per 1000 μ l per well. After 24 h, the plating media were replaced with fresh growth media, followed by the dropwise addition of 100 μ L of complex solution (containing 100 nM bcl-2 siRNA or negative control siRNA complexed with various polymers at N/P ratio of 50). Following 4 h of incubation, free complexes were removed by replacing the medium in each well. After a further 68 h of incubation, the cell culture medium in each well was removed and the cells were subjected to RNA extraction.

Each condition was performed in duplicates to ensure the reproducibility of the results, and each sample was taken from an individual well of a 12 well plate. Total RNA from untreated HeLa cells or those transfected with polymer/bcl-2 siRNA or polymer/negative-control-siRNA complexes was extracted with RNeasy[®] Mini Kit (Qiagen, Singapore) according to the RNeasy[®] Mini Handbook. The total RNA was then reverse-transcribed by SuperScript[™] III Reverse Transcriptase (Invitrogen, Singapore) using oligo(dT)₁₈ primer according to the manufacturer's instructions. The resulting cDNA was subjected to real-time PCR reaction, which was performed with SYBR[®] Green PCR master mix (2x) (Stategene, Singapore) and detected with Rotorgene 6000 (Corbett Research). Custom primers were purchased for Bcl-2 (target gene) and β -Actin (endogenous control), with sequences as follows:

Bcl-2: sense 5'-CGACGACTTCTCCCGCCGCTACCGC-3', antisense 5'-CCGCATGCTGGGGCCGTACAGTTCC-3'; β -Actin, sense 5'-GCTCGTCGTCGACAACGGCTC-3', antisense 5'-CAAACATGATCTGGGTTCATCTTCTC-3'. β -Actin primer sequence is based on Invitrogen primers provided with the Superscript III reverse-transcription kit, and yields a 353-bp product. Custom Bcl-2 primer is based on the literature [257]. A 25 μ L reaction mixture contained 12.5 μ L of SYBR[®] Green I PCR master mix (2 \times), 10 μ M of each primer, 9.5 μ L of DEPC-treated water, and 2 μ L of the cDNA sample. Reaction conditions were set as follows: (1) incubation at 95 $^{\circ}$ C for 10 min; (2) amplified for 45 cycles (95 $^{\circ}$ C for 45 s, 55 $^{\circ}$ C for 45 s, 72 $^{\circ}$ C for 90 s for each cycle); (3) 1 cycle of 72 $^{\circ}$ C for 7 min for final extension; (4) ramp from 72 $^{\circ}$ C to 95 $^{\circ}$ C, 1 degree change per step, 5 s interval between steps. The mean fold change of Bcl-2 gene expression level upon various treatments was normalized against the house-keeping gene β -Actin using the $2^{-\Delta\Delta CT}$ method [258].

3.2.11 Cytotoxicity test

The cytotoxicity of the polymer/DNA and polymer/siRNA complexes was studied using the standard MTT assay protocol. Briefly, HepG2, HeLa, NIH-3T3, MCF7, 4T1, HMSC and keratinocytes were seeded onto 96-well plates at densities of 10000, 5000, 10000, 10000, 10000, 10000 and 10000 cells per well, respectively, and allowed to grow to 60–70% confluence before treatment. Polymer/DNA or polymer/siRNA complexes at various N/P ratios were prepared in water as described in sections 3.2.4. The cells in each well were then incubated with growth medium comprising of 10 μ L of polymer/nucleic acid complexes and 100 μ L of fresh medium for 4 h at 37 $^{\circ}$ C. Following incubation, the medium was replaced with fresh growth medium and incubated further for 68 h. Subsequently, 100 μ L of growth medium and 20 μ L of MTT solution (5 mg/mL in PBS) were added to each well and the cells were incubated for 4 h at 37 $^{\circ}$ C. Formazan crystals formed in each well were solubilized using 150 μ L of DMSO upon removal of growth media. A 100 μ L aliquot from each well was then transferred to a new 96-well plate for determination of absorbance using a microplate spectrophotometer at wavelengths of 550 nm and 690 nm. Relative cell viability was expressed as $[(A_{550}-A_{690})_{\text{sample}} / (A_{550}-A_{690})_{\text{control}}] \times 100\%$. Data were expressed as mean \pm standard deviations of at least eight replicates per N/P ratio.

3.2.12 Organ specific luciferase gene expression in mice

The animal protocols were approved by the Institutional Animal Care and Use Committee (IACUC), Biological Resource Centre, Agency for Science, Technology and

Research (A*STAR), Singapore. 6- to 7- week-old female Balb/c mice (the Jackson Laboratory, Singapore) were maintained under specific pathogen-free conditions. The mice were randomly divided into 10 groups of six mice each: PBS control, PEI/DNA (N/P 10), **G**:PEI-Mannose(1:25)/DNA (N/P 30, 50, 80, 120), **K**:PEI-TMC(1:25)/DNA (N/P 50, 80) and **O**:PEI-ethyl(1:25)/DNA (N/P 50, 80). The polymer/luciferase DNA complexes were formed in PBS according to the protocol mentioned in section 3.2.4, by mixing equal volumes of polymer and luciferase gene solutions at intended N/P ratios, and incubating at room temperature for 30 min. Then a dose of 200 μ l polymer/luciferase gene complexes solution per mouse (contained 4 μ g luciferase plasmid DNA) was injected intravenously via tail vein, with PBS solution as control. After injection, the mice were returned to their cages for 72 h with normal food and water. 72 h later, the various treated and control mice were asphyxiated with CO₂, and heart, liver, spleen, lung and kidney from each sacrificed mouse were excised and stored in -80°C freezer immediately until analysis. When analyzing the luciferase gene expression in each organ, the respective organ tissues were thawed in 4°C fridge for 1 h, rinsed twice in PBS, and 1mL luciferase reporter lysis buffer (1x) (Promega, Singapore) was added to each sample. The tissue was then homogenized in 1 mL of reporter lysis buffer using a EpiShear™ Probe Sonicator (Active Motif, Singapore), and stored on ice. The organ homogenate was then centrifuged for 20 min, at 14000 rpm and 4°C, and the supernatant was transferred to another set of clean 1.5 mL eppendorf tubes. Luciferase measurements were made by adding 100 μ L of freshly reconstituted luciferase assay buffer (Promega, Singapore) to 20 μ L of the supernatant of the organ homogenate. Luciferase activity was measured as RLU using a standard luminometer (Lumat LB9507, Berthold, Germany). The RLU readings were normalized against the protein concentration of the supernatant determined using the BCA protein assay to give the overall luciferase expression efficiency. Luciferase activity in the organs of PBS treated mice was used as negative control, and that in PEI/DNA N/P 10 treated mice were used as a positive control. Data were expressed as mean \pm standard deviations of six replicates.

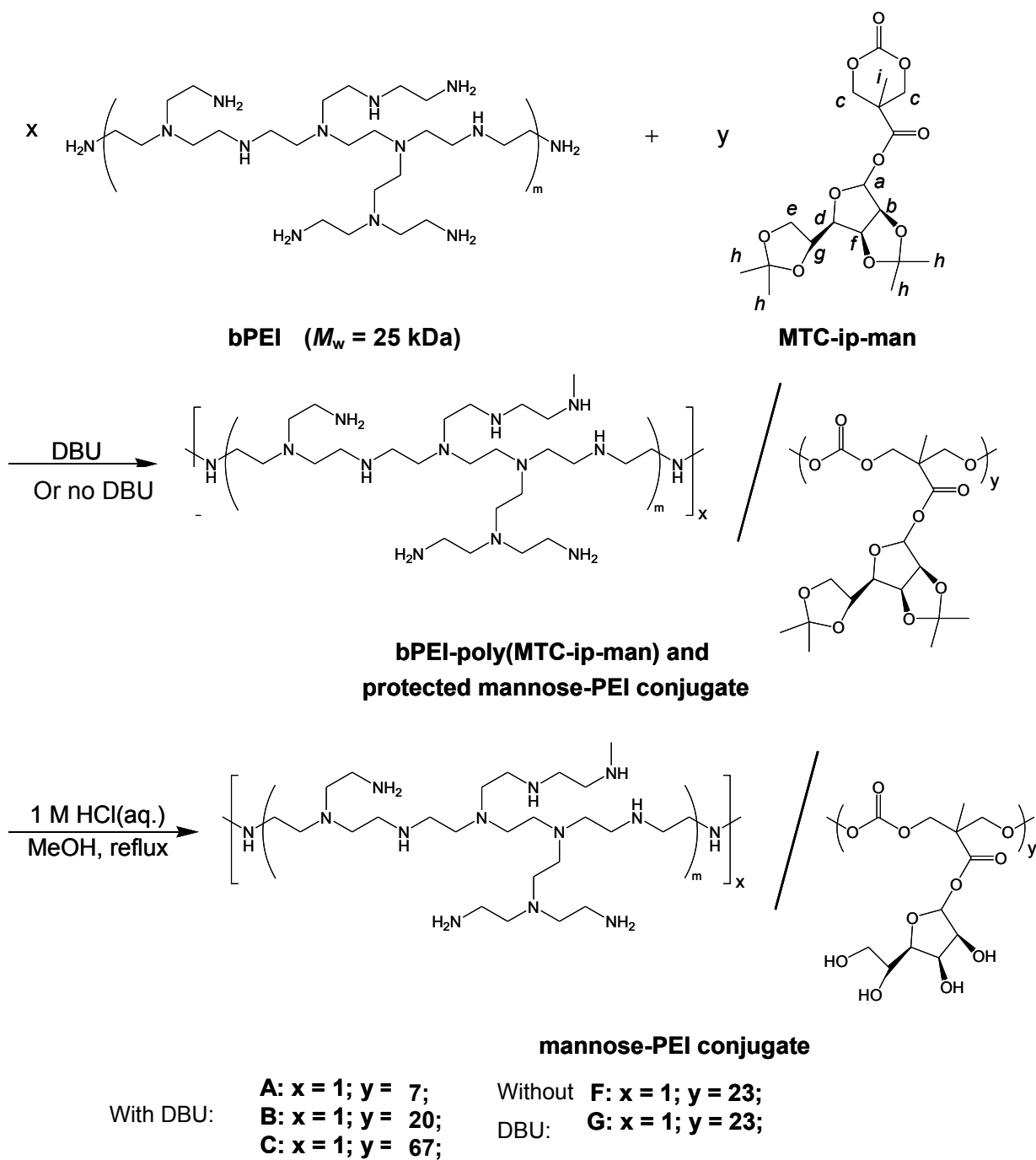
3.2.13 Statistical analysis

All data were presented as mean \pm standard deviation. The statistical analyses between different groups were determined with unpaired Student's t-test and were considered significant if $p < 0.05$.

3.3 Results and Discussion

3.3.1 Polymer synthesis and characterization

In this study, facile nucleophilic addition chemistry was employed to conjugate functionalized cyclic carbonate monomers onto primary amines of PEI. Taking PEI-mannose conjugates for example, Scheme 1 shows the synthesis procedures and structures of some PEI-mannose conjugates. The reaction was conducted in the presence or absence of DBU, giving polymer **A/B/C** or **F/G**, respectively. Quantitative comparisons between the integral intensities of methylene peaks of PEI and those of methyl peaks of MTC-mannose moieties gave the compositions of the polymers (Figure 5). The ^1H NMR results showed that the content of mannose in the polymer was proportional to that in the feed (Table 2a and Table 2b). After substituting primary amines in PEI with the MTC-mannose, a large excess of 1 M HCl/MeOH solution was added to the reaction solution and refluxed for 2 h, removing the protecting groups of mannose moieties. Finally, all the small molecules were removed using ultrafiltration method (MW cut-off of the membrane: 5000 Da). As a result, a series of PEI-mannose conjugates with different feed ratios were synthesized. The resulting polymers, their feed ratios of PEI to mannose monomers, and nitrogen content, etc. were summarized in Table 2a.



Scheme 1. Synthesis procedures and structures of PEI-mannose conjugate.

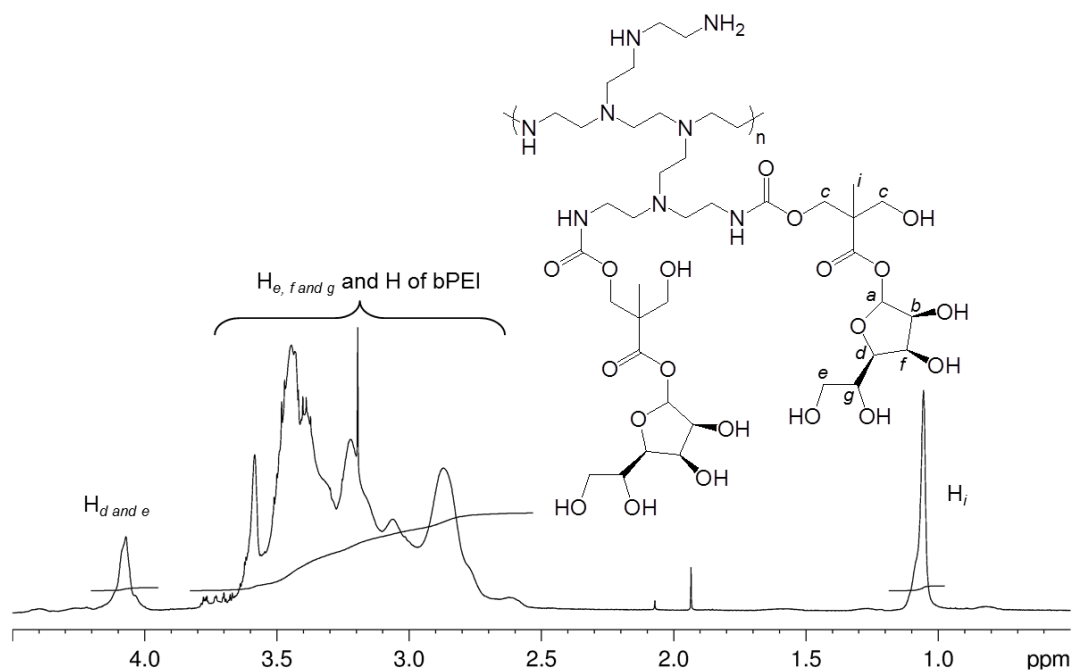


Figure 5. ^1H NMR spectrum of polymer **B** in D_2O .

Table 2. (a) Mannose-PEI conjugates synthesized and used in this thesis. Higher nitrogen content correlates with lower degree of Mannose attachment. Therefore the extent of mannosylation is: $\text{N} > \text{M} > \text{L} > \text{C} > \text{B} = \text{F} = \text{G} > \text{S} > \text{A} > \text{T}$. **B**, **F**, and **G** were synthesized by different methods of mannose conjugation (**B**: reacted for 1 h in the presence of DBU as catalyst; **F**: reacted for 18 h without DBU; **G**: reacted for 1 h without DBU). (PEI: 58 primary amines, 116 secondary amines and 58 tertiary amines)

Modified bPEI Name	Cyclic Monomer	Cyclic Monomer MW	Mass Feed Ratio (bPEI: Cyclic Monomer)	Molar Feed Ratio (bPEI: Cyclic Monomer)	Mol% Cyclic Monomer ^a	Used DBU?	Nitrogen Content (%)
A	MTC-IPMAN	402.15	3:1	1:8	13.7	Yes	24.4
B	MTC-IPMAN	402.15	1:1	1:25	43.1	Yes	16.3
C	MTC-IPMAN	402.15	1:3	1:75	129.3	Yes	8.14
T	MTC-IPMAN	402.15	4:1	1:6	10.3	No	26.2
S	MTC-IPMAN	402.15	2:1	1:12.5	21.6	No	21.7
F	MTC-IPMAN	402.15	1:1	1:25	43.1	No	16.3

G	MTC-IPMAN	402.15	1:1	1:25	43.1	No	16.3
L	MTC-IPMAN	402.15	1:2.3	1:58	100.0	Yes	12.03
M	MTC-IPMAN	402.15	1:5	1:120	206.9	Yes	5.6
N	MTC-IPMAN	402.15	1:16	1:400	689.7	Yes	1.9

^a moles cyclic monomer / moles primary amine groups x 100%.

(b) Summary of the NMR analysis of the mannose- modified PEI (25 kDa) polymers.

Modified bPEI Name	Cyclic Carbonate	Mole Ratio Found (NMR) bPEI: Carbamate Groups ^a	% of bPEI Primary Amine Groups Modified (NMR) ^b	# of bPEI Primary Amine Groups Modified Per Mole bPEI ^{a,c}
A	MTC-IPMAN	1:7	12.1	7
B	MTC-IPMAN	1:20	34.5	20
C	MTC-IPMAN	1:67 ^a	115.5 ^b	67 ^c
T	MTC-IPMAN	1:5.5	9.5	5.5
S	MTC-IPMAN	1:12.2	21.0	12.2
F	MTC-IPMAN	1:23	39.7	23
G	MTC-IPMAN	1:23	39.7	23
L	MTC-IPMAN	1:53	91.4 ^b	53
M	MTC-IPMAN	1:120 ^a	206.9 ^b	120 ^c
N	MTC-IPMAN	NA	NA	NA

^a based on 1 mole bPEI-25 = 10000 g, containing 58 primary amine groups per mole.

^b A value greater than 100% indicates reaction at all active primary amine sites, and reaction of secondary amine groups.

^c A number greater than 58 indicates reaction at all active primary amine sites, and reaction of secondary amine groups.

Using a similar approach, Galactose/Glucose-PEI conjugates were synthesized. The single step, spontaneous ring-opening event allows different amounts of Galactose monomers to be substituted onto PEI, in a precisely controlled manner (Table 3a). Moreover, the ¹H NMR results showed that the content of Galactose/Glucose functional cyclic monomers attached to the PEI was proportional to that in the feed (Table 3b).

Table 3. (a) Galactose/Glucose-PEI conjugates synthesized and used in this thesis.

Modified bPEI Name	Cyclic Monomer	Cyclic Monomer MW	Mass Feed Ratio (bPEI:	Molar Feed Ratio (bPEI:	Mol% Cyclic Monomer ^a	Used DBU?	Nitrogen Content (%)
--------------------	----------------	-------------------	------------------------	-------------------------	----------------------------------	-----------	----------------------

			Cyclic Monomer)	Cyclic Monomer)			
U	MTC-IPGAL	402.15	4:1	1:6	10.3	No	26.2
R	MTC-IPGAL	402.15	2:1	1:12.5	21.6	No	21.7
I	MTC-IPGAL	402.15	1:1	1:25	43.1	No	16.3
H	MTC-IPGLU	402.15	1:1	1:25	43.1	No	16.3

^a moles cyclic monomer / moles primary amine groups x 100%.

(b) Summary of the NMR analysis of the Galactose/Glucose-modified PEI (25 kDa) polymers.

Modified bPEI Name	Cyclic Carbonate	Mole Ratio Found (NMR) bPEI: Carbamate Groups ^a	% of bPEI Primary Amine Groups Modified (NMR) ^b	# of bPEI Primary Amine Groups Modified Per Mole bPEI ^{a,c}
U	MTC-IPGAL	1:6	10.3	6
R	MTC-IPGAL	1:12	20.7	12
I	MTC-IPGAL	1:24	41.4	24
H	MTC-IPGLU	1:23	39.7	23

^a based on 1 mole bPEI-25 = 10000 g, containing 58 primary amine groups per mole.

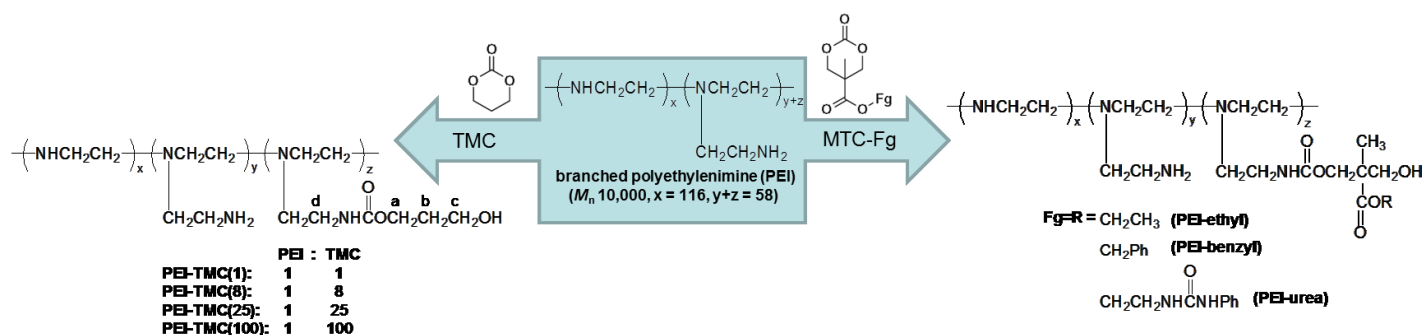
^b A value greater than 100% indicates reaction at all active primary amine sites, and reaction of secondary amine groups.

^c A number greater than 58 indicates reaction at all active primary amine sites, and reaction of secondary amine groups.

Moreover, the incorporation of hydrophobic groups has been suggested to increase polymer/DNA complex interaction with cell membrane and therefore enhance endocytosis of the complexes, which in turn leads to enhanced transfection efficiencies [236]. Commercially available trimethylene carbonate (TMC) was substituted onto PEI at various PEI:TMC ratios (1:1, 1:8, 1:25, and 1:100) to determine the optimum substitution ratio to achieve high transfection efficiency and minimal cytotoxicity.

Reaction of nucleophilic PEI with hydrophobic group functionalized cyclic carbonates was done only for 1 h under ambient conditions without using a catalyst or producing any by-products. The primary amines were converted into carbamate linkages and primary hydroxyl groups during the ring-opening event, while concurrently installing the functionality on the original cyclic carbonate [259, 260] (Scheme 2). The final polymer composition, or degree to which primary amines of PEI were substituted, was readily controlled by PEI:cyclic carbonate

feed ratios (Table 4a). Modification was monitored and quantified using ^1H NMR. For example, by comparing relative integral intensities of PEI methylene signals (2.4-2.9 ppm) and TMC methylene signals (1.83 ppm), the degree of TMC incorporation was determined (Figure 6). The obtained values from ^1H NMR experimentally matched the starting PEI:TMC feed ratio, suggesting the reaction was quantitative (Table 4b). This clean and controlled substitution reaction permitted a structural-functional relationship study between PEI polymer functionalization and resulting transfection capacity. It should be noted that when excess TMC relative to the PEI primary amines was used (PEI contains 58 primary, 116 secondary and 58 tertiary amines [261]), the secondary amines were also found to react with the cyclic carbonates, as in the case of modification with 100 TMC groups (Table 4b, TMC 1:100). With a similar approach, MTC-Ethyl, MTC-Benzyl and MTC-Urea were attached to PEI at a molar ratio of 1:25 (Table 2a).



Scheme 2. Single-step carbamate modification of branched PEI (PEI-TMC, PEI-Ethyl, PEI-Benzyl and PEI-Urea). Reproduced with permission from [149]. Copyright © 2013 WILEY-VCH Verlag GmbH & Co. KGaA, Weinheim.

Table 4. (a) Hydrophobic groups-PEI conjugates synthesized and used in this thesis.

Modified bPEI Name	Cyclic Monomer	Cyclic Monomer MW	Mass Feed Ratio (bPEI: Cyclic Monomer)	Molar Feed Ratio (bPEI: Cyclic Monomer)	Mol% Cyclic Monomer ^a	Used DBU?	Nitrogen Content (%)
V	TMC	102.1	100:1	1:1	1.7	No	16.3
P	TMC	102.1	12:1	1:8	13.7	No	25.92
K	TMC	102.1	4:1	1:25	43.1	No	30.0
J	TMC	102.1	1:1	1:100	172.4	No	32.2
O	MTC-Ethyl	188	2:1	1:25	43.1	No	22.12
aa	MTC-Benzyl	250.25	1.6:1	1:25	43.1	No	20.0
ab	MTC-Urea	322	1.2:1	1:25	43.1	No	18.0

^a moles cyclic monomer moles / primary amine groups x 100%.

(b) Summary of the NMR analysis of the hydrophobic groups-modified PEI (25 kDa) polymers.

Modified bPEI Name	Cyclic Carbonate	Mole Ratio Found (NMR) bPEI: Carbamate Groups ^a	% of bPEI Primary Amine Groups Modified (NMR) ^b	# of bPEI Primary Amine Groups Modified Per Mole bPEI ^{a,c}
V	TMC	1:1	1.7	1
P	TMC	1:7	12.1	7
J	TMC	1:109 ^a	187.9 ^b	109 ^c
K	TMC	1:27	46.6	27
O	MTC-Ethyl	1:27	46.6	27
aa	MTC-Benzyl	1:29	46.6	29
ab	MTC-Urea	1:27	46.6	27

^a based on 1 mole bPEI-25 = 10000 g, containing 58 primary amine groups per mole.

^b A value greater than 100% indicates reaction at all active primary amine sites, and reaction of secondary amine groups.

^c A number greater than 58 indicates reaction at all active primary amine sites, and reaction of secondary amine groups.

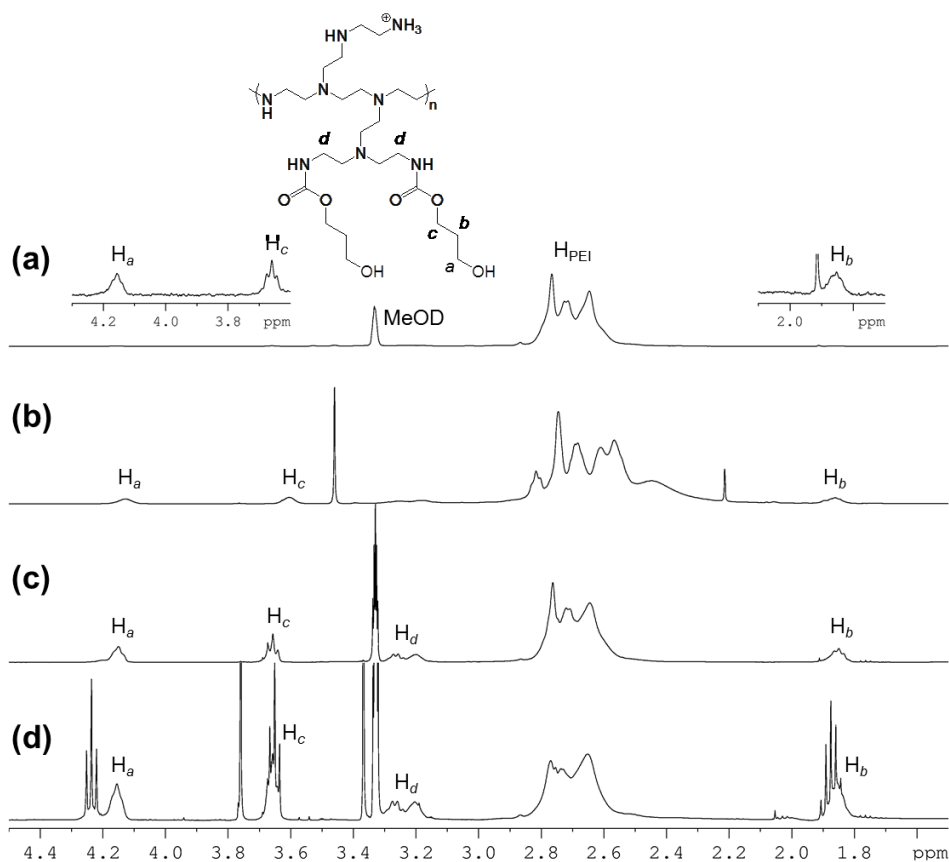


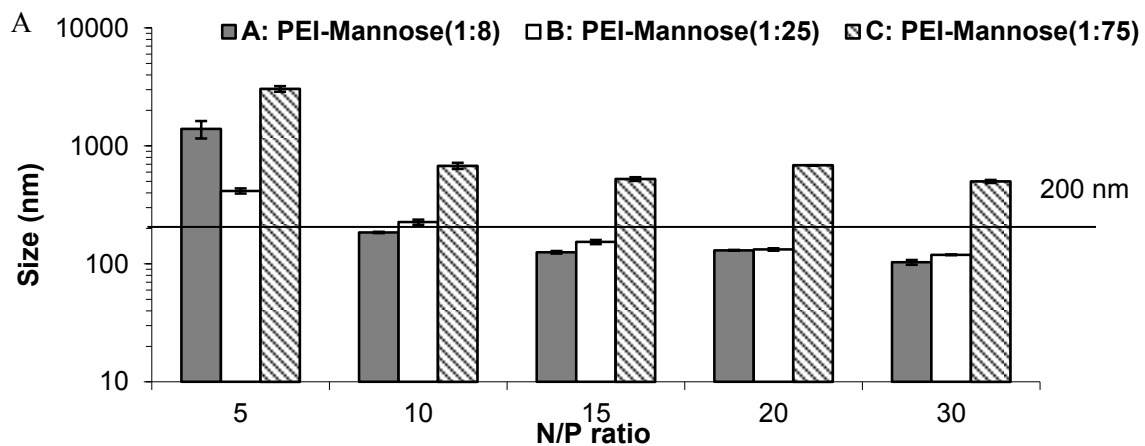
Figure 6. ^1H NMR spectra of PEI-TMC at conjugation degrees of 1, 8, 25 and 100 (a, b, c and d respectively) in MeOD.

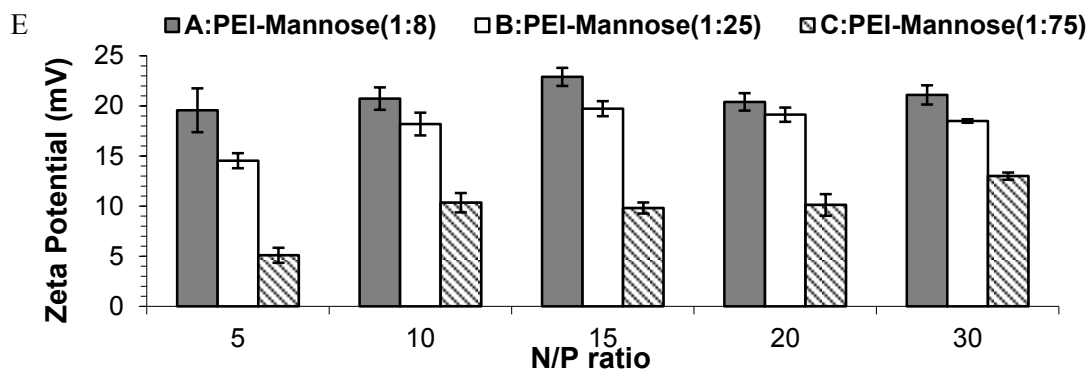
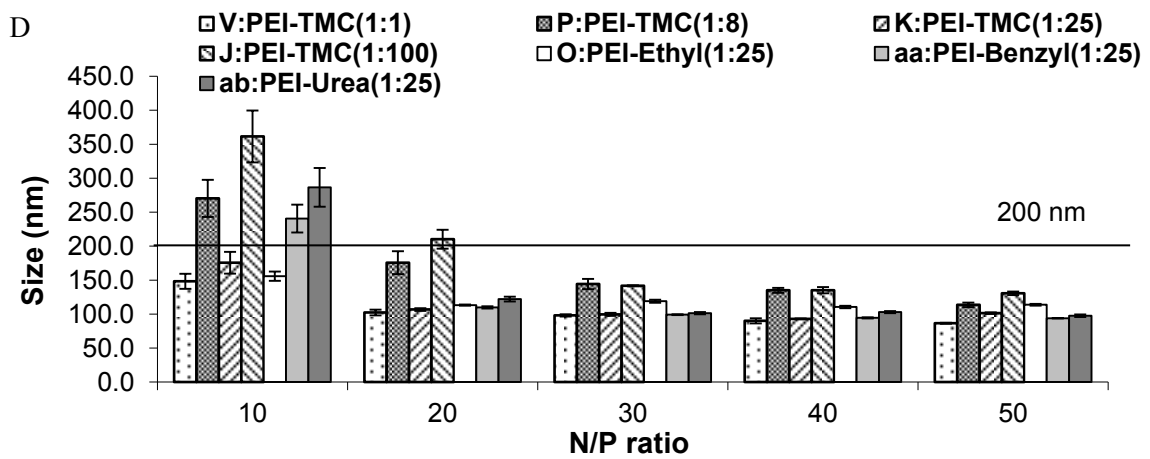
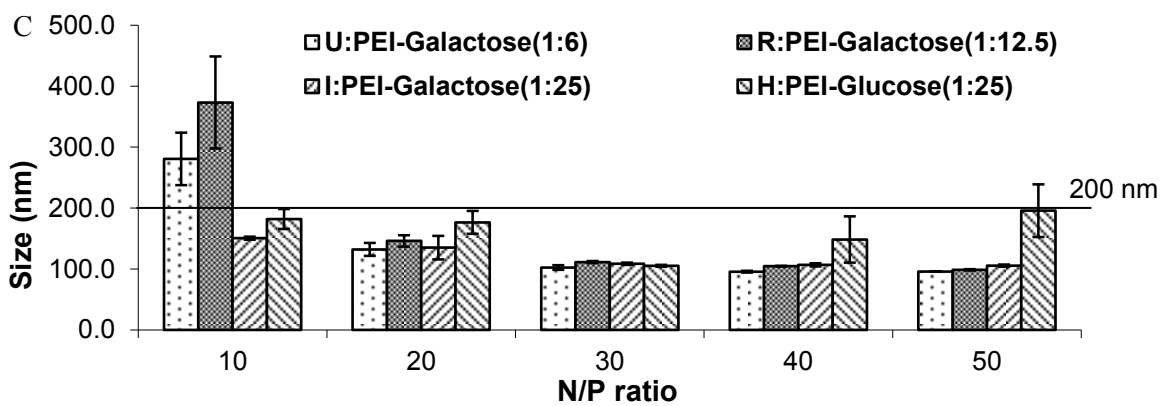
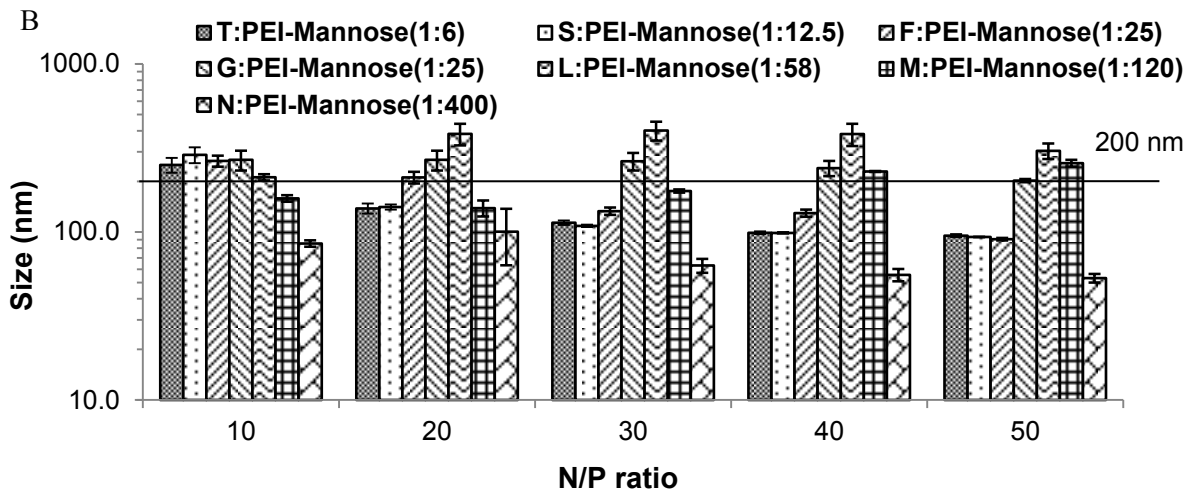
3.3.2 Size and zeta potential of polymer/DNA complexes

Traditionally, small size of nanoparticles within the nano-size range is desirable in drug and gene delivery, as small nanoparticles can take advantage of the presence of 100-200 nm fenestrations along the sinusoidal endothelial wall which permit the extravasation of nanoparticles less than 200 nm into the liver [262]. Moreover, in the case of carcinoma, passive accumulation of the nanoparticles less than 400-600 nm can occur in the tumor via the enhanced permeation and retention (EPR) effect that was first described by Matsumura and Maeda in 1986 [263]. In gene delivery application in this thesis, particle size is an important parameter for dictating cellular uptake by non-specific endocytosis [264]. And here, nanoparticle sizes under 200 nm are considered desirable properties (as indicated by the threshold lines in Figure 7A-D). As can be seen from Figure 7A-D, generally, the size of the DNA complexes decreased with increasing N/P ratio, indicating that stronger electrostatic interaction between the cationic polymer and anionic DNA enabled the formation of more compact complexes. This effect was more prominent in polymers **A**, **B**, **F**, **U**, **R**, **P**, **J**, **aa** and **ab**, whose sizes plunged from over 400 and 1000 nm at N/P 5 to 119 and 103 nm at N/P 30 for **A** and **B**, and from over 250, 280, 370, 270, 260, 240, and 280 nm at N/P 10 to 91, 96, 99, 113, 131, 94, and 98 nm at N/P 50 for **F**, **U**, **R**, **P**, **J**, **aa** and **ab**, respectively. Size of Polymer **G** decreased from 269 nm at N/P 10 to 202 nm at N/P 50, reaching the desired nano-size range. In each of the four graphs (Figure 7A-D), at most of the high N/P ratios, and under the same reaction conditions, the least amount of amine groups in **S/T**, **U** and **V** were used for functional carbonate modification, leading to stronger interactions between **S/T**, **U**, **V** and DNA and thus forming more compact DNA complexes as compared to other polymers. For example, polymer **V** produced the smallest DNA complexes (87 nm) among all the polymers. Polymer **C**, **L** and **M** did not complex DNA as effectively as other polymers, leading to large particles even at high N/P ratios (Figure 7A and B). The size distribution of the **A**/DNA, **B**/DNA, **S**/DNA, **T**/DNA, **F**/DNA, **G**/DNA, **L**/DNA, **U**/DNA, **R**/DNA, **I**/DNA, **H**/DNA, **V**/DNA, **P**/DNA, **J**/DNA, **K**/DNA, **O**/DNA, **aa**/DNA and **ab**/DNA complexes was found to be narrow with polydispersities of 0.178, 0.200, 0.168, 0.104, 0.129, 0.078, 0.150, 0.130, 0.120, 0.207, 0.209, 0.149, 0.075, 0.104, 0.097, 0.123, 0.071 and 0.110, respectively. However, the polydispersities of **M**/DNA and **N**/DNA complexes were large, which were above 0.4 and 0.7, respectively (PDI=0: ideally homogenous; PDI=1: completely heterogeneous). As a comparison, DNA complexes formed with unmodified PEI at N/P 10 also had a small size (84 nm) and low polydispersity (0.120).

The net positive charge of DNA complexes also has a crucial function of interacting with the negatively charged phospholipid surface of the cell membrane, therefore affecting cellular uptake as well as gene transfection efficiency [110]. From Figure 7E-H, **A/DNA**, **B/DNA**, **S/DNA**, **T/DNA**, **F/DNA**, and **G/DNA** complexes had a comparable cationic charge density on the surface at N/P 10-50 as compared to unmodified PEI/DNA complexes at N/P 10 (Zeta potential: ~20-26 mV for **A/DNA**, **B/DNA**, **S/DNA**, **T/DNA**, **F/DNA**, and **G/DNA** complexes and 22 mV for PEI/DNA complexes). **C/DNA**, **L/DNA**, **M/DNA** and **N/DNA** complexes had a significantly lower cationic charge density on the surface at the same N/P ratios (Zeta potential: ~5 to 13 mV for **C/DNA**, -11 to 2 mV for **L/DNA**, -14 to -8 mV for **M/DNA**, and -25 to -14 mV for **N/DNA** complexes). Therefore, given the big particle size and/or low zeta potential, polymer **C**, **L**, **M**, and **N** were expected to be less effective in gene transfection.

For polymers conjugated with galactose, glucose or hydrophobic groups (Figure 7G and H), the zeta potentials were between 7 and 20 mV at all N/P ratios, slightly lower than that of unmodified PEI at N/P ratio of 10 (22 mV). Because positively charged particles are prone to plasma protein and erythrocyte adhesion, which might cause alternative complement pathway activation, limiting *in vivo* applications [169], slightly lower zeta potentials demonstrated by these polymer/DNA complexes at N/P 10-50 were expected to exert less cytotoxicity as compared to the unmodified PEI.





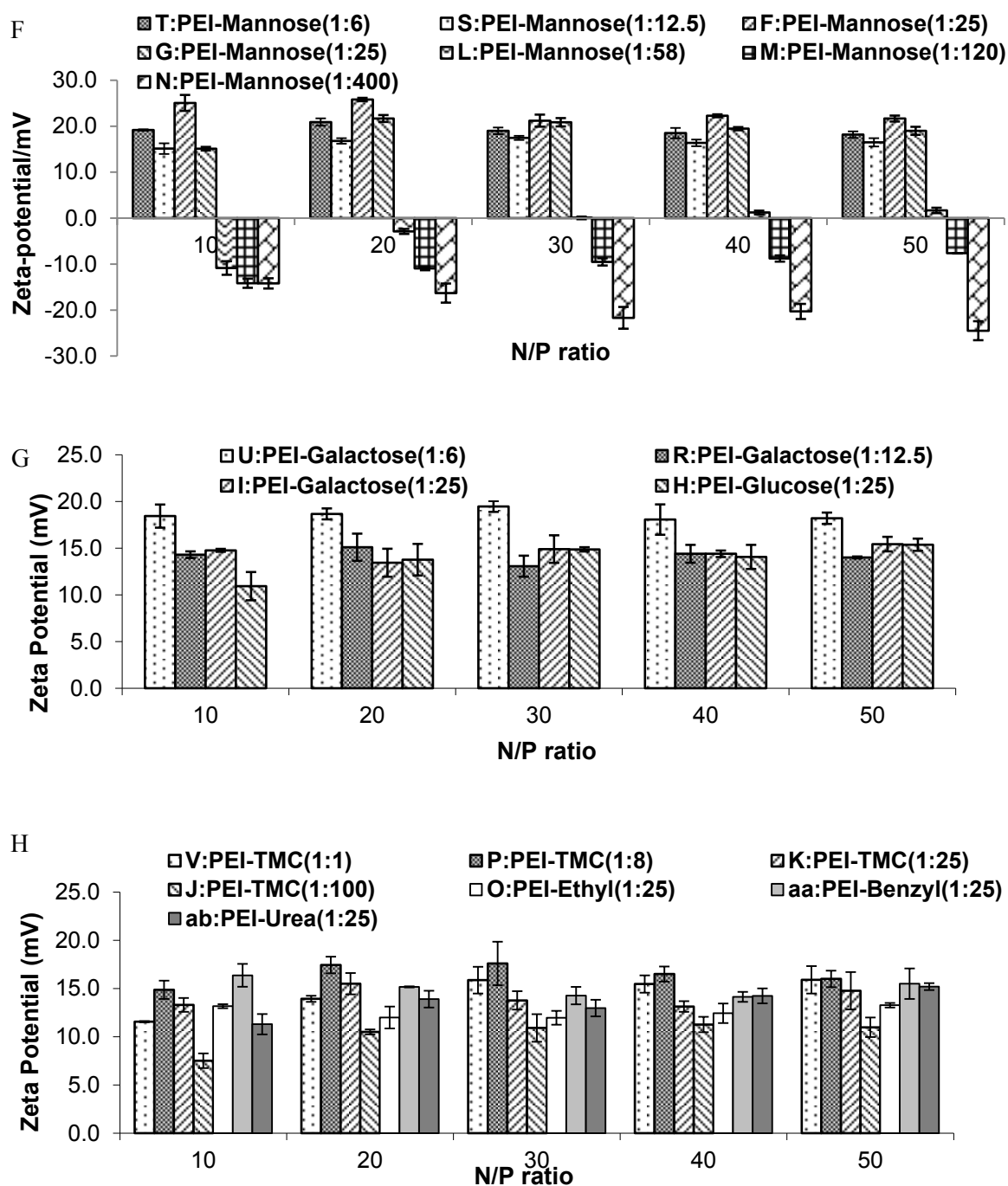
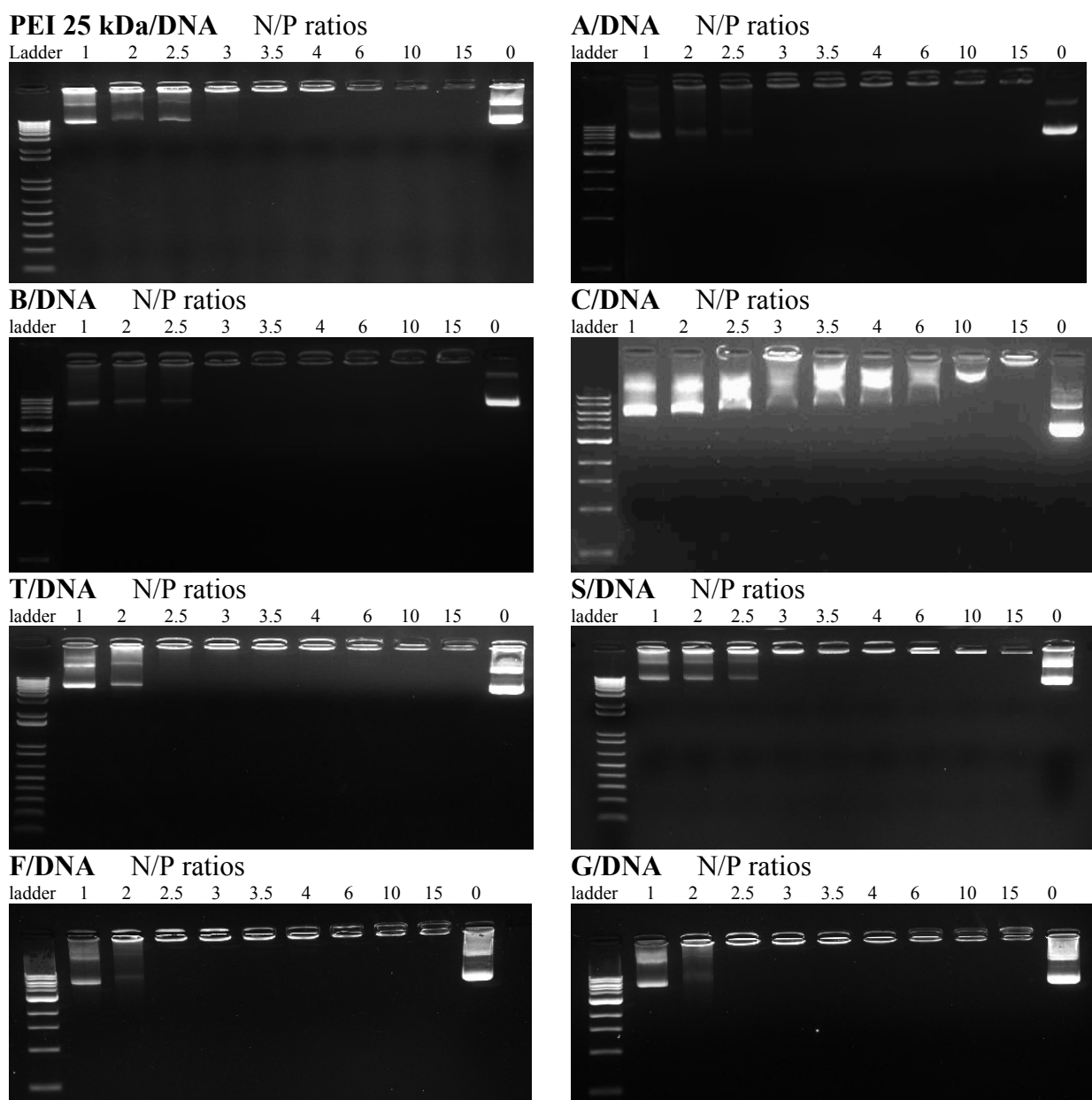


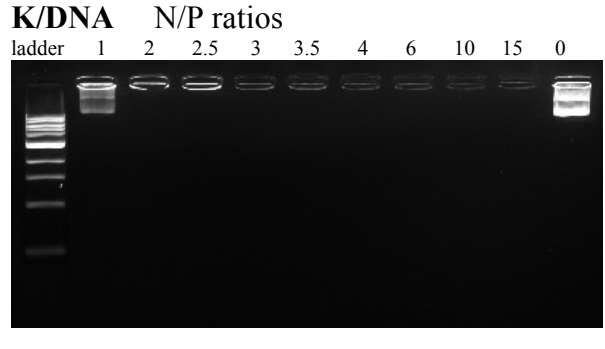
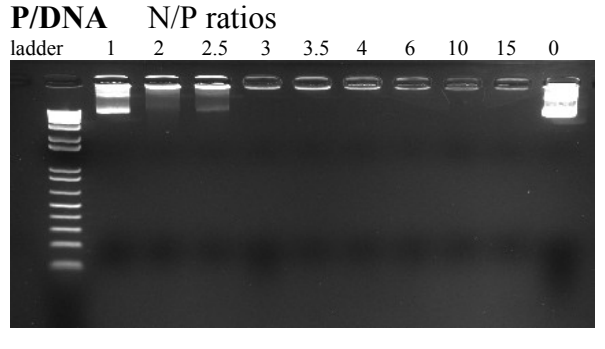
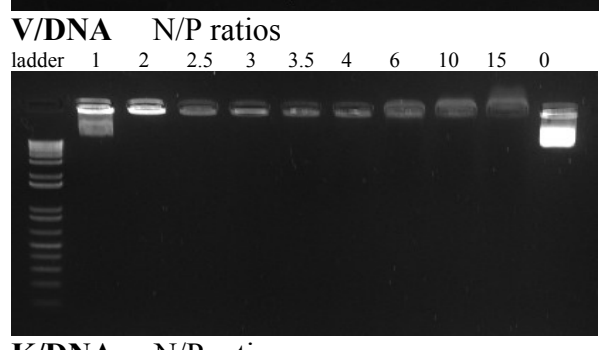
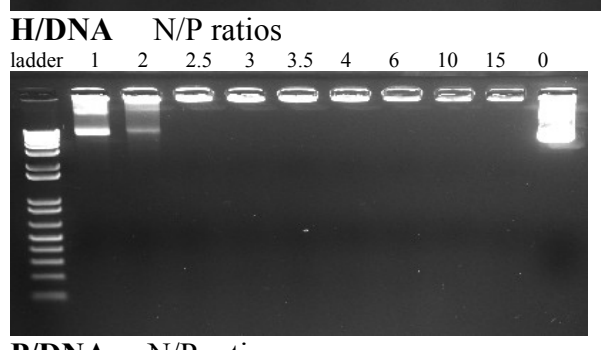
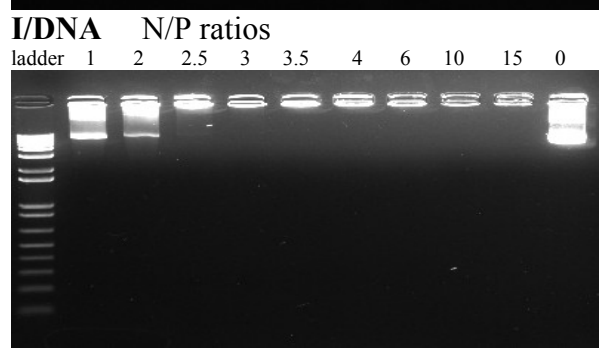
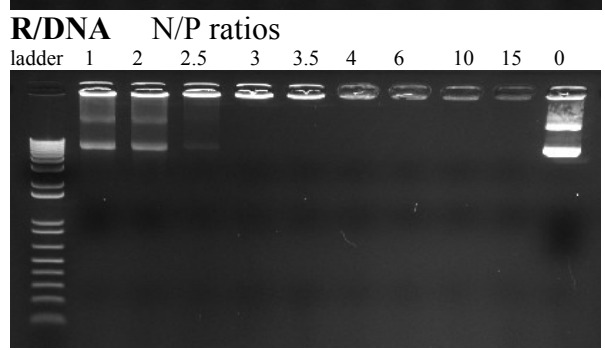
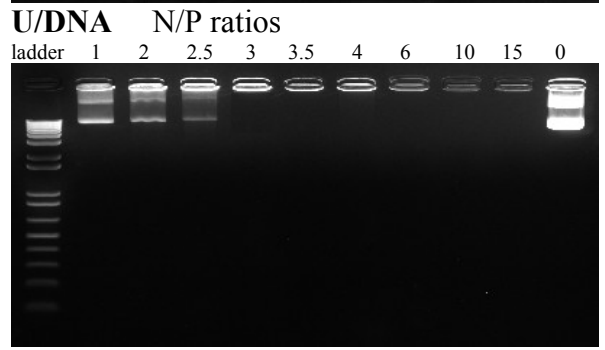
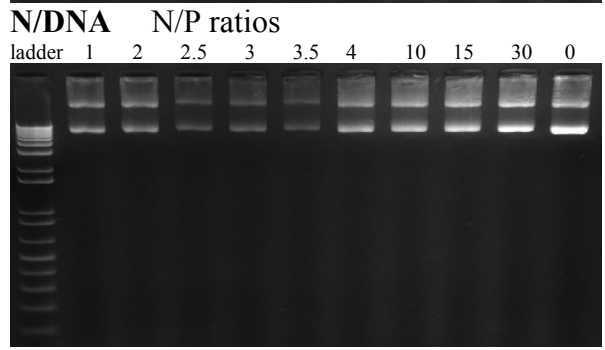
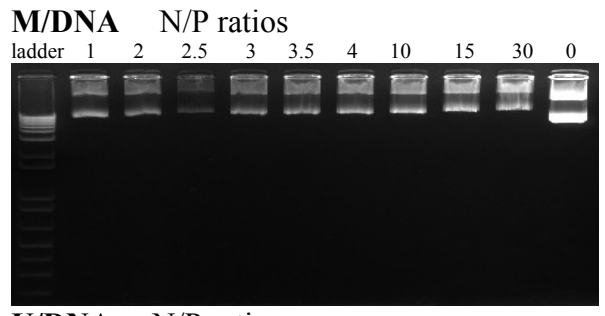
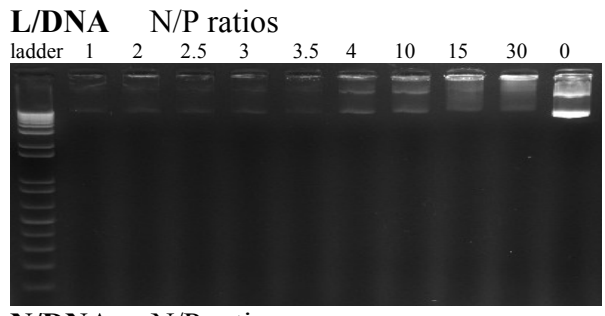
Figure 7. Particle size (A, B, C, D) and zeta-potential (E, F, G, H) of polymer/DNA complexes at various N/P ratios specified. Unmodified PEI(25k)/DNA complexes prepared at N/P ratio of 10 was used as a control, with a size of about 84 nm and a zeta potential of around 22 mV. Data were expressed as mean \pm standard deviations of triplicates.

3.3.3 DNA binding

The condensation of DNA by the polymers to form complexes of appropriate sizes and surface charges is an important requirement for gene delivery. Thus the DNA binding ability is an important parameter determining the efficiency of the polymeric gene delivery. DNA retardation assay was employed to assess the gene binding ability of the various functional

groups-modified PEIs, using the unmodified PEI as positive control. As shown in Figure 8, like the unmodified PEI, polymers **A**, **B**, **S**, **T**, **F**, **G**, **U**, **R**, **I**, **H**, **V**, **P**, **K**, **J**, **O**, **aa** and **ab** were able to effectively bind to and condense DNA. The complete retardation of DNA mobility in the complexes was observed at or below N/P 3 for the above mentioned polymers. On the contrary, **C**, **L**, **M** and **N** had poor DNA binding ability, and complete DNA binding was observed only at N/P 15 for **C**. Moreover, even at N/P 30, **L**, **M** and **N** could not bind to and condense DNA effectively. This was because in these polymers, more amine groups were consumed for carbonate-mannose attachment, leaving insufficient numbers of amines for DNA binding. Finally, as a gold standard, unmodified PEI (25 kDa) also enabled complete DNA binding from a fairly low N/P ratio (i.e. N/P 3) (Figure 8).





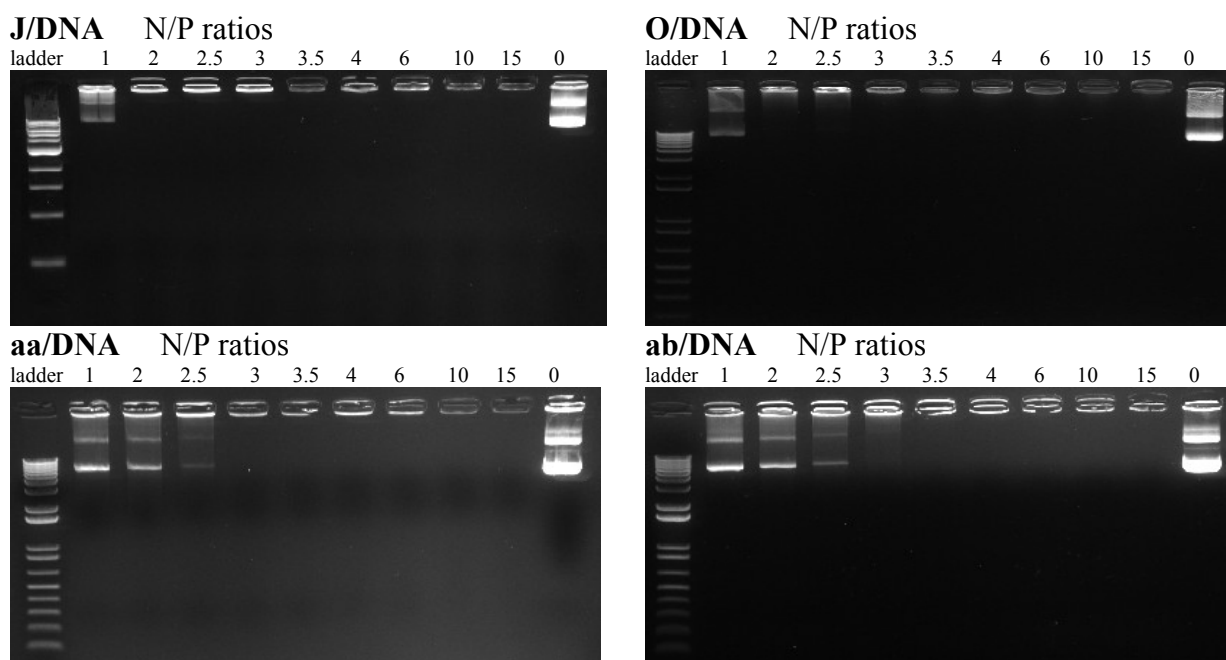


Figure 8. Electrophoretic mobility of DNA in polymer/DNA complexes.

Since the primary amines of PEI are protonated at physiological pH 7.4 to allow PEI to condense negatively charged DNA effectively into nano-sized complexes via electrostatic interactions, conjugating functional groups onto primary amines of PEI might have a negative impact on the gene binding efficiency of the modified PEI. In order to quantitatively investigate the relationship between the degree of PEI primary amine substitution and the amount of DNA bound to the polymer, the gene binding efficiency of TMC-modified PEIs (ratio from 1:1 to 1:100) was studied by measuring the fluorescence emitted by SYBR green dye when bound to free DNA [220]. For most polymers, the relative fluorescence emitted negatively correlated with the N/P ratio, indicating the inaccessibility of the dye to the condensed DNA (Figure 9). Substitution of PEI primary amines with an increasing number of TMC up to 25 slightly increased the IC_{50} value (N/P ratio at which the relative fluorescence is 50%) of the modified PEIs as compared to unmodified PEI (IC_{50} value: ~ 1.8 for PEI, ~ 2.1 for **V**:PEI-TMC(1:1) and **P**:PEI-TMC(1:8), and ~ 2.5 for **K**:PEI-TMC(1:25)), indicating marginally decreased gene binding capacity. In contrast, **J**:PEI-TMC(100) showed a drastic plunge in gene binding ability with an IC_{50} value of more than 10. The reason of this large IC_{50} value is most likely due to the complete blockage of the primary amines in **J**, which are required for DNA binding. Moreover, modification of PEI with cyclic carbonate monomers functionalized with other hydrophobic groups (ethyl, benzyl and urea) at ratio of 1:25 (Figure 9) also increased the IC_{50} values to some extent (~ 2.8 vs. ~ 1.8 for PEI).

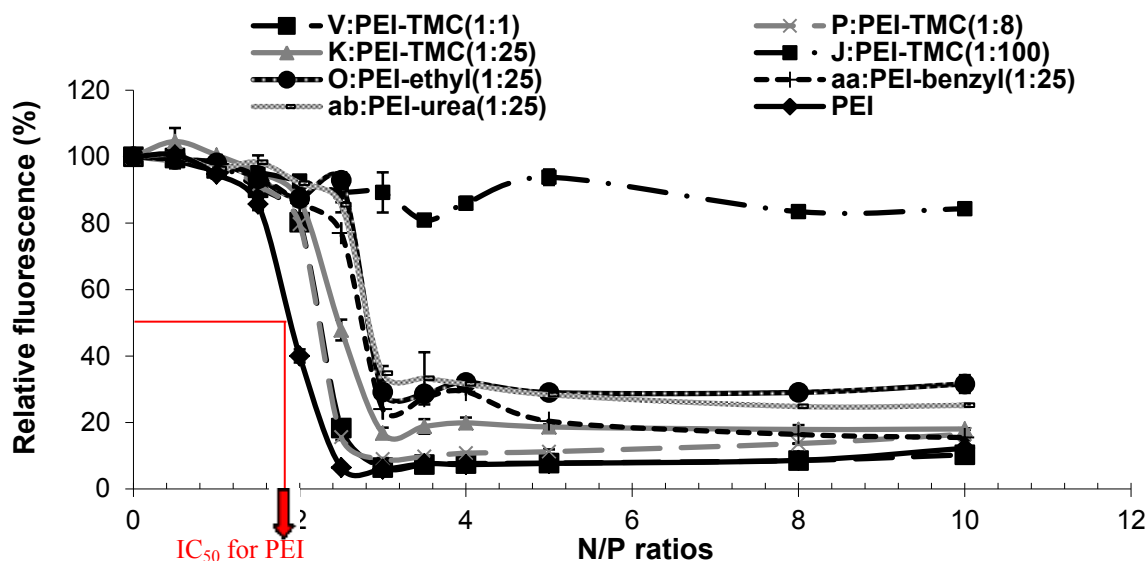


Figure 9. DNA binding analyzed as a decrease in fluorescence of SYBR green dye added to polymer/DNA complexes. A relative fluorescence of 100 represents the fluorescence of SYBR green intercalated with uncomplexed DNA, while 0 corresponds to the fluorescence of non-intercalating SYBR green dye. Data were expressed as mean \pm standard deviations of triplicates. Reproduced with permission from [150], Copyright © 2013 WILEY-VCH Verlag GmbH & Co. KGaA, Weinheim.

3.3.4 *In vitro* GFP gene expression in various cell lines

To assess the suitability of these polymers as gene delivery vectors, *in vitro* GFP and luciferase gene transfection and expression assays were performed in various cell lines: HepG2 (human hepatocellular carcinoma cell line), HeLa (human cervical epithelial cancer cell line), NIH-3T3 (mouse fibroblast cell line), MCF-7 (human breast cancer cell line), 4T1 (mouse breast cancer cell line), HMSC (human mesenchymal stem cell), and keratinocytes (epidermal cell line). In this section we will first present GFP transfection efficiencies achieved by the various polymers. GFP transfection efficiency reflects the percentage of transfected cells. For most gene therapy cases, it is important for gene carriers to transfect a high percentage of cells such that a large number of cells incorporate the therapeutic gene.

3.3.4.1 *In vitro* GFP gene expression in HepG2

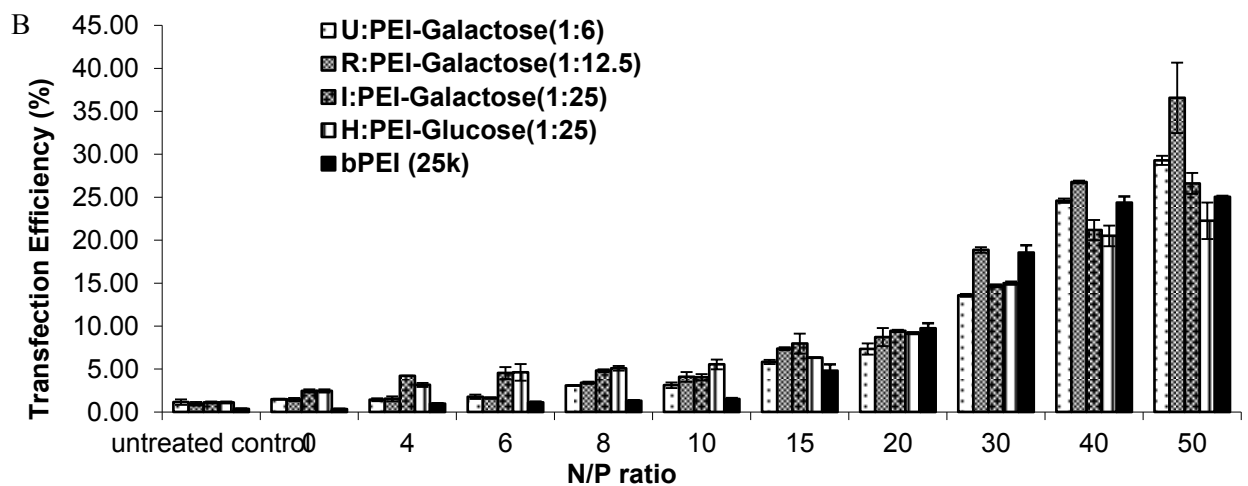
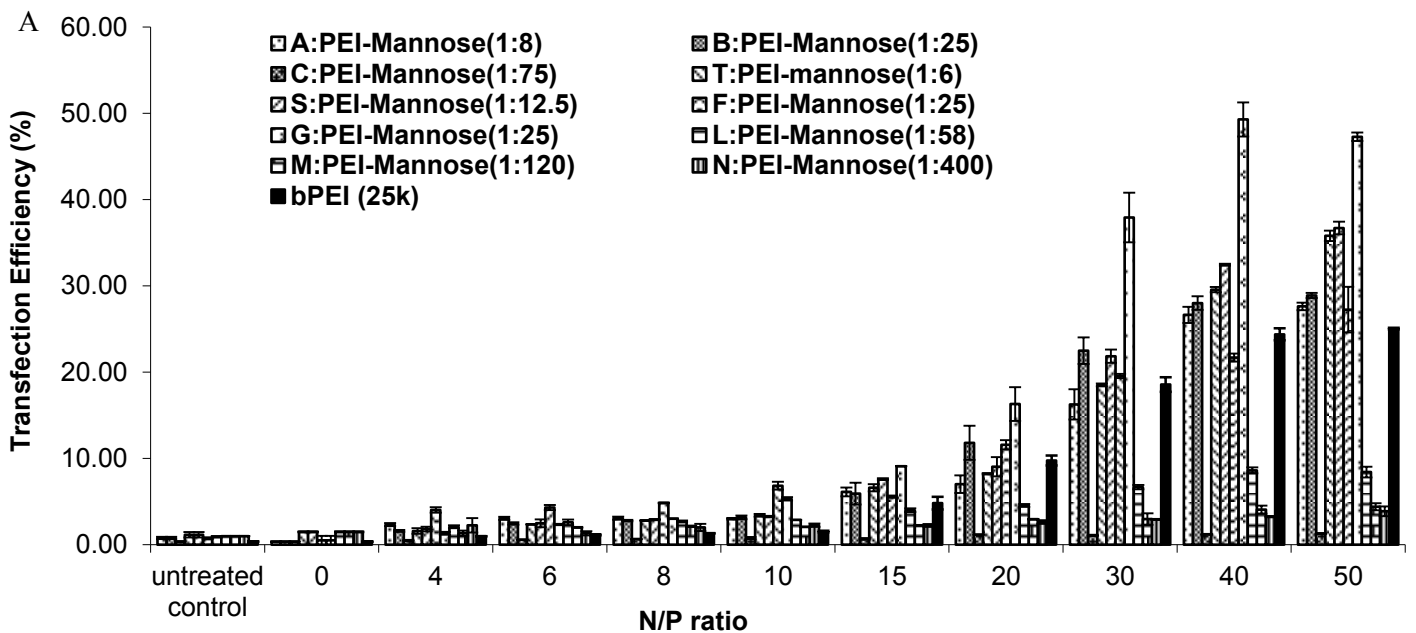
As shown in Figure 10, the polymers mediated high GFP expression in the presence of serum proteins in a polymer- and N/P ratio-dependent manner. Generally, increasing N/P ratio led to higher transfection efficiency. For HepG2 cells, unmodified PEI/DNA transfected 4.8% of the cells with GFP gene at N/P 15, and its transfection efficiency reached a plateau of about 25% at N/P 40 and 50. For the mannose-modified PEIs (Figure 10A), as expected, C/DNA, L/DNA, M/DNA and N/DNA complexes gave much lower transfection efficiency than

unmodified PEI/DNA complexes due to their large particle size with huge size distribution and low cationic charge density on the surface (Figure 7). However, **A** and **B** with fewer amine groups used for MTC-mannose attachment were promising with transfection efficiency comparable to that of unmodified PEI at N/P ratios below 30, but greater than that of unmodified PEI at N/P 30-50. In addition, among all mannose-modified polymers, **S**, **T** and **G** were the best, demonstrating higher transfection efficiency than unmodified PEI at all N/P ratios tested, with the highest value reaching 37%, 36% and 47% at N/P 50, respectively (Figure 10A).

For the glucose and galactose conjugated PEI, polymer **R**:PEI-Galactose(1:12.5) achieved the highest transfection efficiency at N/P 50, which was 37%, compared to polymers **U**:PEI-Galactose(1:6) (30%), **I**:PEI-Galactose(1:25) (27%), and **H**:PEI-Glucose(1:25) (22%), whose transfection efficiencies were comparable to that of the unmodified PEI at N/P 50 (25%) (Figure 10B).

Hydrophobic groups greatly enhanced the transfection efficiency of PEI 25 kDa in HepG2 cells. PEI modified with TMC at different ratios were first used to determine the optimal carbamate functionalization for gene transfection (Figure 10C). It was found that 1:25 was the optimal PEI:cyclic carbonate ratio in terms of GFP transfection efficiency. Polymer **K**:PEI-TMC(1:25), whose transfection efficiency at N/P 50 reached 64%, currently was the highest value achieved among all the polymers in HepG2 cells, which was 5.5-fold higher than that of the unmodified PEI at N/P 20. Also, polymer **P**:PEI-TMC(1:8) had very high transfection efficiency, reaching 35% at N/P 50. Polymer **J**:PEI-TMC(1:100) and **V**:PEI-TMC(1:1) had comparable GFP transfection efficiency (22-26%) with unmodified PEI at N/P 50 (Figure 10C). When this optimized PEI:cyclic carbonate ratio was applied to the modification of PEI with various substituted hydrophobic carbonates, despite the additional hydrophobicity (PEI-ethyl, PEI-benzyl, PEI-urea), and hydrogen bonding capacity provided by urea groups (PEI-urea) [265, 266], PEI functionalized with commercially available TMC proved to be the most effective gene delivery vector (Figure 10D). Polymer **O**:PEI-Ethyl(1:25) also had very high transfection efficiency, reaching 48% at N/P 50, making it the second best in GFP gene transfection among the hydrophobic-groups modified PEI polymers. On the contrary, benzyl and urea conjugation onto PEI only provided a marginal improvement in gene transfection efficiency at N/P 40-50 as compared to unmodified PEI at N/P 20, probably because their hydrophobicity was too high [236]. A similar phenomenon was also observed by

Jia et al. that modification by benzyloxyl trimethylene carbonate (conducted at 70°C for 48 h) did not improve gene transfection efficiency in HepG2 cells significantly [267]. Although the exact mechanism of hydrophobic groups such as TMC and ethyl contributing to increased transfection efficiency is not clear, it was suggested that they favorably modulated the polymer/DNA complexes action with or within cells, such as cell membrane adsorption and cellular uptake, as well as aided in the dissociation of the polymer-DNA complex and subsequent release of DNA, which otherwise would be strongly bound through ionic interactions on the cationic polymers [268]. These favorable features contributed by the hydrophobic modification may result in higher transfection efficiency than polymers depending solely on electrostatic interactions to complex and deliver DNA.



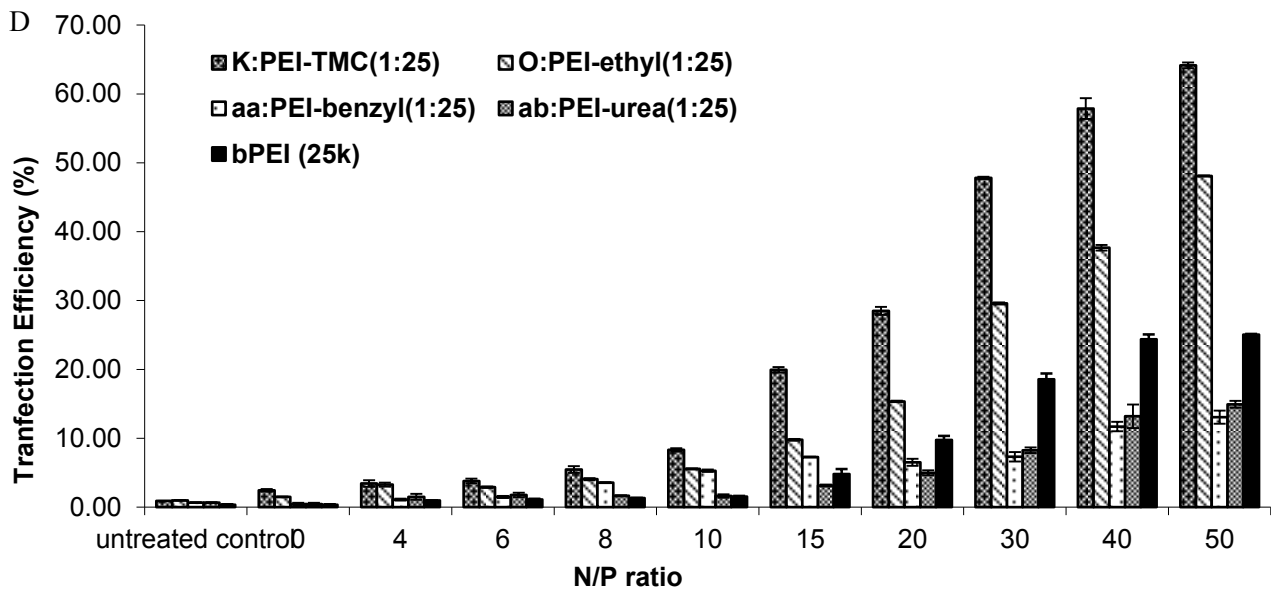
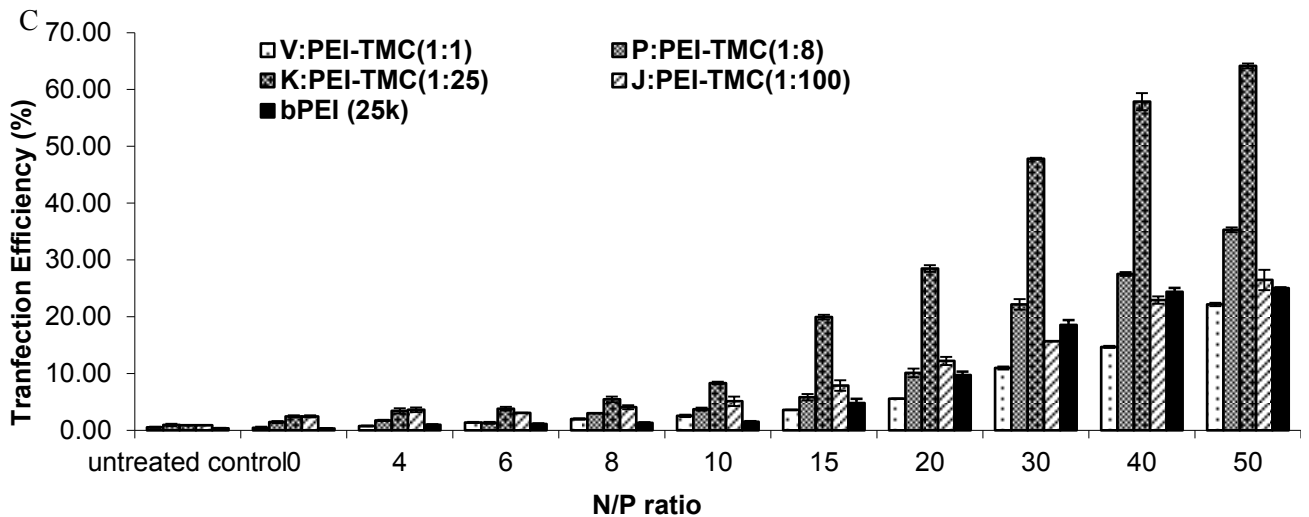
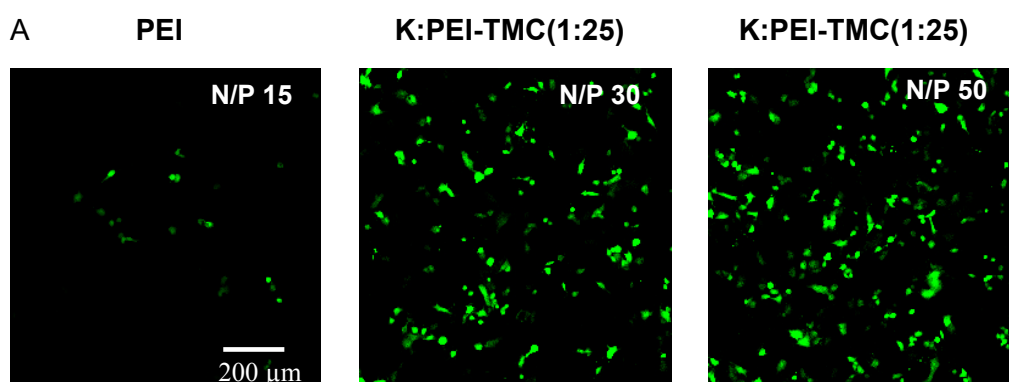


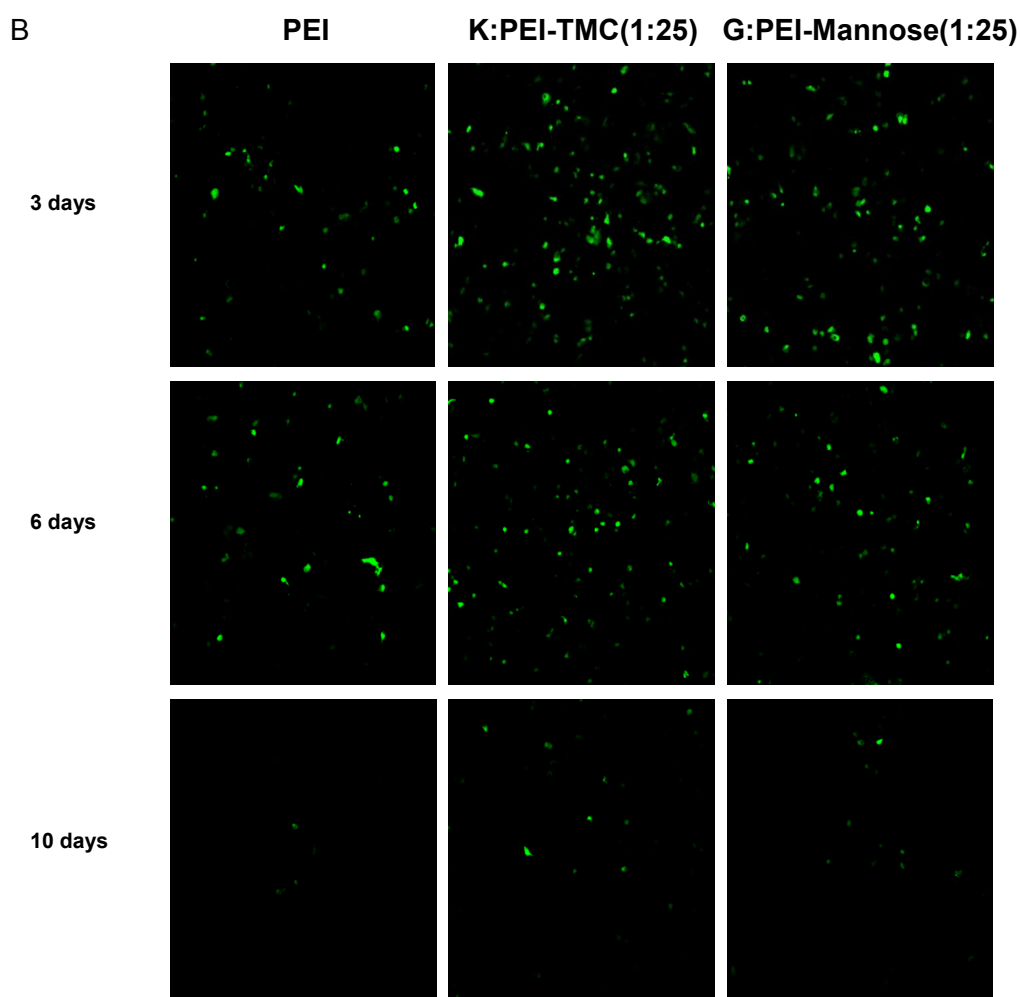
Figure 10. *In vitro* GFP gene transfection efficiency in HepG2 cells mediated by the various polymers at various N/P ratios indicated. Results represent mean \pm standard deviation of triplicates. Polymer concentrations in the order of N/P ratios specified: unmodified PEI - 0, 1.6, 2.4, 3.2, 4.0, 6.0, 8.0, 12.0, 16.0 and 20.0 mg/L. **A** - 0, 2.2, 3.3, 4.4, 5.5, 8.2, 11.0, 16.4, 21.9 and 27.4 mg/L. **B, F, G, H, I, J** - 0, 3.3, 4.9, 6.6, 8.2, 12.3, 16.4, 24.6, 32.8 and 41.0 mg/L. **C** - 0, 6.6, 9.9, 13.1, 16.4, 24.6, 32.8, 49.3, 65.7 and 82.1 mg/L. **K** - 0, 2.1, 3.1, 4.1, 5.2, 7.7, 10.3, 15.5, 20.6 and 25.8 mg/L. **L** - 0, 4.4, 6.7, 8.9, 11.1, 16.7, 22.2, 33.3, 44.4, and 55.5 mg/L. **M** - 0, 9.5, 14.3, 19.1, 23.9, 35.8, 47.7, 71.6, 95.5, and 119.3 mg/L. **N** - 0, 28.1, 42.2, 56.3, 70.3, 105.5, 140.7, 211.0, 281.3, and 351.7 mg/L. **T, U** - 0, 2.0, 3.1, 4.1, 5.1, 7.7, 10.2, 15.3, 20.4, and 25.5 mg/L. **R, S** - 0, 2.5, 3.7, 4.9, 6.2, 9.2, 12.3, 18.5, 24.6, and 30.8 mg/L. **V** - 0, 1.7, 2.5, 3.3, 4.2, 6.2, 8.3, 12.5, 16.6, and 20.8 mg/L. **P** - 0, 1.8, 2.7, 3.6, 4.5, 6.7, 8.9, 13.4, 17.8, and 22.3 mg/L. **O** - 0, 2.4, 3.6, 4.8, 6.0, 9.1, 12.1, 18.1, 24.2, and 30.2 mg/L.

3.3.4.1.1 Confocal imaging of GFP gene expression in HepG2

Confocal images of HepG2 cells transfected with GFP DNA plasmid by **K**:PEI-TMC(1:25) after 3 days were consistent with the flow cytometry data. This result further showed that TMC-modified PEI at the optimal conjugation ratio (1:25) mediated efficient GFP gene transfection of HepG2 cells, and yielded a larger number of cells transfected with green fluorescent GFP gene, at N/P 30 and 50, compared to the unmodified PEI at N/P 15 (Figure 11 A).

In addition, as expected, the expression of the GFP gene transfected by the non-viral polymers (carbamate modified PEIs) into the HepG2 cells was only transient, as the plasmids were not integrated into the HepG2 cell genome, but rather, they were gradually diluted and lost from generation to generation during cell division over time [269]. In order to test the duration of the gene expression, two of the best modified PEIs achieving high transfection efficiency in HepG2 cells were selected: **G**:PEI-Mannose (1:25) in the sugar modification group, and **K**:PEI-TMC(1:25) in the hydrophobic-group modification group. After using these two polymers to transfect GFP gene into HepG2 cells at N/P 50, with PEI (N/P 15) as a control, confocal images were taken at 3, 6, and 10 days after gene transfection to monitor the expression profiles over time. As shown in Figure 11B, the peak of gene expression was at 3 days, and then the expression lasted until 6 days but slowly went off at 10 days. The same trend was observed for all the three polymers tested. These results provided guidance for the approximate effective time frame of the cargo gene expression after delivered by the modified PEIs, and might be useful for designing the gene delivery regime in preclinical/clinical trials in the future.





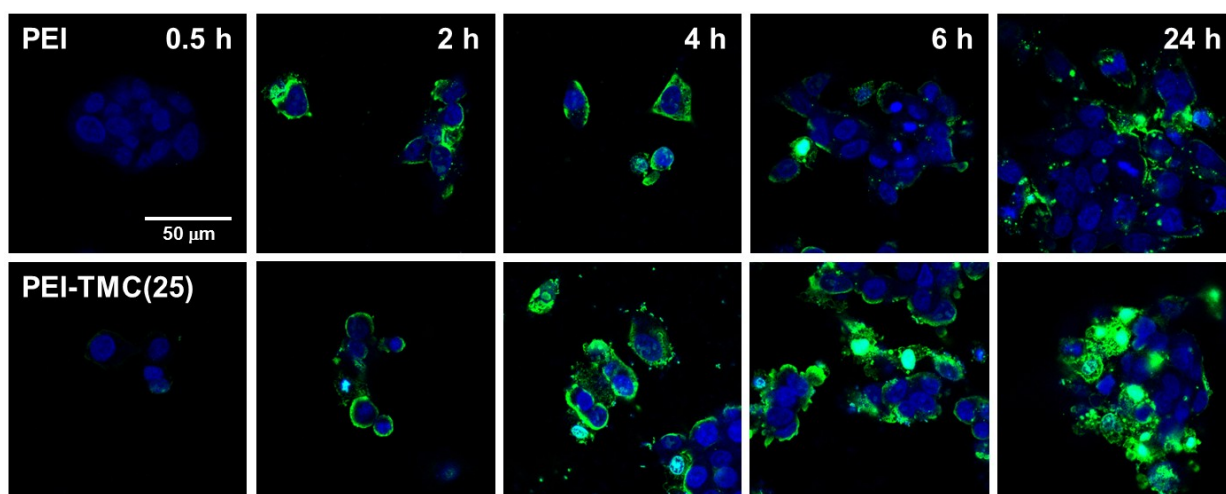
Green: GFP protein expressed from GFP plasmid transfected into the cells

Figure 11. (A) Confocal images of HepG2 cells after incubation with unmodified or modified PEI/DNA complexes formed at various N/P ratios. N/P 15 was used to form PEI/DNA complexes as they were highly toxic at N/P 20-50. Carbamate modifications, especially TMC at PEI:TMC molar ratio of 1:25, increased gene transfection efficiency tremendously. (B) GFP gene delivered by the polymers could be expressed in HepG2 cells over a time of 6 days, however the expression diminished to very low level at day 10 after transfection.

3.3.4.1.2 Intracellular trafficking of polymer/DNA complexes in HepG2

In order to investigate the possible mechanism behind the drastically boosted GFP transfection efficiency provided by TMC modification of PEI at the ratio of 1:25, intracellular trafficking of the polymer/DNA complexes was monitored by confocal microscopy over a 24 h period. Prior to complex formation, the DNA was tagged with YOYO-1, a fluorescent DNA intercalator, which enabled real-time visualization and tracking of DNA localization within HepG2 cells. As is shown in Figure 12, after 2 h of incubation, DNA (green) delivered by both PEI and K:PEI-TMC(1:25) have entered the HepG2 cells but remained in the cytoplasmic region. At 4 h, more DNA was observed to accumulate around the nuclei for both polymer

treated cells. At 6 h, DNA was obvious and abundant in both the cytoplasm and the nuclei (cyan regions in blue-colored Hoechst-stained nuclei) of the cells incubated with **K**:PEI-TMC(1:25) as compared to those incubated with unmodified PEI. Moreover, at 24 h, almost 50% of the cells treated with **K**:PEI-TMC(1:25)/DNA complexes showed DNA accumulation in the nuclei, whereas most of DNA molecules were still trapped in the peri-nuclear region of the cells treated with PEI/DNA complexes, and the amount of DNA entered the PEI treated cells was far less than in those treated by **K**:PEI-TMC(1:25). This result suggested that in contrast to unmodified PEI, **K**:PEI-TMC(1:25) provided more nuclear localization and better cell trafficking kinetics. It was postulated that weaker DNA binding of **K**:PEI-TMC(1:25) (Figure 9) led to more facile intracellular release of DNA allowing it to travel more easily to the nuclei. Furthermore, increased vector hydrophobicity by TMC attachment caused more favorable plasma membrane and nuclear envelope interactions, hence enhancing gene transfection efficiency (Figure 10D).



Blue: Hoechst dye stained nuclei

Green: YOYO-1 dye attached to luciferase plasmid transfected into the cells

Figure 12. Cellular trafficking of DNA. HepG2 cells were treated with unmodified PEI or TMC modified PEI (1:25)/DNA complexes formed at N/P 50. Blue: Hoechst stained nuclei; Green: DNA with YOYO-1 dye. **K**:PEI-TMC(1:25) provided higher nuclear localization and faster cell trafficking kinetics of DNA as compared to unmodified PEI. Reproduced with permission from [150], Copyright © 2013 WILEY-VCH Verlag GmbH & Co. KGaA, Weinheim.

3.3.4.2. *In vitro* GFP gene expression in other cell lines

Based on the GFP gene transfection efficiency in HepG2 cells, the following eight polymers giving comparable or higher transfection efficiency than the unmodified PEI were selected and their gene transfection capacities were further tested in other cell lines: **A**:PEI-Mannose(1:8) (synthesized with DBU), **B**:PEI-Mannose(1:25) (synthesized with DBU), **T**:PEI-

Mannose(1:6) (without DBU), **S**:PEI-Mannose(1:12.5) (without DBU), **F**:PEI-Mannose(1:25) (reaction 18 h without DBU), **G**:PEI-Mannose(1:25) (reaction 1 h without DBU), **K**:PEI-TMC(1:25) (without DBU), and **O**:PEI-ethyl(1:25) (without DBU).

The mannose-modified PEIs (**A**, **B**, **F** and **G**) were tested in HeLa cells for their GFP gene transfection efficiency over three days, using PEI as a positive control and polymer **C**:PEI-Mannose(1:75) as a negative control. **F** gave the highest gene transfection efficiency of 6.9% at N/P 50 among all mannose-modified PEIs tested (Figure 13). Although unmodified PEI yielded higher gene transfection efficiency (8.6%), it was much more cytotoxic than **F** at N/P ratio of 50 (to be shown in the cytotoxicity studies in Section 3.3.6.1). At comparable cell viability, unmodified PEI gave much lower transfection efficiency (< 2% at N/P 20) (Figure 13). Moreover, surprisingly, polymer **G** which achieved the highest transfection in HepG2 cells showed lower GFP transfection efficiency compared to other mannose polymers in HeLa cells (2.8% at N/P 50 for **G**), suggesting that the transfection efficiency achieved using a transfection reagent varies depending on the cell type being transfected and the transfection conditions used. Therefore, the best transfection reagent and conditions for a particular cell type must be empirically and systematically determined because inherent properties of the cell influence the success of any specific transfection method [270, 271].

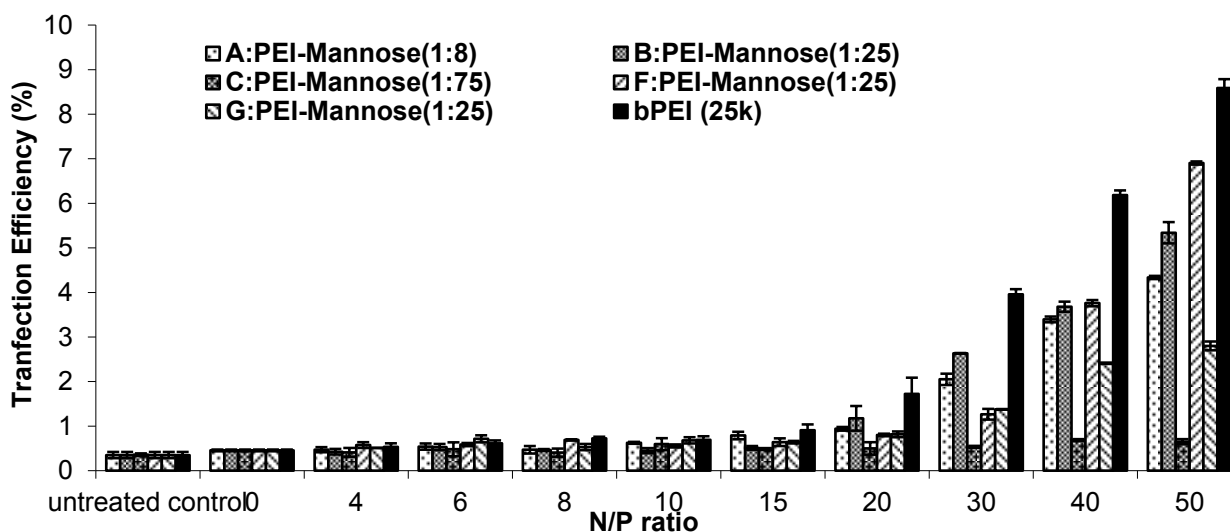


Figure 13. *In vitro* GFP gene transfection efficiency in HeLa cells mediated by polymers at various N/P ratios indicated. Results represent mean \pm standard deviation of triplicates. Polymer concentrations in the order of N/P ratios specified: unmodified PEI - 0, 1.6, 2.4, 3.2, 4.0, 6.0, 8.0, 12.0, 16.0 and 20.0 mg/L. **A** - 0, 2.2, 3.3, 4.4, 5.5, 8.2, 11.0, 16.4, 21.9 and 27.4 mg/L. **B**, **F**, **G** - 0, 3.3, 4.9, 6.6, 8.2, 12.3, 16.4, 24.6, 32.8 and 41.0 mg/L. **C** - 0, 6.6, 9.9, 13.1, 16.4, 24.6, 32.8, 49.3, 65.7 and 82.1 mg/L.

Moreover, polymers **T**, **S**, and **G** were proven highly effective in transfecting GFP gene to the mouse embryonic fibroblast cell line NIH3T3, especially polymer **G**:PEI-Mannose(1:25), whose transfection efficiencies from N/P 20-50 were much higher than those of **T**:PEI-Mannose(1:6) and **S**:PEI-Mannose(1:12.5). It even achieved 89% transfection efficiency at N/P 100, equivalent to that of polymer **T** (Figure 14). Although the unmodified PEI had the highest transfection efficiency among the four polymers tested, especially from N/P 50-100, its high cytotoxicity (to be described in Section 3.3.6.1) compromised its potential clinical application.

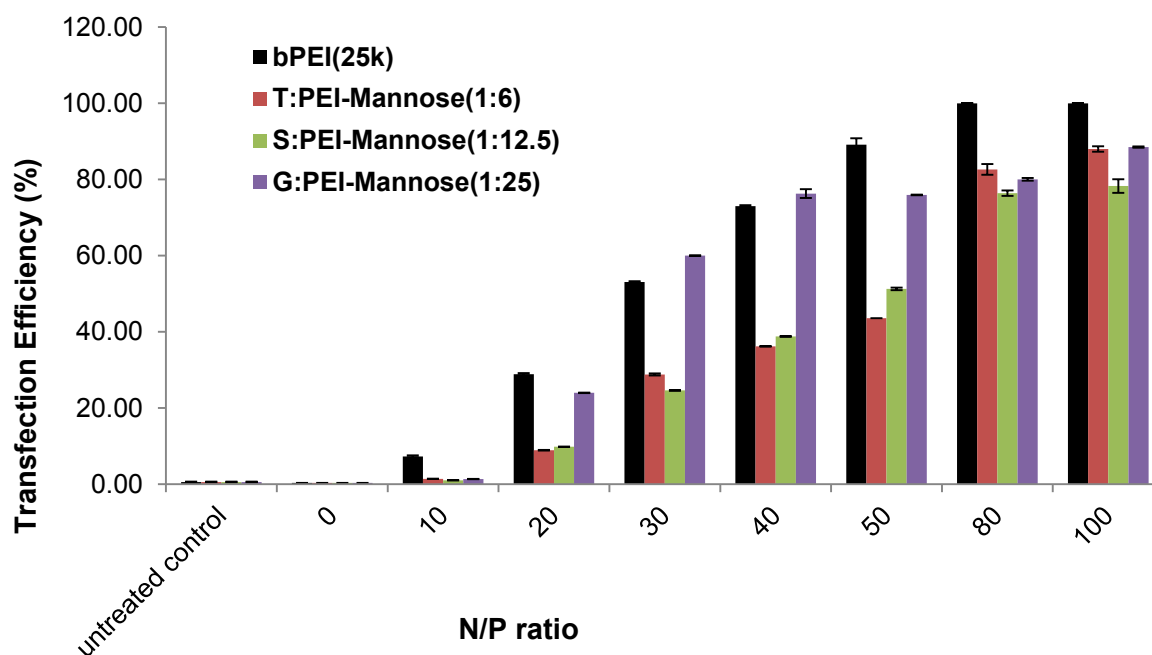


Figure 14. *In vitro* GFP gene transfection efficiency in NIH3T3 cells mediated by polymers at various N/P ratios indicated. Results represent mean \pm standard deviation of triplicates. Polymer concentrations in the order of N/P ratios specified: unmodified PEI - 0, 4.0, 8.0, 12.0, 16.0, 20.0, 32.1, and 40.1 mg/L. T - 0, 5.1, 10.2, 15.3, 20.4, 25.5, 40.8, and 51.0 mg/L. S - 0, 6.2, 12.3, 18.5, 24.6, 30.8, 49.3, and 61.6mg/L. G - 0, 8.2, 16.4, 24.6, 32.8, 41.0, 65.6, and 82.0 mg/L.

In addition, polymers **T**, **S**, **G**, **K** and **O** were tested on MCF7 (human breast cancer) and 4T1 (mouse breast cancer) cells. For MCF7 cells, as can be seen in Figure 15A, except unmodified PEI, polymer **K**:PEI-TMC(1:25) achieved the second highest transfection efficiency (65% vs. 75% for PEI), while the three mannose modified PEIs (**T**, **S**, **G**) showed comparable transfection efficiency of around 45%, at N/P 50. Ethyl modified PEI only made 26% of the MCF7 GFP positive at the highest N/P ratio tested (N/P 50). However, in 4T1 cells, polymer **O**:PEI-ethyl(1:25) was the best polymer, achieving 34% transfection efficiency at N/P 100, which surpassed that of the unmodified PEI (30%). Additionally, in 4T1 cells, the mannose attachment ratio showed an inversed relationship with their transfection efficiency (**T**:

22%, S: 17% and G: 13%) (Figure 15B), which was on the contrary to the relationship between mannose conjugation degrees and transfection efficiencies achieved in HepG2 (T: 36%, S: 37% and G: 47%) (Figure 10A). The different performance of polymers in different cell lines again suggested that to select the best polymer to transfect therapeutic genes in a certain cell line, testing of the transfection efficiency of the selected polymers using a reporter plasmid first was absolutely necessary.

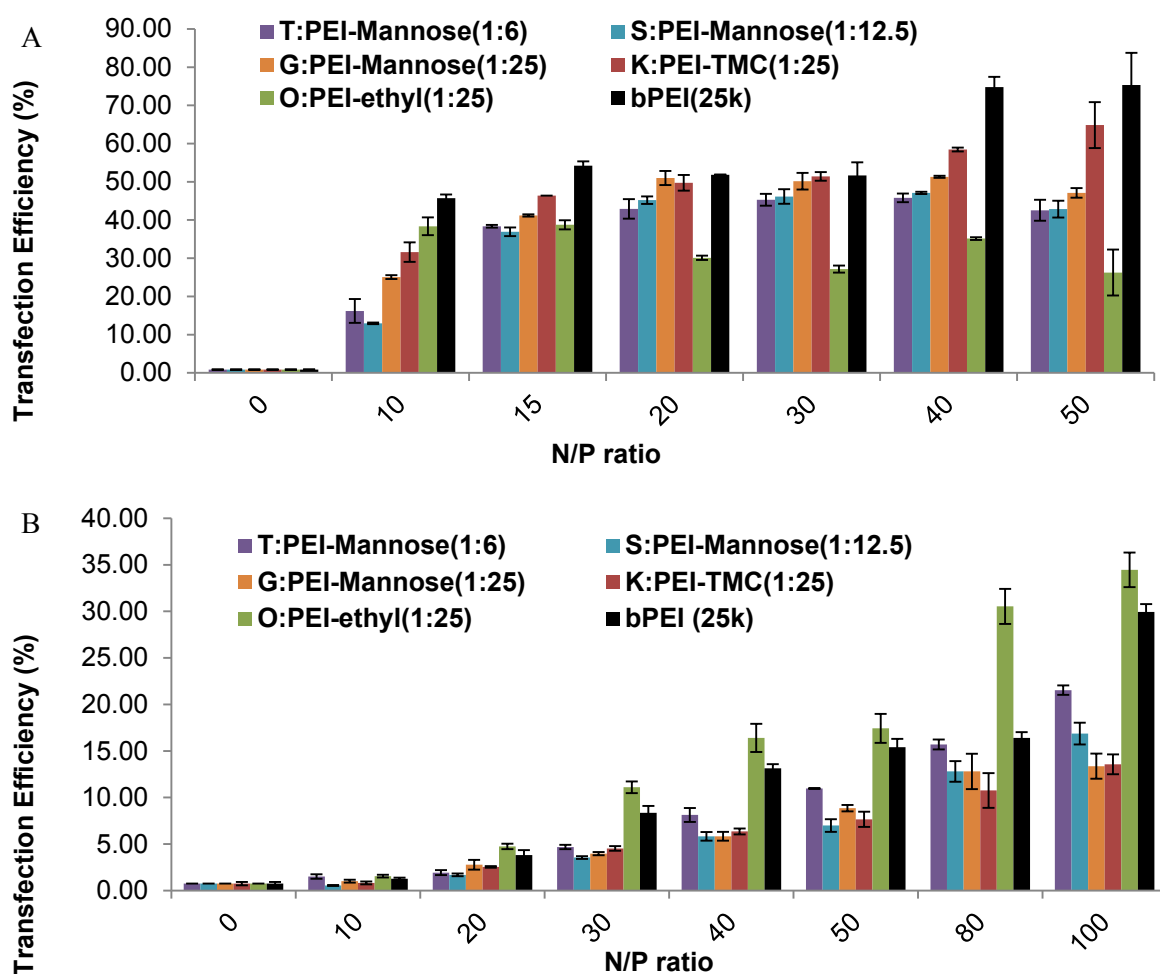


Figure 15. *In vitro* GFP gene transfection efficiency in MCF7 (A) and 4T1 cells (B) mediated by polymers at various N/P ratios indicated. Results represent mean \pm standard deviation of triplicates. Polymer concentrations in the order of N/P ratios specified: unmodified PEI - 0, 4.0, 6.0, 8.0, 12.0, 16.0 and 20.0 mg/L. G - 0, 8.2, 12.3, 16.4, 24.6, 32.8 and 41.0 mg/L. K - 0, 5.2, 7.7, 10.3, 15.5, 20.6 and 25.8 mg/L. T - 0, 5.1, 7.7, 10.2, 15.3, 20.4, 25.5 mg/L. S - 0, 6.2, 9.2, 12.3, 18.5, 24.6, and 30.8 mg/L. O - 0, 6.0, 9.1, 12.1, 18.1, 24.2, and 30.2 mg/L.

3.3.5 *In vitro* luciferase gene expression assay

While GFP transfection efficiency reflects the percentage of cells successfully transfected with the plasmid for GFP expression, luciferase gene expression assay detects the

mean protein expression level in the transfected cells and therefore is also an important parameter of the gene transfection efficiency of the polymers.

Firstly, when polymers **A**, **B** and **C** were used to transfect luciferase DNA plasmid to HepG2 cells, as can be seen in Figure 16, the luciferase expression profiles of **A**, **B** and unmodified PEI were similar, with luciferase expression level positively correlated with the N/P ratio, which reached a plateau of above 10^9 RLU/mg protein from N/P 15 onwards. The luciferase expression level induced by **C** was two magnitudes lower than that mediated by unmodified PEI. The low gene transfection mediated by **C**/DNA complexes correlated well with its size, zeta potential, and DNA binding ability (Figure 7A, 7E, and 8). The large particle size and low positive charge density of the **C**/DNA complexes might lead to low cellular uptake, which together with inefficient DNA binding, might led to poor gene expression.

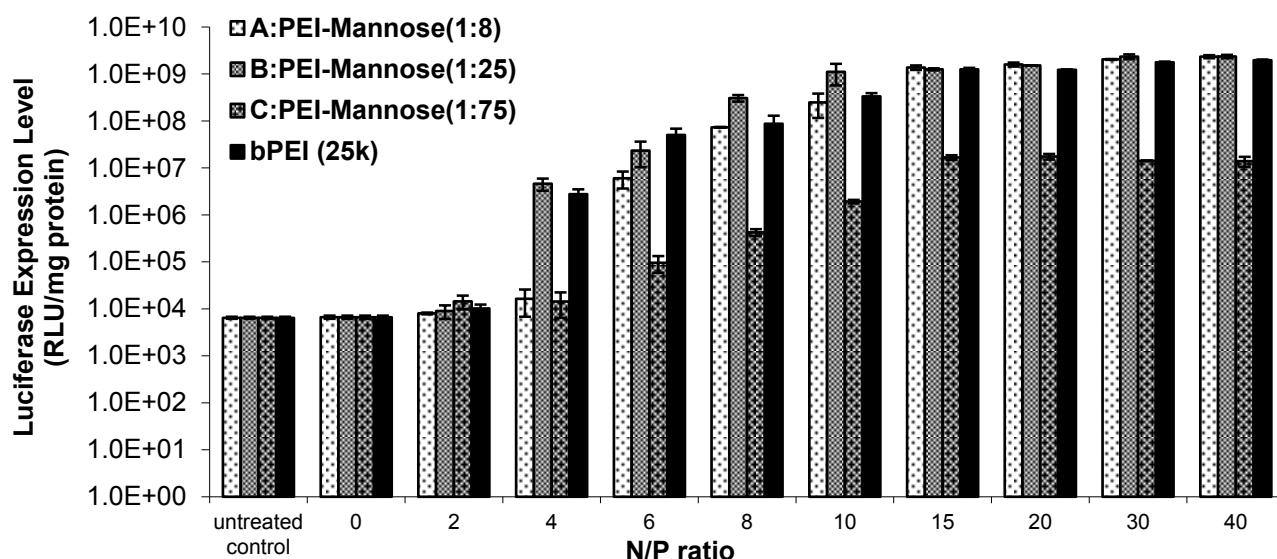


Figure 16. *In vitro* luciferase expression levels in HepG2 cells, mediated by polymers at various N/P ratios indicated. Results represent mean \pm standard deviation of triplicates. Polymer concentrations in the order of N/P ratios specified: unmodified PEI - 0, 1.1, 2.3, 3.4, 4.6, 5.7, 8.6, 11.5, 17.2 and 22.9 mg/L. A - 0, 1.6, 3.1, 4.7, 6.3, 7.8, 11.7, 15.6 23.5 and 31.3 mg/L. B - 0, 2.3, 4.7, 7.0, 9.4, 11.7, 17.6, 23.4, 35.1 and 46.8 mg/L. C - 0, 4.7, 9.4, 14.1, 18.8, 23.5, 35.2, 46.9, 70.4 and 93.8 mg/L.

Furthermore, polymers **T**:PEI-Mannose(1:6), **S**:PEI-Mannose(1:12.5), **G**:PEI-Mannose(1:25), and hydrophobic groups-modified PEIs **K**:PEI-TMC(1:25), and **O**:PEI-ethyl(1:25) were used to deliver luciferase gene to MCF7, 4T1, HMSC, and keratinocytes, respectively. As can be seen in Figure 17A, in MCF7 cells, Polymer **G** proved to be the best in the mannose series of polymers, reaching more than 8×10^9 RLU/mg protein from N/P 15 onwards, while polymer **T** and **S** reached around 10^9 RLU/mg protein at the highest N/P ratio

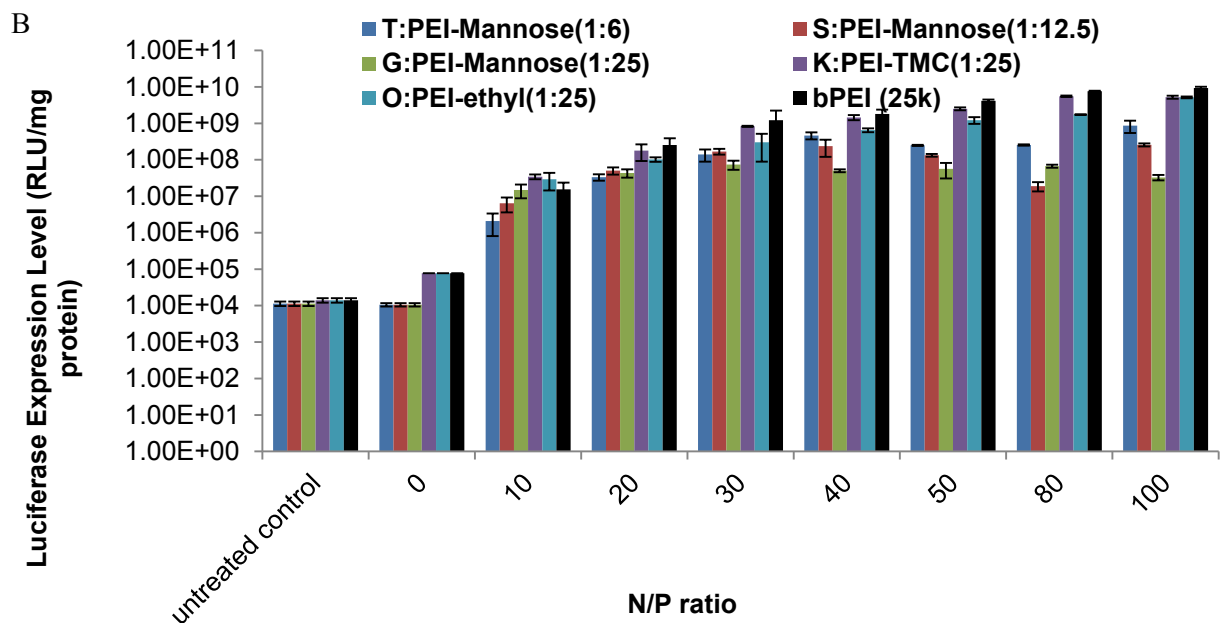
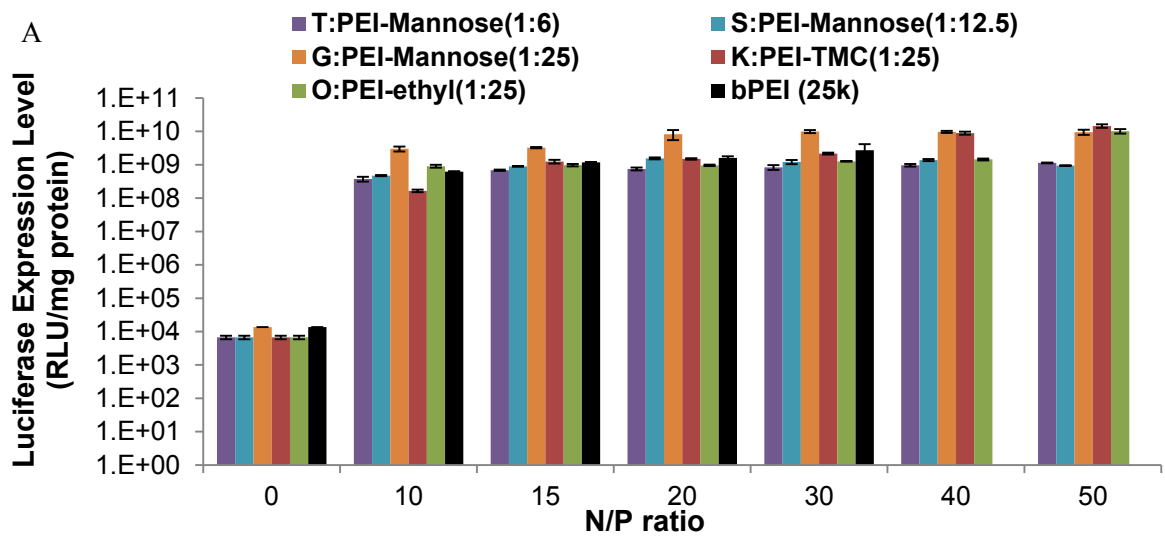
50. **K**:PEI-TMC(1:25) achieved the highest luciferase expression value among all polymers at N/P 50, namely 1.5×10^{10} RLU/mg protein. Additionally, ethyl group modified PEI (1:25) achieved high luciferase gene expression only at N/P 50, which was 1×10^{10} RLU/mg protein, whereas it had similar gene expression levels with polymer **S** and **T** at lower N/P ratios. Moreover, the expression level for unmodified PEI at N/P 40 and 50 was not presented because of the high cytotoxicity induced by PEI, therefore the luciferase expression reading was negligible.

Regarding the mouse breast cancer cell line 4T1, it was shown in Figure 17B that the degree of mannosylation had a negative impact on the luciferase gene transfection efficiency---the larger the mannose attachment ratio, the lower the transfection efficiency of the modified PEI, especially at high N/P ratio of 100, which showed the same trend as the GFP transfection efficiency data in 4T1 (Figure 15B). Moreover, **K**:PEI-TMC(1:25) achieved the highest degree of transfection among all the modified PEIs at N/P 80: 5.5×10^9 RLU/mg protein. However, the luciferase transfection capabilities of the modified PEIs were still inferior as compared to the unmodified PEI, which had the highest gene expression level of 9×10^9 RLU/mg protein, at N/P 100. This matched the GFP transfection data in Figure 15B as well.

However, the luciferase gene expression profiles for these polymers were different in HMSC and keratinocytes. In these two cell lines, **G**:PEI-Mannose(1:25) achieved the highest gene expression level, which was 1.3×10^9 RLU/mg protein at N/P 40 in HMSC (Figure 17C), and 1.8×10^9 RLU/mg protein at N/P 20 in the keratinocytes (Figure 17D), respectively. These values were at least one magnitude higher than those achieved by the unmodified PEI: 2.5×10^7 RLU/mg protein at N/P 40 in HMSC, and 3.8×10^8 RLU/mg protein at N/P 20 in the keratinocytes. Moreover, **T**:PEI-Mannose(1:6) and **S**:PEI-Mannose(1:12.5) achieved luciferase gene expression level which was one magnitude lower than that of **G**:PEI-Mannose(1:25) in both HMSC and the keratinocytes. In addition, **M**:PEI-Mannose(1:120), which was used here as a negative control, much like the case of polymer **C** in HepG2 cells, induced a luciferase expression level which was three magnitudes lower than that mediated by unmodified PEI. The low gene transfection mediated by **M**/DNA correlated well with its zeta potential data (Figure 7F) and DNA retardation gel picture (Figure 8). The negative polyplex charge might lead to low cellular uptake and thus low gene expression. Furthermore, among the hydrophobically modified PEIs, **K**:PEI-TMC(1:25), which achieved the highest luciferase transfection efficiency in the breast cancer cell lines (Figure 17A and B), in this case had comparable

luciferase gene expression level as **S**:PEI-Mannose(1:12.5); and **O**:PEI-ethyl(1:25) had an even lower gene expression level: around 6.5×10^7 RLU/mg protein at N/P 40 and N/P 20, in HMSC and keratinocytes, respectively.

The different behaviors of the polymers in different cell lines again suggested that the nature of cells, and perhaps different cell surface proteins interacting favorably with different modification groups, were a critical factor determining the suitability of using a modified PEI as a gene delivery vector to achieve desirable therapeutic efficacies.



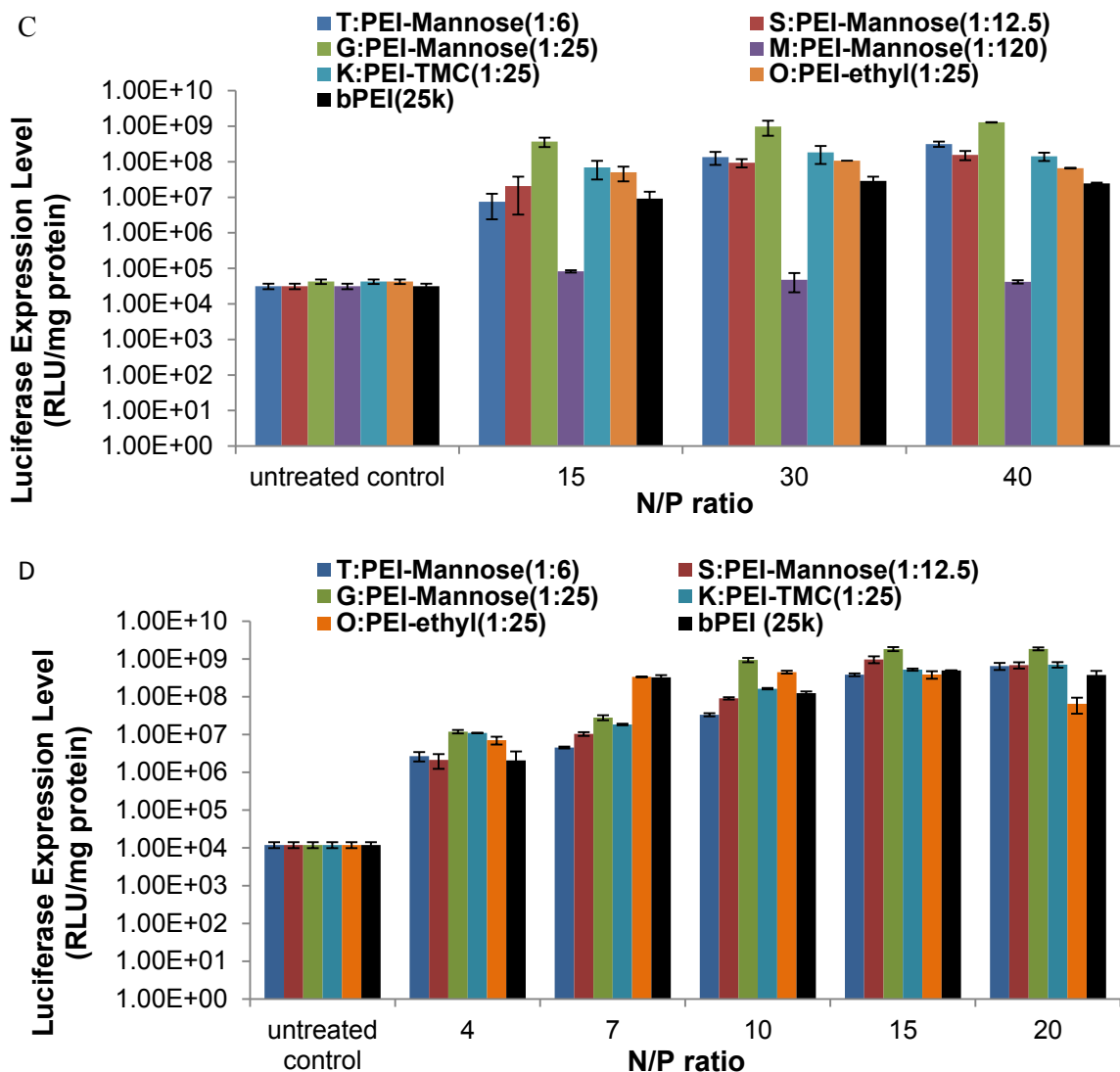


Figure 17. *In vitro* luciferase expression levels in (A) MCF7, (B) 4T1, (C) HMSC, and (D) keratinocytes, mediated by polymers at various N/P ratios indicated. Results represent mean \pm standard deviation of triplicates. Polymer concentrations in the order of N/P ratios specified: (A) unmodified PEI - 0, 5.7, 8.6, 11.5, 17.2, 22.9 and 28.6 mg/L. **T** - 0, 7.3, 10.9, 14.6, 21.9, 29.1 and 36.4 mg/L. **S** - 0, 8.8, 13.2, 17.6, 26.4, 35.2 and 44.0 mg/L. **G** - 0, 11.7, 17.6, 23.4, 35.1, 46.8 and 58.6 mg/L. **K** - 0, 7.4, 11.0, 14.7, 22.1, 29.5 and 36.8 mg/L. **O** - 0, 8.6, 12.9, 17.3, 25.9, 34.5 and 43.2 mg/L. (B) unmodified PEI - 0, 5.7, 11.5, 17.2, 22.9, 28.6, 45.8 and 57.3 mg/L. **T** - 0, 7.3, 14.6, 21.9, 29.1, 36.4, 58.3 and 72.9 mg/L. **S** - 0, 8.8, 17.6, 26.4, 35.2, 44.0, 70.4 and 88.0 mg/L. **G** - 0, 11.7, 23.4, 35.1, 46.8, 58.6, 93.7 and 117.1 mg/L. **K** - 0, 7.4, 14.7, 22.1, 29.5, 36.8, 58.9 and 73.7 mg/L. **O** - 0, 8.6, 17.3, 25.9, 34.5, 43.2, 69.0, and 86.3 mg/L. (C) unmodified PEI - 0, 8.6, 17.2 and 22.9 mg/L. **T** - 0, 10.9, 21.9 and 29.1 mg/L. **S** - 0, 13.2, 26.4 and 35.2 mg/L. **G** - 0, 17.6, 35.1 and 46.8 mg/L. **M** - 0, 51.1, 102.3 and 136.4 mg/L. **K** - 0, 11.0, 22.1 and 29.5 mg/L. **O** - 0, 12.9, 25.9 and 34.5 mg/L. (D) unmodified PEI - 0, 2.3, 4.0, 5.7, 8.6 and 11.5mg/L. **T** - 0, 2.9, 5.1, 7.3, 10.9 and 14.6 mg/L. **S** - 0, 3.5, 6.2, 8.8, 13.2 and 17.6 mg/L. **G** - 0, 4.7, 8.2, 11.7, 17.6 and 23.4 mg/L. **K** - 0, 2.9, 5.2, 7.4, 11.0 and 14.7 mg/L. **O** - 0, 8.6, 12.9, 17.3, 25.9, 34.5 and 43.2 mg/L.

3.3.6 Cytotoxicity test

The cytotoxicity of unmodified PEI was likely due to polymer aggregation on cell surfaces, impairing important membrane functions, as PEI has been reported to induce hole formation or expand the size of pre-existing holes on the cellular membrane [272]. After consecutively feeding a cell with many membrane-disrupting particles, high toxicity was observed, which might be a consequence of the escape of endo/lysosomal enzyme into the cytoplasm, disturbing vital cellular processes [106]. Although PEI mediates high gene transfection efficiency at a low N/P ratio of 10, its high toxicity at higher concentrations impedes its potential *in vivo* application. As the strong positive charge of PEI has been considered to be the main culprit of its high cytotoxicity [273], various functionalized cyclic monomers were used in this thesis to partially shield the primary amines of PEI with the purpose of reducing its toxicity.

In order to evaluate the cytotoxicity of the polymer/DNA complexes, MTT assay was performed on HepG2, HeLa, NIH3T3, MCF7, 4T1, HMSC, and keratinocytes. The GFP plasmid was used for complex formation for treatment of HepG2, HeLa, and NIH3T3 cells, while the luciferase plasmid was used for complex formation and treatment on MCF7, 4T1, HMSC, and keratinocytes.

3.3.6.1 Cytotoxicity test for HepG2, HeLa and NIH3T3 cells

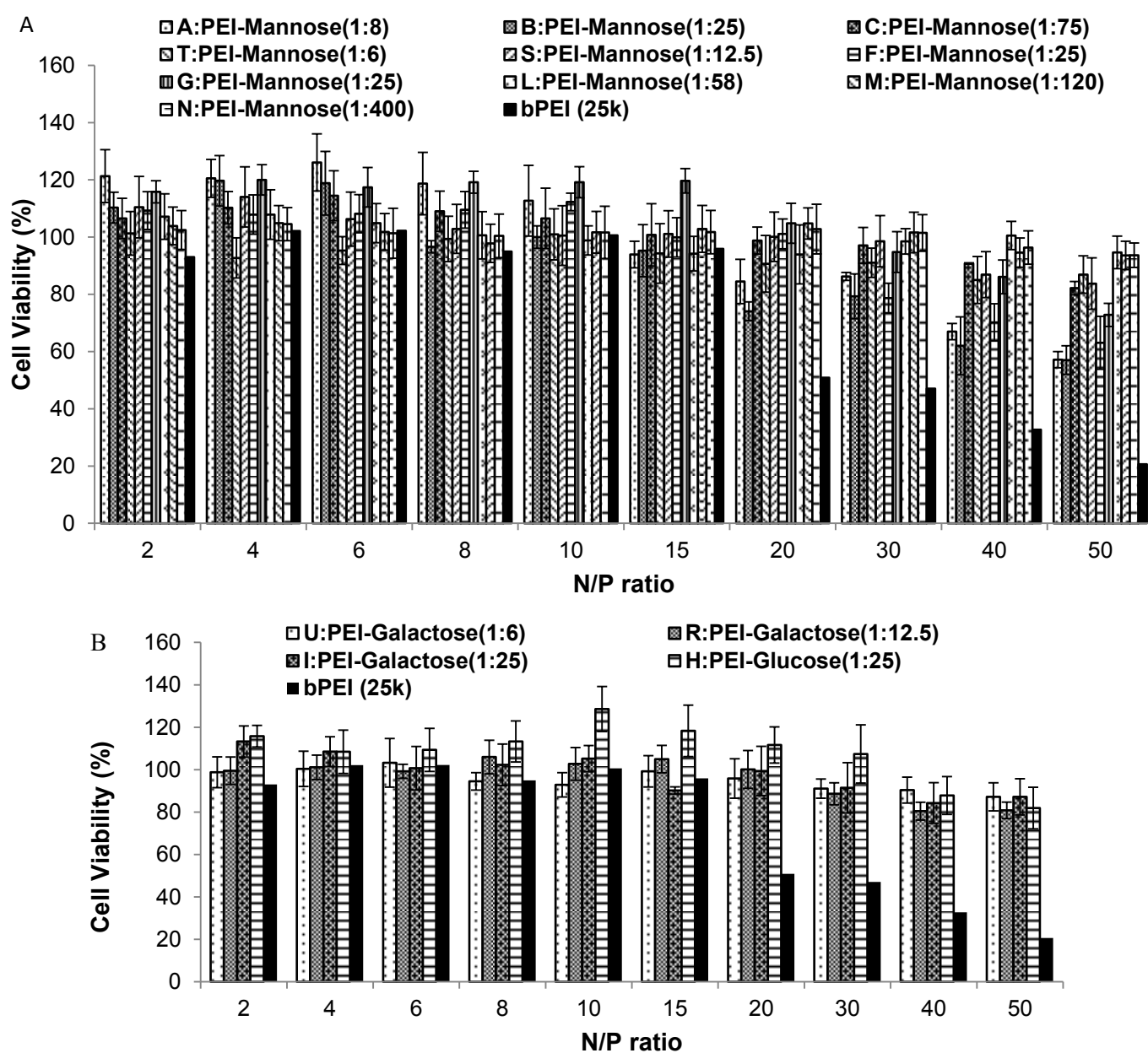
The results of cytotoxicity studies for the modified PEIs are shown as follows. The viability of HepG2 and HeLa cells treated with unmodified PEI/DNA complexes drastically plunged with increasing PEI concentration (or N/P ratio), yielding cell viability of less than 60% at N/P 20 and higher for HepG2 cells (Figure 18A-C) and less than 46% at N/P 30 and higher for HeLa cells (Figure 18D). In particular, at N/P 50, the cell viability was only about 20% for HepG2 and only 4.6% for HeLa after treatment with unmodified PEI/DNA complexes. However, all the modified PEI/DNA complexes were much less cytotoxic than unmodified PEI/DNA complexes at N/P 20-50 in both HepG2 and HeLa cell lines. At N/P 50, the viability of the cells treated with **A, B, C, T, S, F, G, L, M, N, U, R, I, H, V, P, K, J, O, aa, ab**/DNA complexes was 57%, 57%, 82%, 87%, 84%, 63%, 73%, 95%, 94%, 94%, 87%, 81%, 87%, 82%, 75%, 91%, 87%, 89%, 99%, 72%, and 66%, respectively for HepG2 (Figure 18A-C) and nearly 100% for HeLa (Figure 18D).

Similar trend was observed in NIH3T3 cells. Unmodified PEI was highly toxic, with cell viability rapidly dropping from 60% at N/P 40 to 1.3% at N/P 80 and 100 (Figure 18E). Although PEI had over 90% GFP transfection efficiency at N/P 80 and 100 in NIH3T3 (Figure 14), the high cytotoxicity suggest that the high GFP signal observed in flow cytometry might be due to auto-fluorescence of the dead cells which emitted green fluorescent light with a peak intensity around 560 nm [274]. On the contrary, the modified PEIs showed greatly mitigated cytotoxicity. **T**:PEI-Mannose(1:6) and **S**:PEI-Mannose(1:12.5) were only toxic at N/P 80 and 100, giving cell viability of 63% and 28% when treated by **T**/DNA, and 78% and 41% when treated by **S**/DNA. Additionally, higher mannose conjugation ratio significantly improved the cell survival rates, presumably because more primary amine groups were blocked, shielding more positive charges of PEI. Interestingly, when the mannosylation ratio increased to 1:25, polymer **G** totally eliminated the cytotoxicity problem of the unmodified PEI, achieving 100% cell viability even at N/P 100 (Figure 18 E).

In the present study, cell viability was significantly enhanced by simple modification with mannose and other functional sugar carbonates such as galactose and glucose. Mannose is a common metabolite and research has shown direct utilization of mannose for mammalian glycoprotein biosynthesis [275]. Therefore it should not impose any toxic effects on the cells. Indeed, comparing to unmodified PEI, a much higher percentage of HepG2 cells transfected by sugar modified PEIs were healthy even at N/P 30-50 (Figure 18A and B), nearly all HeLa cells treated by them were viable even at N/P 50 (Figure 18D), and nearly all NIH3T3 cells were viable by polymer **G** treatment even at N/P 100 (Figure 18E). Importantly, at these N/P ratios, gene transfection efficiency provided by the modified PEI was significantly higher than that given by unmodified PEI at N/P 15 (Figure 10, 13 and 14). Although cationic polymers with high charge density had strong cell lytic and toxic properties, a reduction of charge density resulted in less cell toxicity [276]. Therefore the significantly reduced cytotoxicity by sugar attachment was most likely due to the shielding of the primary amines of PEI, leading to reduced charge density.

Similarly, hydrophobic group-conjugation and blockage of the primary amines of PEI also accounted for the reduced cytotoxicity for the respective polymers. In fact, even modification with only a single TMC equivalently made **V**:PEI-TMC(1:1) minimally toxic at N/P 50 (75% vs 20% for unmodified PEI) for HepG2 (Figure 18C). The large cytotoxicity reduction could be due to the formation of a hydroxyl shell on the polymer/DNA complexes,

which shielded the cationic surface charge, rendering them less cytotoxic. With increasing TMC conjugation degree of PEI, additional toxicity reduction, albeit relatively mild, was observed. Moreover, modification using other functional hydrophobic carbonates such as ethyl, benzyl and urea also demonstrated cell viability enhancement. Among the hydrophobic group-modified PEIs at 1:25 ratio, **O**:PEI-ethyl(1:25) demonstrated the greatest cytotoxicity reduction at N/P 30-50 in HepG2 (Figure 18C). Despite the lack of the exact mechanism of cytotoxicity reduction, it can be postulated that a decreased quantity of free primary amines diminishes the surface charge density of PEI/DNA nanocomplexes (Figure 7H), hence cell membrane rupture and consequent cytotoxicity was significantly mitigated.



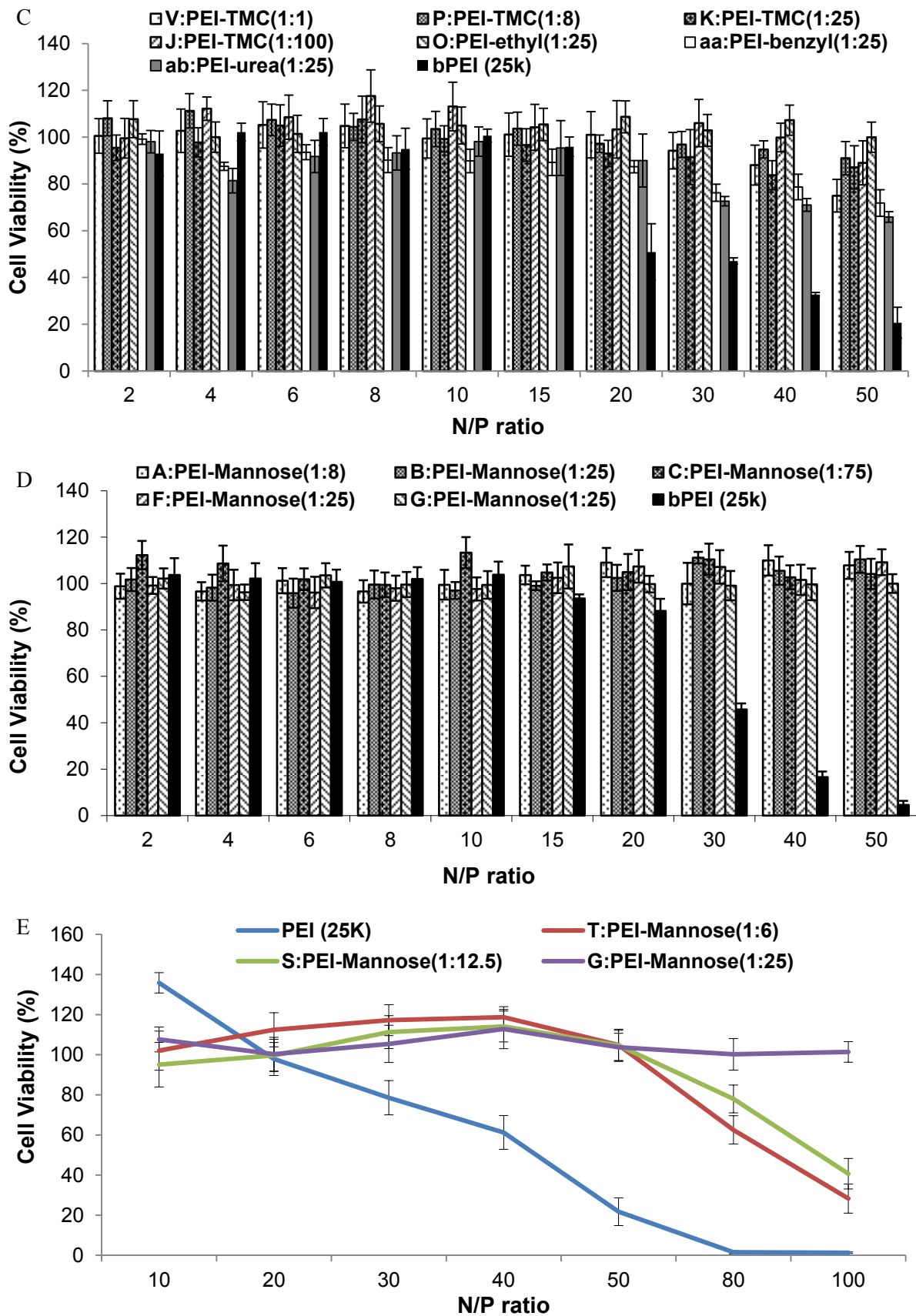


Figure 18. Viability of HepG2 cells (A, B, C), HeLa cells (D), and NIH3T3 cells (E) after incubation with polymer/DNA complexes at various N/P ratios in comparison to unmodified PEI/DNA complexes. Results represent mean \pm standard deviation of at least 8 replicates. (A-D)

Polymer concentrations in the order of N/P ratios specified: unmodified PEI - 0.8, 1.6, 2.4, 3.2, 4.0, 6.0, 8.0, 12.0, 16.0 and 20.0 mg/L. **A** - 1.1, 2.2, 3.3, 4.4, 5.5, 8.2, 11.0, 16.4, 21.9 and 27.4 mg/L. **B, F, G, H, I, J** - 1.6, 3.3, 4.9, 6.6, 8.2, 12.3, 16.4, 24.6, 32.8 and 41.0 mg/L. **C** - 3.3, 6.6, 9.9, 13.1, 16.4, 24.6, 32.8, 49.3, 65.7 and 82.1 mg/L. **K** - 1.0, 2.1, 3.1, 4.1, 5.2, 7.7, 10.3, 15.5, 20.6 and 25.8 mg/L. **L** - 2.2, 4.4, 6.7, 8.9, 11.1, 16.7, 22.2, 33.3, 44.4, and 55.5 mg/L. **M** - 4.8, 9.5, 14.3, 19.1, 23.9, 35.8, 47.7, 71.6, 95.5, and 119.3 mg/L. **N** - 14.1, 28.1, 42.2, 56.3, 70.3, 105.5, 140.7, 211.0, 281.3, and 351.7 mg/L. **T, U** - 1.0, 2.0, 3.1, 4.1, 5.1, 7.7, 10.2, 15.3, 20.4, 25.5 mg/L. **R, S** - 1.2, 2.5, 3.7, 4.9, 6.2, 9.2, 12.3, 18.5, 24.6, and 30.8 mg/L. **V** - 0.8, 1.7, 2.5, 3.3, 4.2, 6.2, 8.3, 12.5, 16.6, and 20.8 mg/L. **P** - 0.9, 1.8, 2.7, 3.6, 4.5, 6.7, 8.9, 13.4, 17.8, and 22.3 mg/L. **O** - 1.2, 2.4, 3.6, 4.8, 6.0, 9.1, 12.1, 18.1, 24.2, and 30.2 mg/L. (E) Polymer concentrations in the order of N/P ratios specified: unmodified PEI -4.0, 8.0, 12.0, 16.0, 20.0, 32.1, and 40.1 mg/L. **T** - 5.1, 10.2, 15.3, 20.4, 25.5, 40.8, and 51.0 mg/L. **S** - 6.2, 12.3, 18.5, 24.6, 30.8, 49.3, and 61.6mg/L. **G** - 0, 8.2, 16.4, 24.6, 32.8, 41.0, 65.6, and 82.0 mg/L.

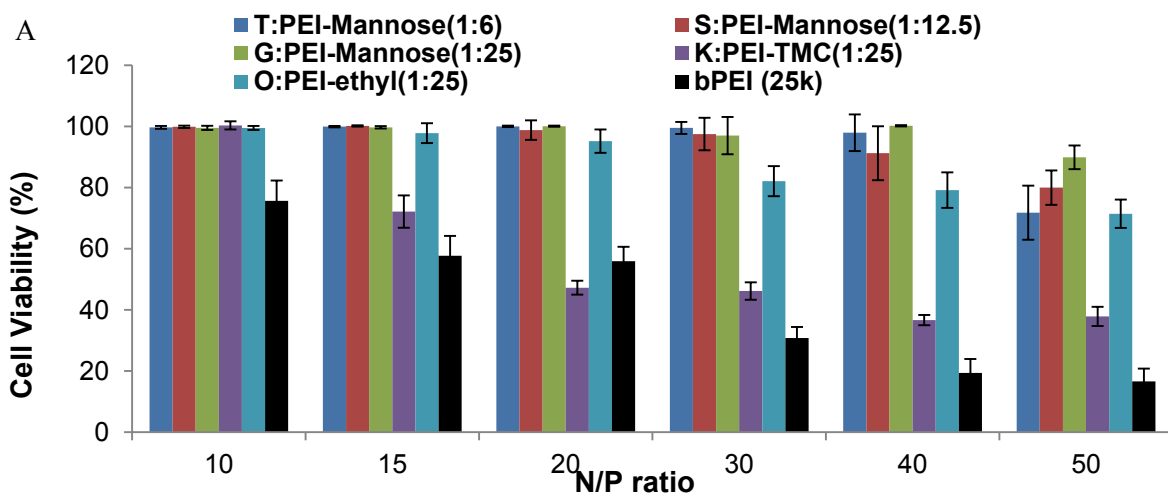
3.3.6.2. Cytotoxicity test in other cell lines

Mannose-modified polymers **T**:PEI-Mannose(1:6), **S**:PEI-Mannose(1:12.5), **G**:PEI-Mannose(1:25), and hydrophobic groups-modified **K**:PEI-TMC(1:25), and **O**:PEI-ethyl(1:25) were used to deliver luciferase gene to MCF7, 4T1, HMSC, and keratinocytes, and the cytotoxicity caused by the polymer/luciferase DNA complexes in these cell lines were tested by MTT assay.

As shown in Figure 19A, unmodified PEI caused very high toxicity in MCF7, with less than 30% viability at N/P 30 and above. The mannose-modified PEI series drastically promoted the viability of the cells, and the survival rate of MCF7 positively correlated with the degree of mannosylation at N/P 50, as the viability of MCF7 treated by **T**/DNA, **S**/DNA and **G**/DNA complexes was 70%, 80%, and 90%, respectively. **O**:PEI-ethyl(1:25) also enhanced the viability of MCF7 to above 70% at all N/P ratios. However, TMC modified PEI at 1:25 did not provide a good relief of the toxicity (40% cell viability at N/P 50). The same phenomenon was observed in TMC-PEI treated HMSC at N/P 40 (Figure 19C), and in this case, **K**:PEI-TMC(1:25) caused even more cytotoxicity compared to the unmodified PEI (viability was 32% for **K** vs. 49% for PEI). Moreover, 4T1 cells, the mouse breast cancer cell line showed more tolerance to the unmodified PEI, as 62% cells survived even at a high N/P ratio of 100. However, in contrast to MCF7, **K**:PEI-TMC(1:25) was completely not toxic in 4T1 cells at all the N/P ratios tested (Figure 19B). **O**:PEI-ethyl(1:25), however, caused even greater toxicity than the unmodified PEI, especially at N/P 80 and 100 (viability was 57%, 27% for **O** vs 66%, 62% for the unmodified PEI). Finally, in keratinocytes, all the modified PEIs decreased the cytotoxicity of the unmodified PEI 25kDa significantly, by at least 25%, at the highest N/P ratio tested (Figure 19D). Although the reason of the toxicity associated with TMC and Ethyl

modifications in these cell lines is still unclear, similar phenomenon was observed before that MCF7 cell viability was seen to decrease with increasing degree of trimethylation on chitosan which delivered drugs and gene to MCF7[277]. Also, it was reported in the literature that addition of aliphatic hydrocarbon (alkyl group) in the structure of hydrophobic substitution for chitosan induced toxicity on cells, while the addition of aromatic hydrocarbon (aryl group) in the hydrophobic substitution reduced toxicity on cells [278]. The difference in cytotoxicity induced by the same polymer between cell lines may be a valuable asset suggesting researchers to preferentially transfect specific cell types with appropriate vectors. Also, when new polymeric materials and derivatives are developed, they need to be tested individually to assess their toxicity and transfection efficiency on the desired cell lines so that a comprehensive understanding of their properties could be attained.

Combined with the luciferase gene transfection results, the best polymers achieving high luciferase protein expression level while maintaining minimal cytotoxicity were: **G**:PEI-Mannose(1:25) for MCF7, HMSC and keratinocytes, and **K**:PEI-TMC(1:25) for 4T1 cells. Furthermore, the low cytotoxicity of polymer **G**/DNA and **K**/DNA complexes in these respective cell lines ensured that luciferase transfection results were reliable without any superficial amplification, as superficial amplification might occur when the RLU of luciferase was normalized against a low protein content of the cells in case a polymer exerts high cytotoxicity, which could be the case of the unmodified PEI at high N/P ratios [279]. Furthermore, **T**:PEI-Mannose(1:6) and **S**:PEI-Mannose(1:12.5) improved the viability in all four cell lines, and their luciferase gene transfection efficiency was slightly lower than the best polymers in the four cell lines.



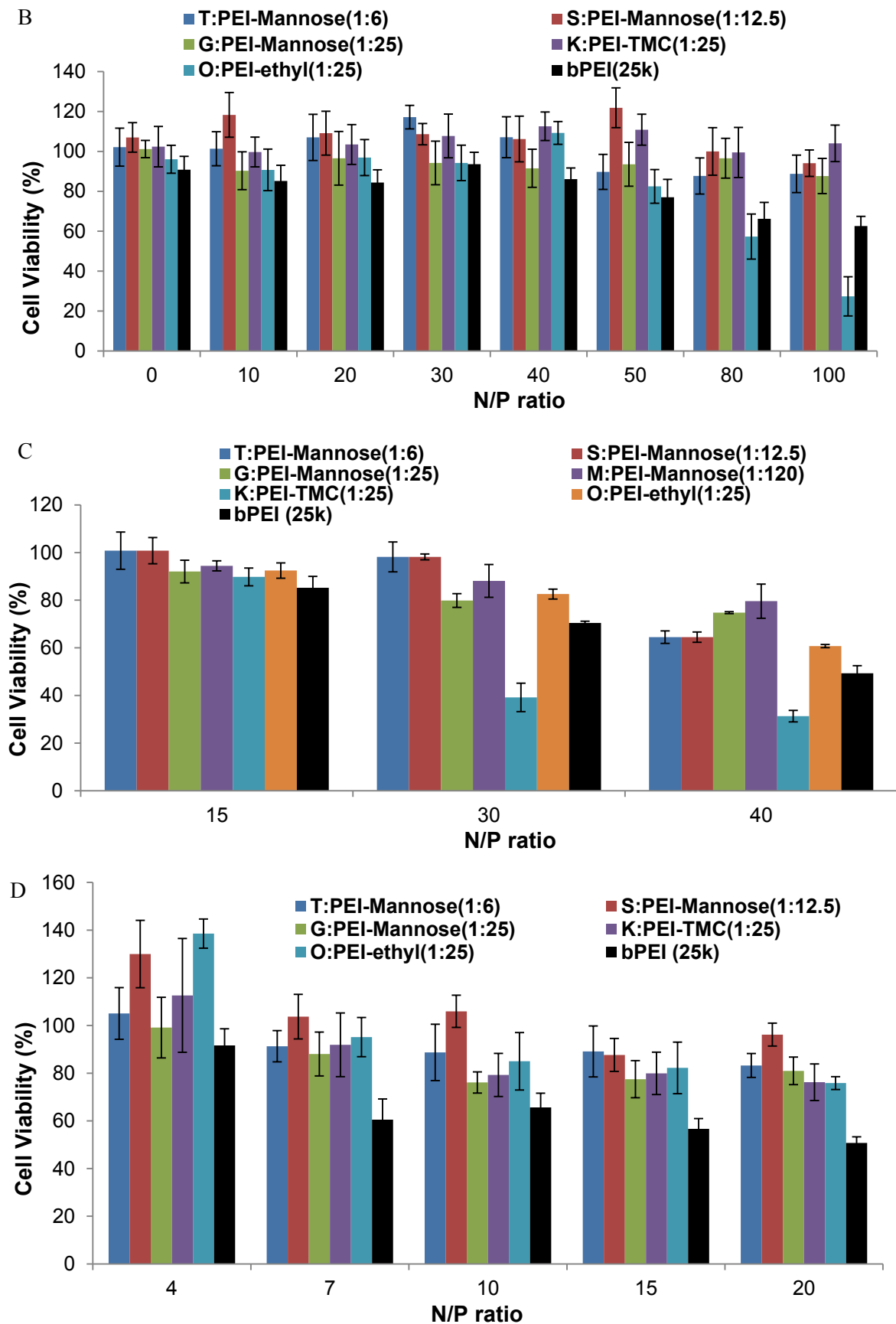


Figure 19. Viability of (A) MCF7, (B) 4T1, (C) HMSC, and (D) keratinocytes after incubation with polymer/DNA complexes at various N/P ratios in comparison to unmodified PEI/DNA

complexes. Results represent mean \pm standard deviation of at least 8 replicates. Polymer concentrations in the order of N/P ratios specified: (A) unmodified PEI - 5.7, 8.6, 11.5, 17.2, 22.9 and 28.6 mg/L. **T** - 7.3, 10.9, 14.6, 21.9, 29.1 and 36.4 mg/L. **S** - 8.8, 13.2, 17.6, 26.4, 35.2 and 44.0 mg/L. **G** - 11.7, 17.6, 23.4, 35.1, 46.8 and 58.6 mg/L. **K** - 7.4, 11.0, 14.7, 22.1, 29.5 and 36.8 mg/L. **O** - 8.6, 12.9, 17.3, 25.9, 34.5 and 43.2 mg/L. (B) unmodified PEI - 0, 5.7, 11.5, 17.2, 22.9, 28.6, 45.8 and 57.3 mg/L. **T** - 0, 7.3, 14.6, 21.9, 29.1, 36.4, 58.3 and 72.9 mg/L. **S** - 0, 8.8, 17.6, 26.4, 35.2, 44.0, 70.4 and 88.0 mg/L. **G** - 0, 11.7, 23.4, 35.1, 46.8, 58.6, 93.7 and 117.1 mg/L. **K** - 0, 7.4, 14.7, 22.1, 29.5, 36.8, 58.9 and 73.7 mg/L. **O** - 0, 8.6, 17.3, 25.9, 34.5, 43.2, 69.0, and 86.3 mg/L. (C) unmodified PEI - 8.6, 17.2 and 22.9 mg/L. **T** - 10.9, 21.9 and 29.1 mg/L. **S** - 13.2, 26.4 and 35.2 mg/L. **G** - 17.6, 35.1 and 46.8 mg/L. **K** - 11.0, 22.1 and 29.5 mg/L. **O** - 12.9, 25.9 and 34.5 mg/L. (D) unmodified PEI - 2.3, 4.0, 5.7, 8.6 and 11.5 mg/L. **T** - 2.9, 5.1, 7.3, 10.9 and 14.6 mg/L. **S** - 3.5, 6.2, 8.8, 13.2 and 17.6 mg/L. **G** - 4.7, 8.2, 11.7, 17.6 and 23.4 mg/L. **K** - 2.9, 5.2, 7.4, 11.0 and 14.7 mg/L. **O** - 8.6, 12.9, 17.3, 25.9, 34.5 and 43.2 mg/L.

3.3.7 siRNA mediated Bcl-2 knockdown in HeLa cells

Since several polymers have been identified which could successfully deliver GFP and luciferase plasmid DNA to various cell lines and at the same time greatly reduce the cytotoxicity caused by the unmodified PEI, it would be interesting to investigate the effectiveness of these polymers to deliver siRNA to the cells and the associated cytotoxicity of the polymer/siRNA complexes, as knocking down erratic gene expression is another crucial aspect of an effective gene therapy. As shown in Figure 20, Bcl-2 siRNA or negative control siRNA was successfully delivered inside HeLa cells using polymers **A** and **B** at N/P ratio of 50, and Bcl-2 down-regulation at the mRNA level was manifest. For Bcl-2 knockdown mediated by **A** and **B**/siRNA complexes, Bcl-2 mRNA expression levels were reduced to 29% and 25% of that in the untreated HeLa cells, respectively, which was comparable to the knockdown level induced by unmodified PEI/siRNA complexes (26%). In a control experiment where negative control siRNA (i.e. scrambled siRNA) was used, no mRNA down-regulation was observed, thus proving the validity of the knockdown results by Bcl-2 siRNA delivery. On the other hand, siRNA delivery using polymer **C** was not successful as the amount of Bcl-2 mRNA was still 85% of that in the untreated cells, which coincided with the inferior GFP gene transfection efficiency mediated by **C** in HeLa cells (Figure 13).

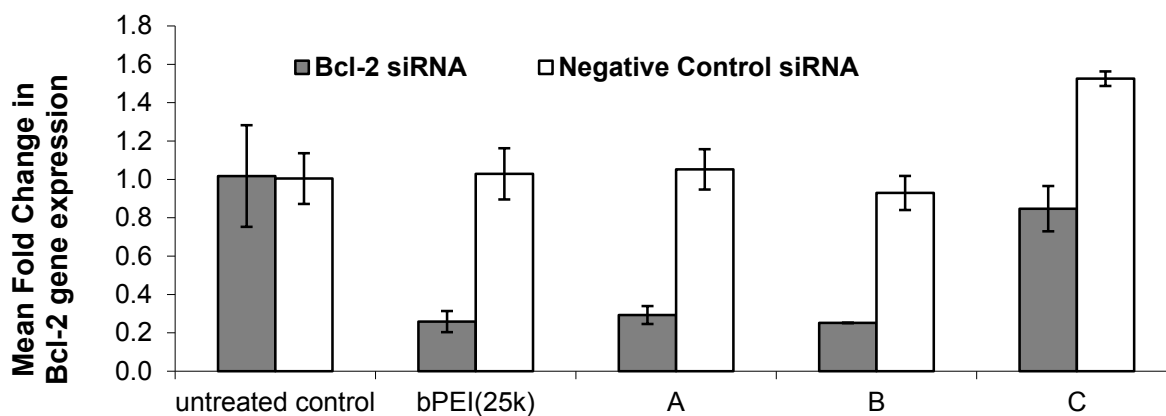


Figure 20. Downregulation of Bcl-2 mRNA in HeLa cells at siRNA concentration of 100 nM and N/P 50. The corresponding polymer concentrations used were: unmodified PEI - 8.4 mg/L; **A** - 11.4 mg/L; **B** - 17.1 mg/L; **C** - 34.3 mg/L. Results represent mean \pm standard deviation of triplicates.

3.3.8 Viability of HeLa cells after being treated with polymer/siRNA complexes

The HeLa cells appeared to be resistant to Bcl-2 siRNA-induced cell death at the siRNA and polymer concentrations tested in this thesis. As can be seen in Figure 21, there was no difference between the cytotoxicity when Bcl-2 siRNA or scrambled siRNA (the negative control) was delivered into HeLa cells at various N/P ratios. Therefore any difference in cell viability was due to the nature of the polymers used. In fact, 82% of the cells were alive after treatment with unmodified PEI/Bcl-2 siRNA complexes (N/P ratio 60). However, when polymers **A**, **B** and **C** were used, nearly 100% of the HeLa cells were viable at N/P 60. All in all, together with the mRNA knockdown data, **A** and **B** were effective in complexing with negatively charged siRNA and mediating siRNA delivery into HeLa cells, leading to successful Bcl-2 mRNA down-regulation to a level comparable to that achieved by unmodified PEI while maintaining excellent cell viability. Although HeLa cells were resistant to death after Bcl-2 mRNA knockdown, this mRNA knockdown was frequently reported to sensitize cancer cells to anticancer drugs [280-283]. Hence, there is huge potential in using the mannose-modified PEIs to deliver Bcl-2 siRNA into HeLa cells as part of a multi-component treatment regime to boost the effect of chemotherapeutic agents such as cisplatin, 5-fluorouracil (5-FU) and 10-hydroxycamptothecin (HCPT).

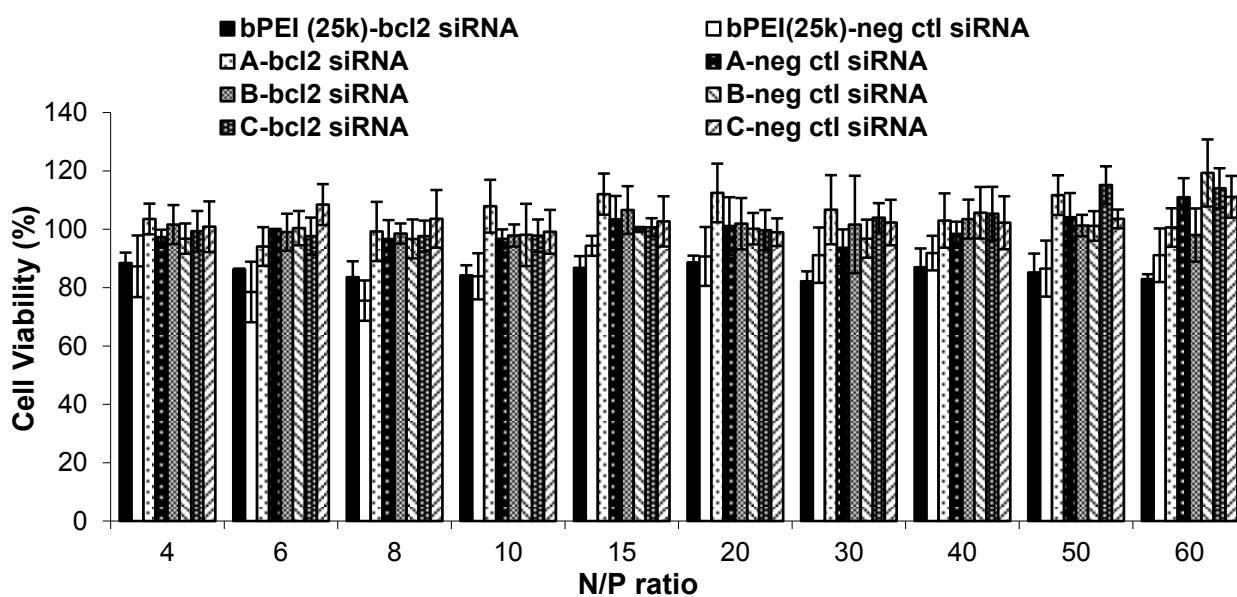


Figure 21. Viability of HeLa cells after being treated with polymer/siRNA complexes at various N/P ratios. siRNA concentration was fixed at 100 nM. Results represent mean \pm standard deviation of 8 replicates. The polymer concentrations corresponding to different N/P ratios used: unmodified PEI - 0.7, 1.0, 1.3, 1.7, 2.5, 3.4, 5.0, 6.7, 8.4 and 10.1 mg/L; **A** - 0.9, 1.4, 1.8, 2.3, 3.4, 4.6, 6.9, 9.2, 11.4 and 13.7 mg/L; **B** - 1.4, 2.1, 2.7, 3.4, 5.1, 6.9, 10.3, 13.7, 17.1 and 20.6 mg/L; **C** - 2.7, 4.1, 5.5, 6.9, 10.3, 13.7, 20.6, 27.4, 34.3 and 41.2 mg/L.

3.3.9 *In vivo* organ-specific luciferase expression in mice

Having investigated the biophysical properties, *in vitro* gene/siRNA delivery efficiency and cytotoxicity of the modified PEIs, their biodistribution and *in vivo* organ specific gene delivery efficiency were studied by tail-vein injection of 4 μ g of luciferase plasmid DNA complexed with selected polymers at various N/P ratios: unmodified PEI (N/P 10), **G**:PEI-Mannose(1:25) (N/P 30, 50, 80, 120), **K**:PEI-TMC(1:25) (N/P 50, 80), and **O**:PEI-ethyl(1:25) (N/P 50, 80). 10 μ g of luciferase plasmid DNA complexed with polymers at the designated N/P ratios was found to cause severe lethality, as more than half of the mice injected with it died within hours after injection. Therefore, a lower, non-lethal 4 μ g DNA dose was used to construct the complexes with various polymers. The polymer concentrations in the nanoparticle complexes solution, as well as the polymer to mice weight/weight ratio (mg/kg) were summarized in Table 5.

Polymer & N/P	PEI 10	G 30	G 50	G 80	G 120	K 50	K 80	O 50	O 80
polymer concentration (mg/L)	25.2	154.6	257.7	412.3	618.4	162.0	259.3	189.9	303.8
Mg polymer/kg mice (20g per mice)	0.25	1.55	2.58	4.12	6.18	1.62	2.59	1.90	3.04

Table 5. The concentrations of various polymers used to deliver 4 µg luciferase DNA intravenously per mouse, and the polymer to mouse weight/weight ratios.

Luciferase expression levels inside the various visceral organs were analysed 72 h after intravenous injection of the polymer/luciferase DNA complexes. As can be seen in Figure 22, generally, the luciferase gene expression level induced by different polymers as well as the unmodified PEI was not significantly higher than the PBS control, especially in hearts, livers, kidneys and spleens. However, there was significantly higher luciferase gene expression observed in the lungs, mediated by unmodified PEI at N/P 10 and polymer **G** at N/P 120, compared to the PBS control, suggesting that these cationic particles were tend to aggregate with serum proteins, erythrocytes, and other blood components to form complexes that can embolize and accumulate in vascular beds of the lung [284, 285]. The lung tropism of unmodified PEI and **G** was consistent with another study by Goula, D., et al., which also showed high levels of luciferase expression in the lung when DNA was complexed with linear, 22 kDa PEI in 5% glucose and administered intravenously, while heart, spleen, liver and kidney remained refractory to PEI mediated luciferase gene transfection [286]. For **G**:PEI-Mannose(1:25), it achieved higher luciferase expression levels when used at higher N/P ratios, especially when complexed with the luciferase DNA at N/P 120, it achieved the highest gene expression in the lung (6×10^3 RLU/mg protein), which was higher than that of unmodified PEI (4.6×10^3 RLU/mg protein), although not significant. However, the luciferase expression level mediated by **G** at N/P 120 was one magnitude higher than those achieved by the hydrophobic groups (TMC and Ethyl)-modified PEIs and the PBS control, and the difference was highly significant according to the statistical analysis ($p < 0.05$). Moreover, relative luciferase expression in the lung induced by **G**:PEI-Mannose(1:25)/DNA complexes formed at N/P 120 was 4-fold higher than the that induced by the same polymer and N/P ratio in the heart, 10-fold higher than that in the kidney and spleen, and 100-fold higher than that in the liver. Therefore, **G**:PEI-Mannose(1:25) could potentially be used for targeted gene delivery to the lung tissue *in vivo* in the future. In addition, although it was reported in the literature that between 50 and 60% of ^{32}P -labelled plasmid/cationic lipid complexes injected into the tail veins of mice were taken up by the liver, the low level of transgene expression in the liver suggested that the complexes were taken by scavenger cells (Kupffer cells) via phagocytosis, resulting in rapid degradation of the plasmid [287]. This result was bolstered by our modified PEIs-mediated organ-specific luciferase gene expression results, which showed no increase in gene expression level in livers compared to the PBS control.

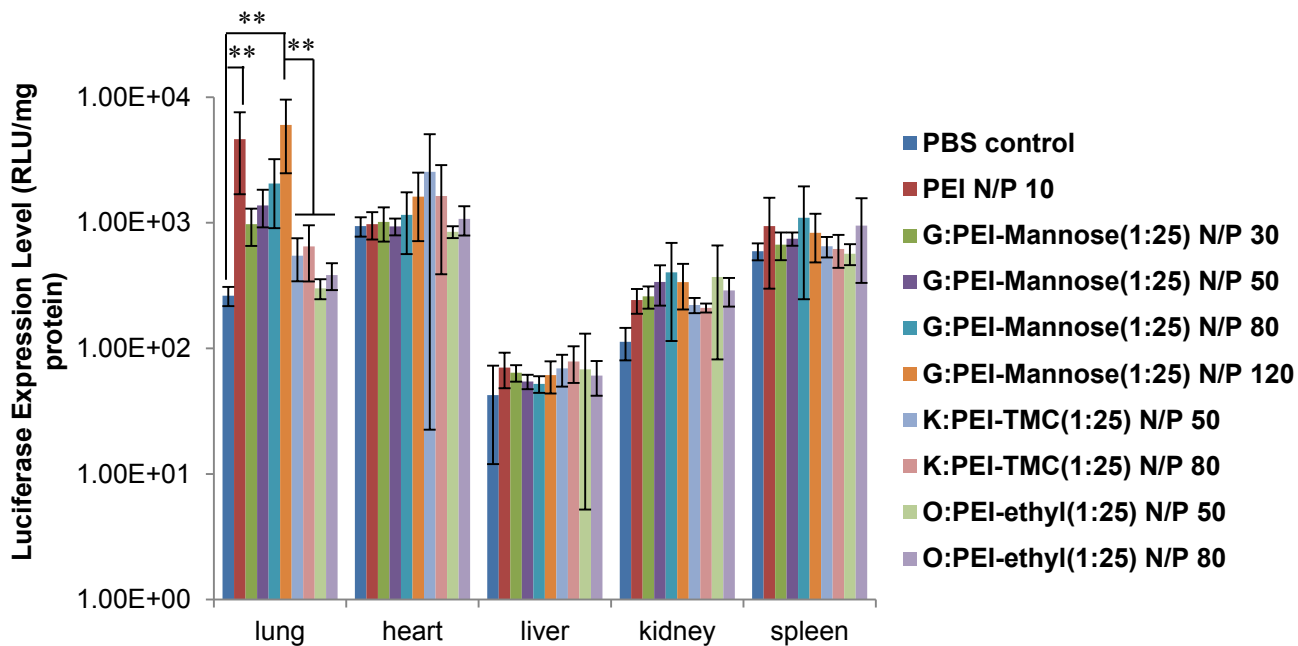


Figure 22. *In vivo* organ specific luciferase gene expression induced 72 h after i.v. injection of selected polymers complexed with luciferase gene at various N/P ratios. PBS was injected as a negative control, and unmodified PEI at N/P 10 was used as a positive control. (** $p < 0.05$) Results represent mean \pm standard deviation of 6 replicates.

3.4 Conclusion

In this study, PEI 25 kDa was successfully modified with cyclic carbonates with mannose/galactose/glucose/hydrophobic groups as functional groups at various feed molar ratios, using a rapid and synthetically facile ring-opening reaction approach. Functionalization of PEI was easily controlled by pre-determined PEI:cyclic carbonate feed ratios and permitted a simple means for the addition of functionality. Polymers **C**, **L**, **M** and **N** with too many primary amines blocked by a higher degree of carbonate-mannose modification did not bind DNA effectively, giving rise to large particles with low positive charges on the surface and thus poor gene transfection efficiency. However, when PEI was modified with functional carbonates at lower degrees (feed molar ratios of PEI-mannose=1:25, 1:12.5 and 1:8; PEI:Galactose=1:25, 1:12.5 and 1:8; PEI:TMC=1:25, 1:8, 1:1; PEI:Ethyl=1:25), the resulting polymers efficiently condensed DNA into nanosized particles with positive zeta potential. Importantly, the cytotoxicity of modified polymers in HepG2, HeLa, NIH-3T3, MCF7, 4T1, HMSC, and keratinocytes was significantly reduced, while the gene transfection efficiency was comparable or higher than unmodified PEI. Especially, GFP gene transfection efficiency was increased by ~ 10 times in HepG2 cells as compared to unmodified PEI, by the commercially available TMC modified PEI (1:25) which was an extremely efficacious gene delivery vector

with minimal cytotoxicity in HepG2. In addition, the mannose-modified polymers effectively delivered Bcl-2 siRNA into HeLa cells and down-regulated Bcl-2 mRNA to one quarter of the normal level without apparent cytotoxicity. And polymer **G**:PEI-Mannose(1:25) even showed targeted gene delivery to the lung 72 h after intravenous injection of **G**/luciferase DNA complexes formed at N/P 120.

This synthesis approach could also be extended to include a plethora of other functional groups such as a targeting signal that recognizes a specific cell type (e.g. mannose towards keratinocytes, macrophages and dendritic cells; galactose targeting liver cells; anti-HER2 antibody targeting breast cancer cell line), PEG for improving serum stability of polymer/DNA complexes, and disulfide linkages for triggered release of other biologically relevant materials. Modified PEIs are envisioned to hold great potential as gene delivery systems due to easy synthesis, scalability, low cost, low cytotoxicity and outstanding transfection capacity.

All in all, careful screening of the various functionalized PEI polymers generated a list of selected polymers with effective gene delivery potential and minimal cytotoxicity which could be used to deliver therapeutic genes and evaluate the biological effects. The details of the therapeutic application of these polymers will be presented in the next two chapters.

CHAPTER 4: DELIVERY OF A GRANZYME B INHIBITOR GENE USING CARBAMATE-MANNOSE MODIFIED PEI TO PROTECT AGAINST NK CELL KILLING

4.1 Introduction

Mass screening of the various functional cyclic carbonate monomer modified PEIs in terms of their physicochemical properties, *in vitro* gene/siRNA transfection efficiency, cytotoxicity, and *in vivo* organ specific luciferase gene delivery capability in Chapter 3 enabled several outstanding polymers to be shortlisted: **A**:PEI-Mannose(1:8) (synthesized with DBU), **B**:PEI-Mannose(1:25) (synthesized with DBU), **T**:PEI-Mannose(1:6) (without DBU), **S**:PEI-Mannose(1:12.5) (without DBU), **G**:PEI-Mannose(1:25) (without DBU), **K**:PEI-TMC(1:25) (without DBU), and **O**:PEI-ethyl(1:25) (without DBU). In this chapter, the potential of using polymers **A** and **B** to deliver PI-9 gene to protect kidney cells from killing by GrB released from a human NK like cell line: YT was examined. Polymer **C**, too many of whose primary amines was blocked by mannose leading to inefficient DNA binding and transfection, was included as a negative control. The reason for selecting mannose-modified PEIs for investigation of the therapeutic gene delivery potential and the associated biological effects was due to the potential possibility of exploitation of the mannose receptor highly expressed on DCs for targeted gene transfer in the future [232], as well as the consistent low cytotoxicity demonstrated by the mannose-PEI conjugates in the various cell lines tested in Chapter 3. Here, facile nucleophilic addition chemistry described in Chapter 3 was employed to substitute primary amines in branched PEI (25 kDa) with roughly 7, 20 or 67 carbamate-mannose groups (determined by NMR spectra), generating polymers **A**, **B** and **C** respectively. The optimal degree of primary amines substitution was determined by a series of tests such as DNA binding, GFP-reporter gene delivery and cytotoxicity on HEK293T (human embryonic kidney cell line), and so on. Finally, the selected polymers with the optimal balance of substituted to free primary amines were further used to deliver PI-9 gene into HEK293T, and the degree of killing by GrB released from YT cells was assessed to investigate the efficacy of protection offered by PI-9 gene transfection.

Part of Chapter 4 has been published in Biomaterials [256], and was reproduced with permission from [256]. Copyright © 2013, rights managed by Elsevier Ltd.

4.2 Materials and Methods

4.2.1 Materials

Branched polyethylenimine with a molecular weight of 25 kDa, MTT for cytotoxicity assay, and other reagents for polymer synthesis were obtained from Aldrich and used without any further purification unless otherwise noted. GFP-reporter gene was obtained from Clontech (U.S.A.). MigR1-PI-9 encoding plasmid DNA was amplified in the *Escherichia coli* strain DH5 α , isolated and purified using a QIAGEN HiSpeed Plasmid Maxi Kit (Qiagen, UK). The concentration of DNA was determined using Nanodrop spectrophotometer (Thermo scientific, UK) by measuring the UV absorption at 260 nm. HEK293T human embryonic kidney and YT human natural killer-like leukemic cell lines were purchased from ATCC (U.S.A.) and cultured according to the instructions on the ATCC website.

4.2.2 Synthesis of protected mannose-functionalized cyclic carbonate (MTC-ipman) and MTC-ipman modified PEI

The protected mannose-functionalized cyclic carbonate (MTC-ipman) and the carbamate mannose-modified PEIs were synthesized by Dr. Chuan Yang in Dr. Yi Yan Yang's lab in IBN, A*STAR, Singapore. A single step, spontaneous ring-opening reaction of the cyclic carbonate generated a carbamate linkage and a primary hydroxyl group together with mannose protected with acetyl group, and the deprotection step revealed each mannose with 5 hydroxyl groups which were expected to reduce positive surface charge and cytotoxicity associated with PEI/DNA complexes. The detailed procedures for the synthesis of the MTC ipman and MTC-ipman modified PEIs, and the characterization of the monomers and polymers using ¹H NMR spectroscopy were described in the appendix.

4.2.3 Cell culture

HEK293T and YT cells were cultured in DMEM (Invitrogen, UK) and RPMI 1640 medium (Invitrogen, UK), respectively. Both growth media were supplemented with 10% (v/v) FBS, (Invitrogen, UK), penicillin at 100 U/mL, streptomycin at 100 μ g/mL, and L-glutamine at 2 mM (Invitrogen, UK), and the cells were cultured at 37 °C, under an atmosphere of 5% CO₂ and 95% humidified air. Both cells were subcultured using 0.25% trypsin/EDTA (1x) (Invitrogen, UK) when reaching 90% confluence.

4.2.4 Preparation, particle size and zeta potential analyses of polymer/DNA complexes

The polymer/DNA complexes were prepared as previously described under Section 3.2.4. Briefly, an equivolume solution of DNA was added to the polymer solution in nuclease free water to achieve the intended N/P ratios, followed by gentle vortexing for about 5 seconds. After equilibration at room temperature for 30 min, the complexes were subjected to particle size and zeta potential analysis, by dynamic light scattering (Brookhaven Instrument Corp., Holtsville, New York, U.S.A.) using a He–Ne laser beam at 658 nm with a scattering angle of 90° and Zetasizer (Malvern Instrument Ltd., Worcestershire, UK), respectively. Immediately prior to the particle size and zeta potential measurement, the polymer/DNA complexes in nuclease free water was diluted 10x in PBS to mimic the dilution in the physiological environment after i.v. administration. Both measurements were repeated for three runs per sample and reported as the mean ± standard deviation of three readings.

4.2.5 Gel retardation assay

DNA binding ability of the polymers was investigated using agarose gel electrophoresis as detailed in Section 3.2.5. Briefly, 20 µL polymer/DNA complexes prepared with N/P ratios ranging from 1 to 15 were electroporated on 1% agarose gel with ethidium bromide staining, which was conducted at 110 V for 50 minutes to detect the relative position of the complexed DNA to the naked DNA.

4.2.6 *In vitro* gene transfection

The *in vitro* gene transfection efficiency of the mannose modified PEIs/DNA complexes was investigated using HEK293 cell line. HEK293T cells were seeded onto 24-well plates at a density of 1×10^5 cells per 500 µL growth media per well, 24 h prior to transfection. Just before transfection, the plating media was replaced 0.5 mL of fresh growth media, and 50 µL of the polymer/GFP plasmid DNA complex solution (containing 1.75 µg DNA) at various N/P ratios was drop-wise added into each well. After 4 h of incubation, free DNA complexes were removed by changing the media in each well. 68 h incubation later, the cells were rinsed once with 0.5 mL of PBS (pH 7.4), and 0.2 mL of 0.25% trypsin-EDTA (1X) (Invitrogen, UK) was added to detach them, followed by adding 0.3 mL fresh growth media and centrifuging at 1500 rpm for 5 min. Two further cell-washing cycles of resuspension and centrifugation were carried out in FACS buffer, and the cell pellet was finally resuspended in FACS buffer for flow cytometry analysis of the percentage of cells transfected by GFP plasmid (FACSCalibur, BD Bioscience, San Jose, CA, USA). 10,000 events were collected, and percentage of cells expressing GFP was reported as mean ± standard deviations of triplicates. Cells were defined

to be GFP positive by setting the gating region to include <0.5% of cells transfected with naked GFP plasmids alone. The data were statistically analyzed for significant differences based on the student's *t* test at $p < 0.0001$.

4.2.7 Confocal imaging for GFP expression in HEK293T cells

HEK293T Cells were treated in the similar fashion as described in Section 4.2.6 with polymer/GFP plasmid DNA complexes at intended N/P ratios (unmodified PEI: N/P 10; polymer **A**, **B** and **C**: N/P 30). After 72 h of transfection, the medium in the wells containing transfected cells was removed, and the cells were washed once with PBS and fixed with paraformaldehyde for 15 min. Then, the cells were washed 3 times with ice cold PBS and imaged using a Motorized Zeiss AxioVert 200M inverted microscope (Carl Zeiss, Germany).

4.2.8 Cytotoxicity test

The cytotoxicity of the polymers was studied using the standard MTT assay protocol. Briefly, HEK293T cells were seeded onto 96-well plates at a density of 10,000 cells per well one day before experiment. Polymer/GFP DNA complexes at various N/P ratios were prepared in nuclease-free water as described in Section 4.2.4. The cells in each well were then transfected with 10 μ L of polymer/DNA complex solution containing 0.35 μ g of GFP plasmid for 4 h at 37 $^{\circ}$ C. Untreated cells were used as control. Then the wells were replaced with fresh growth media and incubated further for 68 h. Subsequently, the cell viability was assessed by replacing all wells with 100 μ L of growth medium and 20 μ L of MTT solution (Sigma, 5 mg/mL in PBS) and incubating the cells for 4 h at 37 $^{\circ}$ C according to the manufacturer's directions. Resultant formazan crystals formed in each well were solubilized using 150 μ L of DMSO after careful aspirating of the growth medium. The absorbance of the solution in each well was measured using a microplate spectrophotometer (PowerWave X, Bio-Tek Inc., Winooski, VT, USA) at wavelengths of 550 nm and 690 nm. Relative cell viability was expressed as $[(A_{550}-A_{690})_{\text{sample}} / (A_{550}-A_{690})_{\text{control}}] \times 100\%$. Data are expressed as mean \pm standard deviations of eight replicates at every N/P ratio.

4.2.9 Characterization of GrB expression level in YT cells

To evaluate the GrB expression level in YT cells, intracellular staining by PE-conjugated anti-GrB antibody and an isotype matched control antibody (Sigma, UK) was carried out. Briefly, 1 million YT cells were incubated in 250 μ L Cytofix/Cytoperm solution (BD Biosciences) at 4 $^{\circ}$ C for 20 min for permeabilization, followed by pelleting and

resuspension in 50 μ L of BD Perm/Wash solution containing a pre-determined optimal concentration of a fluorochrome(PE)-conjugated anti-GrB antibody or the isotype control antibody, and incubated at 4°C for 30 minutes in the dark. After that, cells were washed two times with 1 mL 1 \times BD Perm/Wash solution and resuspended in 300 μ L FACS buffer prior to flow cytometric analysis. The results were analyzed using the Summit software.

4.2.10 *In vitro* protection of HEK293T cells from YT cell killing by transfection with polymer/PI-9 encoding plasmid DNA complexes

The protective effect of polymer/PI-9 plasmid DNA complexes was evaluated by a killing assay in which human natural killer-like leukemic YT cells were used as the effector [288] and HEK293T cells were the target. Calcein-acetoxymethyl (Calcein-AM, Invitrogen, UK), a fluoresceinated molecular probe that is retained within the intact membranes of live cells but excluded by cells with damaged membranes, was used to measure the percentage of cell killing [289]. Briefly, YT cells were collected, washed and re-suspended to 5 \times 10⁶ cells/mL in RPMI, 100 μ L of which was dispensed into each well of a 96 well round bottom plate. Moreover, HEK293T cells were transfected using the polymer/DNA complexes at N/P 10, 20 and 40, respectively, in a 24-well plate as described in Section 4.2.6. Three days after transfection, HEK293T cells were trypsinized, washed and re-suspended at 2 \times 10⁶ cells/mL in RPMI, followed by adding Calcein-AM to reach 15 μ M final concentration, and incubating for 30 min with occasionally mixing. Then the Calcein-AM labelled HEK93T were washed twice with RPMI and re-suspended to 10⁵ cells/mL, 100 μ L of which was dispensed to each well of the 96-well plate containing 5 \times 10⁵ YT cells to reach effector:target (E:T) ratio of 50:1. After incubating the effector and target cells together for 4 h, 100 μ L of the supernatant was removed to be read on a microplate spectrophotometer at excitation and emission wavelengths of 485 nm and 530 nm respectively. Wells for spontaneous release (100 μ L of fresh RPMI medium without YT cells was added) and maximal release (100 μ L of 5% Triton X-100 instead of YT cells for total lysis of the cells was added) of Calcein-AM were included as negative and positive controls respectively. Untreated and empty MigR1 plasmid mock-transfected HEK293T cells were used as the negative controls. The data were expressed as light units per minute (LUPM). The average values were determined from 4 replicates for every N/P ratio and control. Percent cytotoxicity was determined using the following formula:

$$\text{Percent Cytotoxicity} = \frac{\text{Experimental sample (LUPM)} - \text{Spontaneous release (LUPM)}}{\text{Maximum release (LUPM)} - \text{Spontaneous release (LUPM)}} \times 100$$

Statistical analysis was performed using the Student's *t* test, and the differences were considered statistically significant at $p < 0.05$.

4.3 Results and Discussion

4.3.1. Polymer synthesis and composition

Nucleophilic addition between primary amine and a protected mannose-functionalized cyclic carbonate (MTC-ipman) was used to block primary amine groups of PEI in order to reduce its inherent cytotoxicity. Scheme 1 in Section 3.3.1 shows the synthesis procedures and structures of carbamate-mannose modified PEIs (polymer **A**, **B** and **C**). Substitution of MTC-ipman onto primary amines of the PEI was a simple click reaction that was carried out by mixing two feeds in DCM for 1 h, in the presence of the DBU catalyst. It is well known that primary amines are much more nucleophilic than secondary amines. When MTC-ipman concentrations were below the molar concentration of primary amine groups, the ring-opening of the cyclic carbonate generated a carbamate linkage and a primary alcohol, which modified a portion of the primary amines of the branched PEI. However, when MTC-ipman concentrations exceeded the molar concentration of primary amines (in the case of polymer **C**), effectively all primary amine groups were blocked, and part of secondary amine groups were also substituted by the MTC-ipman. After the nucleophilic addition reaction, the protecting groups of mannose moieties were removed by heating and refluxing in methanol and 1 M HCl for 2 h, giving rise to carbamate-mannose modified PEIs. The ^1H NMR analysis allowed quantitative comparisons between the integral intensities of methylene peaks of PEI and those of methyl peaks of carbamate mannose moieties, thus the compositions of the polymers were elucidated (Figure 5 in Section 3.3.1, Table 6). The result showed that the content of mannose in the polymer identified in the ^1H NMR spectrum was proportional to that in the feed.

Table 6. Compositions, nitrogen contents, and ^1H NMR analysis of carbamate-mannose modified PEI. Higher nitrogen content correlates with lower substitution degree. Substitution degree: $A < B < C$. (PEI: 58 primary amines, 116 secondary amines and 58 tertiary amines).

Polymer	Nitrogen Content (%)	Method of mannosylation	Mole Ratio Found (NMR) bPEI: Carbamate Groups ^a	% of bPEI Primary Amine Groups Modified (NMR) ^b	# of bPEI Primary Amine Groups Modified Per Mole bPEI ^{a,c}
A	24.4	bPEI : ipman = 3:1 (mass ratio) (molar ratio = 1:8)	1:7	12.1	7

B	16.3	bPEI : ipman = 1:1 (mass ratio) (molar ratio = 1:25)	1:20	34.5	20
C	8.14	bPEI : ipman = 1:3 (mass ratio) (molar ratio = 1:75)	1:67 ^a	115.5 ^b	67 ^c

^a based on 1 mole bPEI-25 = 10000 g, containing 58 primary amine groups per mole.

^b A value greater than 100% indicates reaction at all active primary amine sites, and reaction of secondary amine groups.

^c A number greater than 58 indicates reaction at all active primary amine sites, and reaction of secondary amine groups.

4.3.2 Size and zeta potential of polymer/DNA complexes

As an important parameter for effective cellular uptake of polymer/DNA complexes, size was investigated using dynamic light scattering [264]. As can be seen from Figure 7A in Chapter 3, generally, the size of the polymer/DNA complexes negatively correlated with N/P ratio, indicating that stronger electrostatic interaction between the anionic polymer and cationic DNA at higher N/P ratio led to the formation of more compact complexes with smaller hydrodynamic sizes. Especially, the sizes of polymers **A** and **B** plunged from over 1000 and 400 nm at N/P 5 to 103 and 119 nm at N/P 30, respectively. Also, as polymer **A** has the least amount of primary amine groups blocked by mannose, under the same reaction conditions, **A** and DNA had stronger electrostatic interaction, and thus formed more compact polymer/DNA complexes than polymers **B** and **C** (103 nm vs. 119 nm and 500 nm for **B** and **C** respectively, at N/P 30). As demonstrated in Figure 7A, polymer **C** which has PEI:MTC-ipman attachment ratio of 1:67 failed to complex DNA as effectively as **A** and **B** due to insufficient free primary amines available, leading to large particles even at high N/P ratios (Figure 7A). Moreover, **A**/DNA and **B**/DNA complexes had small size distribution, as the polydispersity indices of them were found to be 0.200 and 0.178, respectively. As a comparison, DNA complexes formed with unmodified PEI, which conferred high gene transfection efficiencies in various cell lines [106], were found to have a hydrodynamic size of ~84 nm.

The surface charge of gene delivery vectors plays a pivotal role in determining gene transfection efficiency [110]. Extensive studies have demonstrated that DNA condensation and stabilization are enhanced when a carrier possesses a net positive surface charge [102, 290]. Additionally, a net positive surface charge of carrier/DNA complexes is favourable for effective cellular uptake via electrostatic interactions with the negatively charged phospholipid

surface of the cell membrane. Indeed, the cationic mannose-attached PEIs interacted electrostatically with the anionic DNA to give rise to **A**/DNA and **B**/DNA complexes with positive zeta potentials at N/P 10-30 of approximately 18-23 mV in nuclease free water (Figure 7E), which were found to be comparable to the 22 mV obtained with unmodified PEI/DNA formulated at N/P ratio 10. **C**/DNA complexes however, had a significantly lower cationic charge density on the surface at all N/P ratios tested, which was only ~5-13 mV. The high percentage of mannose conjugation on the primary amines on polymer **C**, rendering them unavailable for protonation in the nuclease free water was the most probable reason for this phenomenon. Therefore, taking the smaller particle size and relatively higher zeta potential together, polymers **A** and **B** were expected to be more effective in gene transfection as compared to polymer **C**.

4.3.3 DNA binding ability of polymers

As DNA binding by a gene delivery vector constitutes an important first step for the formation of stable and compact DNA complexes that are essential for efficient cellular uptake, gene binding ability of the polymers was evaluated by gel retardation assay [102]. As shown in Figure 8 in Chapter 3, same as unmodified PEI, polymers **A** and **B** were able to bind to and condense DNA effectively from N/P ratio of 1. The degree of DNA binding and hence the retardation of its movement across the agarose gel was enhanced with increasing concentrations of the cationic polymers **A** and **B**, giving rise to complete retardation of DNA movement at N/P ratio of 3 (Figure 8). In contrast, **C** had poor DNA binding ability, showing complete DNA retardation only at N/P 15. More primary amine groups consumed for carbamate-mannose modification contributed to the poor DNA binding ability of **C**. These results suggested that PEI with 7 or 20 of 56 primary amine groups substituted by the carbohydrate condensed DNA effectively.

4.3.4 *In vitro* GFP transfection efficiency

In order to assess the suitability of using the carbamate-mannose modified PEIs as DNA delivery vectors, we transfected the GFP-reporter gene into HEK293T cells using these polymers. The evaluation of gene transfection in the presence of serum offers a more accurate assessment of the gene delivery efficiency of the polymers in serum protein-containing physiological environments. As shown in Figure 23, the unmodified PEI showed prominent gene transfection capability in HEK93T cells, reaching a plateau of nearly 100% transfection efficiency from N/P 10 onwards. The GFP expression profiles of polymers **A** and **B** in

HEK293 were similar, with GFP expression increasing with N/P ratio. Although the gene transfection efficiency for **A** and **B** at N/P 6-20 was lower than that of the unmodified PEI, **A** and **B** quickly emulated PEI, and reached nearly 100% GFP transfection efficiency at N/P 30 and higher (Figure 23). In sharp contrast, polymer **C** only achieved less than 3% GFP transfection efficiency even at the highest N/P ratio tested: N/P 40 (Figure 23). Furthermore, the GFP gene transfection efficiency by the various polymers assessed by flow cytometry were verified by confocal microscopy studies showing the GFP expressing HEK293T cells 72 h after the cells being transfected by the modified and unmodified PEI (Figure 24). Unmodified PEI (N/P 10), **A**:PEI-Mannose(1:8) (N/P 30) and **B**:PEI-Mannose(1:25) (N/P 30) all showed evident GFP expression inside almost all the cells in the field of view (Figure 24A-F), while **C**:PEI-Mannose(1:75) (N/P 30) hardly mediated any transfection of GFP plasmid into the HEK93T cells (Figure 24G, H). These results were correlated well with polymer gene binding ability, DNA complex size and zeta potential data (Figure 7A, 7E and Figure 8) and met our expectation. All in all, both unmodified PEI and carbamate-mannose modified PEIs with primary amine groups partially blocked at optimal ratios mediated high gene transfection efficiency in HEK93T cells.

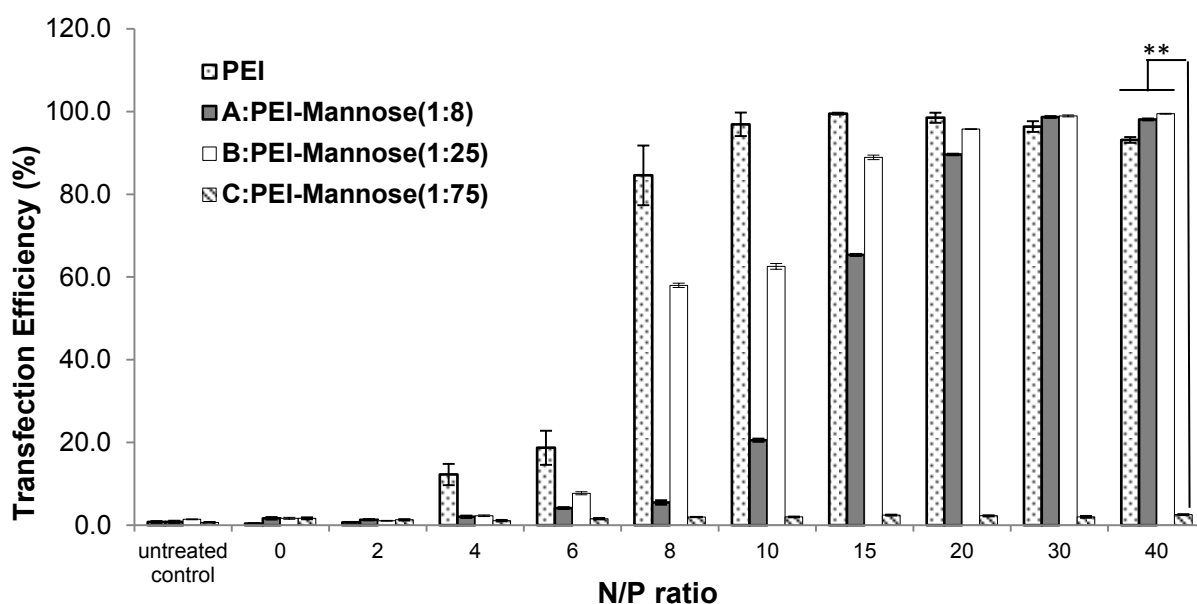


Figure 23. *In vitro* GFP transfection in HEK293T cells. GFP transfection efficiency mediated by various polymers at different N/P ratios. Results represent mean \pm standard deviation of triplicates. Polymer concentrations in the order of N/P ratios specified: PEI - 0, 0.8, 1.6, 2.4, 3.2, 4.0, 6.0, 8.0, 12.0, and 16.0 mg/L. Polymer **A** - 0, 1.1, 2.2, 3.3, 4.4, 5.5, 8.2, 11.0, 16.4, and 21.9 mg/L. Polymer **B** - 0, 1.6, 3.3, 4.9, 6.6, 8.2, 12.3, 16.4, 24.6, and 32.8 mg/L. Polymer **C** - 0, 3.3, 6.6, 9.9, 13.1, 16.4, 24.6, 32.8, 49.3, and 65.7 mg/L. Data are shown as mean \pm SD (n=3);

student's *t* test, $**p < 0.05$). Reproduced with permission from [256]. Copyright © 2013, rights managed by Elsevier Ltd.

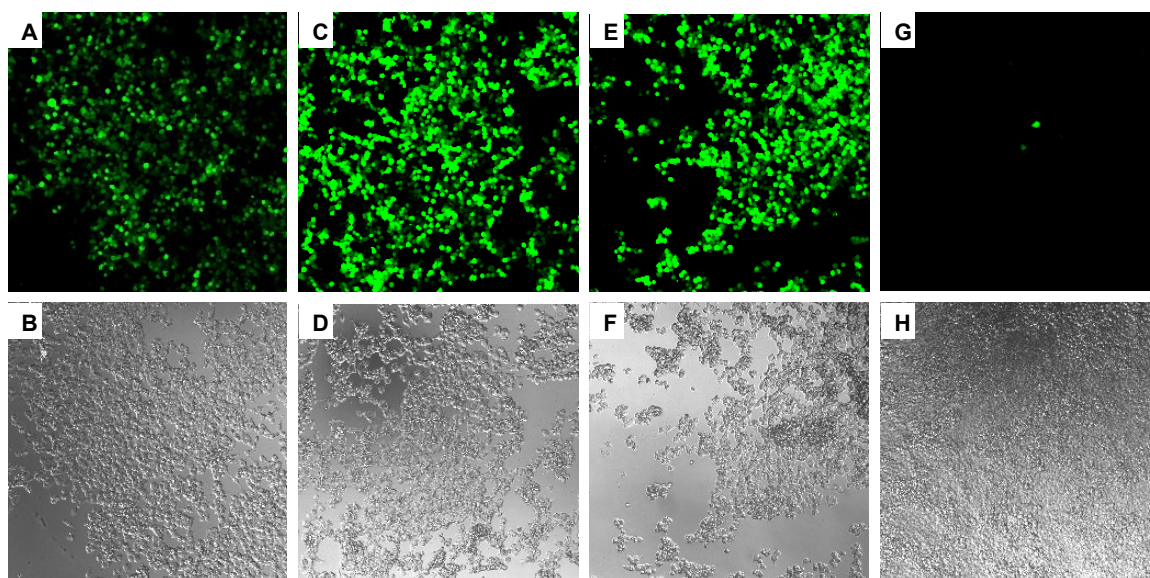


Figure 24. Confocal microscopic images of GFP-transfected HEK293T cells mediated by unmodified PEI at N/P 10 (A and B), polymer **A** at N/P 30 (C and D), polymer **B** at N/P 30 (E and F) and polymer **C** at N/P 30 (G and H). Reproduced with permission from [256]. Copyright © 2013, rights managed by Elsevier Ltd.

4.3.5 Cytotoxicity of unmodified and carbamate-mannose modified PEIs

Overt cellular toxicity remains as one of the biggest challenges to overcome in the quest for a novel and efficient non-viral gene delivery vector [102, 290]. The cytotoxicity of unmodified and modified PEIs was evaluated in HEK293T cells using the standard MTT assay protocol. As demonstrated in Figure 25, the notoriously high cytotoxicity of the “gold standard” unmodified PEI was aptly demonstrated by the viability of HEK293T cells treated with it, which drastically decreased with increasing PEI concentration. Specifically, only approximately 81%, 63% and 43% HEK293T cells were viable after 4 h of incubation with 4.0, 6.0 and 8.0 mg/L of PEI (corresponding to PEI concentrations at N/P 10, 15 and 20), respectively. However, the cytotoxicity problem seemed to be almost completely mitigated by the treatment of all the three carbamate-mannose modified PEIs at all concentrations tested. For example, amazingly, under the same treatment conditions, polymers **A**, **B** and **C** even at the highest concentrations (21.9, 32.8 and 65.7 mg/L respectively) still maintained the HEK293T cell viability at about 100%. This degree of cell viability contrasts very favorably with the significant cytotoxicity obtained with unmodified PEI.

As discussed in Section 3.3.6, feeding a cell with many membrane-disrupting particles consecutively enabled endo/lysosomal enzyme release into the cytoplasm and disturbance of vital cellular processes, resulting in high cytotoxicity [106]. A prominent example is the unmodified PEI, which due to its high surface charge density, interacts favourably with the anionic cell membrane, and even induces hole formation or expands the size of pre-existing defects on the cellular membrane. It was reported that the cell membrane holes due to the action of PEI caused leakage of more significant amounts of the cytosolic enzyme lactate dehydrogenase (LDH) as compared to other cationic polymers such as poly-L-lysine (PLL) in human epithelial KB and rat fibroblast Rat2 cell lines, as PEI possesses a much greater charge/monomer ratio than those counterparts [118]. Therefore, the cytotoxicity of unmodified PEI in HEK293T cells observed in the present study could be very much attributed to the impairment of important membrane functions by PEI [272]. Although the GFP transfection efficiency mediated by PEI was observed to reach the highest level of nearly 100% at a moderately low N/P ratio of 10, its high toxicity in HEK293T cells from N/P 15 onwards hampered its potential *in vivo* application which usually requires a high polymer concentration to achieve distinctive therapeutic effects. Thus, the present study clearly demonstrated the advantage of the modified PEIs as potential *in vivo* gene delivery vectors, whose primary amines were substituted by the carbamate-mannose at various degrees, as they not only significantly enhanced the cellular viability, but also achieved comparable high gene transfection efficiency as compared to the unmodified PEI. Mannose is a common metabolite and well tolerated by the cells. Carbamate-mannose modified PEIs condensed DNA effectively and formed nanoparticles with a mannose shell, which led to reduced charge density and thus mitigated cytotoxicity. Similar phenomenon was reported previously in the literature, which stated that although cationic polymers such as PEI with high charge density had strong cell lytic and toxic properties, a reduction of charge density by reaction with glycidol, which converted primary and secondary amines to secondary and tertiary ones respectively, resulted in less cell toxicity [291].

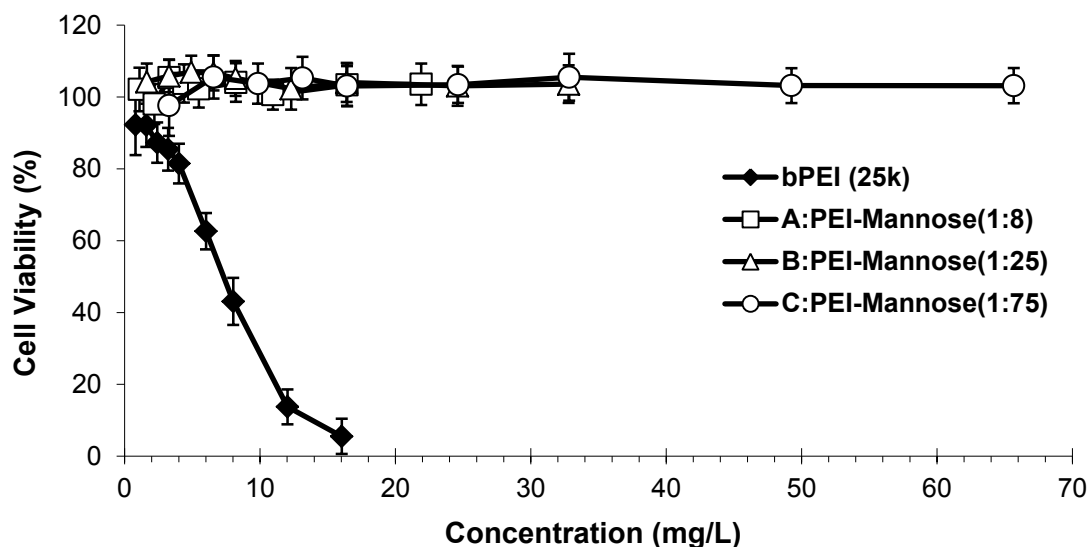


Figure 25. Viability of HEK293T cells after incubation with unmodified PEI/DNA and carbamate-mannose modified PEI/DNA complexes at various concentrations. Results represent mean \pm standard deviation of 8 replicates. Polymer concentrations in the order of N/P ratios (0, 2, 4, 6, 8, 10, 15, 20, 30 and 40): PEI - 0, 0.8, 1.6, 2.4, 3.2, 4.0, 6.0, 8.0, 12.0, and 16.0 mg/L. Polymer **A** - 0, 1.1, 2.2, 3.3, 4.4, 5.5, 8.2, 11.0, 16.4, and 21.9 mg/L. Polymer **B** - 0, 1.6, 3.3, 4.9, 6.6, 8.2, 12.3, 16.4, 24.6, and 32.8 mg/L. Polymer **C** - 0, 3.3, 6.6, 9.9, 13.1, 16.4, 24.6, 32.8, 49.3, and 65.7 mg/L. Reproduced from [256]. Copyright © 2013, rights managed by Elsevier Ltd.

4.3.6 Protection of HEK293T cells from GrB mediated killing

Having demonstrated the high gene transfection efficiency and low cytotoxicity profiles of the carbamate-mannose modified PEIs, especially polymers **A** and **B**, it would be interesting to employ them for *in vitro* biological functional applications. Since PI-9 is a specific and physiologically relevant inhibitor of granzyme B, we examined the ability of PI-9 gene delivered by the modified PEIs into HEK93T cells to protect them against GrB mediated cytotoxicity *in vitro*. In this system, death by GrB was induced by exposure to intact human NK-like leukemic YT cells [288].

YT cells have been reported to express high levels of GrB constantly and thus demonstrate strong killing activity *in vitro* [292-294]. In order to verify that the YT cells used in this study are potent killer cells, intra-cellular staining of GrB by a PE-conjugated anti-GrB antibody was carried out, while isotype-matched control antibody of irrelevant specificity was used to ensure the GrB binding was specific. Figure 26 showed that YT cells in standard culture condition expressed high level of GrB, thus they could potentially function as a potent killer against HEK293T cells.

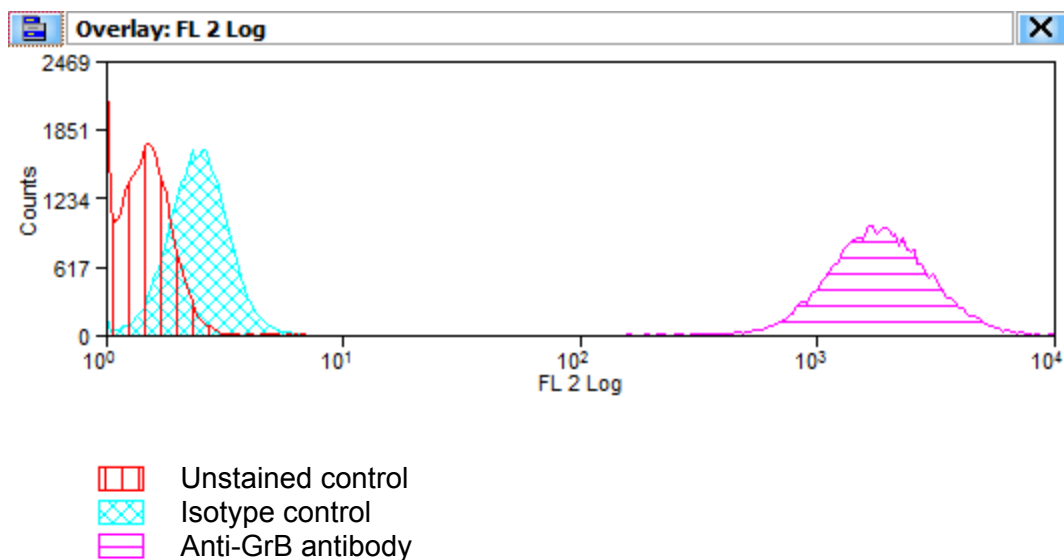


Figure 26. Intracellular staining of GrB on YT cells under standard cell culture condition.

As shown in Figure 27, HEK293T cells as the target cells when transfected with PI-9, showed less cytotoxicity than those transfected with empty plasmids or untreated control when challenged by WT YT killer cells, confirming the inhibitory role of PI-9 against GrB-mediated apoptosis [70]. Moreover, PI-9 delivered by different polymers demonstrated distinct abilities to protect against GrB. Specifically, at effector:target ratio of 50:1, **A** and **B** provided more potent protection of HEK293T cells against GrB-mediated killing, at N/P 20 and 40, where more than 70-80% cells were viable as compared to ~ 30% viability of untreated HEK293T cells. It is worth to be noticed that at N/P 10, the difference in cytotoxicity between **A/B** and **C** was not evident (53.0% for **A**, 47.1% for **B**, and 53.3% for **C**). This was probably due to the fact that the gene transfection efficiency for **A** and **B** at N/P 10 (20.5% and 62.6% respectively) had not reached the threshold of physiologically significant demonstration of protection against GrB-mediated apoptosis. When the threshold of physiologically relevant protection was not reached, the cytotoxicity contributed by bystander and indirect killing unspecific in the cell culture might also account for the insignificant protection by PI-9 delivered at N/P 10 by **A** and **B**. However, when the N/P ratio increased to 20 and 40, gene transfection efficiency shot up to close to 100% for **A** and **B**, while polymer **C** still conferred very low gene transfection efficiency, which was below 3%, and it conferred only slight protection of HEK293T cells against YT cell killing. Thus, the difference in cytotoxicity when challenged with YT cells killing between **A/B** and **C** was obvious and statistically significant (25.6%, 25.5% and 40.5% for **A**, **B** and **C** respectively, at N/P 40). On the other hand, the transfection of PI-9 encoding plasmid into HEK293T cells induced by unmodified PEI at N/P 10 and 20 provided effective

protection of the cells from GrB-mediated killing (Figure 27), which was consistent with its high gene transfection efficiency (Figure 23). However, at N/P 40 (i.e. PEI concentration: 16.0 mg/L), PI-9 lost its potent protective effect, with about 55% cells killed (Figure 27). This was presumably due to PEI's high intrinsic cytotoxicity at high N/P ratio, which hampered its biological usefulness. Therefore, carbamate-mannose modified PEIs at appropriate mannose attachment ratios: polymers **A**:PEI-Mannose(1:8) and **B**:PEI-Mannose(1:25) were superior to unmodified PEI due to PEI's intrinsic cytotoxicity.

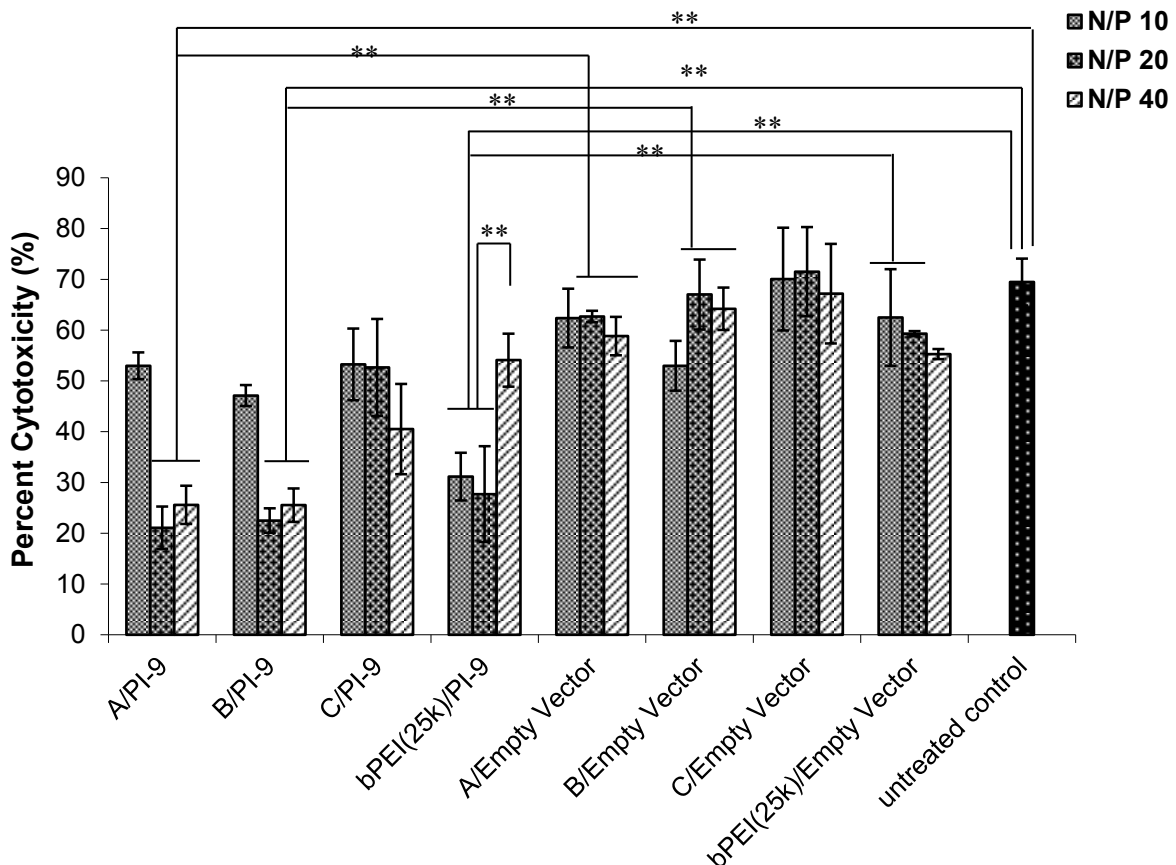


Figure 27. Viability of HEK293T cells after incubation with YT cells for 4 h. HEK293T cells were transfected with PI-9 encoding plasmid using **A**, **B** and **C** at N/P 10, 20 and 40 in comparison with unmodified PEI and empty plasmids (i.e. empty vector). Polymer concentrations in the order of N/P ratios specified: PEI -4.0, 8.0, and 16.0 mg/L. **A** -5.5, 11.0 and 21.9 mg/L. **B** -8.2, 16.4 and 32.8 mg/L. **C** -16.4, 32.8 and 65.7 mg/L. Each data represents mean \pm SD (n=4; student's *t* test, ** $p < 0.05$). Reproduced from [256]. Copyright © 2013, rights managed by Elsevier Ltd.

4.4 Conclusions

In this study, a novel platform for synthetic gene vectors was developed and their biological functions were tested. After successful modification of PEI by selectively blocking a portion of the primary amine groups with a mannose-functionalized cyclic carbonate through

facile nucleophilic addition chemistry, the degree of carbamate-mannose substitution was readily controlled, as evidenced by NMR spectra readings. The polymers **A**:PEI-Mannose(1:8) and **B**:PEI-Mannose(1:25) at the optimal substitution degrees of carbamate-mannose effectively condensed DNA into nanosized complexes with narrow size distribution and positive zeta potential, which induced high gene transfection efficiency and significantly reduced intrinsic cytotoxicity as compared to unmodified PEI. These carbamate-mannose modified PEIs successfully delivered PI-9 encoding plasmid into HEK293T human embryonic kidney cells which were protected from killing by human NK cells (YT cells) to a great extent, compared to the empty-vector transfected and the untreated HEK293T cells. Also, these modified PEIs outperformed the unmodified PEI at relatively high N/P ratio of 40, as effective protection of HEK293T cells by PI-9 gene delivery was evident for **A** and **B** at high N/P ratio, but was lost in the case of unmodified PEI, largely due to its intrinsic cytotoxicity against the target cells, which masked the effect of PI-9, despite its high gene transfection efficiency at N/P 40. These findings suggest that the delivery of PI-9 gene by the modified PEIs has the potential to target pathogenic GrB and so alleviate allograft rejection and other inflammatory diseases. Thus, aim 2 described in Chapter two was partially fulfilled, while the exploration of the potential of using other functionally modified PEIs to deliver the PI-9 gene to other cell types to protect them from GrB released from other killer cells will be presented in the next chapter.

CHAPTER 5: CARBAMATE-MANNOSE MODIFIED PEI DELIVERY OF A GRANZYME B INHIBITOR GENE TO MOUSE FIBROBLAST BALB/3T3 CELLS TO PROTECT AGAINST GrB MEDIATED KILLING

5.1 Introduction

Based on the results in Chapter 4, the degree of primary amines substitution for PEI is a paramount factor determining the satisfactory performance of the modified polymer. When molar feed ratio of 1:75 (PEI:mannose) was applied in the nucleophilic addition reaction, all the primary amines of PEI were consumed, rendering the modified PEI (polymer C) ineffective in DNA condensation and transfection. Therefore during PEI modification by functionalized carbamate, a careful balance must be stricken between the amount of free and substituted amines. This chapter serves as an extension to Chapter 4, where three other mannose-modified PEIs were synthesized at PEI to MTC-ipman monomer conjugation ratios of 1:6, 1:12.5, and 1:25, in the absence of the DBU catalyst, which further simplified the synthesis process as compared to Chapter 4. After investigating the physicochemical properties, GFP reporter gene transfection capability, as well as cytotoxicity of these modified PEIs on mouse fibroblast cell line Balb/3T3, we examined the potential of using them to deliver PI-9 gene to and protect the Balb/3T3 cells from cytotoxicity caused by GrB secreted from allo-specific CTLs from B6 mice or YT cell line. The reason of using two types of killer cells was because they have different killing mechanisms toward the same target cell. Finally, the potential *in vivo* work for measuring the longevity of the PI-9 transfected Balb/3T3 cells after i.v. injection was introduced.

5.2 Materials and Methods

5.2.1 Materials

Branched PEI with a MW of 25 kDa, MTT for cytotoxicity assay, and other reagents for polymer synthesis were obtained from Aldrich and used without any further purification unless otherwise noted. GFP-reporter gene was obtained from Clontech (U.S.A.). pcDNA3.1-hGH vector encoding human growth hormone (hGH) gene and the empty pcDNA3.1 vector were kindly provided by Professor Peter E. Lobie from Cancer Science Institute of Singapore, and contain gene expressing neomycin phosphotransferase, conferring resistance to G418. PI-9 encoding plasmid DNA MigR1-PI9 was amplified in the *Escherichia coli* strain DH5 α , isolated and purified using a QIAGEN HiSpeed Plasmid Maxi Kit (Qiagen, UK). The

concentration of DNA was determined by measuring the UV absorption at 260 nm by Nanodrop spectrophotometer (Thermo scientific, UK). YT human natural killer-like leukemic cell lines were purchased from ATCC (U.S.A.). The immortalised mouse fibroblast cell line Balb/3T3 was stemmed from the clone A31-1-1, and was kindly provided by Dr. Jessica Ponti from European Commission, Joint Research Centre, Institute for Health and Consumer Protection, Nanobiosciences Unit, Ispra, VA, Italy.

5.2.2 Synthesis of mannose-functionalized cyclic carbonate (MTC-ipman) and mannose-modified bPEI-25 in the absence of DBU

The monomers with protected mannose pendent groups is designated MTC-ipman, they and the carbamate mannose-modified PEIs were synthesized by Dr. Chuan Yang in Dr. Yi Yan Yang's lab in IBN, A*STAR, Singapore, according to a protocol reported previously [295]. Briefly, a single step, spontaneous ring-opening reaction of the cyclic carbonate generated a carbamate linkage and a primary hydroxyl group together with mannose protected with acetyl group, and the deprotection step revealed each mannose with 5 hydroxyl groups which were expected to reduce positive surface charge and cytotoxicity associated with PEI/DNA complexes. Polymers **T**, **S** and **G** were synthesized without DBU using a molar feed ratio bPEI-25:MTC-ipman of 1:6, 1:12.5 and 1:25, respectively, and mass feed ratio of 4:1, 2:1 and 1:1, respectively, for 1 hour before acidification. In each case, available primary amine sites exceeded the available MTC-ipman. The PEI:MTC-ipman molar ratio found by NMR for polymer **T**, **S** and **G** was 1:5.5, 1:12.2, and 1: 23, respectively. The detailed procedures for the synthesis of the MTC-ipman and MTC-ipman modified PEIs, and the characterization of the monomers and polymers using ¹H NMR spectroscopy were described in the appendix.

5.2.3 Cell culture

YT cells were cultured in RPMI 1640 medium (Invitrogen, UK) supplemented with 10% (v/v) fetal bovine serum (FBS, Invitrogen, UK) and PSG (v/v) (penicillin at 100 U/mL, streptomycin at 100 µg/mL, and L-glutamine at 2 mM, Invitrogen, UK), and split every two days, when cells reach 90% confluence.

Experimental cultures of the mouse fibroblast cell line Balb/3T3 were prepared from deep-frozen stock vials and always maintained in a sub-confluent state (less than 70% of confluence). Cells were maintained in complete culture medium made by DMEM (Gibco®, UK) added with 10% (v/v) fetal bovine serum and 1% (v/v) PSG.

All cells were maintained under standard cell culture conditions (37 °C, 5% CO₂ and 95% humidity, in GALAXY® DIRECT HEAT CO₂ INCUBATORS, RS Biotech, UK).

5.2.4 DNA handling, transformation of bacteria with recombinant DNA, and maxiprep

pcDNA3.1-hGH vector encoding hGH gene and the empty pcDNA3.1 vector were bound to two pieces of sterile filter paper upon arrival. To extract the DNA, the DNA bound filter paper was transferred to a sterile microcentrifuge tube. 100 µl distilled water was added to the tube and incubated for 1 h at room temperature. The DNA was resuspended by gently pipetting up and down 5-10 times and stored at –20°C till use.

Transformation was carried out in the ultra-competent *E.coli* strain. 50 µl of the competent cells were removed from –70°C and thawed on ice. 1 µL plasmid DNA (around 50 ng) was added to the 50 µl cell suspension, mixed thoroughly in a 1.5 mL autoclaved microcentrifuge tube by finger flicking and incubated on ice for 30 min. After that, the cells were heat-shocked by immersion in a 42°C water bath for 45 seconds without shaking, followed by transferring the tube on ice for 1-2 min. 500 µl of room temperature LB broth was added to the heat-shocked reaction and the tube was then transferred to an agitating incubator at 37°C for 60 min at 700 rpm. The tube was then centrifuged at 8000 rpm for 5 min and the supernatant was removed taking caution not to disturb the pellet. The pellet was resuspended in 300 µl of fresh LB broth, and a volume of 50-200 µl of the bacterial transformation was evenly spread on LB agar plates containing appropriate antibiotics (100 µg/mL ampicillin for pcDNA3.1 and pcDNA3.1-hGH) using a sterile spreader. The agar plate was then placed in a 37°C incubator overnight. Single colonies were isolated on the LB plate and propagated in LB media for plasmid DNA preparation.

Plasmid DNA was prepared according to the protocol provided with QiagenHispeed Plasmid Maxi Kit (Qiagen® Ltd, UK). Briefly, a single colony was picked from a freshly streaked selective plate and inoculated into a starter culture of 2–5 mL LB medium containing the appropriate selective antibiotic (100 µg/mL ampicillin for pcDNA3.1 and pcDNA3.1-hGH), which was incubated for approximately 8 h at 37°C with vigorous shaking (approximately 300 rpm). The starter culture was then diluted 1000 times into selective LB medium. For high-copy plasmids like pcDNA3.1, 150 µL starter culture was inoculated into 150 mL medium, which was then incubated at 37°C for 12–16 h with vigorous shaking (approx. 300 rpm). A volume of 100 mL of bacteria was harvested by centrifugation at 6000 x g for 15 min at 4°C in a Sorval

SS34 rotor (Du Pont Instruments, UK). The pellet was resuspended in 10 mL Buffer P1 (50 mM Tris HCL [pH 8.0], 10 mM EDTA, 100 µg/mL RNase A) and the bacteria were lysed by 10 mL Buffer P2 (0.2 M Sodium hydroxide, 1% SDS) by vigorously inverting the sealed tube 4–6 times, and incubating at room temperature (15–25°C) for 5 min. The mixture was neutralized with 10 mL chilled Buffer P3 (3 M KAc, [pH 5.5]), and the resulting precipitate of protein and genomic DNA was poured into the barrel of the QIAfilter Cartridge and incubated at room temperature for 10 min. Then the plunger was inserted into the QIAfilter Maxi Cartridge and the cell lysate was filtered into the previously equilibrated HiSpeed Tip (equilibrated with 10 mL Buffer QBT), and allowed to pass through the resin by gravity flow. The column was then washed with 60 mL Buffer QC (1 M NaCl, 50 mM MOPS [pH 7.0] and 15% isopropanol) and bound plasmid DNA was eluted with 15 mL Buffer QF (1.25 M NaCl, 50 mM MOPS [pH 7.0] and 15% isopropanol). Eluted plasmid DNA was then precipitated with 10.5 mL (0.7 volumes) room temperature isopropanol, mixed and incubated at room temperature for 5 min. The Eluate/isopropanol mixture was then transferred into a 30 mL syringe with a QIAprecipitator Maxi Module attached onto the outlet nozzle, filtered through the QIAprecipitator using constant pressure. Subsequently, 2 mL 70% ethanol was added to the syringe and pressed through the QIAprecipitator using constant pressure to wash the DNA. The DNA was dried by pressing air through the QIAprecipitator quickly and forcefully for a few times and eluted by 1 mL of Buffer TE. The final plasmid DNA concentration was accurately determined by Nanodrop spectrophotometer (Thermoscientific, UK).

5.2.5 Generation of stable cell transfectants

In order to generate stable Balb/3T3 cells expressing and secreting hGH protein, pcDNA3.1 vector alone and pcDNA3.1-hGH vector were stably transfected into Balb/3T3 cells by the use of Lipofectamine[®] 2000 (Invitrogen, UK) and the stably transfected cells were selected by Geneticin[®] Selective Antibiotic (G418 Sulfate, Invitrogen, UK). These gene plasmid vectors contain gene expressing neomycin phosphotransferase, conferring resistance to G418. As the selection condition for each specific cell type and each batch of G418 needs to be established experimentally, first of all, the minimum level of G418 to be added to the culture medium to prevent Balb/3T3 cell growth was determined. Balb/3T3 cells were split into 60 mm tissue culture plates in the density of 2×10^5 cells in 2 mL DMEM without G418 per well. The next day, the medium was replaced with fresh DMEM containing increasing concentrations of G418 (G418 in a range of 0.1 mg/mL to 1.0 mg/mL was added to the cells). Cells were fed every 3 days with the selection medium and observed under light microscopy

every day to check cell death. The concentration which caused complete cell death in 7-14 days was chosen as the appropriate G418 concentration for selection: 0.4 mg/mL.

Then, Balb/3T3 cells were seeded into 60 mm tissue culture plates (BD Falcon™, UK) at 8×10^5 cells per well in 5 mL DMEM medium with 10% (v/v) heat-inactivated FBS but without antibiotics. The next day, to prepare the Lipofectamine® 2000 transfection, for each well of cells, 15 µL DNA (1mg/mL in sterile molecular biology water, pcDNA3.1 or pcDNA3.1-hGH) was diluted into 250µL OptiMEM® Medium (Invitrogen, UK); 20 µL Lipofectamine® 2000 reagent was diluted into 250 µL OptiMEM® Medium as well, and incubated for 5 min at room temperature. After that, the diluted Lipofectamine® 2000 reagent was combined with the DNA by gentle pipetting, and the mixture was allowed to sit undisturbed for 20 minutes at room temperature for DNA-Lipofectamine® 2000 complexes to form. Finally the complexes were distributed over the Balb/3T3 cells. A plate of untransfected Balb/3T3 cells was used as a negative control. The medium was replaced by fresh one 6 h after transfection, and the cells were allowed to grow and express the protein for G418 resistance under non-selective conditions for 48 hours. Then, cells were split 1:10 and cultivated in the selection medium (standard medium with supplements and G418 at 0.4 mg/mL) for the selection of stably expressing cells. Cell growth was observed every day and the medium was replaced with fresh selection medium every 3 days for a total of 15 days. In the well containing untransfected cells, there should be no sign of living cells, while outgrowth of resistant cells was observed in pcDNA3.1-hGH and pcDNA3.1 transfected wells.

In order to generate single clones of hGH expressing Balb/3T3 cells, cells from pcDNA3.1-hGH and pcDNA3.1 transfected wells 15 days after G418 selection were harvested using trypsin. The living cells were counted by trypan blue staining, then 100, 1000, and 10000 living cells were into T-160 tissue culture flasks (BD Falcon™, UK) containing 0.4 mg/mL G418. Cells were incubated at 37 °C, 5% CO₂ and 95% humidity for 7-10 days, and observed under the microscope. Cells in the non-transfected control plates should be completely dead, while large, healthy and well separated colonies were observed in the flasks containing pcDNA3.1-hGH and pcDNA3.1 transfected cells. To isolate these colonies, the locations of the colonies were marked by a marker pen, and the medium in the flasks was carefully removed. Trypsin-soaked Scienceware® cloning discs (3mm, Sigma-Aldrich, UK) were put directly on the surface of the cell colonies and left there for around 2 min. Then the paper discs containing cells from different clones were transferred to wells of 24 well plate for growth in fresh

selection medium. After three days, clones that reach ~80% confluence were split into 12-well plate, and hGH protein secretion in the medium of the wells of the 24 well plate was assessed by enzyme-linked immunosorbent assay (Roch, Singapore). The hGH expression positive clones were further expanded using 6 well plate and T25 tissue culture flasks, and stored in liquid nitrogen till use in the future.

Cells stably transfected with pcDNA3.1-hGH were designated Balb/3T3-hGH, whereas cells stably transfected with pcDNA3.1 were designated Balb/3T3-empty.

5.2.6 Preparation, particle size and zeta potential analyses of polymer/DNA complexes

Polymer/DNA complexes were prepared as previously described under Section 3.2.4. The particle sizes and zeta potentials of the post-equilibrated polymer/DNA complexes were measured by dynamic light scattering (Brookhaven Instrument Corp., Holtsville, New York, U.S.A.) using a He–Ne laser beam at 658 nm with a scattering angle of 90° and Zetasizer (Malvern Instrument Ltd., Worcestershire, UK), respectively, at a set temperature of 25 °C. Immediately prior to the particle size and zeta potential measurement, the polymer/DNA complexes in nuclease free water was diluted 10x in PBS to mimic the dilution in the physiological environment after i.v. administration. Particle size and zeta potential measurements were repeated for three runs per sample and reported as the mean ± standard deviation of three readings.

5.2.7 Titration experiments

The buffering capacity of the unmodified and modified PEIs was analyzed as described previously [296]. Briefly, the polymer (0.1 mmol nitrogen atoms) was first dissolved in 5 mL of NaCl solution (150 mmol). Then, 15 mL of 0.01 M HCl was added to the solution to reduce the pH to 2, and the solution was titrated against 0.01 M NaOH until reaching pH 11 using an auto titrator (Spectralab Instruments). The unmodified PEI was used as a control. The buffering capacity is defined as the percentage of amine groups which get protonated over the pH of 4.8–7.2 and is calculated by the following equation: buffering capacity (%) = $100 \times (\Delta V_{\text{NaOH}} \times 0.01 \text{ mol}) / N \text{ mol}$.

Where ΔV_{NaOH} is the volume of NaOH (0.01 M) which is required to increase the pH from 4.8 to 7.2 and N mol is the total moles of protonable amines.

5.2.8 Gel retardation assay

DNA binding ability of the polymers was investigated using agarose gel electrophoresis as detailed in Section 3.2.5. Briefly, various formulations of polymer/DNA complexes were prepared with N/P ratios ranging from 1 to 30. Post-equilibration, the complexes were electrophoresed on 1% agarose gel (stained with 5 μ L of 10 mg/mL ethidium bromide per 60 mL of agarose solution) in 1 \times TBE buffer at 110 V for 50 min. The gel was then analyzed under an UV illuminator (Chemi Genius, Evolve, Singapore) to reveal the relative position of the complexed DNA to the naked DNA.

5.2.9 *In vitro* GFP gene transfection

The *in vitro* gene transfection efficiency of the polymer/DNA complexes was investigated using the GFP reporter gene in mouse fibroblast cell line Balb/3T3. Briefly, Balb/3T3 cells were seeded onto 24-well plates at a density of 5×10^4 cells per 500 μ L per well. 24 h later, the plating DMEM media were replaced with 0.5 mL fresh growth media, followed by the drop-wise addition of 50 μ L of the polymer/GFP-reporter plasmid DNA complex solution (containing 1.75 μ g DNA) at various N/P ratios. Following 8 h of incubation, free DNA complexes were removed by replacing the media in each well. After a further 64 h of incubation, cells were harvested for analysis by first washing with 1 mL of PBS and then detaching with 0.3 mL of trypsin (0.5 g/L in PBS). The cell suspension was then centrifuged at 1500 rpm for 5 minutes, followed by one more round of wash by 1 mL PBS. The cell pellet was again collected and finally resuspended in 300 μ L PBS for flow cytometry (FACSCalibur, BD Bioscience, San Jose, CA, USA). Prior to FACS analysis, 10 μ L of Propidium Iodide (PI) Nucleic Acid Stain (Molecular Probes, UK) (10 μ g/mL diluted in PBS) was added to a control tube of otherwise unstained cells, mixed gently and incubated for 1 minute in the dark. Then the data for unstained cells and single-color positive controls (GFP single positive and PI single positive) were acquired with the flow cytometer. Subsequently, 10 μ L of PI staining solution was added to each sample just prior to analysis. 30000 total events were recorded and the percentage of viable (PI negative) cells expressing GFP was reported as a mean \pm standard deviation ($n \geq 3$). Cells were defined to be GFP positive by setting the gating region to include less than 0.5% of the un-transfected cells. In all *in vitro* gene expression experiments, naked DNA was used as a negative control, and unmodified PEI/DNA complexes prepared were used as the positive control.

5.2.10 Cytotoxicity test

The cytotoxicity of the polymer/DNA complexes was studied using the standard MTT assay protocol detailed in Section 3.2.11. Cells were seeded in 96 well plates at 1×10^4 per 100 μL per well, for Balb/3T3 cells. And polymer/DNA complexes were removed after 8 h incubation with the cells. Data are expressed as mean \pm standard deviations from two independent experiments performed in eight replicates per N/P ratio.

5.2.11 Mixed Lymphocyte Reaction (MLR)

WT B6 and Balb/c mice (6-8 weeks old) were obtained from the Jackson Laboratory. Mice were kept in a standard animal housing setting at the CBS facilities at St Mary's Hospital, Imperial College London. In the mixed lymphocyte reaction (MLR), suspensions of responder T cells (lymphocytes isolated from non-immunized B6 mouse spleen) were cultured with allogeneic stimulator lymphocytes isolated from Balb/c mouse spleen. The activating stimulus is the foreign histocompatibility antigen (usually MHC class I or class II molecules) expressed on the allogeneic stimulator cells. Responder cells needed not be primed because a sufficiently high number of T cells in the MLR will respond to the stimulator population.

Mice were humanly killed by cervical dislocation. Single-cell suspensions from the spleen of both B6 and Balb/c mice were aseptically prepared in the sensitization medium: RPMI +10% (v/v) FCS +1% (v/v) PSG +1mM sodium pyruvate +1% (v/v) nonessential amino acids +0.1% (v/v) beta-mercaptoethanol (2ME). The stimulator cells isolated from Balb/c mice spleen was treated by 3000 rad gamma irradiation (Gammacell Irradiator, UK) to block cell division. The B6 splenocytes were pelleted at 1600 rpm, 5 min at 4 °C, and 3 mL 1x RBC lysis buffer (eBioscience, UK) was added to the pellet. After a brief vortex, the cell suspension was incubated at room temperature for 10 min. 7 mL fresh medium was added to the suspension followed by pelleting and resuspension in 5 mL medium. Viable cells were then counted by trypan blue staining. After that, responder B6 spleen cells (7×10^6) and irradiated stimulator Balb/c spleen cells (1×10^6) were cultured together in 2 ml of the sensitization medium in 24-well plates, for 5 days in a humidified 37°C, 5% CO₂ incubator. Mouse recombinant IL-2 (10 U/mL) was added when cultures were initiated to enhance the generation of CTL activity. On day 5, non-adherent effector cells were harvested from each well by vigorous pipetting, washed once with PBS, and resuspended in 10 mL serum free RPMI. Then they were spun over lympholyte gradients to remove dead cells. Briefly, Lympholyte-M Cell Separation Media (Isolation of lymphocytes from Mouse lymphoid tissue) (VH Bio Ltd. UK) was equilibrated to the room temperature, 2 mL of which was added to the bottom of the cell suspension using a

Pasteur pipette. The tube was centrifuged at room temperature, 2000 rpm for 20 min without brake, so that a well defined lymphocyte layer (buffy coat) was formed at the interface of the medium and lympholyte-M. The lymphocyte layer was removed carefully using a pipette and washed once with PBS, and the viable CD8 cells were counted using trypan blue staining. Finally, the cells were characterized by flow cytometry after being stained by anti-mouse CD8-PB (Biolegend, UK), and intracellular anti-GrB-PE (Sigma, UK) FACS antibodies. For the immunostaining of GrB, cells were incubated for 20 min in 250 μ L Cytotfix/Cytoperm solution (BD Biosciences) at 4°C for permeabilization, followed by pelleting and thorough resuspension in 50 μ l of BD Perm/Wash solution containing a pre-determined optimal concentration of a fluorochrome(PE)-conjugated anti-GrB antibody, and the cells were incubated at 4°C for 30 minutes in the dark. After that, cells were washed twice with 1 mL 1 \times BD Perm/Wash solution and resuspended in FACS buffer prior to flow cytometry analysis. Auto-compensation was done using the Summit software.

5.2.12 *In vitro* protection of Balb/3T3 cells from YT cell or allo-specific CTL killing by transfection with polymer/PI-9 encoding plasmid DNA complexes

The protective effect of polymer/PI-9 plasmid DNA complexes was evaluated by a killing assay using human natural killer-like leukemic YT cells [288] or allo-specific CTL generated from section 5.2.11 as the effector, and Balb/3T3 cells as the target. Calcein-acetoxymethyl (Calcein-AM, Invitrogen, UK) which is a fluoresceinated molecular probe retained only by live cells with intact membranes, was used to assess the percentage of cell killing [289]. Briefly, YT cells or allo-specific CTL generated from B6 mouse spleen were washed and re-suspended to 5×10^6 cells/mL in RPMI, 100 μ L of which was dispensed into each well of a 96 well plate (round-bottom). Balb/3T3 cells were transfected using the polymer/PI-9 DNA complexes at various N/P ratios in a 24-well plate as described in Section 5.2.9. After 72 h of incubation, the target cells were trypsinized, washed and re-suspended at 2×10^6 cells/mL in RPMI. Calcein-AM was added to target cell suspension to a final concentration of 15 μ M and the cells were incubated for 30 min with occasionally mixing. Then they were washed twice with the medium and re-suspended to 10^5 cells/mL, 100 μ L of which was dispensed to each well of the 96-well plate containing 5×10^5 allo-specific CTLs or YT cells to achieve effector:target (E:T) ratio of 50:1. Subsequently, the target and effector cells were incubated together for designated period of time, and centrifuged at 1000 rpm for 5 min, before 100 μ L of the supernatant was removed to be read on a microplate spectrophotometer at excitation and emission wavelengths of 485 nm and 530 nm respectively.

Wells for spontaneous release (100 μ L of fresh RPMI medium without effector cells was added) and maximal release (100 μ L of 5% Triton X-100 instead of effector cells was added for complete lysis of cells) of Calcein-AM were included as negative and positive controls, respectively. Untreated and empty MigR1 plasmid-transfected target cells were used as the negative controls. The data were expressed as light units per minute (LUPM). The average values were determined from 4 replicates for every N/P ratio and control. Percent cytotoxicity was determined using the following formula:

$$\text{Percent Cytotoxicity} = \frac{\text{Experimental sample (LUPM)} - \text{Spontaneous release (LUPM)}}{\text{Maximum release (LUPM)} - \text{Spontaneous release (LUPM)}} \times 100$$

5.2.13 Statistical Analysis

Results were analyzed using the two-tailed Student's *t*-test to determine statistical significance (Microsoft Excel). The difference between mean readings was considered to be statistically significant when $p < 0.05$.

5.3 Results and Discussion

5.3.1 Polymer synthesis

To study the structure-function relationship between the modification groups and the modified PEI (25 kDa) polymer properties, the MTC monomer was modified with mannose. In addition, the protected MTC-ipman monomers were able to react with the primary amines of PEI (25 kDa) in a typical ring-opening reaction. The synthesis procedures and structures of carbamate-mannose modified PEIs (polymers **T**, **S** and **G**) were shown in Scheme 1 in Section 3.3.1. The reaction went smoothly without the help of the DBU catalyst, and it was highly controllable, fast, and correlated well to feed molar ratios of PEI to MTC-ipman monomers as verified by ^1H NMR analysis. Specifically, the conjugation degree of MTC-ipman to PEI was found to be at molar ratios of 1:5.5, 1:12.2, and 1:23 for **T**:PEI-Mannose(1:6), **S**:PEI-Mannose(1:12.5), and **G**:PEI-Mannose(1:25) by comparing relative integral intensities of methyl signals of MTC-ipman and PEI methylene signals on NMR (Figure 28), and the molar ratios on NMR were proportional to those in the feed. The reaction is highly advantageous as it enabled the synthesis of well-defined polymers which permitted an accurate study of structure-function relationships. The compositions and nitrogen contents of carbamate-mannose modified PEI synthesized without the DBU catalyst (polymers **T**, **S** and **G**) were summarized in Table 7.

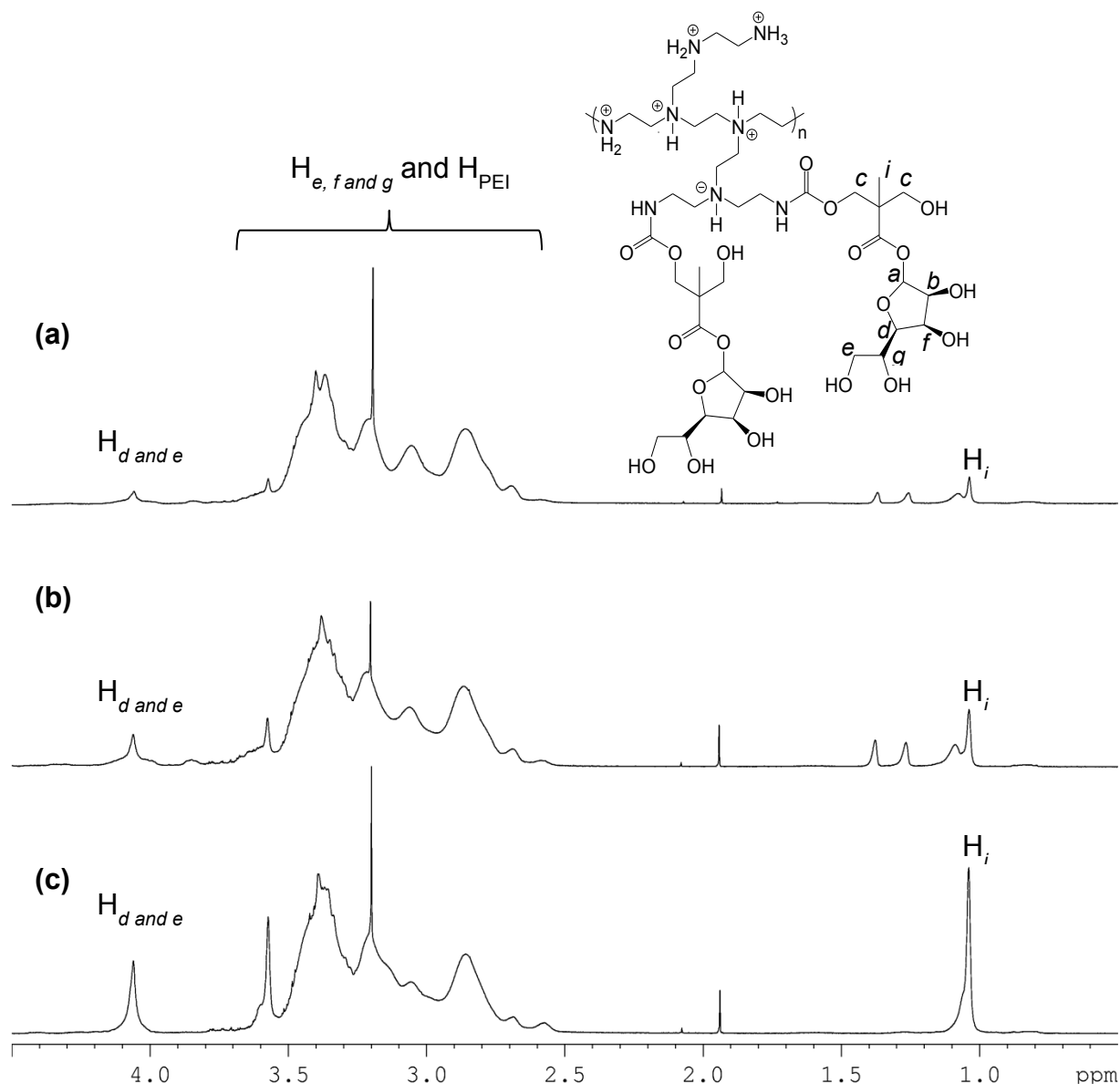


Figure 28. ^1H NMR spectra of PEI-mannose at conjugation degrees of 6, 12.5 and 25 (a, b and c, corresponding to polymers **T**, **S** and **G**, respectively) in D_2O .

Table 7. Compositions and nitrogen contents of carbamate-mannose modified PEI synthesized without the DBU catalyst, and their buffering capacity. Higher nitrogen content correlates with lower substitution degree. Substitution degree: **T**<**S**<**G**. (PEI: 58 primary amines, 116 secondary amines and 58 tertiary amines)

Polymer	Nitrogen Content (%)	Method of mannosylation	Buffering Capacity (%)
T	26.2	bPEI : ipman = 1:6 (molar ratio); Actual molar ratio from NMR: 1:5.5	19.7
S	21.7	bPEI : ipman = 1:12.5 (molar ratio); Actual molar ratio from NMR: 1:12.2	20.0
G	16.3	bPEI : ipman = 1:25 (molar ratio); Actual molar ratio from NMR: 1:23	22.3

bPEI (25 kDa)	33.3	21.2
---------------	------	------

As there are approximately 58 primary amine, 116 secondary amine and 58 tertiary amine groups in every PEI (25 kDa) molecule, the degree of mannose conjugation on the primary amine groups of PEI in this chapter was varied from 6 to 25 in order to determine an optimal number of conjugated mannose monomer. As shown in Chapter 3, modified PEI with all the primary amines blocked---**C**:PEI-Mannose(1:75), **L**:PEI-Mannose(1:58), **M**:PEI-Mannose(1:120), and **N**:PEI-Mannose(1:400) were inferior in gene transfection efficiency in various cell lines such as HepG2 and HMSC, due to inefficient DNA binding and condensation, and therefore they were excluded in this chapter.

5.3.2 Buffering Capacity

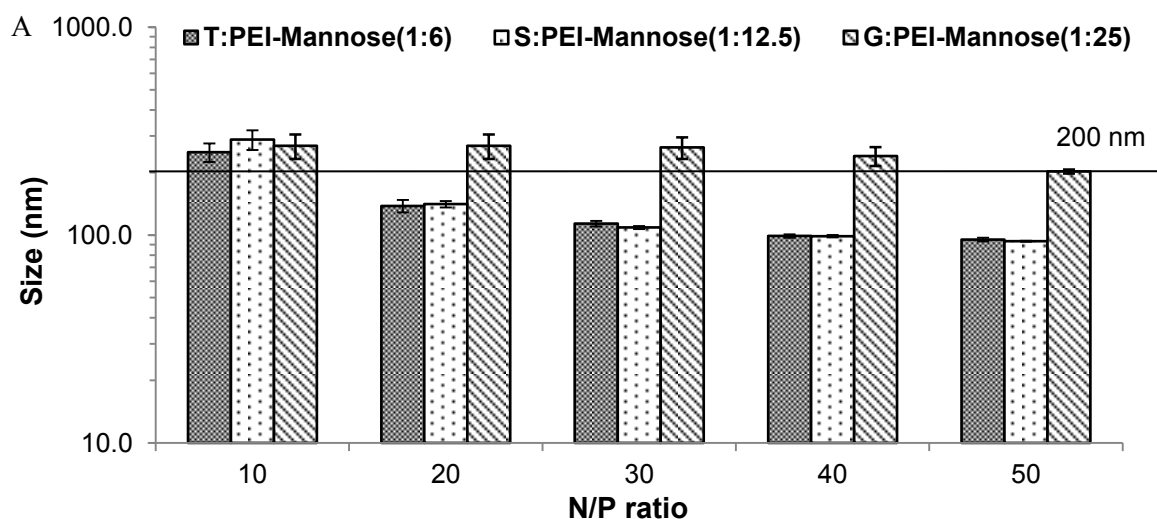
Increasing the conjugation degree not only decreased the number of free primary amines, it might also affect the pKa values of the available amines [297]. Altered pKa might in turn have an impact on the endosomal buffering properties and thus the ability of endosomal escape of the DNA/polymer complex [298]. In order to evaluate whether the buffering capacity of the PEI 25 kDa was modified by the MTC-ipman conjugation, acid-base titration experiments were performed. As a result, the buffering capacity of polymers **T**:PEI-Mannose(1:6), **S**:PEI-Mannose(1:12.5), and **G**:PEI-Mannose(1:25) with different mannose conjugation degrees were found to be 19.7%, 20.0% and 22.3%, respectively, which were comparable to unmodified PEI (21.2%) (Table 7). The unaltered buffering capacity of the mannose modified PEIs suggested that the majority of conjugation reactions took place at the primary amine sites of PEI, leaving the secondary and tertiary amines intact and available to sequester protons in the acidic environment of endosomes [299]. Therefore, mannose modification could largely conserve the prominent endosomal escape capabilities of the gold standard PEI 25 kDa, while other properties of the modified PEI remained to be explored in the following sections.

5.3.3 Size and zeta potential of polymer/DNA complexes

Nanoparticles with sizes less than 200 nm are ideal as they have been reported to exploit the clathrin-mediated endocytosis to enter and accumulate in cells, in a better and more efficient way than larger sized particles [300]. The size and zeta potential of the polymer/DNA complexes formed using mannose modified PEI (25kDa) synthesized without the use of

catalyst and the unmodified PEI were measured by dynamic light scattering. For polymers **T**:PEI-Mannose(1:6) and **S**:PEI-Mannose(1:12.5), they had lower percentages of primary amine groups modified with cyclic mannose carbonate monomer, as compared to polymer **G**:PEI-Mannose(1:25). Therefore, more compact DNA complexes formed by them were observed as compared to polymer **G** in Figure 29A, especially at higher N/P ratios (~93 nm at N/P 50 to ~250 nm at N/P 10 for **T**, **S**; and 202 nm at N/P 50 to 268 nm at N/P 10 for **G**). As a comparison, DNA complexes formed with unmodified PEI at N/P 10 also had a small size (~84 nm). In addition, the modified PEI/DNA complexes displayed low polydispersity index (PDI) values ranging from 0.078 to 0.186, indicating uniform particle sizes.

In addition to having a small size, a net positive surface charge is also beneficial as it aids in electrostatic interaction with the negatively charged cellular membrane, mainly through proteoglycans, such as syndecan on cell surfaces, enhancing the chance of cellular uptake [301]. From Figure 29B, **T**/DNA, **S**/DNA and **G**/DNA complexes had a comparable or slightly lower cationic charge density on their surfaces at N/P 20-50 as compared to unmodified PEI/DNA complexes at N/P 10 (Zeta potential: ~18-22 mV for **T**/DNA and **G**/DNA complexes, ~16-18 mV for **S**/DNA complexes, and ~22 mV for PEI/DNA complexes). This could be explained by the fact that primary amine groups responsible for being protonated in PBS (pH 7.4) were partially blocked by the mannose cyclic carbonate in the modified polymers, therefore reducing the net positive charge of the modified polymer/DNA complexes. A similar phenomenon was also reported in lipoic acid modified LMW PEI (1.8 kDa), which showed comparable and slightly lower zeta potential than the unmodified PEI 1.8 kDa, demonstrated stronger DNA binding ability and mediated nontoxic and highly potent *in vitro* gene transfection in HeLa and HEK293T cells [296].



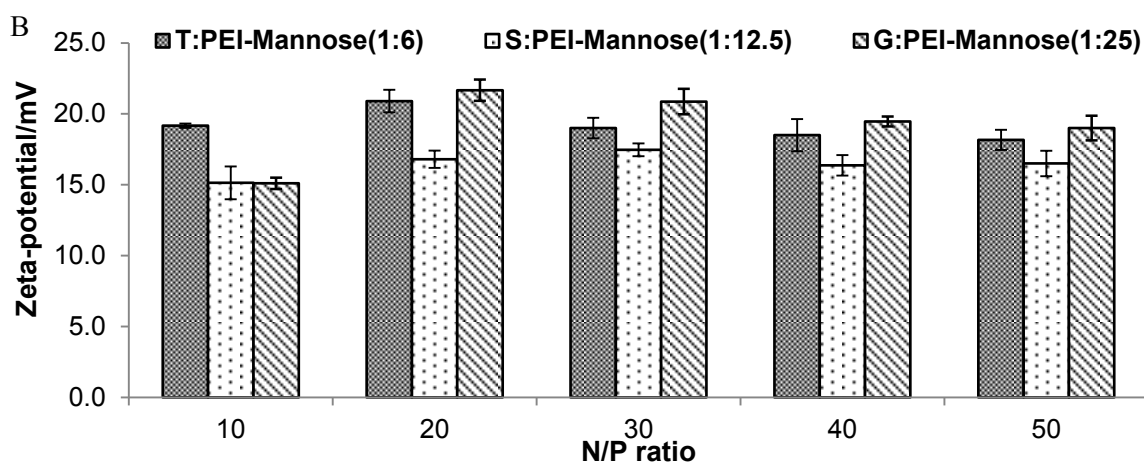


Figure 29. Particle size (A) and zeta potential (B) of polymer/DNA complexes at various N/P ratios as specified. Unmodified PEI/DNA complexes prepared at N/P 10 were used as a control. Results represent mean \pm standard deviation of triplicates.

5.3.4 DNA binding ability of polymers

To determine whether the mannose modified PEI (25kDa) could effectively bind DNA to form compact complexes for easy cellular uptake, agarose gel electrophoresis was performed to evaluate the gene binding capacity of the polymers. As shown in Figure 30, like unmodified PEI, which enabled complete DNA binding from a fairly low N/P ratio (i.e. N/P 3) (Figure 30D), polymers **T**, **S** and **G** condensed DNA effectively. The complete retardation of DNA mobility in the complexes was observed at N/P 3 for **S**, and N/P 2.5 for both **T** and **G** (Figure 30A, B and C). These results suggested that PEI with 5.5, 12.2 or 23 of 56 primary amine groups substituted by mannose still condensed DNA effectively.

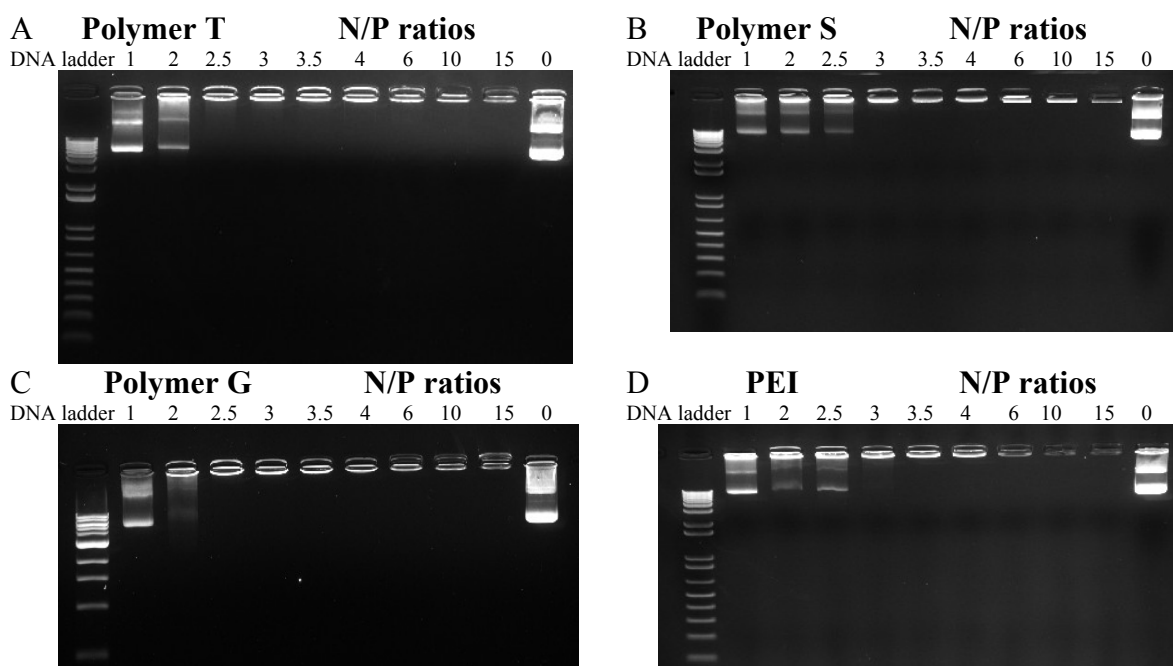


Figure 30. Electrophoretic mobility of DNA in polymer/DNA complexes. A, B, C and D represent polymer **T**, **S**, **G**, and the unmodified PEI, respectively.

5.3.5 Cytotoxicity of unmodified and carbamate-mannose modified PEIs

The cytotoxicity of unmodified and modified PEIs was evaluated against Balb/3T3 cells using the MTT cell viability assay. As demonstrated in Figure 31, the unmodified PEI caused extensive cytotoxicity over the range of concentrations tested, especially at high N/P ratios of 50 and above, where less than 25% of the Balb/3T3 survived after 8 h incubation with the unmodified PEI. On the contrary, although demonstrating a trend of decreasing cell viability with increasing N/P ratio, all three mannose-modified PEI polymers were much less cytotoxic against Balb/3T3 cells than unmodified PEI at all N/P ratios. Balb/3T3 cells demonstrated strong tolerance to the mannose-modified PEIs, Especially **G**:PEI-Mannose(1:25), which caused almost 0% cytotoxicity from N/P 10-50, and more than 80% cell survived when treated by **G**/DNA complexes at N/P 60. Moreover, the same treatment conditions of the cells with **T**, **S** and **G** even at the highest concentrations corresponding to N/P 100 (51.0, 61.6 and 82.0 mg/L, respectively) led to 42%, 40%, and 61% cell viability. Furthermore, in the present study, cell viability correlated positively with the increasing degrees of carbamate-mannose substitution, further proved that mannose moieties successfully shielded the primary amines of PEI and reduced the high positive charges associated with strong cell lytic and toxic properties. Taken together, the MTT assay demonstrated the potential of the mannose-modified PEIs to be safe gene delivery vectors.

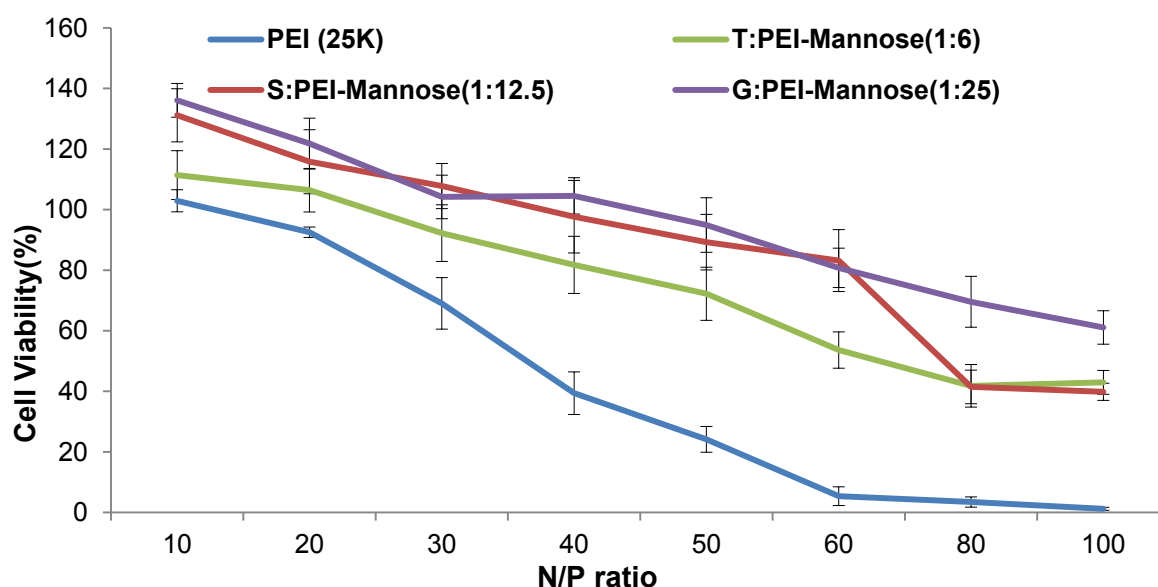


Figure 31. Viability of Balb/3T3 cells after incubation with unmodified PEI/DNA and carbamate-mannose modified PEI/DNA complexes at various concentrations. Results represent mean \pm standard deviation of 8 replicates. Polymer concentrations in the order of N/P ratios specified: unmodified PEI - 4.0, 8.0, 12.0, 16.0, 20.0, 24.1, 32.1, and 40.1 mg/L. T - 5.1, 10.2, 15.3, 20.4, 25.5, 30.6, 40.8, and 51.0 mg/L. S - 6.2, 12.3, 18.5, 24.6, 30.8, 37.0, 49.3, and 61.6mg/L. G - 8.2, 16.4, 24.6, 32.8, 41.0, 49.2, 65.6, and 82.0 mg/L.

5.3.6 *In vitro* GFP gene transfection efficiency

The percentage of Balb/3T3 cells successfully transfected with the reporter gene encoding for GFP by the various polymers was quantified using flow cytometry. DNA/polymer complexes were formed at N/P ratios ranging from 10 to 100, cells were incubated with the complexes for a period of 8 h which corresponded to the polymer treatment time in the MTT viability assay, and the GFP expression was analyzed 72 h after transfection. As the unmodified PEI caused extensive cytotoxicity at N/P 40 and above, the false positive GFP signal caused by auto-fluorescence of the dead cells needed to be eliminated [274]. To achieve this, 30000 total Balb/3T3 cells were acquired by fluorescence-activated cell sorting (FACS), and gating was first performed on forward scatter and side scatter double-positive cells, then on propidium iodide (PI) negatively-stained cells, therefore most of the dead cells were eliminated to avoid interference with the genuineness of the GFP transfection efficiency.

As shown in Figure 32A, although the unmodified PEI caused a peak of 59% GFP positive cells at N/P 30 and 40, its transfection efficiency drastically plunged at N/P 50 and above, presumably because of its high intrinsic toxicity at high concentrations. The transfection efficiency of the mannose-modified PEIs increased with increasing mannose attachment degree at each N/P ratio, suggesting that mannose-conjugation had a positive influence on the gene transfection ability. Polymers **T** and **S** demonstrated the highest transfection efficiency at N/P 50, where 42% and 54% GFP transfection efficiency was achieved in the presence of serum by **T** and **S**, respectively (Figure 32A). But their transfection efficiency dropped at higher N/P ratios, suggesting that their elevated cytotoxicity at N/P 80-100 (~40% cell viability for both polymers, Figure 31) had a negative impact on the percentage of GFP positive cells. In the contrast, polymer **G** mediated around 65% transfection efficiency even at the highest N/P 100, and the peak of its transfection efficiency occurred at N/P 80 (66%) (Figure 32A). Furthermore, when counting the absolute number of GFP positive cells transfected by the various polymers at the N/P ratios tested, the negative impact of the polymer cytotoxicity on the effectiveness of gene transfection was even more obvious. As can be seen in Figure 32B, the unmodified PEI led to ~5400 live GFP positive cells out of 30000 total cells, which corresponded to the high

cell viability of 93% at N/P 20 (Figure 31). When the cell viability dropped to below 40% from N/P 40 and above, only less than 630 GFP positive cells were managed to be collected. Moreover, ~40% cell viability at N/P 80 and 100 also made the amount of GFP positive cells collected at these two N/P ratios very low for Polymer T and S (200 and lower). In sharp contrast to these, polymer G enabled more than 3900 viable GFP positive cells to be collected even at N/P 100, which was significantly higher than those achieved by other polymers at such a high N/P ratio, largely due to its compatibility with Balb/3T3 cells at high concentrations. All in all, the favourable data in Sections 5.3.5 and 5.3.6 suggested that carbamate-mannose modified PEIs with primary amine groups partially blocked, especially G:PEI-Mannose(1:25), was potentially a very useful gene delivery vector with high gene transfection efficiency and very well contained cytotoxicity, even at high N/P ratios.

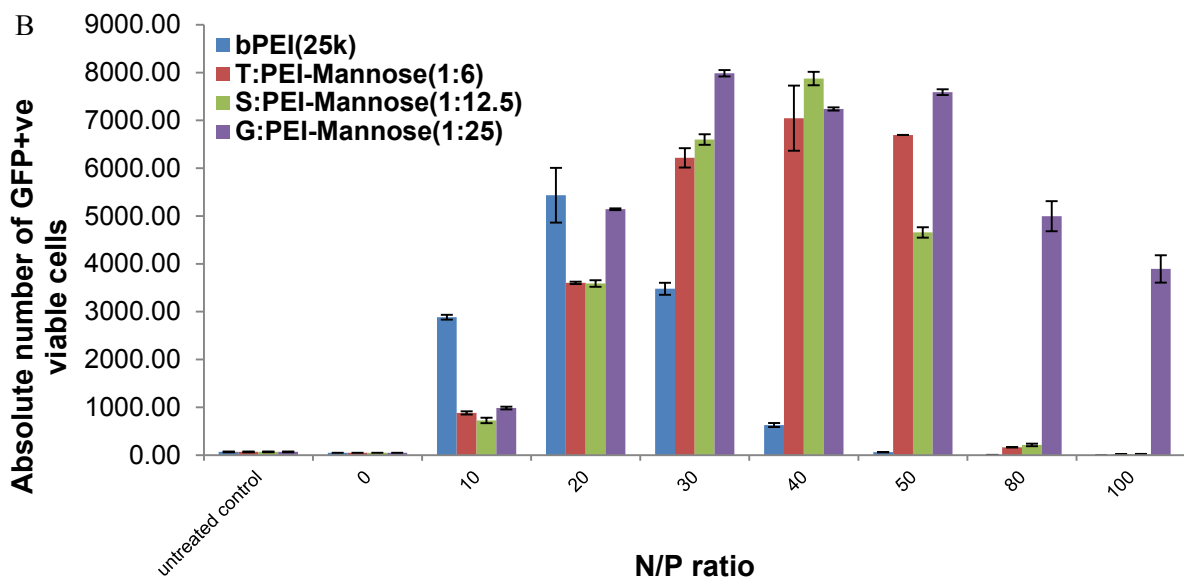
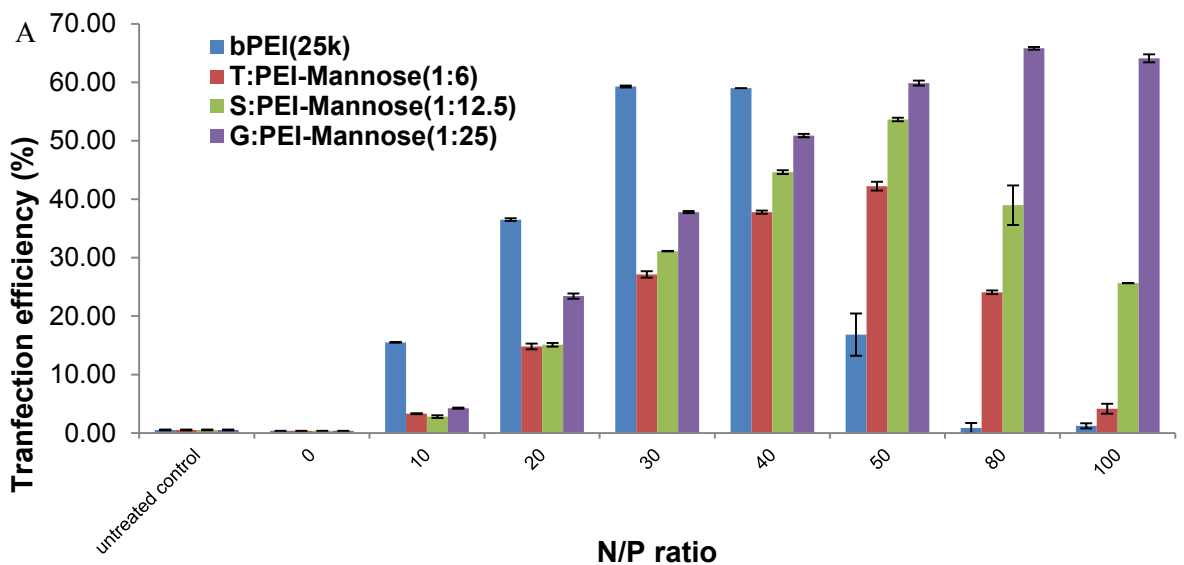


Figure 32. *In vitro* GFP transfection in viable Balb/3T3 cells. (A) GFP transfection efficiency mediated by various polymers at different N/P ratios. (B) Absolute number of GFP^{+ve} viable cells transfected by the various polymers. Results represent mean \pm standard deviation of triplicates. Polymer concentrations in the order of N/P ratios specified: unmodified PEI - 0, 4.0, 8.0, 12.0, 16.0, 20.0, 32.1, and 40.1 mg/L. T - 0, 5.1, 10.2, 15.3, 20.4, 25.5, 40.8, and 51.0 mg/L. S - 0, 6.2, 12.3, 18.5, 24.6, 30.8, 49.3, and 61.6mg/L. G - 0, 8.2, 16.4, 24.6, 32.8, 41.0, 65.6, and 82.0 mg/L.

5.3.7 Protection of Balb/3T3 cells from allo-specific CTL and YT cell killing

Given the high gene transfection efficiency and low cytotoxicity of the carbamate-mannose modified PEIs, especially polymer **G**, they were used to transfect PI-9 encoding plasmid into Balb/3T3 cells in order to protect them from GrB mediated killing. In order to carry the study a step further, the source of GrB used to kill Balb/3T3 used in Chapter 5 was designed to be allo-specific CTLs generated from the spleen of a mouse of a different strain (B6), rather than human NK-like leukemic YT cells as in Chapter 4. The killing of target cells by sensitized T lymphocytes is an important type of cell-mediated immunity, which is antigen specific and requires contact between the specific effector T lymphocyte and a target cell carrying the appropriate cell surface antigen. Effector/killer cells were generated in a manner analogous to the generation of antibody-forming cells in which antigens stimulate specific T lymphocyte precursors to proliferate and differentiate. In this study, mixed lymphocyte responses (MLR) was carried out whereby two populations of allogeneic lymphoid cells (isolated from Balb/c and B6 mice spleens respectively, and Balb/c splenocytes were γ -irradiated to block proliferation) were mixed together, resulting in B6 T cell proliferation. Cell surface antigens encoded by genes of the MHC are the major stimuli of this response. As Balb/c and C57BL/6 mice have different H2 haplotypes: H2-d for Balb/c, and H2-b for C57BL/6 [302], the cell surface antigens displayed by γ -irradiated Balb/c splenocytes were able to stimulate the proliferation and differentiation of C57BL/6 T lymphocyte precursors, and the stimulated B6 CTLs incubated for 5 days in MLR culture were specific against cells displaying antigens of the Balb/c mice origin, in this case, Balb/3T3 cells.

7×10^6 Responder B6 spleen cells and irradiated (3000 rad) stimulator Balb/c spleen cells (1×10^6) were cultured together in 2 ml sensitization medium containing 10 U/mL IL-2 in 24-well plates, for 5 days at 37°C. After five days, lympholyte-M gradient recovered the effective T lymphocytes, and they were analyzed by flow cytometry for CD8 and GrB expression. According to Figure 33, 5-day MLR culture successfully generated B6 strain CTLs

expressing high levels of CD8 and GrB, which are presumably potent killer of cells of the Balb/c mouse strain.

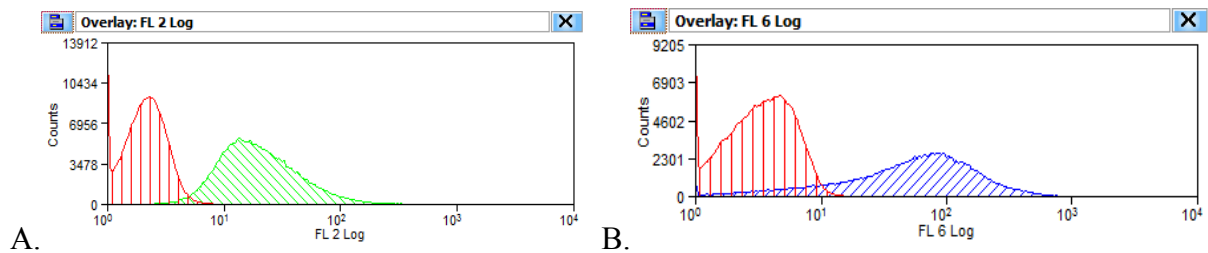


Figure 33. Expression profiles of intracellular GrB (A) and cell surface CD8 (B) markers of B6 CTLs, which were generated by a 5-day MLR culture with γ -irradiated Balb/c splenocytes. Red line denotes unstained control, Green line denotes cells expressing GrB, and Blue line denotes cells expressing CD8.

Then, serial dilutions of cytolytic effector cell populations (B6 CTLs) were incubated with a constant number of Calcein-AM dye labelled target cells (WT Balb/3T3), at a range of effector-to-target ratios (50:1, 25:1, 12.5:1, 6:1, 3:1, 1.5:1). However, no killing was observed even at the highest effector-to-target ratio of 50:1, after a 72 h co-incubation. The apparent impotency of the allo-specific B6 CTLs against Balb/3T3 could be explained by the nature of Balb/3T3 cells provided. The Balb/3T3 provided by Dr. Ponti from European Commission was stemmed from the clone A31-1-1. Although it is not tumorigenic in immunosuppressed mice, it did form colonies in semisolid medium [303]. Also, research showed that Balb/c mouse embryo lines maintained in culture with minimal cell-to-cell contact remained non-tumorigenic for over 200 generations, however, when extensive cell contact was allowed during cell culture, cells could become tumor-producing within 30 generations [304]. Loss of contact inhibition of Balb/3T3 in this study was constantly observed throughout cell culture, therefore the Balb/3T3 cells used in this experiment probably have acquired tumor-like properties, critical in determining the effectiveness of killing by the allo-specific CTLs, which will be illustrated below.

In healthy individuals, tumor cells and virus-infected cells are eliminated by CTLs and NK cells of the adaptive and innate immune system. Both the killer cells use the same basic mechanisms for destroying their targets, although they are triggered by different receptors, and the expression of cytolytic molecules is constitutive in NK cells, but regulated in CTLs [305]. CTL recognizes its target through engagement of its TCR-CD3 complex with a specific target cell antigen bound with class I MHC molecules expressed on the target cell surface; also, its CD8 binds to the constant portion of the class I MHC molecule, associated signalling

molecules cluster, and other larger molecules such as CD2 and leukocyte function-associated antigen 1 (LFA 1), forming a well-organized immunological synapse [59]. Then the cytotoxic granules which are dispersed throughout the cytosol migrate towards the synapse, and activated granzymes enter target cells through holes formed by perforin, triggering apoptosis of the target cells. Given the important roles played by CTLs in controlling tumor growth or viral infection, it is unsurprising that many tumors/viruses have evolved mechanisms for immune evasion, for example, down-regulation or even loss of expression of a particular MHC class I molecule, rendering tumor cells unrecognizable by CTLs [48]. This explains the inefficiency of allo-specific CTLs in killing Balb/3T3 cells in this study. In order to induce more potent GrB mediated killing of the Balb/3T3 cells and test the efficiency of protection of Balb/3T3 apoptosis by polymeric delivery of the PI-9 gene, NK cells (YT, human NK like cell line) were used as the GrB source instead. NK cells are activated in a simpler fashion, by direct engagement of activating receptors on the NK cell surface with ligands that are expressed on the surface of tumor/virus-infected cells [306] or by exposure to cytokines, such as interferon produced by other immune cells in response to viral infection [307]. Both activating and inhibitory receptors are expressed on the NK cell surface, which recognize different determinants on the target cell surfaces of infected cells. The inhibitory receptors recognize mainly major histocompatibility complex (MHC) class I molecules, while the activating NK receptors recognize stress-induced ligands and viral products. NK cell activity thus is determined by a combination of signals perceived by both activating and inhibitory receptors [308, 309]. As the inhibitory receptor engages MHC class I molecules [306], NK-mediated autoimmunity is prevented as all nucleated cells in the body express MHC class I, which are capable of engaging an NK inhibitory receptor, and rendering NK cells inactive. Down-regulation of MHC class I molecules from the cell surface by oncogenic transformation or virus infection, although makes the target cells less sensitive to CD8 CTLs, renders these cells more susceptible to attack by NK cells. This mechanism is called “missing-self” hypothesis, which proposes that loss of signalling from the inhibitory receptors for “self” MHC class I molecules activate the NK cells [310] (Figure 34A).

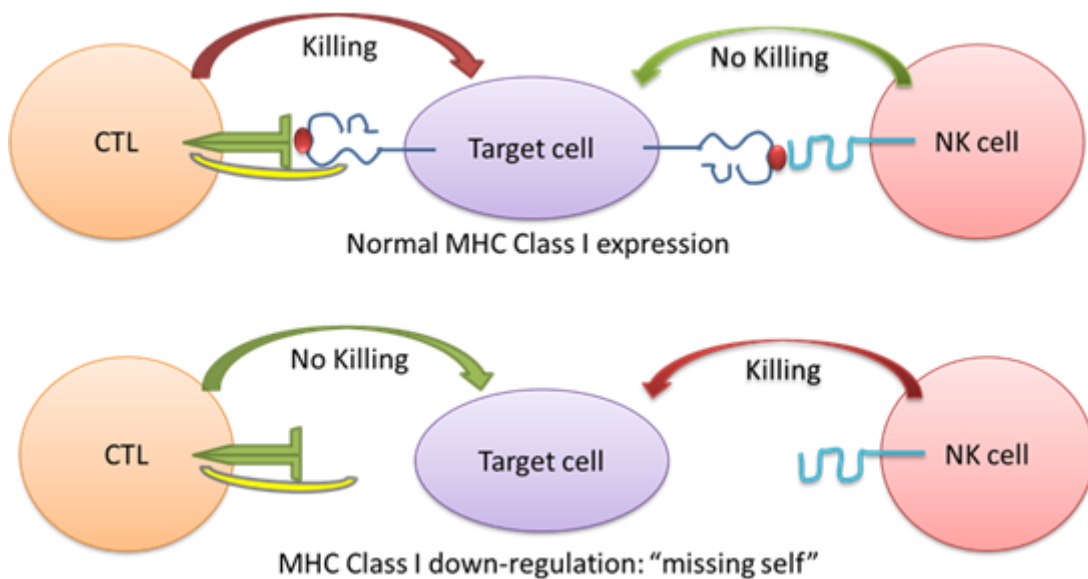
Another reason to justify the use of NK cells for increased Balb/3T3 killing is the “KIR-HLA mismatch” model. The killing by NK cells is regulated by their inhibitory, co-stimulatory, and activating receptors. Killer immunoglobulin-like receptors (KIRs) are NK cell surface proteins that regulate NK cell activation and function. Inhibitory KIRs are distinguished from activating KIRs by the inclusion of an immune-receptor tyrosine-based

inhibitory motif (ITIM) in the cytoplasmic signalling domain, leading to a potent inhibition of multiple cell processes upon engagement [311]. Inhibitory KIRs recognize Class I human leukocyte antigen (HLA-I) molecules, which are expressed by all nucleated cells, and thus NK effector function against HLA-expressing autologous normal cells is inhibited by the expression of inhibitory KIRs [312]. KIR genes and HLA-I genes are encoded on chromosomes 19q13.4 and 6p21.3 respectively and therefore inherited independently [311]. Moreover, a great degree of polymorphism of KIR and HLA-I genes among individuals can cause some individuals to have NK cells that express KIRs for which that same individual has no corresponding HLA, a situation designated by Leung et al. as “KIR-HLA mismatch” [313]. Various reports of clinical trials have suggested that an autologous KIR/HLA mismatch occurs in approximately 60% of patients undergoing allogeneic hematopoietic stem cell transplant (HSCT) [313-315], and the clinical benefit of autologous KIR/HLA mismatch in paediatric patients that received HSCT for lymphoma or solid tumors has been demonstrated [313]. In a retrospective study of 169 patients, Venstrom et al. (2009) found a significantly lower risk of death and disease progression in HSCT patients lacking one or more autologous HLA compared to patients who were fully autologous KIR/HLA matched [316]. Applying the model to the NK cell killing experiment, the mouse MHC I molecules expressed on the target (Balb/3T3) cells would very probably mismatch the inhibitory KIRs on the human NK cell line YT, leading to YT cell activation and killing of Balb/3T3 cells (Figure 34B). This effect has already been demonstrated in xenotransplantation experiments. A review by Auchincloss & Sachs [317] showed that human NK cells were able to kill porcine targets due to the failure of pig MHC class I molecules to interact with human HLA class I-specific inhibitory receptors. In this context, it is likely that the NK-mediated cytotoxicity in xenografts may be the result of the failure to engage HLA-specific inhibitory human receptors (due to inappropriate MHC ligands) together with the NK-mediated recognition of xenogeneic ligands (possibly via NKp46) [318].

NKp46 was observed to express on YT cells as an activating receptor. Recognition by NKp46 is required to lyse cells expressing haemagglutinin of influenza virus and the haemagglutinin-neuraminidase of parainfluenza virus [319]. Moreover, YT cells kill B7⁺ targets in a non-MHC-restricted, CD28-dependent manner. CD28 ligation on the surface of YT cells caused CD28 receptor association with phosphatidylinositol 3-kinase (PI3-K), a rapid increase in the tyrosine phosphorylation of PI3-K, and induction of PI3-K activity [320]. The association of PI3-K with CD28 requires the interaction of SH2 domains of the PI3-K

regulatory subunit with the phosphotyrosine motif p¹⁷³YMNM within the CD28 cytoplasmic tail. And it was suggested that the src-family protein tyrosine kinase (PTK), Lck and Fyn, are capable of phosphorylating CD28 *in vitro*, leading to CD28/PI3-K binding and eventually NK killing [321]. Furthermore, generally, NK cell-mediated killing can be triggered by a number of pathways, and the most potent mechanism for triggering degranulation is linked to antibody recognition through the Fc receptor CD16 on NK cells, which can trigger antibody - dependent cellular cytotoxicity (ADCC) by NK cells without other signals, and it has the potential to overcome inhibition by inhibitory KIRs [322]. Other NK cell activating receptors must be engaged in combinations in order to trigger cytotoxicity, and activating receptors with different types of motifs constitute the most synergistic combinations. For instance, Ly49 (Ly49D,-H -P and -W) and CD94/NKG2 (NKG2C and NKG2E) receptors associate with DAP12, which has an ITAM motif [323, 324]; while NKG2D recognizing a number of stress-induced and virally expressed ligands associates with DAP10, which has a YINM motif [325]. Also, several of the activating NK cell receptors have unknown but widely expressed ligands, such that not all of the receptors engaged in an activating NK synapses can be known at present. A complete review of the various activation receptors with their respective ligands involved in cytotoxic activity of NK cells as well as the different intracellular signalling molecules was presented by Vyas et al. [326]. The activating receptors specifically employed by YT cells to recognize and kill its target cells, except from NKp46 and CD28, need to be further explored.

A



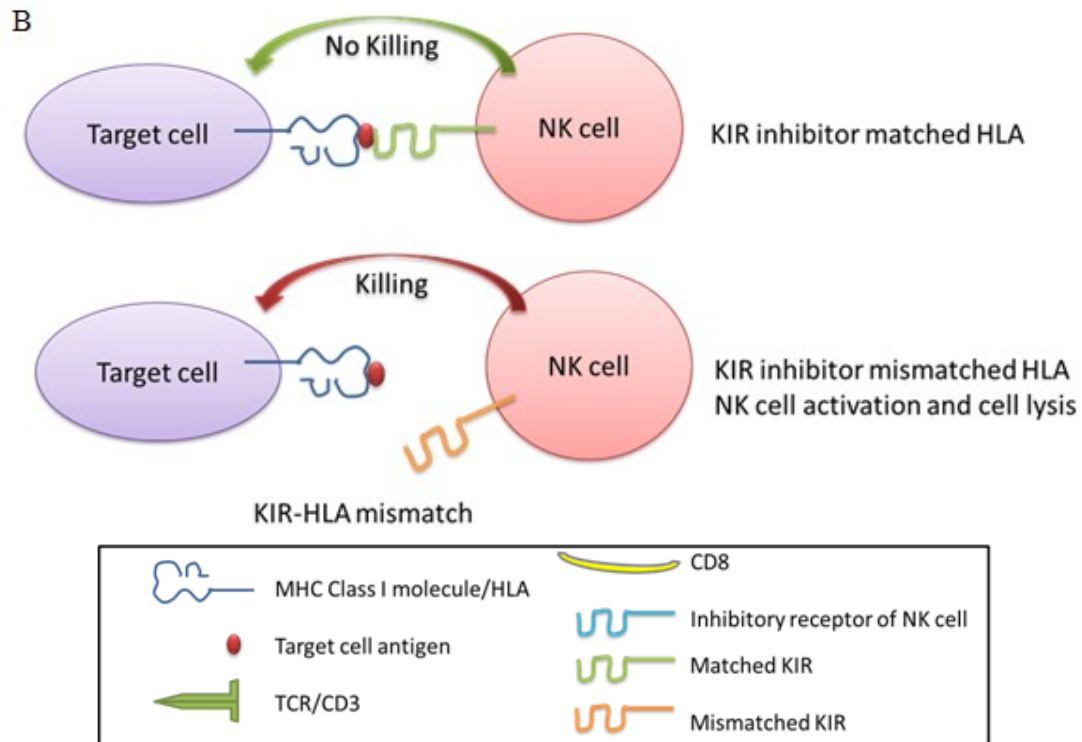


Figure 34. A. “Missing self” hypothesis. MHC Class I molecule is crucial in displaying tumor or viral antigens to the TCR on CTLs to induce activation of CTLs and killing of the malignant or infected cells. However, both tumors and viruses adapt to this by chronic down-regulation of MHC class I molecules on the target cell surface, rendering them impervious to CTL mediated immune surveillance. NK cells, however, are believed to evolve as a counteraction to this tumor/viral adaption [306]. According to the ‘missing-self’ hypothesis originally proposed by Klas Kärre, when cells down-regulate MHC class I on their cell surface, they become more prone to be recognized and eliminated by NK cells, because they are unable to engage the NK cell inhibitory receptors for MHC class I, and NK cells will no longer be inhibited [327]. B. KIR-HLA mismatch model. NK cell function is regulated by KIR interactions with matched HLA class I alleles. In the case for inhibitory KIRs, binding with matching HLA prevents donor NK cell activation to self. If HLA is mismatched, NK cells are relieved from inhibition and induce cell lysis.

In order to test the killing efficiency of YT cells, a killing assay against Calcein-AM labelled Balb/3T3 cells was performed. As shown in Figure 35A, when WT Balb/3T3 cells were exposed to different amounts of YT cells in a series of effector:target ratios from 50:1 to 0.39:1, over a time course of 8 h, the percentage of Balb/3T3 killed by GrB released by the YT cells positively correlated with the effector:target ratio, suggesting the effectiveness of YT as a killer of the target cell. Although the killing efficiency was not high compared to that of YT killing HEK293T (13.6% at E/T 50, 8 h incubation for Balb/3T3; compared to 69.5% at E/T 50, 4 h incubation for HEK293T, Figure 27, Chapter 4), it did show more effective killing of Balb/3T3 by YT than by allo-specific CTLs, and the killing by YT might be attributed to the “missing self” and “KIR-HLA mismatch” mechanism discussed above. The apparent higher

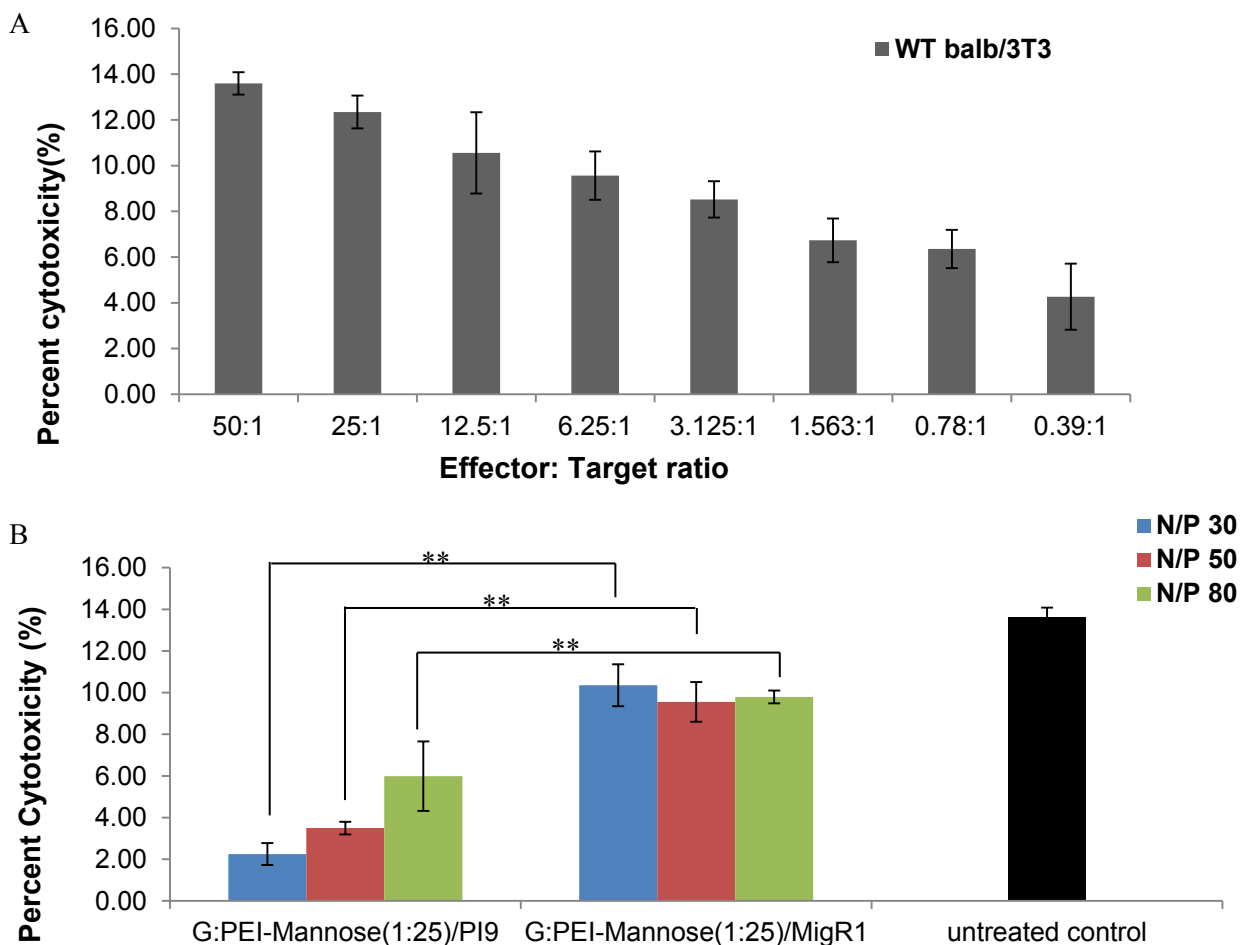
resistance to killing by YT for Balb/3T3 compared to HEK293T might be due to the different expression levels of the ligands on the target cell surfaces which engage the activation or inhibitory receptors of the NK cells, resulting in a more activation-prone integrated signal for HEK293T. Moreover, to test the effectiveness of PI-9 mediated protection of Balb/3T3 against GrB induced apoptosis, MigR1-PI-9 plasmid was transfected into Balb/3T3 by polymers **T**, **S**, **G** and the unmodified PEI, at the following N/P ratios: N/P 20, 50 and 80 for the unmodified PEI, N/P 30, 40, and 80 for **T** and **S**, N/P 30, 50, and 80 for **G**. According to Figure 32B, N/P 20 for PEI, N/P 30 and 40 for **T** and **S**, N/P 30 and 50 for **G** gave the highest absolute number of GFP^{+ve} Balb/3T3 cells 72 h after GFP gene transfection, and N/P 80 was included for each polymer to evaluate the influence of polymer cytotoxicity at high N/P ratio on the effectiveness of PI-9 mediated apoptosis protection.

As shown in Figure 35, generally, Balb/3T3 transfected with PI-9 gene demonstrated greater viability than those transfected with empty MigR1 plasmids or the untreated control when challenged by wild type YT cells, confirming the protective role of PI-9 against GrB-mediated apoptosis [70]. To compare the protective effects of PI-9 delivered by different polymers, at effector:target ratio of 50:1, **G** provided very effective protection of Balb/3T3 cells against GrB-mediated killing, at all three N/P ratios tested: N/P 30, 50, and 80, where only 2.3%, 3.5%, and 6.0% cells were killed (Figure 35B) as compared to 13.6% of killed untreated Balb/3T3 cells (Figure 35A). The effective protection correlated with the high gene transfection efficiency of polymer **G**, which caused 8000, 7600, and 5000 absolute GFP^{+ve} cells out of 30000 total cells acquired by FACS at N/P 30, 50, and 80, respectively, and 8000 was the highest GFP^{+ve} cell number achieved among all the polymers tested (Figure 32B). However, in the GrB mediated killing assay, the higher percentage of dead cells at N/P 80 when challenged by YT compared to N/P 30 and 50 ($p < 0.05$) was probably due to the higher inherent cytotoxicity of polymer **G** at N/P 80 (70% at N/P 80 vs. 95% at N/P 50 and 104% at N/P 30) (Figure 31).

Moreover, consistent with the high gene transfection efficiency, the transfection of PI-9 encoding plasmid into Balb/3T3 cells by polymers **S** and **T** at N/P 30 and 40 also protected the cells from GrB-mediated killing, compared to the empty plasmid transfected Balb/3T3 (Figure 35 C and D). However, at N/P 80 (i.e. polymer concentrations: 60.2 mg/L for **S**, and 49.9 mg/L for **T**), PI-9 lost its potent protective effect, with about 10.8% and 25.1% cells treated by **S** and **T** killed by YT, which were significantly higher than the cell death rates at N/P 30 and 40.

Again, this could be explained by the relatively higher cytotoxicity of **S** and **T** at high N/P ratios (~ 41% cell viability at N/P 80 vs. ~90-100% viability at N/P 30 and 40, for both polymers, Figure 31).

Finally, when unmodified PEI was used to deliver PI-9 gene to protect the Balb/3T3, consistent with its high cytotoxicity from N/P 40 onwards, and its relatively low gene transfection efficiency compared to the mannose-modified PEIs, it conferred slightly less protection of Balb/3T3 against YT cell killing at N/P 20 (4.4% killed), compared to the protection conferred by PI-9 delivered by mannose-modified PEIs (2.3%, 3.3%, and 3.3% cells killed for **G**, **S**, and **T**) at N/P 30. However, at N/P 50 and 80, due to PEI's severe inherent cytotoxicity, PI-9 totally lost its potent protective effect, with about 23.0% and 34.6% cells killed, which were higher than the death rate of the WT Balb/3T3 when challenged by YT (Figure 35E). Therefore, polymer **G**, **S**, and **T** were superior to unmodified PEI due to PEI's huge intrinsic cytotoxicity.



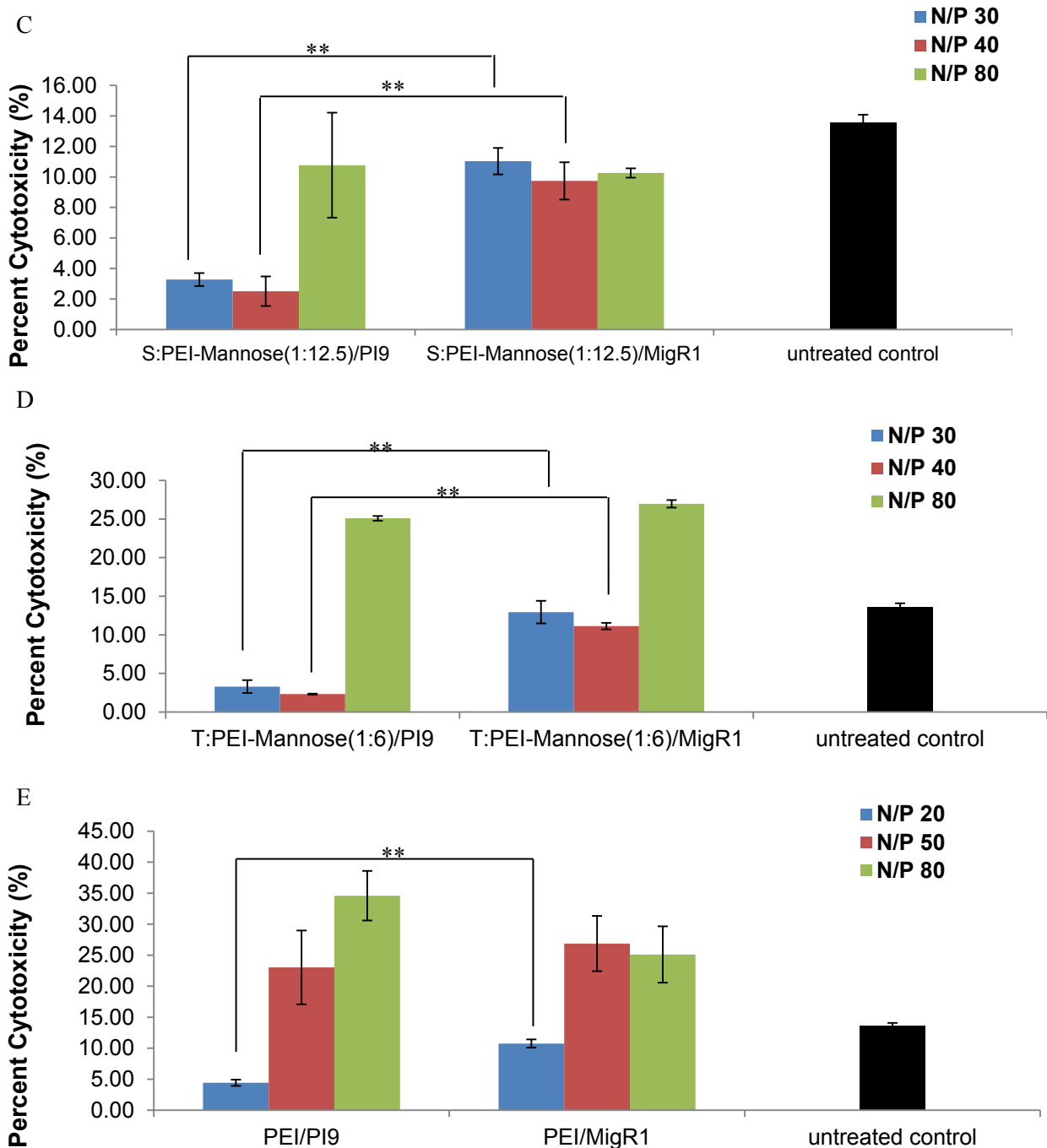


Figure 35. Viability of Balb/3T3 cells after incubation with YT cells for 8 h. Balb/3T3 cells were transfected with PI-9 encoding plasmid using **T**, **S**, **G**, and unmodified PEI at N/P ratios which gave the highest GFP transfection efficiency, and the GrB killing efficiency of the PI-9 or MigR1 empty plasmids transfected Balb/3T3 by the various polymers were compared. Polymer concentrations in the order of N/P ratios specified: PEI -14.7, 24.5, and 39.2mg/L. **T** - 18.7, 31.2, and 49.9mg/L. **S** -22.6, 37.6, and 60.2mg/L. **G** -30.1, 50.1, and 80.2mg/L. Each data represents mean \pm SD (n=4; student's *t* test, ** $p < 0.05$).

The fact that Balb/3T3 cells, a murine fibroblast cell line could be killed by the human NK cell line YT was supported by evidence in the literature [328]. Usually, different natural cytotoxicity receptors (NCR) on NK cells cooperate in target cell recognition and killing.

Blocking experiments demonstrated that when NK clones were assessed for cytotoxicity against Fc receptor negative, NK-susceptible target cells, blocking of individual NCR using an anti-NCR mAb only resulted in partial inhibition of cytotoxicity [329, 330]. Only the combined use of mAbs directed to different NCRs resulted in strong inhibition of cytolysis [331]. Thus, the cooperation of the different NCRs strongly suggested that most target cells expressed multiple ligands recognized by these receptors. However, there was an infrequently encountered case that a single triggering receptor was sufficient for the lysis of a given target cell. One such example is killing of xenogeneic (murine) target cells. Indeed, lysis of murine cells by human NK cells only involved NKp46-mediated recognition. Various blocking experiments demonstrated that NKp46 blocking by anti-NKp46 mAb prevented killing of murine target cells such as YAC, BW15.02, or P815 [331, 332]. Also, a murine (m) NKp46 homologue was discovered in 1999 by Biassoni et al., suggesting that this particular receptor/ligand interaction might be conserved during evolution [333]. Nonetheless, the simultaneous engagement of different NCRs usually resulted in a more efficient target cell lysis, which suggested that a given human NK cell clone would kill human target cells more efficiently than murine target cells, further corroborating the higher killing efficiency of YT cells against HEK293T versus Balb/3T3 cells.

5.4 Future work

We have demonstrated that the mannose-modified PEIs synthesized without the DBU catalyst could effectively deliver PI-9 gene into Balb/3T3 cells with minimal cytotoxicity, and protected them from GrB mediated apoptosis *in vitro* by decreasing the cell death rate by 11.3% compared to the untreated cells. In the future, it would be interesting to assess the role of PI-9 gene delivered by the mannose-modified PEIs in the survival of Balb/3T3 cells *in vivo*. In order to quantitatively measure the *in vivo* longevity of the PI-9 transfected cells, a pcDNA3.1-hGH plasmid construct containing the gene expressing neomycin phosphotransferase, which was kindly provided by Professor Peter E. Lobie from Cancer Science Institute of Singapore, was stably transfected into Balb/3T3 cells. The stably transfected cell clones were successfully selected by G418 antibiotics, and the hGH expressed and secreted in the cell culture medium was assessed by the hGH ELISA kit from Roche.

The protocol for measuring the longevity of the PI-9 transfected Balb/3T3 will be adopted from [334]. Cells stably transfected with pcDNA3.1-hGH were designated Balb/3T3-hGH, whereas cells stably transfected with pcDNA3.1 were designated Balb/3T3-empty. PI-9

gene will be transfected into them using the unmodified and modified PEIs, at different N/P ratios as in Section 5.3.7. After 72 h of transfection, they will be injected into two groups of syngeneic (Balb/c) and allogeneic (C57BL/6) recipient mice. Mice serum will be collected at 1, 3, 6, 10, and 13 days after injection, and the hGH in the serum will be used as an indicator for Balb/3T3-hGH survival after injection. 1×10^6 cells will be injected per animal. Balb/3T3-empty will be used as a negative control to make sure that the background signal of hGH in the serum is low when measured by the ELISA kit. The reason for injecting the transfected Balb/3T3-hGH in a syngeneic background is to assess the possibility of hGH triggering an immune response from the recipient and influencing Balb/3T3-hGH survival. Ideally this should not be the case and the cells should be surviving fairly well in the syngeneic setting. Moreover, in order to rule out the possibility of the viability of Balb/3T3-hGH being affected by the various treatments such as the gene transfection, cells will be injected to humanized NOD-SCID IL-2 γ^{null} mice [335], which are immune-deficient mice lacking NK activity and thus alloimmunity or innate immunity. The serum hGH will be assessed at the same time points as for allogeneic and syngeneic injections, and a stable hGH serum concentration at all time points will be expected. Furthermore, for the cells injected into allogeneic mice, the levels and lengths of expression of hGH in the serum will be compared, for mannose-modified PEIs-treated and unmodified PEI-treated Balb/3T3-hGH. Given that mannose-modified PEIs enabled more effective gene transfection into Balb/3T3 and caused much less cytotoxicity compared to the unmodified PEI, especially at high N/P ratios such as N/P 80, a longer survival would be expected for the BALB/c 3T3-hGH transfected with PI-9 by the mannose-modified PEIs.

5.5 Conclusions

In this study, PEI was successfully modified by selectively blocking a portion of the primary amine groups with a mannose-functionalized cyclic carbonate through a simple ring-opening of functional carbonate monomers based on nucleophilic addition chemistry, without the help of the DBU catalyst. The compositions of the modified PEI (25kDa) polymers correlated well with the mannose monomer and PEI feed ratios, and thus allowed an accurate study of how mannose affected PEI's physicochemical properties, transfection efficiency and cytotoxicity. The modified PEIs had similar buffering capacity as the unmodified PEI, were able to condense DNA into nanosized complexes with narrow size distribution and positive zeta potential, resulted in higher gene transfection efficiency and significantly reduced cytotoxicity as compared to unmodified PEI. They could also deliver PI-9 encoding plasmid

effectively into Balb/3T3 mouse embryonic fibroblast cells which were protected from GrB mediated killing by human NK cells (YT cells). Moreover, hGH plasmid was stably transfected into Balb/3T3 cells, which provided a feasible readout to test the *in vivo* longevity of PI-9 delivered Balb/3T3 cells in the future. These findings provided insights into modification of PEI for the development of effective and non-toxic non-viral vectors, which could mediate delivery of various therapeutic genes to target different diseases.

CHAPTER 6: CONCLUSIONS AND FUTURE PERSPECTIVES

The overall aim of this thesis was to design and evaluate a novel class of carbamate modified branched PEIs (25 kDa) synthesized by facile one-step ring-opening reaction, and use them in gene delivery applications, i.e. protection against cytotoxic lymphocyte killing. We tested the hypothesis that the well-defined cationic polymers with predictable molecular weights and narrow polydispersities conferred by the simple reaction are safe and effective synthetic non-viral gene carriers. In aim (1), we provided an important proof-of-concept that rationally designed hydrophobic-groups or sugar-functionalized MTC monomers could be attached to the primary amines of PEI at precisely controlled ratios. And at optimized PEI:monomer ratios, the resulting modified PEIs can effectively condense DNA to form complexes with highly desirable physicochemical properties. It was demonstrated that the polymer/DNA complexes mediated GFP/luciferase reporter gene expression that was comparable or superior to the 25 kDa branched PEI benchmark, while inducing minimal cytotoxicity even at relatively high N/P ratios for gene transfection in a panel of mammalian cell lines.

In aim (2), mannose-modified PEIs synthesized with or without the DBU catalyst at optimal mannose conjugation degrees were used to deliver plasmids encoding PI-9, a potent GrB inhibitor to HEK293T cells (Chapter 4) and Balb/3T3 cells (Chapter 5). These transfected cells were then subjected to killing by GrB releasing killer cells such as YT cells (Chapter 4 and 5) and/or allo-specific CTLs (Chapter 5). PI-9 expression in the target cells successfully inhibited GrB induced apoptosis, especially when the PI-9 gene was delivered by the modified PEIs, as the inherent high toxicity of the unmodified PEI caused undesirable cytotoxicity on the target cells, masking the protective effect of PI-9 against GrB. Thus, the findings suggested that the modified PEIs could be potentially used for PI-9 delivery to inhibit GrB and alleviate conditions such as allograft rejection.

This present work has raised several issues and identified potential opportunities that can be pursued in future investigations. Firstly, through our preliminary *in vivo* study performed in Chapter 3, the modified PEIs which demonstrated superior *in vitro* transfection efficiency and significantly reduced cytotoxicity did not achieve satisfactory organ-specific luciferase gene expression level 72 h after i.v. injection. The relatively higher luciferase gene expression in the lungs might suggest aggregation of the modified PEIs in the body. Therefore in the future, polymer/DNA complexes stabilization strategies could be explored, such as

tagging PEG molecules on the polymer to provide more serum stability. Otherwise, the modified PEIs could be employed for *ex vivo* gene delivery, for example, delivery of PI-9 gene to the tissue/organ before it was transplanted into the recipient's body.

Another inherent problem lying in the modified PEIs is that they are not biodegradable. Therefore the potential difficulty of eliminating them from the body after administration needs to be addressed. Recently, biodegradable polymers have emerged as highly attractive gene delivery vehicles as they are able to reduce long term accumulations in the body following repeated administrations, as well as to facilitate DNA release in the intracellular milieu. A bio-friendly synthetic method therefore is imperative to allow control over MW and composition of the polymers which have favorable pharmacological profiles. Once reported in the literature, reductively cleavable disulphide-bond containing moieties incorporated via primary amines of PEI was able to facilitate DNA release and reduce cytotoxicity [235]. In the future, disulfide bonds could be introduced into the backbone or side chain of the modified PEIs to enhance its biodegradability and DNA release efficiency. Also, LMW PEI, which was properly modified with functional carbamate could be cross-linked to form biodegradable HMW PEI to overcome the problems of accumulation of non-degradable polymers inside the body and the associated toxicity.

Furthermore, with regard to the application aspect in this thesis, which is to use the modified PEIs to deliver PI-9 gene to protect target cells from cytotoxic killing, the results in Chapter 5 suggested that the degree of killing was influenced by the nature of the target and killer cells and the killer-target engagement mechanism. Target cells with normal MHC I expression are normally subjected to killing by allo-specific CTLs, while those with down-regulated MHC I expression could be killed by NK cells via "missing self" mechanism. Also, mismatched KIR-HLA interaction could result in killing by NK cells. The unexpected low killing of BALB/c 3T3 cells by allo-specific B6 CTLs in Chapter 5 suggested that further investigations in a wider range of target cells should be performed to validate the relationship between MHC I expression level and efficiency of killing by either CTLs or NKs. Specifically, for example, primary mouse hepatocytes isolated from healthy liver tissue obtained from Balb/c mouse will be used as target cells. Their MHC I expression will be measured using anti-MHC I mAb to make sure the expression level is high. Allo-specific CTLs generated from B6 mouse lymphocytes by MLR using irradiated Balb/c hepatocytes as stimulators will be used as effector cells. Effector cells will be co-cultured for 4 hours with target cells stained with 15 μ M

Calcein-AM, and the degree of killing at various effector:target ratios will be determined by a spectrofluorometer. When an appropriate level of killing of the WT target cell is achieved (e.g. 50% killing at E:T ratio of 50), PI-9 gene or the MigR1 empty plasmid could be transfected into the WT target cells to evaluate the degree of protection against killing by the effector cells. In this way, a proper *in vitro* cell-killing system could be established for more effective identification of the most optimal polymer system for gene delivery.

All in all, the findings of this thesis have supported the hypothesis that rationally designed carbamate modified branched PEIs (25 kDa) with well-defined molecular architectures and narrow polydispersities conferred by one-step ring opening reaction are highly effective and non-toxic non-viral gene vectors which compare favorably with the commercially available 25 kDa branched PEI benchmark. Through functional biological assays in Chapter 4 and Chapter 5, we have clearly demonstrated that the modified PEIs with optimal primary-amine conjugation degree, and at optimal N/P ratios, could deliver PI-9 gene encoding the GrB inhibitor into target cells and prevent them from GrB mediated killing. Moreover, the current strategy of employing polymeric nanoparticles to deliver PI-9, the GrB inhibitor gene for allograft rejection prevention has not been reported previously in the literature, and it demonstrated superiority as compared to other strategies targeting AAR or CAR. For instance, immunosuppressive drugs have been associated with increasing patient intolerance and toxicity [30]; nanotechnology such as co-precipitation of polymers and immunosuppressive drugs experienced formulation challenges, for example, burst release of drugs and systemic toxicities [336]; also, strategies such as donor specific transfusion of CD47 mediated repression of recipient DC activation and subsequent allograft rejection could potentially compromise the ability of the recipient to combat other infections [337]. In contrast, our strategy of inhibiting GrB by PI-9 gene delivery has the advantage that it specifically targets the CTLs and NK cells responsible for allograft rejection, and the polymeric gene delivery vector based on PEI (25 kDa) is safe, well-modulated, synthetically facile and reproducible. Given the valid *in vitro* evaluation of biological functions of PI-9 gene-loaded nanoparticles using a cell killing assay (Chapter 4 and 5), with further optimization of the vector design, and evaluation of the *in vivo* longevity of PI-9 transfected Balb/3T3 cells in the future, the nanoparticles could be finally used to evaluate allograft rejection alleviation in a mouse chronic heart allograft rejection (CHAR) model. Specifically, hearts from CD11c-DTR-GFP mice (C57BL/6; GFP is linked to the CD11c promoter to identify dDC) will be transplanted into allogeneic recipients under co-stimulatory blockade using anti-CD154. The effective dose and frequency of administration of

PI-9 gene needed to increase the lifespan of GFP^{+ve} dDC for up to 30-100 days after transplantation will be examined. Immunohistology (IH) on multiple heart sections and secondary lymphoid tissues will be used to measure the number of GFP^{+ve} dDC. If this approach fails, the alternative approach of delivery of nanoparticles loaded with PI-9 gene by heart perfusion in donors via inferior vena cava over a range of concentrations (10-0.3 micromolar) will be performed. Donor DC will be measured before hearts being transplanted to C57BL/6 recipients. Heart allograft survival will be compared in the anti-CD154 alone vs. anti-CD154 and PI-9 treated groups. Rejection will be determined by complete cessation of cardiac contractility. Heart allografts recovered at day 60 and 100 post transplantation will be examined for chronic rejection histologically. An expert in the field will blindly evaluate and score CHAR using established procedures and criteria. The criterion of success would be PI-9 delivered by the nanoparticles proven effective in the CHAR model. All in all, pending successful *in vivo* proof-of-concept, the modified PEI platform may potentially facilitate the widespread use of gene therapy for various genetic and acquired diseases in the clinical setting.

LIST OF PUBLICATIONS AND PRESENTATIONS

Journal Publications:

1. C. Yang, J. P. K. Tan, W. Cheng, A. Bte Ebrahim Attia, C. Y. T. Tan, A. Nelson, J. L. Hedrick and Y. Y. Yang, "Supramolecular Nanostructures Designed for High Cargo Loading Capacity and Kinetic Stability," *Nano Today*, 5 (2010) 515-523
2. W. Cheng*, C. Yang*, J. L. Hedrick, D. F. Williams, Y. Y. Yang, P. G. Ashton-Rickardt, "Delivery Of A Granzyme B Inhibitor Gene Using Carbamate-Mannose Modified PEI Protects Against Cytotoxic Lymphocyte Killing," *Biomaterials*, 34 (2013) 3697-3705
3. C. Yang*, W. Cheng*, P. Y. Teo, A. C. Engler, D. J. Coady, Y. Y. Yang, J. L. Hedrick, "Mitigated Cytotoxicity and Tremendously Enhanced Gene Transfection Efficiency of PEI through Facile One-Step Carbamate Modification" *Advanced Healthcare Materials*. 2013 Mar 18. doi: 10.1002/adhm.201300046

*: co-first author

Patents:

1. "Branched Polyamines for Delivery of Biologically Active Materials", Y. Y. Yang, C. Yang, W. Cheng, P. Y. Teo, J. L. Hedrick, D. J. Coady, A. C. Engler, Patent submitted.
2. "Low Molecular Weight Branched Polyamines for Delivery of Biologically Active Materials", Y. Y. Yang, P. Y. Teo, C. Yang, W. Cheng, J. L. Hedrick, D. J. Coady, A. C. Engler, Patent submitted.

Conference Proceedings:

1. C. Yang, J. P. K. Tan, W. Cheng, A. BteEbrahimAttia, C. Y. T. Tan, A. Nelson, J. L. Hedrick and Y. Y. Yang, "Supramolecular nanostructures designed for high cargo loading capacity and kinetic stability". 2011 MRS Fall Meeting & Exhibit, Boston, MA, U.S.A., Oral Presentation.
2. Wei Cheng, Chuan Yang, Philip G Ashton-Rickardt and Yi Yan Yang, "Delivery of gene encoding Granzyme B inhibitor using polymer-based non-viral vector for prevention of chronic allograft rejection". E-MRS 2012 Fall Meeting, Warsaw, Poland. Oral Presentation.
3. Wei Cheng, Chuan Yang, Philip G Ashton-Rickardt and Yi Yan Yang, "Delivery of gene encoding Granzyme B inhibitor using polymer-based non-viral vector for prevention of chronic allograft rejection". European Polymer Federation (EPF) 2013, Pisa, Italy. Poster Presentation.

REFERENCES

1. Trulock, E.P., et al., *Registry of the International Society for Heart and Lung Transplantation: twenty-fourth official adult lung and heart-lung transplantation report-2007*. J Heart Lung Transplant, 2007. **26**(8): p. 782-95.
2. George, M.B.a.D., *Renal allograft pathology: The Banff classification*. Kidney International 1999. **56**: p. 1602-1603.
3. Nankivell, B.J., et al., *Natural history, risk factors, and impact of subclinical rejection in kidney transplantation*. Transplantation, 2004. **78**(2): p. 242-9.
4. Solez, K., et al., *International standardization of criteria for the histologic diagnosis of renal allograft rejection: the Banff working classification of kidney transplant pathology*. Kidney Int, 1993. **44**(2): p. 411-22.
5. Anthony J. Demetris, R.J.D., John J. Fung, Noriko Murase, Michael A. Nalesnik, and Parmjeet Randhawa *Pathophysiology of Chronic Allograft Rejection*. Medscape Education, N.D.
6. Viklicky, O., et al., *SDZ-RAD prevents manifestation of chronic rejection in rat renal allografts*. Transplantation, 2000. **69**(4): p. 497-502.
7. Janeway CA Jr, T.P., Walport M, et al., *Immunobiology: The Immune System in Health and Disease*. . 5 ed. Responses to alloantigens and transplant rejection. 2001, New York: Garland Science.
8. Schulman, L.L., et al., *Mismatches at the HLA-DR and HLA-B loci are risk factors for acute rejection after lung transplantation*. Am J Respir Crit Care Med, 1998. **157**(6 Pt 1): p. 1833-7.
9. Quantz, M.A., et al., *Does human leukocyte antigen matching influence the outcome of lung transplantation? An analysis of 3,549 lung transplantations*. J Heart Lung Transplant, 2000. **19**(5): p. 473-9.
10. Vilchez, R.A., et al., *Parainfluenza virus infection in adult lung transplant recipients: an emergent clinical syndrome with implications on allograft function*. Am J Transplant, 2003. **3**(2): p. 116-20.
11. Kumar, D., et al., *Clinical impact of community-acquired respiratory viruses on bronchiolitis obliterans after lung transplant*. Am J Transplant, 2005. **5**(8): p. 2031-6.
12. Glanville, A.R., et al., *Chlamydia pneumoniae infection after lung transplantation*. J Heart Lung Transplant, 2005. **24**(2): p. 131-6.
13. Palmer, S.M., et al., *Genetic regulation of rejection and survival following human lung transplantation by the innate immune receptor CD14*. Am J Transplant, 2007. **7**(3): p. 693-9.
14. Zheng, H.X., et al., *The impact of pharmacogenomic factors on acute persistent rejection in adult lung transplant patients*. Transpl Immunol, 2005. **14**(1): p. 37-42.
15. Fadili, W., M. Habib Allah, and I. Laouad, *Chronic renal allograft dysfunction: risk factors, immunology and prevention*. Arab J Nephrol Transplant, 2013. **6**(1): p. 45-50.
16. Pascual, J., et al., *Chronic renal dysfunction in kidney transplant recipients. Consensus Document. Spanish Consensus Group on Renal Dysfunction in Kidney Transplantation Patients*. Nefrologia, 2012. **32 Suppl 2**: p. 1-28.
17. Terasaki, P.I. and M. Ozawa, *Predictive value of HLA antibodies and serum creatinine in chronic rejection: results of a 2-year prospective trial*. Transplantation, 2005. **80**(9): p. 1194-7.
18. Ferlicot, S., et al., *The role of replicative senescence in chronic allograft nephropathy*. Hum Pathol, 2003. **34**(9): p. 924-8.
19. Pratschke, J., et al., *Influence of donor brain death on chronic rejection of renal transplants in rats*. J Am Soc Nephrol, 2001. **12**(11): p. 2474-81.
20. Ojo, A.O., et al., *Long-term survival in renal transplant recipients with graft function*. Kidney Int, 2000. **57**(1): p. 307-13.

21. Clipstone, N.A. and G.R. Crabtree, *Identification of calcineurin as a key signalling enzyme in T-lymphocyte activation*. Nature, 1992. **357**(6380): p. 695-7.
22. Nankivell, B.J. and D.R. Kuypers, *Diagnosis and prevention of chronic kidney allograft loss*. Lancet, 2011. **378**(9800): p. 1428-37.
23. Inkinen, K., et al., *Cytomegalovirus enhance expression of growth factors during the development of chronic allograft nephropathy in rats*. Transpl Int, 2005. **18**(6): p. 743-9.
24. Martinu, T., D.N. Howell, and S.M. Palmer, *Acute cellular rejection and humoral sensitization in lung transplant recipients*. Semin Respir Crit Care Med, 2010. **31**(2): p. 179-88.
25. Yousem, S.A., et al., *Can immunohistological analysis of transbronchial biopsy specimens predict responder status in early acute rejection of lung allografts?* Hum Pathol, 1994. **25**(5): p. 525-9.
26. Lau, C.L., et al., *Lung transplantation at Duke University Medical Center*. Clin Transpl, 1998: p. 327-40.
27. Shennib, H., et al., *Efficacy of OKT3 therapy for acute rejection in isolated lung transplantation*. J Heart Lung Transplant, 1994. **13**(3): p. 514-9.
28. Kirk, A.D., et al., *Treatment with humanized monoclonal antibody against CD154 prevents acute renal allograft rejection in nonhuman primates*. Nat Med, 1999. **5**(6): p. 686-93.
29. Vo, A.A., et al., *Rituximab and intravenous immune globulin for desensitization during renal transplantation*. N Engl J Med, 2008. **359**(3): p. 242-51.
30. Sandovici, M., et al., *Towards graft-specific immune suppression: Gene therapy of the transplanted kidney*. Adv Drug Deliv Rev, 2010. **62**(14): p. 1358-68.
31. Marcen, R., *Immunosuppressive drugs in kidney transplantation: impact on patient survival, and incidence of cardiovascular disease, malignancy and infection*. Drugs, 2009. **69**(16): p. 2227-43.
32. Bedi, D.S., et al., *Animal models of chronic allograft injury: contributions and limitations to understanding the mechanism of long-term graft dysfunction*. Transplantation, 2010. **90**(9): p. 935-44.
33. Takemoto, S.K., et al., *National conference to assess antibody-mediated rejection in solid organ transplantation*. Am J Transplant, 2004. **4**(7): p. 1033-41.
34. Flechner, S.M., et al., *Kidney transplantation without calcineurin inhibitor drugs: a prospective, randomized trial of sirolimus versus cyclosporine*. Transplantation, 2002. **74**(8): p. 1070-6.
35. Nianqiao G, X.C., Zhao D, Changsheng M, Xiaoping C., *Chronic allograft Nephropathy: the Mechanisms and Strategies*. Hong Kong J Nephrol, 2007. **9**(2): p. 58-69.
36. Lechler, R.I., et al., *Organ transplantation--how much of the promise has been realized?* Nat Med, 2005. **11**(6): p. 605-13.
37. Joffre, O., et al., *Prevention of acute and chronic allograft rejection with CD4+CD25+Foxp3+ regulatory T lymphocytes*. Nat Med, 2008. **14**(1): p. 88-92.
38. Pasquet, L., et al., *Long-term prevention of chronic allograft rejection by regulatory T-cell immunotherapy involves host Foxp3-expressing T cells*. Blood, 2013. **121**(21): p. 4303-10.
39. Bai, J.P., L.J. Lesko, and G.J. Burckart, *Understanding the genetic basis for adverse drug effects: the calcineurin inhibitors*. Pharmacotherapy, 2010. **30**(2): p. 195-209.
40. Metalidis, C. and D.R. Kuypers, *Emerging immunosuppressive drugs in kidney transplantation*. Curr Clin Pharmacol, 2011. **6**(2): p. 130-6.
41. Ueno, T., et al., *Divergent role of donor dendritic cells in rejection versus tolerance of allografts*. J Am Soc Nephrol, 2009. **20**(3): p. 535-44.
42. Tepperman, E., et al., *Surgical biology for the clinician: vascular effects of immunosuppression*. Can J Surg, 2010. **53**(1): p. 57-63.
43. Willoughby, C.A., et al., *Discovery of potent, selective human granzyme B inhibitors that inhibit CTL mediated apoptosis*. Bioorg Med Chem Lett, 2002. **12**(16): p. 2197-200.

44. Femke Broere, S.G.A., Michail V. Sitkovsky and Willem van Eden, *Principles of Immunopharmacology: 3rd revised and extended edition*. T cell subsets and T cell-mediated immunity, ed. F.P.N.a.M.J. Parnham. 2011: Springer Basel.
45. Swain, S.L., K.K. McKinstry, and T.M. Strutt, *Expanding roles for CD4(+) T cells in immunity to viruses*. *Nat Rev Immunol*, 2012. **12**(2): p. 136-48.
46. Joncker, N.T. and D.H. Raulet, *Regulation of NK cell responsiveness to achieve self-tolerance and maximal responses to diseased target cells*. *Immunol Rev*, 2008. **224**: p. 85-97.
47. Ljunggren, H.G. and K. Karre, *In search of the 'missing self': MHC molecules and NK cell recognition*. *Immunol Today*, 1990. **11**(7): p. 237-44.
48. Janeway, T., Walport, and Shlomchik, *Immunobiology, the immune system in health and disease*. 6 ed. Failures of Host Defense Mechanisms. 2005.
49. Raja, S.M., S.S. Metkar, and C.J. Froelich, *Cytotoxic granule-mediated apoptosis: unraveling the complex mechanism*. *Curr Opin Immunol*, 2003. **15**(5): p. 528-32.
50. Kam, C.M., D. Hudig, and J.C. Powers, *Granzymes (lymphocyte serine proteases): characterization with natural and synthetic substrates and inhibitors*. *Biochim Biophys Acta*, 2000. **1477**(1-2): p. 307-23.
51. Sutton, V.R., et al., *Caspase activation by granzyme B is indirect, and caspase autoprocessing requires the release of proapoptotic mitochondrial factors*. *Immunity*, 2003. **18**(3): p. 319-29.
52. Zhang, D., et al., *Granzymes A and B directly cleave lamins and disrupt the nuclear lamina during granule-mediated cytolysis*. *Proc Natl Acad Sci U S A*, 2001. **98**(10): p. 5746-51.
53. Choy, J.C., *Granzymes and perforin in solid organ transplant rejection*. *Cell Death Differ*, 2010. **17**(4): p. 567-76.
54. Isaaz, S., et al., *Serial killing by cytotoxic T lymphocytes: T cell receptor triggers degranulation, re-filling of the lytic granules and secretion of lytic proteins via a non-granule pathway*. *Eur J Immunol*, 1995. **25**(4): p. 1071-9.
55. Walden, P.R. and H.N. Eisen, *Cognate peptides induce self-destruction of CD8+ cytolytic T lymphocytes*. *Proc Natl Acad Sci U S A*, 1990. **87**(22): p. 9015-9.
56. Hanon, E., et al., *Fatricide among CD8(+) T lymphocytes naturally infected with human T cell lymphotropic virus type I*. *Immunity*, 2000. **13**(5): p. 657-64.
57. Huang, J.F., et al., *TCR-Mediated internalization of peptide-MHC complexes acquired by T cells*. *Science*, 1999. **286**(5441): p. 952-4.
58. Ida, H., et al., *Granzyme B leakage-induced cell death: a new type of activation-induced natural killer cell death*. *Eur J Immunol*, 2003. **33**(12): p. 3284-92.
59. Ashton-Rickardt, P.G., *Serine protease inhibitors and cytotoxic T lymphocytes*. *Immunol Rev*, 2010. **235**(1): p. 147-58.
60. Silverman, G.A., et al., *The serpins are an expanding superfamily of structurally similar but functionally diverse proteins. Evolution, mechanism of inhibition, novel functions, and a revised nomenclature*. *J Biol Chem*, 2001. **276**(36): p. 33293-6.
61. Zhang, M., et al., *Serine protease inhibitor 6 protects cytotoxic T cells from self-inflicted injury by ensuring the integrity of cytotoxic granules*. *Immunity*, 2006. **24**(4): p. 451-61.
62. Ansari, A.W., et al., *Serine protease inhibitor 6 protects iNKT cells from self-inflicted damage*. *J Immunol*, 2010. **185**(2): p. 877-83.
63. Ludewig, B., et al., *Perforin-independent regulation of dendritic cell homeostasis by CD8(+) T cells in vivo: implications for adaptive immunotherapy*. *Eur J Immunol*, 2001. **31**(6): p. 1772-9.
64. Medema, J.P., et al., *Expression of the serpin serine protease inhibitor 6 protects dendritic cells from cytotoxic T lymphocyte-induced apoptosis: differential modulation by T helper type 1 and type 2 cells*. *J Exp Med*, 2001. **194**(5): p. 657-67.
65. Opferman, J.T., B.T. Ober, and P.G. Ashton-Rickardt, *Linear differentiation of cytotoxic effectors into memory T lymphocytes*. *Science*, 1999. **283**(5408): p. 1745-8.
66. Phillips, T., et al., *A role for the granzyme B inhibitor serine protease inhibitor 6 in CD8+ memory cell homeostasis*. *J Immunol*, 2004. **173**(6): p. 3801-9.

67. Zhang, M., et al., *Differential survival of cytotoxic T cells and memory cell precursors*. J Immunol, 2007. **178**(6): p. 3483-91.
68. Liu, N., et al., *NF-kappaB protects from the lysosomal pathway of cell death*. EMBO J, 2003. **22**(19): p. 5313-22.
69. Liu, N., et al., *Serine protease inhibitor 2A is a protective factor for memory T cell development*. Nat Immunol, 2004. **5**(9): p. 919-26.
70. Hirst, C.E., et al., *The intracellular granzyme B inhibitor, proteinase inhibitor 9, is up-regulated during accessory cell maturation and effector cell degranulation, and its overexpression enhances CTL potency*. J Immunol, 2003. **170**(2): p. 805-15.
71. Hermans, I.F., et al., *CD8+ T cell-dependent elimination of dendritic cells in vivo limits the induction of antitumor immunity*. J Immunol, 2000. **164**(6): p. 3095-101.
72. Rowshani, A.T., et al., *Hyperexpression of the granzyme B inhibitor PI-9 in human renal allografts: a potential mechanism for stable renal function in patients with subclinical rejection*. Kidney Int, 2004. **66**(4): p. 1417-22.
73. Hameed, A., et al., *Immunohistochemical localization of granzyme B antigen in cytotoxic cells in human tissues*. Am J Pathol, 1991. **138**(5): p. 1069-75.
74. Clement, M.V., et al., *Perforin and granzyme B as markers for acute rejection in heart transplantation*. Int Immunol, 1991. **3**(11): p. 1175-81.
75. Kummer, J.A., et al., *Expression of granzyme A and B proteins by cytotoxic lymphocytes involved in acute renal allograft rejection*. Kidney Int, 1995. **47**(1): p. 70-7.
76. Vasconcellos, L.M., et al., *Cytotoxic lymphocyte gene expression in peripheral blood leukocytes correlates with rejecting renal allografts*. Transplantation, 1998. **66**(5): p. 562-6.
77. Buzza, M.S., et al., *Extracellular matrix remodeling by human granzyme B via cleavage of vitronectin, fibronectin, and laminin*. J Biol Chem, 2005. **280**(25): p. 23549-58.
78. Singh, N., J. Pirsch, and M. Samaniego, *Antibody-mediated rejection: treatment alternatives and outcomes*. Transplant Rev (Orlando), 2009. **23**(1): p. 34-46.
79. Uber, W.E., et al., *Acute antibody-mediated rejection following heart transplantation*. Am J Transplant, 2007. **7**(9): p. 2064-74.
80. Nencioni, A., et al., *Dendritic cells transfected with tumor RNA for the induction of antitumor CTL in colorectal cancer*. Cancer Gene Ther, 2003. **10**(3): p. 209-14.
81. Van Tendeloo, V.F., P. Ponsaerts, and Z.N. Berneman, *mRNA-based gene transfer as a tool for gene and cell therapy*. Curr Opin Mol Ther, 2007. **9**(5): p. 423-31.
82. Breckpot, K., et al., *Exploiting dendritic cells for cancer immunotherapy: genetic modification of dendritic cells*. J Gene Med, 2004. **6**(11): p. 1175-88.
83. Smits, E.L., et al., *Dendritic cell-based cancer gene therapy*. Hum Gene Ther, 2009. **20**(10): p. 1106-18.
84. Banchereau, J. and A.K. Palucka, *Dendritic cells as therapeutic vaccines against cancer*. Nat Rev Immunol, 2005. **5**(4): p. 296-306.
85. Cao, J., et al., *DNA vaccines targeting the encoded antigens to dendritic cells induce potent antitumor immunity in mice*. BMC Immunol, 2013. **14**(1): p. 39.
86. Chen, J., et al., *Generation of CTL responses against pancreatic cancer in vitro using dendritic cells co-transfected with MUC4 and survivin RNA*. Vaccine, 2013.
87. Vik-Mo, E.O., et al., *Therapeutic vaccination against autologous cancer stem cells with mRNA-transfected dendritic cells in patients with glioblastoma*. Cancer Immunol Immunother, 2013.
88. Anguille, S., et al., *Interleukin-15 dendritic cells as vaccine candidates for cancer immunotherapy*. Hum Vaccin Immunother, 2013. **9**(9).
89. Banchereau, J., et al., *Immunobiology of dendritic cells*. Annu Rev Immunol, 2000. **18**: p. 767-811.
90. Reis e Sousa, C., *Dendritic cells in a mature age*. Nat Rev Immunol, 2006. **6**(6): p. 476-83.

91. Xu, D.L., et al., *Marked prolongation of murine cardiac allograft survival using recipient immature dendritic cells loaded with donor-derived apoptotic cells*. Scand J Immunol, 2004. **59**(6): p. 536-44.
92. Wang, Q., et al., *Anti-ICAM-1 antibody and CTLA-4Ig synergistically enhance immature dendritic cells to induce donor-specific immune tolerance in vivo*. Immunol Lett, 2003. **90**(1): p. 33-42.
93. Wu, L., et al., *RelB is essential for the development of myeloid-related CD8alpha- dendritic cells but not of lymphoid-related CD8alpha+ dendritic cells*. Immunity, 1998. **9**(6): p. 839-47.
94. Cejas, P.J., et al., *Regulation of RelB expression during the initiation of dendritic cell differentiation*. Mol Cell Biol, 2005. **25**(17): p. 7900-16.
95. Burkly, L., et al., *Expression of relB is required for the development of thymic medulla and dendritic cells*. Nature, 1995. **373**(6514): p. 531-6.
96. Zanetti, M., et al., *The role of relB in regulating the adaptive immune response*. Ann N Y Acad Sci, 2003. **987**: p. 249-57.
97. Ardeshtna, K.M., et al., *The PI3 kinase, p38 SAP kinase, and NF-kappaB signal transduction pathways are involved in the survival and maturation of lipopolysaccharide-stimulated human monocyte-derived dendritic cells*. Blood, 2000. **96**(3): p. 1039-46.
98. Walsh, C.E., *Gene therapy progress and prospects: gene therapy for the hemophilias*. Gene Ther, 2003. **10**(12): p. 999-1003.
99. Ferrari, M., *Nanovector therapeutics*. Curr Opin Chem Biol, 2005. **9**(4): p. 343-6.
100. McNeish, I.A., S.J. Bell, and N.R. Lemoine, *Gene therapy progress and prospects: cancer gene therapy using tumour suppressor genes*. Gene Ther, 2004. **11**(6): p. 497-503.
101. Alexis, F., et al., *New frontiers in nanotechnology for cancer treatment*. Urol Oncol, 2008. **26**(1): p. 74-85.
102. Pack, D.W., et al., *Design and development of polymers for gene delivery*. Nat Rev Drug Discov, 2005. **4**(7): p. 581-93.
103. Cavazzana-Calvo, M., et al., *Gene therapy of human severe combined immunodeficiency (SCID)-X1 disease*. Science, 2000. **288**(5466): p. 669-72.
104. Thomas, C.E., A. Ehrhardt, and M.A. Kay, *Progress and problems with the use of viral vectors for gene therapy*. Nat Rev Genet, 2003. **4**(5): p. 346-58.
105. Raper, S.E., et al., *Fatal systemic inflammatory response syndrome in a ornithine transcarbamylase deficient patient following adenoviral gene transfer*. Mol Genet Metab, 2003. **80**(1-2): p. 148-58.
106. Boussif, O., et al., *A versatile vector for gene and oligonucleotide transfer into cells in culture and in vivo: polyethylenimine*. Proc Natl Acad Sci U S A, 1995. **92**(16): p. 7297-301.
107. Wood, K.C., et al., *A family of hierarchically self-assembling linear-dendritic hybrid polymers for highly efficient targeted gene delivery*. Angew Chem Int Ed Engl, 2005. **44**(41): p. 6704-8.
108. Wood, K.C., et al., *Tumor-targeted gene delivery using molecularly engineered hybrid polymers functionalized with a tumor-homing peptide*. Bioconjug Chem, 2008. **19**(2): p. 403-5.
109. Allen, M.H., et al., *Tailoring charge density and hydrogen bonding of imidazolium copolymers for efficient gene delivery*. Biomacromolecules, 2011. **12**(6): p. 2243-50.
110. Ong, Z.Y., et al., *Rational design of biodegradable cationic polycarbonates for gene delivery*. J Control Release, 2011. **152**(1): p. 120-6.
111. Hemp, S.T., et al., *Phosphonium-containing diblock copolymers for enhanced colloidal stability and efficient nucleic acid delivery*. Biomacromolecules, 2012. **13**(8): p. 2439-45.
112. N.A. *Gene therapy clinical trials worldwide*. 2011 1 August 2013]; Available from: <http://www.wiley.com/legacy/wileychi/genmed/clinical/>.
113. Wang, W., et al., *Polyethylenimine-mediated gene delivery into human bone marrow mesenchymal stem cells from patients*. J Cell Mol Med, 2011. **15**(9): p. 1989-98.
114. Sharon Y. Wong, J.M.P., David Putnam, *Polymer systems for gene delivery—Past, present, and future*. Progress in Polymer Science, 2007. **32**(8-9): p. 799–837.

115. Abdelhady, H.G., et al., *Direct real-time molecular scale visualisation of the degradation of condensed DNA complexes exposed to DNase I*. Nucleic Acids Res, 2003. **31**(14): p. 4001-5.
116. Schaffer, D.V. and D.A. Lauffenburger, *Optimization of cell surface binding enhances efficiency and specificity of molecular conjugate gene delivery*. J Biol Chem, 1998. **273**(43): p. 28004-9.
117. Burckbuchler, V., et al., *DNA compaction into new DNA vectors based on cyclodextrin polymer: surface enhanced Raman spectroscopy characterization*. Biopolymers, 2006. **81**(5): p. 360-70.
118. Hong, S., et al., *Interaction of polycationic polymers with supported lipid bilayers and cells: nanoscale hole formation and enhanced membrane permeability*. Bioconjug Chem, 2006. **17**(3): p. 728-34.
119. Leroueil, P.R., et al., *Wide varieties of cationic nanoparticles induce defects in supported lipid bilayers*. Nano Lett, 2008. **8**(2): p. 420-4.
120. Park, T.G., J.H. Jeong, and S.W. Kim, *Current status of polymeric gene delivery systems*. Adv Drug Deliv Rev, 2006. **58**(4): p. 467-86.
121. Leblond, J., et al., *Design, synthesis, and evaluation of enhanced DNA binding new lipopolythioureas*. Bioconjug Chem, 2006. **17**(5): p. 1200-8.
122. Wang, J., H.Q. Mao, and K.W. Leong, *A novel biodegradable gene carrier based on polyphosphoester*. J Am Chem Soc, 2001. **123**(38): p. 9480-1.
123. Zugates, G.T., et al., *Synthesis of poly(beta-amino ester)s with thiol-reactive side chains for DNA delivery*. J Am Chem Soc, 2006. **128**(39): p. 12726-34.
124. Oster, C.G., et al., *Cationic microparticles consisting of poly(lactide-co-glycolide) and polyethylenimine as carriers systems for parental DNA vaccination*. J Control Release, 2005. **104**(2): p. 359-77.
125. Kong, H.J., et al., *Design of biodegradable hydrogel for the local and sustained delivery of angiogenic plasmid DNA*. Pharm Res, 2008. **25**(5): p. 1230-8.
126. Ando, S., et al., *PLGA microspheres containing plasmid DNA: preservation of supercoiled DNA via cryopreparation and carbohydrate stabilization*. J Pharm Sci, 1999. **88**(1): p. 126-30.
127. Fu, K., et al., *Visual evidence of acidic environment within degrading poly(lactic-co-glycolic acid) (PLGA) microspheres*. Pharm Res, 2000. **17**(1): p. 100-6.
128. Jeong, J.H., S.W. Kim, and T.G. Park, *Biodegradable triblock copolymer of PLGA-PEG-PLGA enhances gene transfection efficiency*. Pharm Res, 2004. **21**(1): p. 50-4.
129. Gary, D.J., N. Puri, and Y.Y. Won, *Polymer-based siRNA delivery: perspectives on the fundamental and phenomenological distinctions from polymer-based DNA delivery*. J Control Release, 2007. **121**(1-2): p. 64-73.
130. Sung, S.J., et al., *Effect of polyethylene glycol on gene delivery of polyethylenimine*. Biol Pharm Bull, 2003. **26**(4): p. 492-500.
131. Mullen, P.M., et al., *Strength of conjugate binding to plasmid DNA affects degradation rate and expression level in vivo*. Biochim Biophys Acta, 2000. **1523**(1): p. 103-10.
132. Miyata, K., et al., *Block cationic polyplexes with regulated densities of charge and disulfide cross-linking directed to enhance gene expression*. J Am Chem Soc, 2004. **126**(8): p. 2355-61.
133. Saito, G., J.A. Swanson, and K.D. Lee, *Drug delivery strategy utilizing conjugation via reversible disulfide linkages: role and site of cellular reducing activities*. Adv Drug Deliv Rev, 2003. **55**(2): p. 199-215.
134. Mislick, K.A. and J.D. Baldeschwieler, *Evidence for the role of proteoglycans in cation-mediated gene transfer*. Proc Natl Acad Sci U S A, 1996. **93**(22): p. 12349-54.
135. Zanta, M.A., et al., *In vitro gene delivery to hepatocytes with galactosylated polyethylenimine*. Bioconjug Chem, 1997. **8**(6): p. 839-44.
136. Diebold, S.S., et al., *Efficient gene delivery into human dendritic cells by adenovirus polyethylenimine and mannose polyethylenimine transfection*. Human Gene Therapy, 1999. **10**(5): p. 775-786.
137. Zou, S.M., et al., *Systemic linear polyethylenimine (L PEI) mediated gene delivery in the mouse*. The journal of gene medicine, 2000. **2**(2): p. 128-134.

138. Lam, J., et al., *Folate conjugated phosphorylcholine-based polycations for specific targeting in nucleic acids delivery*. Journal of Drug Targeting, 2009. **17**(7): p. 512-523.
139. Ogris, M., et al., *PEGylated DNA/transferrin-PEI complexes: reduced interaction with blood components, extended circulation in blood and potential for systemic gene delivery*. Gene Therapy, 1999. **6**(4): p. 595.
140. Li, S., et al., *Targeted gene delivery to pulmonary endothelium by anti-PECAM antibody*. American Journal of Physiology-Lung Cellular and Molecular Physiology, 2000. **278**(3): p. L504.
141. Chiu, S.J., N.T. Ueno, and R.J. Lee, *Tumor-targeted gene delivery via anti-HER2 antibody (trastuzumab, Herceptin®) conjugated polyethylenimine*. Journal of Controlled Release, 2004. **97**(2): p. 357-369.
142. Kim, W.J., et al., *Soluble Flt-1 gene delivery using PEI-g-PEG-RGD conjugate for anti-angiogenesis*. Journal of Controlled Release, 2005. **106**(1-2): p. 224-234.
143. Kunath, K., et al., *Integrin targeting using RGD PEI conjugates for in vitro gene transfer*. The journal of gene medicine, 2003. **5**(7): p. 588-599.
144. Blessing, T., et al., *Different strategies for formation of pegylated EGF-conjugated PEI/DNA complexes for targeted gene delivery*. Bioconjugate Chemistry, 2001. **12**(4): p. 529-537.
145. Han, L., et al., *Plasmid pORF-hTRAIL and doxorubicin co-delivery targeting to tumor using peptide-conjugated polyamidoamine dendrimer*. Biomaterials, 2011. **32**(4): p. 1242-1252.
146. von Gersdorff, K., et al., *The internalization route resulting in successful gene expression depends on both cell line and polyethylenimine polyplex type*. Mol Ther, 2006. **14**(5): p. 745-53.
147. Rejman, J., A. Bragonzi, and M. Conese, *Role of clathrin- and caveolae-mediated endocytosis in gene transfer mediated by lipo- and polyplexes*. Mol Ther, 2005. **12**(3): p. 468-74.
148. Bettinger, T., et al., *Peptide-mediated RNA delivery: a novel approach for enhanced transfection of primary and post-mitotic cells*. Nucleic Acids Res, 2001. **29**(18): p. 3882-91.
149. Lee, H., J.H. Jeong, and T.G. Park, *PEG grafted polylysine with fusogenic peptide for gene delivery: high transfection efficiency with low cytotoxicity*. Journal of Controlled Release, 2002. **79**(1-3): p. 283-291.
150. Yang, C., et al., *Mitigated Cytotoxicity and Tremendously Enhanced Gene Transfection Efficiency of PEI through Facile One-Step Carbamate Modification*. Adv Healthc Mater, 2013.
151. Erbacher, P., et al., *Putative role of chloroquine in gene transfer into a human hepatoma cell line by DNA/lactosylated polylysine complexes*. Exp Cell Res, 1996. **225**(1): p. 186-94.
152. Cheung, C.Y., et al., *A pH-sensitive polymer that enhances cationic lipid-mediated gene transfer*. Bioconjug Chem, 2001. **12**(6): p. 906-10.
153. Dauty, E. and A.S. Verkman, *Actin cytoskeleton as the principal determinant of size-dependent DNA mobility in cytoplasm: a new barrier for non-viral gene delivery*. J Biol Chem, 2005. **280**(9): p. 7823-8.
154. Vaughan, E.E. and D.A. Dean, *Intracellular trafficking of plasmids during transfection is mediated by microtubules*. Mol Ther, 2006. **13**(2): p. 422-8.
155. Kichler, A., et al., *Efficient DNA transfection mediated by the C-terminal domain of human immunodeficiency virus type 1 viral protein R*. J Virol, 2000. **74**(12): p. 5424-31.
156. Moffatt, S., S. Wiehle, and R.J. Cristiano, *A multifunctional PEI-based cationic polyplex for enhanced systemic p53-mediated gene therapy*. Gene Ther, 2006. **13**(21): p. 1512-23.
157. Pante, N. and M. Kann, *Nuclear pore complex is able to transport macromolecules with diameters of about 39 nm*. Mol Biol Cell, 2002. **13**(2): p. 425-34.
158. Duverger, E., et al., *Nuclear import of glycoconjugates is distinct from the classical NLS pathway*. J Cell Sci, 1995. **108 (Pt 4)**: p. 1325-32.
159. Grosse, S., et al., *Which mechanism for nuclear import of plasmid DNA complexed with polyethylenimine derivatives?* J Gene Med, 2006. **8**(7): p. 845-51.
160. Klink, D.T., et al., *Nuclear translocation of lactosylated poly-L-lysine/cDNA complex in cystic fibrosis airway epithelial cells*. Mol Ther, 2001. **3**(6): p. 831-41.

161. Brunner, S., et al., *Cell cycle dependence of gene transfer by lipoplex, polyplex and recombinant adenovirus*. *Gene Ther*, 2000. **7**(5): p. 401-7.
162. Brunner, S., et al., *Overcoming the nuclear barrier: cell cycle independent nonviral gene transfer with linear polyethylenimine or electroporation*. *Mol Ther*, 2002. **5**(1): p. 80-6.
163. Jeong, J.H., S.W. Kim, and T.G. Park, *Molecular design of functional polymers for gene therapy*. *Progress in Polymer Science*, 2007. **32**(11): p. 1239-1274.
164. Wong, S.Y., J.M. Pelet, and D. Putnam, *Polymer systems for gene delivery--Past, present, and future*. *Progress in Polymer Science*, 2007. **32**(8-9): p. 799-837.
165. Pichon, C., et al., *Poly[Lys-(AEDTP)]: a cationic polymer that allows dissociation of pDNA/cationic polymer complexes in a reductive medium and enhances polyfection*. *Bioconjug Chem*, 2002. **13**(1): p. 76-82.
166. Read, M.L., et al., *Vectors based on reducible polycations facilitate intracellular release of nucleic acids*. *J Gene Med*, 2003. **5**(3): p. 232-45.
167. de Las Heras Alarcon, C., S. Pennadam, and C. Alexander, *Stimuli responsive polymers for biomedical applications*. *Chem Soc Rev*, 2005. **34**(3): p. 276-85.
168. Cheng, N., et al., *A study of thermoresponsive poly(N-isopropylacrylamide)/polyarginine bioconjugate non-viral transgene vectors*. *Biomaterials*, 2006. **27**(28): p. 4984-92.
169. Plank, C., et al., *Activation of the complement system by synthetic DNA complexes: a potential barrier for intravenous gene delivery*. *Hum Gene Ther*, 1996. **7**(12): p. 1437-46.
170. Davis, M.E. and M.E. Brewster, *Cyclodextrin-based pharmaceuticals: past, present and future*. *Nat Rev Drug Discov*, 2004. **3**(12): p. 1023-35.
171. Park, I.K., et al., *Supramolecular assembly of cyclodextrin-based nanoparticles on solid surfaces for gene delivery*. *Langmuir*, 2006. **22**(20): p. 8478-84.
172. Pun, S.H., et al., *Cyclodextrin-modified polyethylenimine polymers for gene delivery*. *Bioconjug Chem*, 2004. **15**(4): p. 831-40.
173. Hunter, A.C., *Molecular hurdles in polyfectin design and mechanistic background to polycation induced cytotoxicity*. *Adv Drug Deliv Rev*, 2006. **58**(14): p. 1523-31.
174. Liu, Y., et al., *Biophysical characterization of hyper-branched polyethylenimine-graft-polycaprolactone-block-mono-methoxyl-poly(ethylene glycol) copolymers (hy-PEI-PCL-mPEG) for siRNA delivery*. *J Control Release*, 2011. **153**(3): p. 262-8.
175. Forrest, M.L., J.T. Koerber, and D.W. Pack, *A degradable polyethylenimine derivative with low toxicity for highly efficient gene delivery*. *Bioconjug Chem*, 2003. **14**(5): p. 934-40.
176. Borchard, G., *Chitosans for gene delivery*. *Adv Drug Deliv Rev*, 2001. **52**(2): p. 145-50.
177. Howard, K.A., et al., *RNA interference in vitro and in vivo using a novel chitosan/siRNA nanoparticle system*. *Mol Ther*, 2006. **14**(4): p. 476-84.
178. Roy, K., et al., *Oral gene delivery with chitosan--DNA nanoparticles generates immunologic protection in a murine model of peanut allergy*. *Nat Med*, 1999. **5**(4): p. 387-91.
179. Xenariou, S., et al., *Low-frequency ultrasound increases non-viral gene transfer to the mouse lung*. *Acta Biochim Biophys Sin (Shanghai)*, 2010. **42**(1): p. 45-51.
180. Nguyen-Hoai, T., et al., *HER2/neu DNA vaccination by intradermal gene delivery in a mouse tumor model: Gene gun is superior to jet injector in inducing CTL responses and protective immunity*. *Oncoimmunology*, 2012. **1**(9): p. 1537-1545.
181. McNeil, P.L., et al., *A method for incorporating macromolecules into adherent cells*. *J Cell Biol*, 1984. **98**(4): p. 1556-64.
182. Luo, D. and W.M. Saltzman, *Synthetic DNA delivery systems*. *Nat Biotechnol*, 2000. **18**(1): p. 33-7.
183. Parker, A.L., et al., *Nonviral gene delivery: techniques and implications for molecular medicine*. *Expert Rev Mol Med*, 2003. **5**(22): p. 1-15.
184. Kay, M.A., J.C. Glorioso, and L. Naldini, *Viral vectors for gene therapy: the art of turning infectious agents into vehicles of therapeutics*. *Nat Med*, 2001. **7**(1): p. 33-40.

185. Lundstrom, K., *Latest development in viral vectors for gene therapy*. Trends Biotechnol, 2003. **21**(3): p. 117-22.
186. Gardlik, R., et al., *Vectors and delivery systems in gene therapy*. Med Sci Monit, 2005. **11**(4): p. RA110-21.
187. Rosenberg, S.A., et al., *Human gene marker/therapy clinical protocols*. Hum Gene Ther, 2000. **11**(6): p. 919-79.
188. Halene, S. and D.B. Kohn, *Gene therapy using hematopoietic stem cells: Sisyphus approaches the crest*. Hum Gene Ther, 2000. **11**(9): p. 1259-67.
189. Edelstein, M.L., et al., *Gene therapy clinical trials worldwide 1989-2004-an overview*. J Gene Med, 2004. **6**(6): p. 597-602.
190. Hacein-Bey-Abina, S., et al., *LMO2-associated clonal T cell proliferation in two patients after gene therapy for SCID-X1*. Science, 2003. **302**(5644): p. 415-9.
191. Bonini, C., et al., *HSV-TK gene transfer into donor lymphocytes for control of allogeneic graft-versus-leukemia*. Science, 1997. **276**(5319): p. 1719-24.
192. Vigna, E. and L. Naldini, *Lentiviral vectors: excellent tools for experimental gene transfer and promising candidates for gene therapy*. J Gene Med, 2000. **2**(5): p. 308-16.
193. Mitrophanous, K., et al., *Stable gene transfer to the nervous system using a non-primate lentiviral vector*. Gene Ther, 1999. **6**(11): p. 1808-18.
194. Yang, Y., et al., *Cellular and humoral immune responses to viral antigens create barriers to lung-directed gene therapy with recombinant adenoviruses*. J Virol, 1995. **69**(4): p. 2004-15.
195. Balague, C., et al., *Sustained high-level expression of full-length human factor VIII and restoration of clotting activity in hemophilic mice using a minimal adenovirus vector*. Blood, 2000. **95**(3): p. 820-8.
196. Flotte, T.R., *Recombinant adeno-associated virus vectors for cystic fibrosis gene therapy*. Curr Opin Mol Ther, 2001. **3**(5): p. 497-502.
197. Krisky, D.M., et al., *Development of herpes simplex virus replication-defective multigene vectors for combination gene therapy applications*. Gene Ther, 1998. **5**(11): p. 1517-30.
198. Liu, H., et al., *Preclinical evaluation of herpes simplex virus armed with granulocyte-macrophage colony-stimulating factor in pancreatic carcinoma*. World J Gastroenterol, 2013. **19**(31): p. 5138-43.
199. Yenari, M.A., et al., *Gene therapy with HSP72 is neuroprotective in rat models of stroke and epilepsy*. Ann Neurol, 1998. **44**(4): p. 584-91.
200. Crystal, R.G., *Transfer of genes to humans: early lessons and obstacles to success*. Science, 1995. **270**(5235): p. 404-10.
201. Schatzlein, A.G., *Non-viral vectors in cancer gene therapy: principles and progress*. Anticancer Drugs, 2001. **12**(4): p. 275-304.
202. Behr, J.P., et al., *Efficient gene transfer into mammalian primary endocrine cells with lipopolyamine-coated DNA*. Proc Natl Acad Sci U S A, 1989. **86**(18): p. 6982-6.
203. Lee, E.R., et al., *Detailed analysis of structures and formulations of cationic lipids for efficient gene transfer to the lung*. Hum Gene Ther, 1996. **7**(14): p. 1701-17.
204. Scheule, R.K., et al., *Basis of pulmonary toxicity associated with cationic lipid-mediated gene transfer to the mammalian lung*. Hum Gene Ther, 1997. **8**(6): p. 689-707.
205. Hui, S.W., et al., *The role of helper lipids in cationic liposome-mediated gene transfer*. Biophys J, 1996. **71**(2): p. 590-9.
206. Koltover, I., et al., *An inverted hexagonal phase of cationic liposome-DNA complexes related to DNA release and delivery*. Science, 1998. **281**(5373): p. 78-81.
207. Sternberg, B., et al., *Ultrastructural characterization of cationic liposome-DNA complexes showing enhanced stability in serum and high transfection activity in vivo*. Biochim Biophys Acta, 1998. **1375**(1-2): p. 23-35.
208. Simoes, S., et al., *Cationic liposomes for gene delivery*. Expert Opin Drug Deliv, 2005. **2**(2): p. 237-54.

209. Kwoh, D.Y., et al., *Stabilization of poly-L-lysine/DNA polyplexes for in vivo gene delivery to the liver*. *Biochim Biophys Acta*, 1999. **1444**(2): p. 171-90.
210. Choi, Y.H., et al., *Polyethylene glycol-grafted poly-L-lysine as polymeric gene carrier*. *J Control Release*, 1998. **54**(1): p. 39-48.
211. Midoux, P., et al., *Specific gene transfer mediated by lactosylated poly-L-lysine into hepatoma cells*. *Nucleic Acids Res*, 1993. **21**(4): p. 871-8.
212. Harada-Shiba, M., et al., *Polyion complex micelles as vectors in gene therapy--pharmacokinetics and in vivo gene transfer*. *Gene Ther*, 2002. **9**(6): p. 407-14.
213. Harada, A., H. Togawa, and K. Kataoka, *Physicochemical properties and nuclease resistance of antisense-oligodeoxynucleotides entrapped in the core of polyion complex micelles composed of poly(ethylene glycol)-poly(L-lysine) block copolymers*. *Eur J Pharm Sci*, 2001. **13**(1): p. 35-42.
214. Wiradharma, N., Y.W. Tong, and Y.Y. Yang, *Self-assembled oligopeptide nanostructures for co-delivery of drug and gene with synergistic therapeutic effect*. *Biomaterials*, 2009. **30**(17): p. 3100-9.
215. Wu, G.Y. and C.H. Wu, *Receptor-mediated in vitro gene transformation by a soluble DNA carrier system*. *J Biol Chem*, 1987. **262**(10): p. 4429-32.
216. Suh, W., et al., *Anti-JL1 antibody-conjugated poly (L-lysine) for targeted gene delivery to leukemia T cells*. *J Control Release*, 2001. **72**(1-3): p. 171-8.
217. Mislick, K.A., et al., *Transfection of folate-polylysine DNA complexes: evidence for lysosomal delivery*. *Bioconjug Chem*, 1995. **6**(5): p. 512-5.
218. Tang, M.X. and F.C. Szoka, *The influence of polymer structure on the interactions of cationic polymers with DNA and morphology of the resulting complexes*. *Gene Ther*, 1997. **4**(8): p. 823-32.
219. Gunther, M., et al., *Polyethylenimines for RNAi-mediated gene targeting in vivo and siRNA delivery to the lung*. *Eur J Pharm Biopharm*, 2010. **77**(3): p. 438-49.
220. Godbey, W.T., K.K. Wu, and A.G. Mikos, *Poly(ethylenimine) and its role in gene delivery*. *J Control Release*, 1999. **60**(2-3): p. 149-60.
221. Zuber, G., et al., *Towards synthetic viruses*. *Adv Drug Deliv Rev*, 2001. **52**(3): p. 245-53.
222. Nel, A.E., et al., *Understanding biophysicochemical interactions at the nano-bio interface*. *Nat Mater*, 2009. **8**(7): p. 543-57.
223. Gebhart, C.L. and A.V. Kabanov, *Evaluation of polyplexes as gene transfer agents*. *Journal of Controlled Release*, 2001. **73**(2-3): p. 401-416.
224. Abdallah, B., et al., *A powerful nonviral vector for in vivo gene transfer into the adult mammalian brain: polyethylenimine*. *Human Gene Therapy*, 1996. **7**(16): p. 1947-1954.
225. Gautam, A., et al., *Aerosol gene therapy for metastatic lung cancer using PEI-p53 complexes*. *Methods Mol Med*, 2003. **75**: p. 607-18.
226. Futami, K., et al., *Anticancer activity of RecQL1 helicase siRNA in mouse xenograft models*. *Cancer Sci*, 2008. **99**(6): p. 1227-36.
227. Ogris, M., et al., *PEGylated DNA/transferrin-PEI complexes: reduced interaction with blood components, extended circulation in blood and potential for systemic gene delivery*. *Gene Ther*, 1999. **6**(4): p. 595-605.
228. Chollet, P., et al., *Side-effects of a systemic injection of linear polyethylenimine-DNA complexes*. *J Gene Med*, 2002. **4**(1): p. 84-91.
229. Neu, M., D. Fischer, and T. Kissel, *Recent advances in rational gene transfer vector design based on poly(ethylene imine) and its derivatives*. *J Gene Med*, 2005. **7**(8): p. 992-1009.
230. Ito, T., et al., *DNA/polyethyleneimine/hyaluronic acid small complex particles and tumor suppression in mice*. *Biomaterials*, 2010. **31**(10): p. 2912-8.
231. Jiang, H.L., et al., *Efficient gene delivery using chitosan-polyethylenimine hybrid systems*. *Biomed Mater*, 2008. **3**(2): p. 025013.
232. Diebold, S.S., et al., *Mannose polyethylenimine conjugates for targeted DNA delivery into dendritic cells*. *J Biol Chem*, 1999. **274**(27): p. 19087-94.

233. Meng Zheng CY, M.F., Peng Rui, Zhong Zhiyuan. , *pH-Sensitive degradable hydrophobe modified 1.8 kDa branched polyethylenimine as "artificial viruses" for safe and efficient intracellular gene transfection.* . *Macromol Res*, 2012. **20**(3): p. 327-334.
234. Tripathi, S.K., et al., *Synthesis and evaluation of N-(2,3-dihydroxypropyl)-PEIs as efficient vectors for nucleic acids.* *Mol Biosyst*, 2012. **8**(5): p. 1426-34.
235. Wang, Y., et al., *Branched polyethylenimine derivatives with reductively cleavable periphery for safe and efficient in vitro gene transfer.* *Biomacromolecules*, 2011. **12**(4): p. 1032-40.
236. Thomas, M. and A.M. Klibanov, *Enhancing polyethylenimine's delivery of plasmid DNA into mammalian cells.* *Proc Natl Acad Sci U S A*, 2002. **99**(23): p. 14640-5.
237. Gabrielson, N.P.P., D. W., *Acetylation of polyethylenimine enhances gene delivery via weakened polymer/DNA interactions.* *Biomacromolecules*, 2006. **7**(8): p. 2427-35.
238. Tian, H., et al., *N-isopropylacrylamide-modified polyethylenimines as effective gene carriers.* *Macromol Biosci*, 2012. **12**(12): p. 1680-8.
239. Fischer, D., et al., *A novel non-viral vector for DNA delivery based on low molecular weight, branched polyethylenimine: effect of molecular weight on transfection efficiency and cytotoxicity.* *Pharm Res*, 1999. **16**(8): p. 1273-9.
240. Fischer, D., et al., *Copolymers of ethylene imine and N-(2-hydroxyethyl)-ethylene imine as tools to study effects of polymer structure on physicochemical and biological properties of DNA complexes.* *Bioconjug Chem*, 2002. **13**(5): p. 1124-33.
241. Godbey, W.T., K.K. Wu, and A.G. Mikos, *Size matters: molecular weight affects the efficiency of poly(ethylenimine) as a gene delivery vehicle.* *J Biomed Mater Res*, 1999. **45**(3): p. 268-75.
242. Xiang, S., et al., *Biscarbamate cross-linked low molecular weight PEI for delivering IL-1 receptor antagonist gene to synoviocytes for arthritis therapy.* *Biomaterials*, 2012. **33**(27): p. 6520-32.
243. Choosakoonkriang, S., et al., *Biophysical characterization of PEI/DNA complexes.* *Journal of Pharmaceutical Sciences*, 2003. **92**(8): p. 1710-1722.
244. Intra, J. and A.K. Salem, *Characterization of the transgene expression generated by branched and linear polyethylenimine-plasmid DNA nanoparticles in vitro and after intraperitoneal injection in vivo.* *Journal of Controlled Release*, 2008. **130**(2): p. 129-138.
245. Wightman, L., et al., *Different behavior of branched and linear polyethylenimine for gene delivery in vitro and in vivo.* *The journal of gene medicine*, 2001. **3**(4): p. 362-372.
246. Welton, F.J.S.T., *Metal-containing dendritic polymers.* *Polyhedron*, 1999. **18**(27): p. 3575-3591.
247. Russ, V., et al., *Oligoethylenimine-grafted polypropylenimine dendrimers as degradable and biocompatible synthetic vectors for gene delivery.* *J Control Release*, 2008. **132**(2): p. 131-40.
248. Lee, C.C., et al., *Designing dendrimers for biological applications.* *Nat Biotechnol*, 2005. **23**(12): p. 1517-26.
249. Lin, C., et al., *Novel bio-reducible poly(amido amine)s for highly efficient gene delivery.* *Bioconjug Chem*, 2007. **18**(1): p. 138-45.
250. Y.B. Lim, C.H.K., K. Kim, S.W. Kim, J.S. Park, 122 (2000), *Development of a safe gene delivery system using biodegradable polymer, poly[alpha-(4-aminobutyl)-L-glycolic acid]*. *J. Am. Chem. Soc.* , 2000. **122**: p. 6524- 6525.
251. Lim, Y.B., et al., *Biodegradable polyester, poly[alpha-(4-aminobutyl)-L-glycolic acid], as a non-toxic gene carrier.* *Pharm Res*, 2000. **17**(7): p. 811-6.
252. Ko, K.S., et al., *Combined administration of plasmids encoding IL-4 and IL-10 prevents the development of autoimmune diabetes in nonobese diabetic mice.* *Mol Ther*, 2001. **4**(4): p. 313-6.
253. Gosselin, M.A., W. Guo, and R.J. Lee, *Efficient gene transfer using reversibly cross-linked low molecular weight polyethylenimine.* *Bioconjug Chem*, 2001. **12**(6): p. 989-94.
254. Kim, Y.H., et al., *Polyethylenimine with acid-labile linkages as a biodegradable gene carrier.* *J Control Release*, 2005. **103**(1): p. 209-19.
255. Mintzer, M.A. and E.E. Simanek, *Nonviral vectors for gene delivery.* *Chem Rev*, 2009. **109**(2): p. 259-302.

256. Cheng, W., et al., *Delivery of a granzyme B inhibitor gene using carbamate-mannose modified PEI protects against cytotoxic lymphocyte killing*. *Biomaterials*, 2013. **34**(14): p. 3697-705.
257. Huang, S.L., et al., *Inhibition of Bcl-2 expression by a novel tumor-specific RNA interference system increases chemosensitivity to 5-fluorouracil in HeLa cells*. *Acta Pharmacol Sin*, 2006. **27**(2): p. 242-8.
258. Livak, K.J. and T.D. Schmittgen, *Analysis of relative gene expression data using real-time quantitative PCR and the 2(-Delta Delta C(T)) Method*. *Methods*, 2001. **25**(4): p. 402-8.
259. Pratt, R.C., et al., *Tagging alcohols with cyclic carbonate: a versatile equivalent of (meth)acrylate for ring-opening polymerization*. *Chem Commun (Camb)*, 2008(1): p. 114-6.
260. Sanders, D.P., et al., *A simple and efficient synthesis of functionalized cyclic carbonate monomers using a versatile pentafluorophenyl ester intermediate*. *J Am Chem Soc*, 2010. **132**(42): p. 14724-6.
261. C. R. Dick , G.E.H., *Characterization of Polyethylenimine*. *Journal of Macromolecular Science: Part A - Chemistry*, 1970. **4**(6): p. 1301-1314.
262. Jacobs, F., E. Wisse, and B. De Geest, *The role of liver sinusoidal cells in hepatocyte-directed gene transfer*. *Am J Pathol*, 2010. **176**(1): p. 14-21.
263. Matsumura, Y. and H. Maeda, *A new concept for macromolecular therapeutics in cancer chemotherapy: mechanism of tumoritropic accumulation of proteins and the antitumor agent smancs*. *Cancer Res*, 1986. **46**(12 Pt 1): p. 6387-92.
264. Nimesh, S., et al., *Enhanced gene delivery mediated by low molecular weight chitosan/DNA complexes: effect of pH and serum*. *Mol Biotechnol*, 2010. **46**(2): p. 182-96.
265. Versteegen, R.M., Sijbesma, R.P. & Meijer, E.W., *Synthesis and characterization of segmented copoly(ether urea)s with uniform hard segments*. *Macromolecules*, 2005. **38**(8): p. 3176-3184.
266. Kim, S.H., et al., *Hydrogen bonding-enhanced micelle assemblies for drug delivery*. *Biomaterials*, 2010. **31**(31): p. 8063-71.
267. Hui-zhen Jia, X.-h.L., Han Cheng, Juan Yang, Cao Li, Chen-Wei Liu, Jun Feng, Xian-zheng Zhang and Ren-xi Zhuo., *Extraordinarily enhanced gene transfection and cellular uptake by aromatic hydrophobicization to PEI25K*. *J. Mater. Chem.*, 2012. **22**: p. 24092-24101
268. Xu, Q., C.H. Wang, and D.W. Pack, *Polymeric carriers for gene delivery: chitosan and poly(amidoamine) dendrimers*. *Curr Pharm Des*, 2010. **16**(21): p. 2350-68.
269. N.A. *Transfection and Infection of Mammalian Cells Handout*. *Mammalian and Plant Cell Culture Module 5 N.D.* [cited 2013 30 August]; Available from: <http://web.mnstate.edu/provost/biotech/Transfection%20and%20Infection%20of%20Mammalian%20Cells%20Handout.pdf>.
270. UK, P. *Transfection*. *Protocols and Applications Guide 2013* [cited 2013 28 August]; Available from: [http://www.promega.co.uk/resources/product-guides-and-selectors/protocols-and-applications-guide/transfection/?_utma=1.1383559151.1380536998.1380536998.1380536998.1&_utmb=1.0.10.1380536998&_utmcc=1&_utmx=-&_utmv=1.1380536998.1.1.utmcsr=google|utmccn=\(organic\)|utmcmd=organic|utmctr=\(not%20provided\)&_utmh=-&_utmk=89684507](http://www.promega.co.uk/resources/product-guides-and-selectors/protocols-and-applications-guide/transfection/?_utma=1.1383559151.1380536998.1380536998.1380536998.1&_utmb=1.0.10.1380536998&_utmcc=1&_utmx=-&_utmv=1.1380536998.1.1.utmcsr=google|utmccn=(organic)|utmcmd=organic|utmctr=(not%20provided)&_utmh=-&_utmk=89684507).
271. Laboratories, B.-R. *Transfection*. *Applications & Technologies 2013* [cited 2013 28 August]; Available from: <http://www.bio-rad.com/en-uk/applications-technologies/technologies/transfection>.
272. Peng, Q., et al., *Enhanced gene transfection capability of polyethylenimine by incorporating boronic acid groups*. *Chem Commun (Camb)*, 2010. **46**(32): p. 5888-90.
273. Zintchenko, A., et al., *Simple modifications of branched PEI lead to highly efficient siRNA carriers with low toxicity*. *Bioconjug Chem*, 2008. **19**(7): p. 1448-55.
274. Dittmar, R., et al., *Assessment of cell viability in three-dimensional scaffolds using cellular auto-fluorescence*. *Tissue Eng Part C Methods*, 2012. **18**(3): p. 198-204.

275. Alton, G., et al., *Direct utilization of mannose for mammalian glycoprotein biosynthesis*. *Glycobiology*, 1998. **8**(3): p. 285-95.
276. Carreño-Gómez, B.a.D., R. , *Evaluation of the biological properties of soluble chitosan and chitosan microspheres*. *International Journal of Pharmaceutics*, 1997. **148**(2): p. 231-240.
277. Kean, T., S. Roth, and M. Thanou, *Trimethylated chitosans as non-viral gene delivery vectors: cytotoxicity and transfection efficiency*. *J Control Release*, 2005. **103**(3): p. 643-53.
278. Kowapradit, J., et al., *In vitro permeability enhancement in intestinal epithelial cells (Caco-2) monolayer of water soluble quaternary ammonium chitosan derivatives*. *AAPS PharmSciTech*, 2010. **11**(2): p. 497-508.
279. Teo, P.Y., et al., *Hydrophobic modification of low molecular weight polyethylenimine for improved gene transfection*. *Biomaterials*, 2013. **34**(32): p. 7971-9.
280. Wacheck, V., et al., *Small interfering RNA targeting bcl-2 sensitizes malignant melanoma*. *Oligonucleotides*, 2003. **13**(5): p. 393-400.
281. Feng, L.F., et al., *Bcl-2 siRNA induced apoptosis and increased sensitivity to 5-fluorouracil and HCPT in HepG2 cells*. *J Drug Target*, 2006. **14**(1): p. 21-6.
282. Beh, C.W., et al., *Efficient delivery of Bcl-2-targeted siRNA using cationic polymer nanoparticles: downregulating mRNA expression level and sensitizing cancer cells to anticancer drug*. *Biomacromolecules*, 2009. **10**(1): p. 41-8.
283. Zhang, L., et al., *Enhanced chemotherapy efficacy by sequential delivery of siRNA and anticancer drugs using PEI-grafted graphene oxide*. *Small*, 2011. **7**(4): p. 460-4.
284. Zou, S.M., et al., *Systemic linear polyethylenimine (L-PEI)-mediated gene delivery in the mouse*. *J Gene Med*, 2000. **2**(2): p. 128-34.
285. Trubetskoy, V.S., et al., *Recharging cationic DNA complexes with highly charged polyanions for in vitro and in vivo gene delivery*. *Gene Ther*, 2003. **10**(3): p. 261-71.
286. Goula, D., et al., *Polyethylenimine-based intravenous delivery of transgenes to mouse lung*. *Gene Ther*, 1998. **5**(9): p. 1291-5.
287. Mahato, R.I., et al., *Physicochemical and pharmacokinetic characteristics of plasmid DNA/cationic liposome complexes*. *J Pharm Sci*, 1995. **84**(11): p. 1267-71.
288. Classen, C.F., et al., *The granzyme B inhibitor PI-9 is differentially expressed in all main subtypes of pediatric acute lymphoblastic leukemias*. *Haematologica*, 2004. **89**(11): p. 1314-21.
289. Bratosin, D., et al., *Novel fluorescence assay using calcein-AM for the determination of human erythrocyte viability and aging*. *Cytometry A*, 2005. **66**(1): p. 78-84.
290. De Laporte, L., J. Cruz Rea, and L.D. Shea, *Design of modular non-viral gene therapy vectors*. *Biomaterials*, 2006. **27**(7): p. 947-54.
291. Shihui Wen, F.Z., Mingwu Shen, Xiangyang Shi, *Surface modification and PEGylation of branched polyethyleneimine for improved biocompatibility*. *Journal of Applied Polymer Science*, 2013. **128**(6): p. 3807-3813.
292. Trapani, J.A., et al., *Immunopurification of functional Asp-ase (natural killer cell granzyme B) using a monoclonal antibody*. *Biochem Biophys Res Commun*, 1993. **195**(2): p. 910-20.
293. Huang, M., et al., *Detection of apoptosis-specific autoantibodies directed against granzyme B-induced cleavage fragments of the SS-B (La) autoantigen in sera from patients with primary Sjogren's syndrome*. *Clin Exp Immunol*, 2005. **142**(1): p. 148-54.
294. Sun, J., et al., *A cytosolic granzyme B inhibitor related to the viral apoptotic regulator cytokine response modifier A is present in cytotoxic lymphocytes*. *J Biol Chem*, 1996. **271**(44): p. 27802-9.
295. Suriano, F., et al., *Synthesis of a family of amphiphilic glycopolymers via controlled ring-opening polymerization of functionalized cyclic carbonates and their application in drug delivery*. *Biomaterials*, 2010. **31**(9): p. 2637-45.
296. Zheng, M., et al., *Lipoic acid modified low molecular weight polyethylenimine mediates nontoxic and highly potent in vitro gene transfection*. *Mol Pharm*, 2011. **8**(6): p. 2434-43.

297. Amanda C. Engler, D.K.B., Hilda G. Buss, Eva Y. Cheung and Paula T. Hammond *The synthetic tuning of clickable pH responsive cationic polypeptides and block copolypeptides*. *Soft Matter*, 2011. **7**: p. 5627-5637.
298. Akinc, A., et al., *Exploring polyethylenimine-mediated DNA transfection and the proton sponge hypothesis*. *J Gene Med*, 2005. **7**(5): p. 657-63.
299. Sonawane, N.D., F.C. Szoka, Jr., and A.S. Verkman, *Chloride accumulation and swelling in endosomes enhances DNA transfer by polyamine-DNA polyplexes*. *J Biol Chem*, 2003. **278**(45): p. 44826-31.
300. Rejman, J., et al., *Size-dependent internalization of particles via the pathways of clathrin- and caveolae-mediated endocytosis*. *Biochem J*, 2004. **377**(Pt 1): p. 159-69.
301. Kopatz, I., J.S. Remy, and J.P. Behr, *A model for non-viral gene delivery: through syndecan adhesion molecules and powered by actin*. *J Gene Med*, 2004. **6**(7): p. 769-76.
302. Lefranc, A.T.a.M.-P. *Mouse H2 haplotypes and polymorphisms*. Mouse strain H2 haplotypes 2002 [cited 2013 4 September]; Available from: http://www.imgt.org/IMGTrepertoireMHC/Polymorphism/haplotypes/mouse/MHC/Mu_haplotypes.html.
303. Aaronson, S.A. and G.J. Todaro, *Development of 3T3-like lines from Balb-c mouse embryo cultures: transformation susceptibility to SV40*. *J Cell Physiol*, 1968. **72**(2): p. 141-8.
304. Aaronson, S.A. and G.J. Todaro, *Basis for the acquisition of malignant potential by mouse cells cultivated in vitro*. *Science*, 1968. **162**(3857): p. 1024-6.
305. Lieberman, J., *The ABCs of granule-mediated cytotoxicity: new weapons in the arsenal*. *Nat Rev Immunol*, 2003. **3**(5): p. 361-70.
306. Lodoen, M.B. and L.L. Lanier, *Viral modulation of NK cell immunity*. *Nat Rev Microbiol*, 2005. **3**(1): p. 59-69.
307. Krug, A., et al., *Herpes simplex virus type 1 activates murine natural interferon-producing cells through toll-like receptor 9*. *Blood*, 2004. **103**(4): p. 1433-7.
308. Lanier, L.L., *NK cell receptors*. *Annu Rev Immunol*, 1998. **16**: p. 359-93.
309. Lanier, L.L., *NK cell recognition*. *Annu Rev Immunol*, 2005. **23**: p. 225-74.
310. Ljunggren, H.G. and K. Karre, *Host resistance directed selectively against H-2-deficient lymphoma variants. Analysis of the mechanism*. *J Exp Med*, 1985. **162**(6): p. 1745-59.
311. Purdy, A.K., and Campbell, K. S., *Natural killer cells and cancer: regulation by the killer cell Ig-like receptors (KIR)*. *Cancer Biol. Ther.*, 2009. **8**: p. 2211-2220.
312. Vilches, C., and Parham, P. , *KIR: diverse, rapidly evolving receptors of innate and adaptive immunity*. *Annu. Rev. Immunol.* , 2002. **20**: p. 217-251.
313. Leung, W., Handgretinger, R., Iyengar, R., Turner, V., Holladay, M. S., and Hale, G. A. , *Inhibitory KIR-HLA receptor-ligand mismatch in autologous haematopoietic stem cell transplantation for solid tumour and lymphoma*. . *Br. J. Cancer* 2007. **97**: p. 539-542.
314. Moretta, L., and Moretta, A. , *Killer immunoglobulin-like receptors*. . *Curr. Opin. Immunol.* , 2004. **16**: p. 626-633.
315. Delgado, D.C., Hank, J. A., Kolesar, J., Lorentzen, D., Gan, J., Seo, S., Kim, K., Shusterman, S., Gillies, S. D., Reisfeld, R. A., Yang, R., Gadbow, B., Desantes, K. B., London, W. B., Seeger, R. C., Maris, J. M., and Sondel, P. M. , *Genotypes of NK cell KIR receptors, their ligands, and Fc gamma receptors in the response of neuroblastoma patients to Hu14.18-IL2 immunotherapy*. . *Cancer Res.*, 2010. **70**: p. 9554-9561.
316. Venstrom, J.M., Zheng, J., Noor, N., Danis, K. E., Yeh, A. W., Cheung, I. Y., Dupont, B., O'Reilly, R. J., Cheung, N. K., and Hsu, K. C. , *KIR and HLA genotypes are associated with disease progression and survival following autologous hematopoietic stem cell transplantation for high-risk neuroblastoma*. . *Clin. Cancer Res.* , 2009. **15**: p. 7330-7334.
317. Auchincloss H Jr, S.D., *Xenogeneic transplantation*. . *Annu. Rev. Immunol.*, 1998. **16**: p. 433-470.

318. Inverardi L, S.M., Motterlini R, Mangili F, Bender JR, Pardi R. , *Early recognition of a discordant xenogeneic organ by human circulating lymphocytes*. J. Immunol., 1992. **149**: p. 1416-1423.
319. Ofer Mandelboim, N.L., Marianna Lev, Lada Paul, Tal I. Arnon, Yuri Bushkin, Daniel M. Davis, Jack L. Strominger, Jonathan W. Yewdell & Angel Porgador, *Recognition of haemagglutinins on virus-infected cells by NKp46 activates lysis by human NK cells*. Nature, 2001. **409**: p. 1055-1060.
320. Yiling Lu, R.R., Jay Bjorndahl, Catherine A. Phillips and James M. Trevillyan, *CD28-dependent killing by human YT cells requires phosphatidylinositol3-kinase activation*. Eur. J. Immunol. , 1996. **26**: p. 1278-1284.
321. Raab, M., Cai, Y., Bunnell, S., Heyeck, S., Berg, L. and Rudd, C. E., , *p56Lck and p59Fyn regulate CD28 binding to phosphatidylinositol 3-kinase, growth factor receptor-bound protein GRB-2, and T cell-specific protein-tyrosine kinase ITK: implications for T-cell costimulation*. Proc Natl Acad Sci U S A., 1995. **92**(19): p. 8891-8895.
322. Long, M.L.D.a.E.O., *Cytotoxic immunological synapses*. Immunol Rev. , 2010. **235**(1): p. 24-34.
323. Smith, K.M., Wu, J., Bakker, A. B., Phillips, J. H. and Lanier, L. L. , *Ly -49D and Ly -49H associate with mouse DAP12 and form activating receptors*. . J. Immunol. , 1998. **161**(1): p. 7-10.
324. Sofia E. Johansson, H.H., Jens Björklund and Petter Höglund, *Broadly impaired NK cell function in non - obese diabetic mice is partially restored by NK cell activation in vivo and by IL - 12/IL - 18 in vitro*. Int. Immunol. , 2004. **16**(1): p. 1-11.
325. Wu, J., Song, Y., Bakker, A. B., Bauer, S., Spies, T., Lanier, L. L. and Phillips, J. H. , *An activating immunoreceptor complex formed by NKG2D and DAP10*. Science, 1999. **285**(5428): p. 730-732
326. Yatin M. Vyas, H.M., Bo Dupont, *Visualization of signaling pathways and cortical cytoskeleton in cytolytic and noncytolytic natural killer cell immune synapses*. Immunological Reviews, 2002. **189**(1): p. 161-178.
327. Karre, K., et al., *Selective rejection of H-2-deficient lymphoma variants suggests alternative immune defence strategy*. Nature, 1986. **319**(6055): p. 675-8.
328. Moretta A, B.C., Vitale M, Pende D, Cantoni C, Mingari MC, Biassoni R, Moretta L., *Activating receptors and coreceptors involved in human natural killer cell-mediated cytotoxicity*. Annu Rev Immunol., 2001. **19**: p. 197-223.
329. Pende D, P.S., Pessino A, Sivori S, Augugliaro R, Morelli L, Marcenaro E, Accame L, Malaspina A, Biassoni R, Bottino C, Moretta L, Moretta A. , *Identification and molecular characterization of NKp30, a novel triggering receptor involved in natural cytotoxicity mediated by human natural killer cells*. J. Exp. Med., 1999. **190**: p. 1505-1516.
330. Vitale M, B.C., Sivori S, Sanseverino L, Castriconi R, Marcenaro R, Augugliaro R, Moretta L, Moretta A. , *NKp44, a novel triggering surface molecule specifically expressed by activated Natural Killer cells is involved in non-MHC restricted tumor cell lysis*. . J. Exp. Med., 1998. **187**: p. 2065-2072.
331. Moretta A, B.R., Bottino C, Mingari MC, Moretta L. , *Natural cytotoxicity receptors that trigger human NK-mediated cytotoxicity*. Immunol. Today, 2000. **21**: p. 228-234.
332. Pessino A, S.S., Bottino C, Malaspina A, Morelli L, Moretta L, Biassoni R, Moretta A., *Molecular cloning of NKp46: a novel member of the immunoglobulin superfamily involved in triggering of natural cytotoxicity*. J. Exp. Med., 1998. **188**: p. 953-960.
333. Biassoni R, P.A., Bottino C, Pende D, Moretta L, Moretta A., *The murine homologue of the human NKp46, a triggering receptor involved in the induction of natural cytotoxicity*. . Eur. J. Immunol., 1999. **29**: p. 1014-1020.
334. El Haddad, N., et al., *Mesenchymal stem cells express serine protease inhibitor to evade the host immune response*. Blood, 2011. **117**(4): p. 1176-83.
335. Greiner, D.L., R.A. Hesselton, and L.D. Shultz, *SCID mouse models of human stem cell engraftment*. Stem Cells, 1998. **16**(3): p. 166-77.

336. Matsumura, Y., et al., *Phase I clinical trial and pharmacokinetic evaluation of NK911, a micelle-encapsulated doxorubicin*. Br J Cancer, 2004. **91**(10): p. 1775-81.
337. Wang, H., et al., *CD47 is required for suppression of allograft rejection by donor-specific transfusion*. J Immunol, 2010. **184**(7): p. 3401-7.

APPENDIX A

Synthetic procedures and characterization of functionalized methylcarboxytrimethylene carbonate (MTC) monomers and carbamate modified PEIs

1. Synthesis of sugar-functionalized cyclic carbonate (MTC-ip-sugar) (Figure S1)

The monomers with protected sugar pendent groups include MTC-ipman, MTC-ipgal and MTC-ipglu and they were prepared according to the protocol reported previously [A1]. The details of the procedure for preparation of MTC-ipman are given below as a typical example. Briefly, a solution of oxalyl chloride (2.48 mL, 19.0 mmol) in 50 mL of dry tetrahydrofuran (THF) was drop-wisely added into a solution of MTC-OH (5-Methyl-5-carboxyl-1,3-dioxan-2-one) (2.75 g, 17.2 mmol) in 50 mL of dry THF, followed by adding a catalytic amount (3 drops) of anhydrous dimethylformamide (DMF) over 30 min under N₂ atmosphere. The reaction solution was stirred for 1 h with N₂ bubbled through to remove volatiles. After the reaction, the solvent was evaporated under vacuum. The solid residue (intermediate product MTC-Cl) was then dissolved in 50 mL of dry dichloromethane (DCM), and a mixture of 2,3;5,6-di-O-isopropylidene-D-mannofuranose (ipman, 4.13 g, 15.8 mmol) and triethylamine (2.8 mL, 20.6 mmol) in 50 mL of dry DCM was stepwise dropped into the solution over 30 min at room temperature. Then, the reaction mixture was heated to 40 °C and reacted for 48 h. After cooled down to room temperature, the reaction solution was concentrated and 100 mL THF was added to precipitate triethylamine salt. After evaporating the filtrate, the crude product was passed through a silica gel column by gradient, eluted of ethyl acetate and hexane (20/80 to 50/50) to provide the product as sticky colorless oil that slowly solidified to a white solid (5.85 g, 85%). ¹H-NMR (400MHz, CDCl₃, 22 °C): δ 6.17 (s, 1H, H-a), 5.79 (dd, 1H, H-b), 4.83 (m, 1H, H-d), 4.66 (d, 2H, H-c), 4.41 (m, 1H, H-g), 4.22 (m, 2H, H-c), 4.03 (m, 2H, H-e + H-f), 3.73 (m, 1H, H-e), 1.33-1.50 (m, 15H, H-h + H-i). By changing the alcohol with 1,2;3,4-Di-O-isopropylidene-D-galactopyranose or 1,2;5,6-Di-O-isopropylidene-D-glucofuranose, the following monomers, MTC-ipgal and MTC-ipglu, were also obtained.

MTC-ipgal, Yield, 81%, ¹H-NMR (400MHz, CDCl₃, 22 °C): δ 5.54 (d, 1H, H-a), 4.70 (m, 2H, H-c), 4.62 (m, 1H, H-b), 4.41 (m, 1H, H-f), 4.33 (m, 2H, H-d and H-e), 4.26 (m, , 3H, H-c and H-g), 4.03 (m, 1H, H-g), 1.32-1.49 (5 s, 15H, H-h + H-i).

MTC-ipglu, Yield, 75%, $^1\text{H-NMR}$ (400MHz, CDCl_3 , 22 $^\circ\text{C}$): δ 5.90 (d, 1H, H-a), 5.39 (d, 1H, H-b), 4.69 (d, 2H, H-c), 4.46 (d, 1H, H-g), 4.18 (m, 2H, H-c), 4.06 (m, 2H, H-e and H-f), 4.00 (m, 1H, H-e), 1.30-1.52 (5 s, 15H, H-h + H-i).

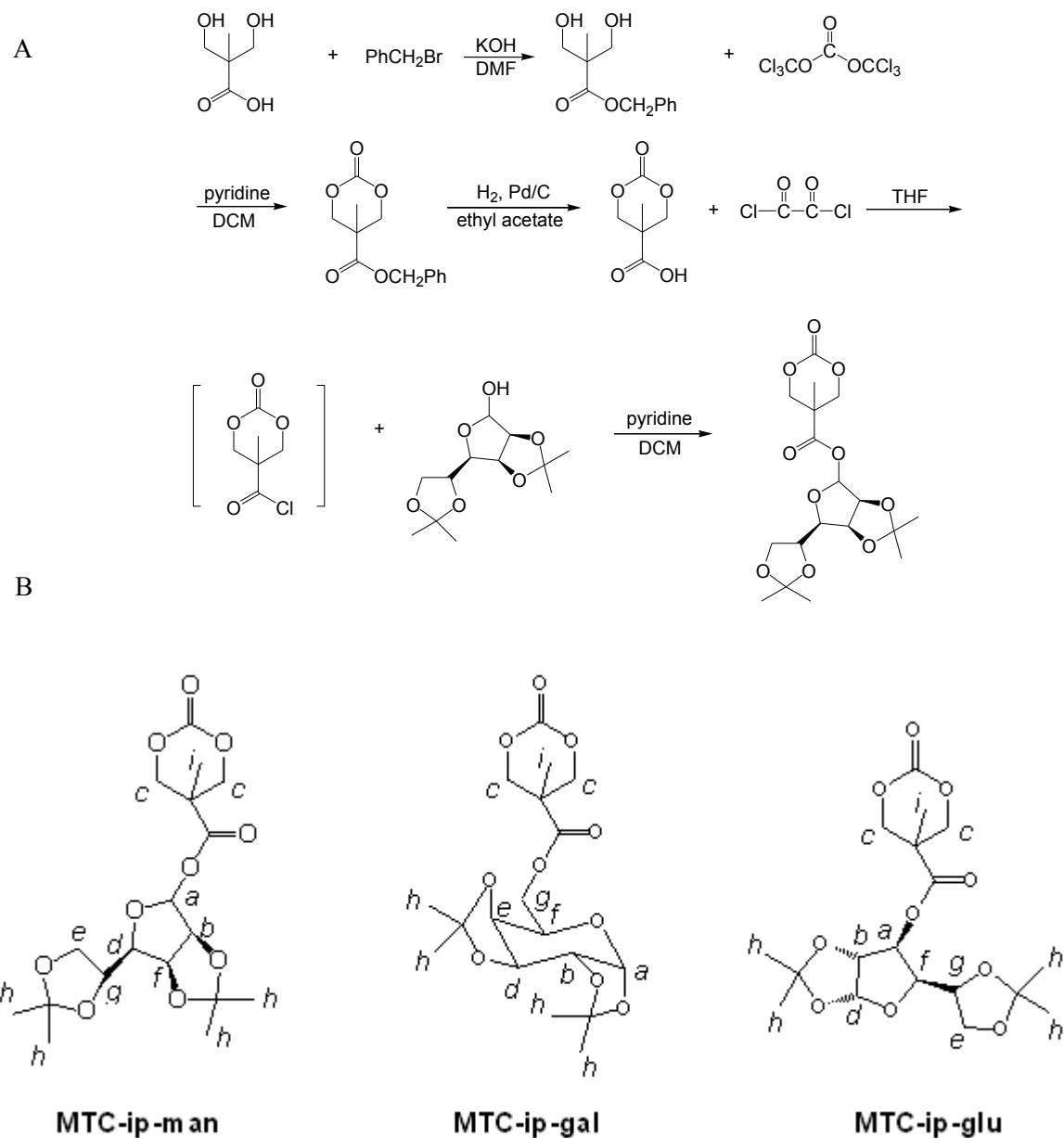


Figure S1. (A) Synthesis of protected mannose-functionalized cyclic carbonate (MTC-ipman). (B) Chemical structures of sugar-functionalized cyclic carbonates.

2. Synthesis of hydrophobic groups-functionalized cyclic carbonate (MTC-benzyl, MTC-ethyl, and MTC-urea)

The detailed preparation protocol of functional MTC monomers, including MTC-benzyl, MTC-ethyl and MTC-urea, was reported previously [A2-A4]. As shown in Figure S2a, they were synthesized via coupling reaction of the corresponding substrates with hydroxyl

group and cyclic carbonate, MTC-OH. MTC-OH was prepared using the standard procedures reported previously [A2]. The synthetic procedure of MTC-urea is given below as a typical example. MTC-urea was synthesized by tagging phenylureaethanol with MTC-OH. In order to prepare phenylureaethanol, ethanolamine (2.96 g, 48.5 mmol) was dissolved in dry THF (30 mL) and cooled to 0°C using an ice bath. Phenylisocyanate (5.19 g, 4.74 mL, 43.6mmol) in dry THF (30 mL) was added dropwise during a period of 30 min. The resulting solution was allowed to warm to the ambient temperature (~ 22°C) and stirred for an additional 16 h. Then, THF was evaporated. The crude product was re-crystallized from ethyl acetate and stirred rigorously for 4 h. The product was collected by filtration, washed with ethyl acetate and dried until a constant weight was reached (7.0g, ~86%). ¹H NMR (400 MHz, DMSO-d₆, 22 °C): δ 8.59 (s, 1H, PhNH), 7.39 (d, 2H, PhH), 7.21 (t, 2H, PhH), 6.95 (t, 1H, PhH), 6.10 (t, 1H, PhNHC(O)NH), 4.78 (t, 1H, -OH), 3.43 (q, 2H, -CH₂OH), 3.17 (q, 2H, -NHCH₂CH₂OH). MTC-OH (3.04 g, 19 mmol) was converted to MTC-Cl using the standard procedure with oxalyl chloride [A2]. MTC-Cl was dissolved in dry methylene chloride (50 mL) and charged in a funnel. In a dry 500 mL round bottom flask equipped with a stir bar was charged phenylureaethanol (4.10 g, 22.8 mmol), pyridine (1.81 g, 1.85 mL, 22.8 mmol) and dry methylene chloride (150 mL) and cooled to 0 °C using an ice bath. The MTC-Cl solution was added dropwise during a period of 30 min and stirred for 30 min. Then, the ice bath was removed, and the solution was allowed to gently warm to the ambient temperature and left under stirring for an additional 16 h. The crude product was purified by column chromatography. Ethyl acetate/hexane (1/1) was initially used as eluent before gently increasing the polarity and finishing with ethyl acetate. The product fractions were collected, and the solvent was removed through rotational evaporation. The isolated product (MTC-urea) was dried under vacuum until a constant weight was reached, yielding 6.0 g of an off white/slight yellow oil which crystallized upon standing (~80%). ¹H NMR (400 MHz, CDCl₃, 22 °C): δ 7.39 (d, 2H, PhH), 7.25 (m, 2H, PhH), 7.02 (t, 1H, PhH), 4.68 (d, 2H, -CH₂OCOO), 4.30 (t, 2H, -COOCH₂-), 4.20 (d, 2H, -CH₂OCOO), 3.55 (t, 2H, -CH₂NHC(O)NHPh), 1.30 (s, 3H, -CH₃).

As shown in Figure S2b, MTC-ethyl was synthesized using the following protocol.

(i) Bis-MPA (22.1 g, 0.165 mol) was added in ethanol (150 mL) with Amberlyst-15 (6.8 g) and refluxed overnight. The resins were then filtered out and the filtrate was evaporated. Methylene chloride (200 mL) was added to the resulting viscous liquid to filtrate the unreacted

reagent and byproduct. After the solution was dried over MgSO_4 and evaporated, ethyl 2,2-bis(methylol)propionate was obtained as a clear and colorless liquid (24.3 g, 91%). ^1H NMR (400 MHz, CDCl_3 , 22 °C): δ 4.09 (q, 2H, $-\text{OCH}_2\text{CH}_3$), 3.74 (d, 2H, $-\text{CH}_2\text{OH}$), 3.57(d, 2H, $-\text{CH}_2\text{OH}$), 1.18 (t, 3H, $-\text{OCH}_2\text{CH}_3$), 0.98 (s, 3H, $-\text{CH}_3$).

(ii) A solution of triphosgene (11.7 g, 0.039 mol) in CH_2Cl_2 (150 mL) was added dropwise to a methylene chloride solution (150 mL) of ethyl 2,2-bis(methylol)propionate (12.6 g, 0.078mol) and pyridine (39 mL, 0.47 mol) over 30 min at -75 °C with dry ice/acetone under N_2 atmosphere. The reaction mixture was kept stirring for another 2 h under the chilled condition and then allowed to warm to room temperature. The reaction was quenched by addition of saturated aqueous NH_4Cl (75 mL), after which the organic layer was washed with 1 M aqueous HCl (3×100 mL), saturated aqueous NaHCO_3 (1×100 mL), dried over MgSO_4 , filtered and evaporated. The residue was re-crystallized from ethyl acetate to give MTC-ethyl as white crystals (8.0 g, 55%). ^1H NMR (400 MHz, CDCl_3 , 22 °C): δ 4.67 (d, 2H, $-\text{CH}_2\text{OCOO}$), 4.25 (q, 2H, $-\text{OCH}_2\text{CH}_3$), 4.19 (d, 2H, $-\text{CH}_2\text{OCOO}$), 1.30 (s, 3H, $-\text{CH}_3$), 1.27 (t, 3H, $-\text{OCH}_2\text{CH}_3$).

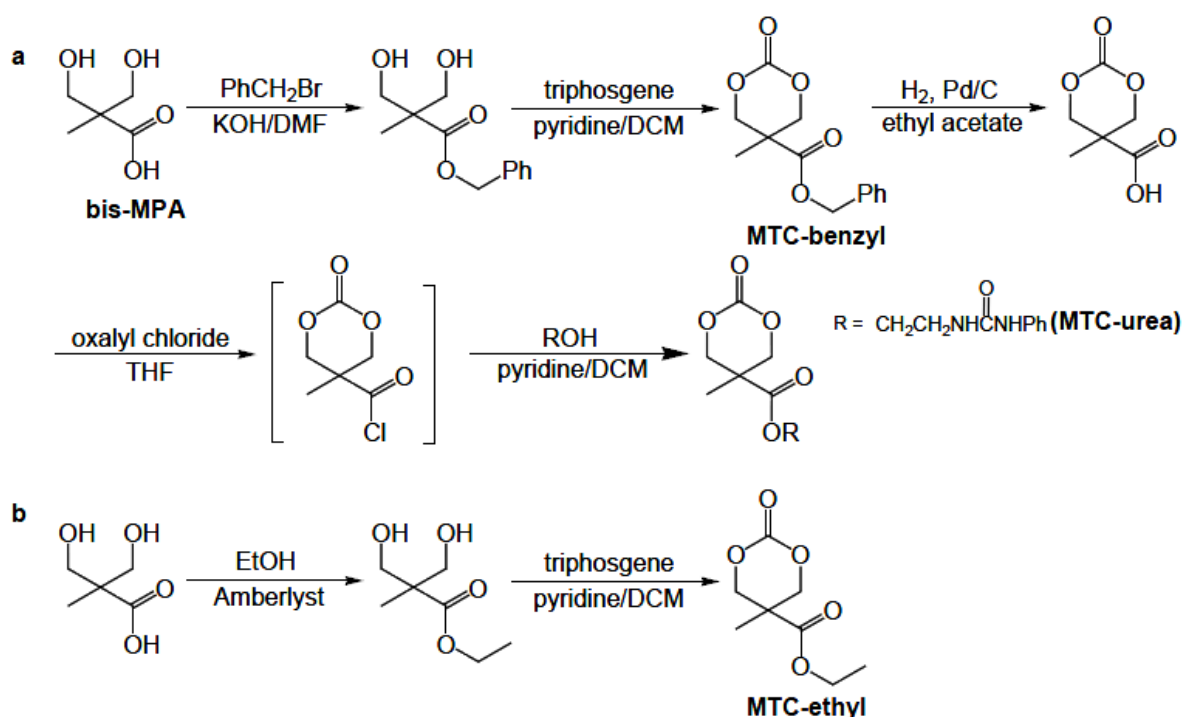


Figure S2. Synthesis of functional MTC-urea (a) and MTC-ethyl (b) monomers.

3. Synthesis of sugar-modified PEI (25 kDa)

The details of the procedure for ring-opening polymerization of MTC-ipman with PEI (molar feed ratio 1:25, polymer **B**) are given as a typical example. In a glove box, MTC-ipman (0.25 g, 0.625 mmol) was added to the solution of PEI ($M_n = 10$ kDa, 0.25 g, 0.025 mmol) in 2 mL of DCM, followed by adding DBU (4.7 μ L, 0.031 mmol). The reaction solution was stirred for 1 h. And then 10 mL of methanol and 10 mL of 1 M HCl (aq.) were added. The resulting reaction mixture was heated to reflux and last for 2 h before cooled down to room temperature. Finally, the above mixture was purified by ultrafiltration in a Vivaspin 20 concentrator (MWCO = 5 k, Sartorius AG, Goettingen, Germany), washed 3 times with de-ionized (DI) water, and freeze-dried (0.36 g, 80%). $^1\text{H-NMR}$ (400MHz, D_2O , 22 $^\circ\text{C}$): δ : 4.08 (s, 40H, H-d and H-e), 2.70-3.65 (br, m, 992H, H-e, H-f, H-g and H of bPEI), 1.06 (s, 61H, H-i).

Using a similar protocol, polymer **A**, **C**, **L**, **M**, and **N** were synthesized at PEI to mannose-carbonate molar feed ratios of 1:8, 1:75, 1: 58, 1:120, and 1:400.

For polymer **F** and **G**, they were synthesized with the PEI to mannose-carbonate molar ratio of 1:25 in the absence of DBU, and reacted for 18 h and 1 h respectively before acidification.

For polymer **T** and **S**, they were synthesized with the PEI to mannose-carbonate molar ratio of 1:6 and 1:12.5 in the absence of DBU, and 1 h before acidification.

For polymer **H**, **I**, **R** and **U**, they were synthesized with the PEI to glucose-carbonate molar ratio of 1:25 (**H**), PEI to galactose-carbonate molar ratio of 1:25 (**I**), 1:12.5 (**R**), and 1:6 (**U**), and reacted for 1 h in the absence of DBU before acidification and purification by ultrafiltration.

4. Synthesis of hydrophobic groups functionalized carbamate-modified PEI

For polymer **P**, **V**, **J**, **K**, **O**, **aa**, and **ab**, they were synthesized with different hydrophobic monomers (TMC, MTC-ethyl, MTC-benzyl, and MTC-urea) at various molar ratios of monomer to PEI, and reacted for 1 h in the absence of DBU. The detailed procedure for modifying PEI with TMC at feed molar ratio of 1:25 (**K**:PEI-TMC(1:25)) was given as a typical example. TMC (64 mg, 0.625 mmol) was added to the 2 mL DCM solution of PEI ($M_n = 10$ kDa, 0.25 g, 0.025 mmol) and the reaction solution was stirred for 1 h before being

concentrated to dryness and dried *in vacuo*. $^1\text{H-NMR}$ (400MHz, MeOD, 22 °C): δ 4.13 (s, 54H, H-a), 3.62 (t, 54H, H-c), 3.21 (br, d, 54H, H-d), 2.50-2.82 (br, m, 930H, H of bPEI), 1.83 (s, 54H, H-b). Using a similar protocol, **V**:PEI-TMC(1:1), **P**:PEI-TMC(1:8), and **J**:PEI-TMC(1:100) were synthesized at the PEI to TMC molar feed ratios of 1:1, 1:8 and 1:100 respectively.

ab:PEI-urea(1:25), $^1\text{H-NMR}$ (400 MHz, MeOD, 22 °C): δ 7.39 (s, 54H, PhH), 7.27 (t, 54H, PhH), 7.00 (s, 27H, PhH), 4.23 (s, 108H, H of $-\text{CH}_2\text{OCOO}$ and $-\text{COOCH}_2-$), 3.69 (s, 54H, $-\text{CH}_2\text{OCOO}$), 3.49 (s, 54H, $-\text{CH}_2\text{NHC(O)NHPH}$), 2.40-2.87 (br, m, 930H, H of bPEI), 1.22 (s, 81H, $-\text{CH}_3$).

aa:PEI-benzyl(1:25), $^1\text{H-NMR}$ (400MHz, MeOD, 22 °C): δ 7.35 (s, 145H, PhH), 5.16 (s, 58H, Ph CH_2-), 4.23 (s, 58H, $-\text{CH}_2\text{OCOO}$), 3.70 (s, 58H, $-\text{CH}_2\text{OCOO}$), 2.50-2.82 (br, m, 930H, H of bPEI), 1.22 (s, 87H, $-\text{CH}_3$).

O:PEI-ethyl(1:25), $^1\text{H-NMR}$ (400MHz, MeOD, 22 °C): δ 4.16 (m, 54H, H of $-\text{OCH}_2\text{CH}_3$ and $-\text{CH}_2\text{OCOO}$), 3.64 (t, 54H, $-\text{CH}_2\text{OCOO}$), 2.50-2.82 (br, m, 930H, H of bPEI), 1.25 (s, 54H, $-\text{CH}_3$).

5. Characterization of monomers and polymers using ^1H NMR spectroscopy

^1H NMR spectra were obtained on a Bruker Advance 400 NMR spectrometer at 400 MHz at room temperature. The ^1H NMR measurements were carried out with an acquisition time of 3.2 s, a pulse repetition time of 2.0 s, a 30° pulse width, 5208-Hz spectral width, and 32 K data points. Chemical shifts were referred to the solvent peaks ($\delta = 7.26$, 3.33 and 2.50 ppm for CDCl_3 , MeOD and $\text{DMSO-}d_6$, respectively).

[A1] Suriano, F., et al., *Synthesis of a family of amphiphilic glycopolymers via controlled ring-opening polymerization of functionalized cyclic carbonates and their application in drug delivery*. *Biomaterials*, 2010. **31**(9): p. 2637-45.

[A2] Pratt, R.C., et al., *Tagging alcohols with cyclic carbonate: a versatile equivalent of (meth)acrylate for ring-opening polymerization*. *Chem Commun (Camb)*, 2008(1): p. 114-6.



[A3] Fukushima, K., et al., *Organocatalytic approach to amphiphilic comb-block copolymers capable of stereocomplexation and self-assembly*. *Biomacromolecules*, 2008. **9**(11): p. 3051-6.

[A4] Kim, S.H., et al., *Hydrogen bonding-enhanced micelle assemblies for drug delivery*. *Biomaterials*, 2010. **31**(31): p. 8063-71.

APPENDIX B

Permission to republish all the third party copyrighted works in this thesis

1.



Thank You For Your Order!

Dear Ms. WEI CHENG,

Thank you for placing your order through Copyright Clearance Center's RightsLink service. Elsevier has partnered with RightsLink to license its content. This notice is a confirmation that your order was successful.

Your order details and publisher terms and conditions are available by clicking the link below:
<http://s100.copyright.com/CustomerAdmin/PLF.jsp?ref=ae8a4527-1173-412a-99ae-4a1f2773e0c4>

Order Details
Licensee: WEI CHENG
License Date: Aug 18, 2013
License Number: 3211870234023
Publication: Progress in Polymer Science
Title: Polymer systems for gene delivery-Past, present, and future
Type Of Use: reuse in a thesis/dissertation
Total: 0.00 GBP

To access your account, please visit <https://myaccount.copyright.com>.

Please note: Online payments are charged immediately after

order confirmation; invoices are issued daily and are payable immediately upon receipt.

To ensure we are continuously improving our services, please take a moment to complete our [customer satisfaction survey](#).

B.1:v4.2

+1-877-622-5543 / Tel: +1-978-646-2777



2.

RightsLink



Thank You For Your Order!

Dear Ms. WEI CHENG,

Thank you for placing your order through Copyright Clearance Center's RightsLink service. Nature Publishing Group has partnered with RightsLink to license its content. This notice is a confirmation that your order was successful.

Your order details and publisher terms and conditions are available by clicking the link below:

<http://s100.copyright.com/CustomerAdmin/PLF.jsp?ref=4d2d64a1-6f87-477b-86e4-7fb70139933a>

Order Details

Licensee: WEI CHENG

License Date: Aug 17, 2013

License Number: 3211350263685

Publication: Cell Death and Differentiation

Title: Granzymes and perforin in solid organ transplant rejection

Type Of Use: reuse in a thesis/dissertation

Total: 0.00 GBP

To access your account, please visit <https://myaccount.copyright.com>.

Please note: Online payments are charged immediately after order confirmation; invoices are issued daily and are payable immediately upon receipt.

To ensure we are continuously improving our services, please take a moment to complete our [customer satisfaction survey](#).

B.1:v4.2

+1-877-622-5543 / Tel: +1-978-646-2777



3.

RightsLink



Thank You For Your Order!

Dear Ms. WEI CHENG,

Thank you for placing your order through Copyright Clearance Center's RightsLink service. Nature Publishing Group has partnered with RightsLink to license its content. This notice is a confirmation that your order was successful.

Your order details and publisher terms and conditions are available by clicking the link below:

<http://s100.copyright.com/CustomerAdmin/PLF.jsp?ref=3f33ab52-f3ba-4d8c-88ba-71acccb17b6>

Order Details

Licensee: WEI CHENG

License Date: Sep 1, 2013
License Number: 3220381406104
Publication: Nature Medicine
Title: Viral vectors for gene therapy: the art of turning infectious agents into vehicles of therapeutics
Type Of Use: reuse in a thesis/dissertation
Total: 0.00 GBP

To access your account, please visit <https://myaccount.copyright.com>.

Please note: Online payments are charged immediately after order confirmation; invoices are issued daily and are payable immediately upon receipt.

To ensure we are continuously improving our services, please take a moment to complete our [customer satisfaction survey](#).

B.1:v4.2

+1-877-622-5543 / Tel: +1-978-646-2777



4.

RightsLink



Thank You For Your Order!

Dear Ms. WEI CHENG,

Thank you for placing your order through Copyright Clearance Center's RightsLink service. Elsevier has partnered with RightsLink to license its content. This notice is a confirmation that your order was successful.

Your order details and publisher terms and conditions are available by clicking the link below:

<http://s100.copyright.com/CustomerAdmin/PLF.jsp?ref=a6ffbc1c-6a01-4a14-95fa-b14473a52130>

Order Details

Licensee: WEI CHENG

License Date: Sep 15, 2013

License Number: 3230280494825

Publication: Biomaterials

Title: Delivery of a granzyme B inhibitor gene using carbamate-mannose modified PEI protects against cytotoxic lymphocyte killing

Type Of Use: reuse in a thesis/dissertation

Total: 0.00 GBP

To access your account, please visit <https://myaccount.copyright.com>.

Please note: Online payments are charged immediately after order confirmation; invoices are issued daily and are payable immediately upon receipt.

To ensure we are continuously improving our services, please take a moment to complete our [customer satisfaction survey](#).

B.1:v4.2

+1-877-622-5543 / Tel: +1-978-646-2777



JOHN WILEY AND SONS LICENSE TERMS AND CONDITIONS

May 13, 2013

This is a License Agreement between WEI CHENG ("You") and John Wiley and Sons ("John Wiley and Sons") provided by Copyright Clearance Center ("CCC"). The license consists of your order details, the terms and conditions provided by John Wiley and Sons, and the payment terms and conditions.

All payments must be made in full to CCC. For payment instructions, please see information listed at the bottom of this form.

License Number	3147080823499
License date	May 13, 2013
Licensed content publisher	John Wiley and Sons
Licensed content publication	Advanced Healthcare Materials
Licensed content title	Mitigated Cytotoxicity and Tremendously Enhanced Gene Transfection Efficiency of PEI through Facile One-Step Carbamate Modification
Licensed copyright line	Copyright © 2013 WILEY-VCH Verlag GmbH & Co. KGaA, Weinheim
Licensed content author	Chuan Yang, Wei Cheng, Pei Yun Teo, Amanda C. Engler, Daniel J. Coady, James L. Hedrick, Yi Yan Yang
Licensed content date	Mar 18, 2013
Start page	n/a
End page	n/a
Type of use	Dissertation/Thesis
Requestor type	Author of this Wiley article
Format	Electronic
Portion	Full article
Will you be translating?	No
Total	0.00 USD